UW-Madison.
SSEC Publication No.92.07.R1.

Hubble Space Telescope
High Speed Photometer
Science Verification Test Report

Space Science and Engineering Center

and

Space Astronomy Laboratory

University of Wisconsin
Madison, Wisconsin

July 1992

1. Purpose of HSP SV Final Report

The purpose of this report is to summarize the results of the HSP Science Verification (SV) tests, the status of the HSP at the end of the SV period, and the work remaining to be done. The HSP OV report (November 1991) covered all activities (OV, SV, and SAO) from launch to the completion of phase III alignment, OV 3233 performed in the 91154 SMS, on June 8, 1991. This report covers subsequent activities though May 1992.

2. Executive Summary

The performance of the HSP has continued, with one exception, to be as designed with no failures or anomalies. The exception is that the VIS detector (IDT #3) has apparently lost sensitivity. There are indications that the loss is about a factor of two from the pre-launch ground calibrations but it is difficult to quantify. Between April 21 and July 20 the total flux observered from the same target (VID998) decreased by 10.7%. The reason for this loss is not known. The other detectors, including the POL detector (same IDT configuration as the VIS) have not shown any loss of sensitivity. More recently, the VIS detector did not show any additional loss of sensitivity between the first and second calibration tests (2912) performed in early March and late April 1992.

The short term photometric stability test (1389) data shows a small orbital variation in the measured signal from a star, the cause of which is not understood. There appear to be two effects: one having an orbital period and another with a much longer period that appears as a monotonically increasing linear component. Neither effect can be explained at present.

As of the end of 1991, all Orbital and Science Verification (OV and SV) activities had been successfully completed with the following exceptions:

1. The instrumental polarization test (1386) was delayed when the first run of a prior aperture position test (3377) failed because the target was not seen in most of the observations. This was because the HST step and dwell scan ramp up and ramp down time was not properly accounted for in the SMS. The problem was subsequently corrected and the aperture position test was re-run successfully in December 1991. There were problems finding guide stars for the target that further delayed the beginning of the test until March 1992. Presently the test has been partially completed and is scheduled to be fully completed by the end of June 1992.

2. The apertures used in the PRISM mode were not adequately mapped in the originally planned OV and SV tests. A new test for mapping the PRISM mode apertures was written after it was determined that the standard aperture mapping tests did not produce sufficient data to determine the prism mode aperture locations to the required accuracy. This test was run, data were analyzed and the locations of the PRISM apertures were updated in the project data base.

3. HSP Performance

HSP performance is nominal. There have been no failures of any hardware or software and the HSP continues to operate in the original pre-launch configuration; there have been no redundant unit reconfigurations. Other than those given in the OV report, there have been no more incidents of single event upsets or bright object safing. Thermal performance, power consumption, and general operation have been as expected.

3.1 Thermal

HSP thermal performance continues to be nominal. Several capabilities built into the HSP thermal control system remain untested in orbit including "software thermostats". Should there ever be a need to control detector or bulkhead temperatures more precisely, the capability exists.

3.2 Power

HSP power consumption continues to be nominal.

3.3 Electrical and Mechanical

There have been no electrical problems. The HSP continues to operate on the primary (prelaunch) set of redundant electronics, including the RIUs. There have been no electrical reconfigurations.

There is, however, a known EMI problem which may or may not require additional work. The reply bus driver is in the RIU and produces significant conducted emission. There has been some indication that reply bus noise can be found in certain detector data. The reply bus can be turned off if needed during critical observations. A test of this scheme was written (SV 2749) and submitted but still awaits implementation; the required commanding has not yet been incorporated into SOGS.

3.4 Depressurization

The HSP has no pressure gauge. There has been no evidence of any significant partial pressure in the HSP at any time.

3.5 Flight Software

Flight software has operated as expected with no anomalies and no revisions. Especially noteworthy was that at its first use the flight software calculated correctly the magnitude and direction of the small angle maneuver required for target acquisition. No corrections or modifications were required. As indicated above, the heater control application processor has been only partially exercised.

3.6 Detectors

All five detectors have continued to operate satisfactorily except, as explained above, the VIS detector has shown a loss of sensitivity of about 10.7% between April and July 1991, but none between March and April 1992.

OV testing has shown that the order of the filter strips on the POL detector was reversed from that shown on the drawings. The same drawings define the orientations of the polarizing strips, which have not been verified yet in the OV or SV program, but will be in later tests. The SV polarization tests have been delayed, first by a problem in HST step and dwell scan timing calculations, then by scheduling problems in the polarization test itself. The test requires a +/- 30 degree spacecraft roll so the observations must be spaced by about 60 days which makes scheduling a suitable target difficult.

3.7 Alignments

Alignment of the HSP apertures to the HST focal plane, FGS-to-SI alignment, has proven during SV to be stable and predictable enough to reliably place targets in apertures. The aperture positions of the image dissector tubes are now known to within 0.02 arc seconds, which is better accuracy than was anticipated before launch.

The GTO program 1092, observations of Z-Chamaeleontis, has shown variations in the pointing of HST that are dependent on the particular FGS configuration used. (see Appendix G)

3.8 Magnetic Shielding and effects

The HSP detectors have double magnetic shielding. HSP instrument level acceptance tests verified the detectors would be insensitive to the effects of the earth's magnetic field or HST ICD level fields. There have been no specific OV or SV tests performed to verify magnetic field sensitivity but no evidence has been found to date of any measurable sensitivity.

3.9 Sensitivity to SAA

Tests have been proposed to measure HSP sensitivity to the SAA but none have been approved or scheduled. Most HSP data have been collected outside the SAA but data taken near the SAA has been examined carefully and no sensitivity to it has been found.

3.10 Contamination

There is no evidence to date in the SV test data of any contamination effects. There is no evidence that the VIS detector sensitivity loss is related to contamination because the VIS detector sensitivity loss is seen in all VIS filters and there is no loss in any other detector. Contamination, although unlikely, cannot be absolutely ruled out as a contributing factor to the VIS tube sensitivity loss.

3.11 Throughput

A few (two or three) filters, F551W for example, have shown evidence of degraded throughput. The VIS detector (all filters) has apparently lost sensitivity but by exactly how much is not known until calibration tests are completed.

3.12 Sensitivity to bright objects

There have been no bright object safing events in the period covered by this report

4. Program Development, Execution, and Results

4.1 Program Development

The HSP SV program is an extension of the ground test program beginning at the sub-box level and extending though VAP, A&V at LMSC, the various GSTs at LMSC and KSC, and OV. The Science Verification program was designed to characterize the performance of the HSP, determine positions of the apertures in both deflection and focal plane coordinates, and to verify photometric performance.

The HSP OV and SV test periods overlapped to a considerable degree because there were problems with specific tests that had to be revised and rescheduled and others that were affected by the difficulties in SI to FGS alignment. The HSP OV report covered the period from launch through early June 1991. This HSP SV report covers the subsequent period from early June 1991 through May 1992. Some SV tests were performed before June 1991 and a few OV tests (by the original defininition: see Appendix A for the designation of each HSP test) were performed in the period covered by this report. For most purposes, the distinction between OV and SV is not significant.

4.2 OV/SV Events in Chronological Order

Launch (liftoff) of HST occurred on April 24, 1990 at 12:32:52 UT. See the HSP OV report for events through May 1991. The major events in the period between June 1991 and May 1992 are listed below:

Test number	Test Name	SMS	Date
3233 - POL	Fine Alignment - POL	911547D3	6/3/91
1385	Photometric Performance	911547D3	6/5/91
3233 - VIS	Fine Alignment - VIS	911547D3	6/8/91
2769	Color Transformation UV	911687AB	6/17/91
2769	Color Transformation VIS	911757AB	6/24/91
3006*	Centering	911827AF	7/5/91
3362	Fine Alignment-UV-Visit 2	911897AK	7/8/91
3362	Fine Alignment-VIS-Visit 2	911967D4	7/19/91
3377	HSP POL Test - part 1	912177D1	8/9/91
1474	Photometric Performance	912317D2	8/19/91
1389	Short Term Photometric Stability	912317D2	8/22/91
3119	Aperture Map	912387C1	8/26/91
3377 - Part II	POL Map and Align	912387C1	8/30/91
3120	Aperture Map - VIS	912457D4	9/3/91
2771	Occultation - rings	912457D4	9/5/91

3119 - visit II	Aperture Map	912527E5	9/9/91
1095***	Variability of High Lum.	912527E5	9/13/91
3362 - Det 1	Fine Alignment - POL	912527E5	9/15/91
1095***	Variability of High Lum	912597B1	9/19/91
3135	Aperture Map - UV	912667C4	9/23/91
3120	Aperture Map - VIS	912667C4	9/23/91
3382	Photometric Performance	912667C4	9/23/91
1386	Instrumental Polarization	912667C4	9/24/91
1081	Saturn Ring Dynamics	912737C6	10/1/91
2769	Color Transformation (repeat)	912807ai	10/11/91
3383	OLT Jitter Test - revised	912807AI	10/13/91
1383	Time Resolved Photometry	912877D1	10/17/91
3378	Color Transformation (VIS)	913157A9	11/11/91
3377	HSP POL Test-Part II repeat	913297B7	11/19/91
3425	Color Transformation VIS	913507DG	12/20/91
1101***	Optical & UV Obs of Radio Pulsars	920207AA	1/21/91
3383**	Revised OLT Jitter	920277AB	1/28/91
1092***	Eclipses of cataclysmic variable stars (note 1)	920277AB	1/28/92
2912	HSP Photometric Calibration	920627c2	3/2/92
3996	Prism Mode Test	920627c2	3/2/92
3985	Instrumental Polarization (revised)	920697ci	3/14/92
2912	HSP Photometric Calibration	921187e4	4/29/92
3985	Instrumental Polarization (revised)	921187e4	4/28/92
3996	Prism Mode Test	921187e4	5/1/92
3985	Instrumental Polarization (revised)	921257e4	5/4/92
1086	Pluto Rings	921397d1	5/20/92
1098 ***	Supernova Remnants	921537a5	6/2/92

*SAO Test
** OLT Test
*** GTO
Note 1: 1092 executed in every SMS between 92027 and 92153

4.3 Test Specific Performance

The SV tests described in the following sections in chronological order were performed after June 8, 1991. All HSP OV, SV, and SAO tests performed on or before June 8 are described in the HSP OV report.

2769 - Color Transformation

A set of targets are observed in several different filters so that the throughput of the various HSP filters can be related. The observations are short and in the single color photometry mode. The VIS and UV detectors were the subjects of this test. Some of the observations were corrupted by jitter and were later repeated.

3006 - Centering

This test is intended to determine the effect of centering errors on photometric response. A small dwell scan was executed with the target in a one arc second aperture while collecting data.

3362 - Fine Alignment

This test is the second visit of the HSP fine alignment test. It is identical to the first visit except that the target acquisition is entirely on-board (Mode II). The test ran as planned, produced high quality data, and confirmed the aperture positions determined earlier. Both UV detectors and the VIS detector were mapped.

3377 - HSP POL Aperture Map and Alignment Test

This test was added to the SV program when it was determined that the original test (3152) did not produce data of sufficient precision. The reason, discussed at greater length in the HSP OV report, is that there are fewer apertures in the POL tube and therefore fewer data points to define the parameters for the position

model. This test is performed in two parts: the first part is a flat field (bright earth or Orion Nebula) aperture mapping test and the second part is similar to 3362 except for the size of the scans.

1474 - Photometric Performance

This proposal verified the dynamic range, limiting magnitude, linearity and digital-to-analog relatability and overlap of the visual IDT (VIS, IDT#3) on HSP. Five (5) photometric standards which span a large range in brightness (5 < V < 14mag.)were observed in the analog and/or digital, single and/or star-sky modes . The results verified the relevant CEI specifications and the deadtime corrections in the pulse counting mode.

1389 - Short Term Photometric Stability

This test has proven to be one of the most interesting of the entire OV & SV program. The test was designed to find any effects on the photometric stability of HSP data. Data are collected in single color photometry mode for as long an observation time with as short an integration time as possible. About five and one half hours were collected with an integration time of 83 milliseconds. The data show two unexpected effects: a sinusoidal oscillation with a 92 minute period and a monotonic linearly increasing offset. Both the zero to peak amplitude of the 92 minute oscillation and the total amplitude of the monotonic linear ramp are about one percent.

3119 - Aperture Map

The exposure times of this test, the SV aperture map test, were slightly modified from those in the OV version of the test, 3093, but is otherwise identical. The Orion nebula or the bright earth is used as a flat field for mapping the HSP image dissector tube apertures in deflection coordinates.

3377 - Part II - POL Map and Alignment

In part I of this test the apertures were mapped in deflection space using a technique similar to the standard aperture mapping test but a bright star was used instead of a flat field. There is sufficient light from the wings of the degraded image to map the apertures. In part II, a technique similar to that used in 3233, HSP Fine Alignment, was used to determine the positions of the apertures in V2/V3 coordinates. The star is observed in a continuous single color photometry data collection while the HST performs a step and dwell scan. The size of the step and dwell scan pattern is optimized for the POL tube. The test did not execute as planned because the HST step and dwell scan ramp up and down times were not properly taken into account in proposal transformation (SMS implementation) Because there were repeated step and dwell scans, the error grew to the point the target moved out of view.

3120 - Aperture Map - VIS

This test is identical to 3119 but is a repeat and was therefore given a new number for scheduling reasons.

2771 - Occultation - Rings

This was the first attempt to observe an occultation of a star by a planet by the HSP. The execution of the test was not as intended because there were errors in transformation resulting from confusion about the proper SMS syntax for specification of scan parameters. However, some occultation data were obtained. Interpretation was made difficult by the loss of background scans.

3119 - Visit II - Aperture Map

This is a repeat of the flat field deflection space aperture map test.

1095 - Variability of High Luminosity Stars

Three targets were observed for about 30 minutes each in the single color photometry mode with 0.1 second integration time. This was an HSP GTO, executed as planned, and provided good data.

3135 - Aperture Map - UV

This is another repeat of the flat field deflection space aperture map test.

3120 - Aperture Map - VIS

This is another repeat of the flat field deflection space aperture map test

3382 - Photometric Performance

This was a repeat of the 1385 test to observe 13th and 15th magnitude targets that were adversely affected by solar array induced jitter in the first attempt.

1386 - Instrumental Polarization

The test executed properly but unfortunately the pre-requisite test, 3377, POL alignment was not completed successfully. It was too late to reschedule the test. Also, the target precession done by the ST ScI did not match the epoch for which the coordinates were correct on the target list. The polarization test was subsequently successfully run as 3985.

1081 - Saturn Ring Dynamics

This was the first HSP GTO of a planetary ring occultation. The following summary is by Amanda Bosh:

On 2-3 October 1991, Saturn occulted the star GSC6323-01396 on its way toward the stationary point of its retrograde loop. This unusually slow occultation was observed with the High Speed Photometer over a period of 20 hours (13 orbits) during ring emersion. Earth occultations, SAA passages, and guide star reacquisitions reduced the actual exposure time, for an exposure efficiency of 34% The losses due to SAA passage were minimized by resuming data collection after SAA on two of the orbits. Whenever possible, simultaneous two-color photometry was obtained using the HSP's photomultiplier tube (PMT, 7500 Angstroms) and visible (VIS, 3200 Angstroms) detectors with an integration time of 0.15 sec. Although the star is not extremely bright (V = 11.9) compared with Saturn's rings, its angular diameter is correspondingly small so that the radial resolution of our observation was determined by diffraction (~2 km, the Fresnel limit).

2769 - Color Transformation

A variety of targets were observed in various filters on all detectors to determine the relative response of the HSP filters. (See section 4.4.2 for discussion of analysis and results)

3383 - OLT Jitter Test - Revised

Excerpts from a "Summary of Jitter Test Execution" by Olivia Lupie, ST ScI

> The Jitter test was executed this weekend (October 13, 1991). The test was very difficult and had only partial success. It appeared that all the special commanding and tape recorder movement executed exactly as planned. The HSP worked flawlessly. The communications contacts were all successful. The OSS support was absolutely exceptional. The method, with some modification based on experience from this test, is sound. The preparatory support of this test by Commanding, the MOC, the HSP IDT, SPSS and OSS all proved to be essential, successful and exactly right -- and are greatly appreciated.
>
> 1. First Jitter exposure on V2 edge - completed. Core was off the edge so sensitivity was reduced. Some information will be acquired but sensitivity is somewhat reduced.
>
> 2. Second Jitter - star and edge were aligned with wonderful precision. LOSS of lock caused complete failure. The science data clearly showed gyro drift.

3. Jitter in aperture center as control - completed and count rates were consistent with the star being centered in the read beam in the aperture center. Successful.

4. First jitter on V2 edge - Lost to LOSS of lock.

5. Second Jitter on V2 edge - the core and edge were not coincident, the count rates are extremely low and unusable.

6. The Spatial scan across the V2/V3 edge were successful and will be used to determine the edges and star positioning.

RECOMMENDATIONS

1. Because of the astrometry observations (to move the servos), LOSS OF LOCK recovery was apparently disabled and the remainder of observation would be taken on gyro control. GET RID OF THE ASTROMETRY activities in subsequent tests.

2. LOSS OF LOCK occurred during orbital midnight on several occasions as well as the transition periods. Recommend to look into that - perhaps these particular guide stars were bad.

3. The scattered light off the aperture edge and the large size of the PSF made interpretation of the 2x2 arcsec images difficult down in OSS. Enlarge the size of the 2x2's next time. Use the PSF data from this run to study the PSF and edge characteristics for next time.

4. The placement of the core on the edge must be calibrated in real-time as we initially construed but opted not to perform in this jitter revision. I have devised a simplified method as a result of experience from this test.

5. Analyze the FGS and HSP data from this test in order to reconstruct the PCS problems. Determine if the alignment of the deflection system and the V2V3 system - in both the command instruction, the proposal instructions, and the PDB -- were all consistent and correct. We may be able to extract some of this information from the data during the jitter test.

1383 - Time Resolved Photometry

This test is one of the most interesting and taxing of the HSP SV program. The data volume is large because there are four observations of 30 minutes each with 11 microsecond integration time. The target was the Crab Pulsar. There were some missing packets for which an HSTAR was written, but the data were otherwise of high quality. The missing packets were restored in later processing.

The analysis and results have been described in Appendix L, *High Speed Photometer Pulsar Timing and Light Curve Reduction* , Jeff Percival, May 19, 1992.

3378 - Color Transformation - VIS

This is a repeat of 2769 for the VIS detector for one 9th magnitude target that was corrupted by jitter in the first run of 2769. The test ran as expected and the data were of good quality.

3377 - HSP POL Test - Part II - Repeat

The second part of this test, the POL fine alignment test using a step and dwell scan to determine V2/V3 aperture positions, had to be repeated because the target was lost in the first attempt. The target drifted out of view because the step and dwell ramp up and ramp down time was not properly taken into account. Because there were repeated step and dwell scans, the error grew to the point the target moved out of view. In this repeat, the ramp times were correctly considered so the test ran as designed. The results provided the information required.

3425 - Color Transformation - VIS

This is a repeat of 2769 for the VIS detector for four stars in the magnitude range 11 to 12.

1101 - Optical & UV Observations of Radio Pulsars

This GTO proposal is the first of a planned series of pulsar observations in the UV. The target for this observation was the Crab Pulsar. The test ran successfully and good data were collected.

3383 - OLT Jitter Test - Second Revision

The first run of the revised OLT jitter test, 3383, did not execute exactly as planned. (see previous discussion in 3383 - OLT Jitter Test - Revised) The test was modified for this repeat to correct the problems encounted in the first execution. The test ran as planned and good data were collected.

1092 - Eclipses of Cataclysmic Variable Stars

This GTO is a long series of about twice-weekly observations of Z-Chamaeleontis using UV1. Each observation is about a half hour long with one second integration time. The observations are timed to catch the eclipse during most observations but to avoid the eclipse during a few.

2912 - Photometric Calibration

This calibration is planned to be run about monthly. It is a series of single color photometric observations of standard stars in a standard set of filters. The objective is to calibrate the photometric response of the HSP as a function of time.

3996 - Prism Mode Test

This test is intended to map the locations of the prism mode apertures in both deflection and V2/V3 space more precisely than is possible using the standard aperture mapping tests.

The 3996 test was constructed and run in two parts. The first portion of the test consisted of a 3x3 dwell scan of the target centered on the two apertures, with area scans of the apertures at each dwell point. The primary goal of the portion of the test was to determine the h,v deflection coordinates of the apertures which were not well determined by the Aperture Mapping tests from SV. A secondary use of the data was to have been a rough calculation of the best pointing for the prism apertures.

This first portion of the test was not sucessfull. The assumed V2,V3 location of the aperture was taken from earlier calibration of the locations of the HSP apertures in the MSC Phase III VS tests and their follow on observations. This calibration had proven usable for many other apertures on the 3 detectors and was assumed would yield a workable pointing for the PRISM apertures. This assumption was in error, and the cores of the stellar images did not appear in the prism apertures during the step-and-dwell portion of the test. However, enough light from the wings of the PSF appeared so that the assumed h,v deflections of the apertures could be checked. Although the data were not good enough to refine the deflection coordinates of the apertures, it was sufficient to verify that the coordinates currently in the PDB were good to better that 4 deflection steps. No PDB updates resulted from this portion of the test.

The second portion of the test was a continuous scan of the target in the entrance aperture to the HSP PRISM's. The HSP was configured in the PRISM mode and data were collected at both PRISM apertures during the scan. The continuous scan was a 21 line scan 5" on a side. This portion of the test was sucessfull in that the star image appeared in both PRISM apertures on all three HSP PRISM assemblies. Concurrently with the science data, FGS telemetry was recorded to provide a good V2,V3 calibration of the HSP science data. These two sets of data were then combined to determine the V2,V3 locations of the six different PRISM mode apertures. The orientation of the scans was then rotated 90 degrees and the apertures re-scanned similarly to the first orientation, and the locations of the aperture again calculated. The results are as follows:

Detector	Aperture	Observation ID	V2 wings	V3 Wings	V2 Core	V3 Core
UV1	Finding	v0vn0203	179.130	-493.212		
UV1	Star	v0vn0204	136.20	-444.35	136.20	-444.35
UV1	Sky	v0vn0204	135.92	-444.67	136.04	-444.67
UV1	Star	v0vn0205	136.20	-444.33	136.20	-444.23
UV1	Sky	v0vn0205	135.95	-444.63	136.03	-444.69
UV2	Finding	v0vn0403	493.273	-158.052		
UV2	Star	v0vn0404	428.24	-162.95	428.26	-163.14
UV2	Sky	v0vn0404	428.38	-163.13	428.44	-163.18
UV2	Star	v0vn0405	428.25	-162.98	428.25	-163.25
UV2	Sky	v0vn0405	428.39	-163.14	428.49	-163.26
VIS	Finding	v0vn0603	375.763	-361.975		
VIS	Star	v0vn0604	315.47	-337.18	315.49	-337.35
VIS	Sky	v0vn0604	315.73	-337.42	315.74	-337.45
VIS	Star	v0vn0605	315.47	-337.26	315.48	-337.32
VIS	Sky	v0vn0605	315.74	-337.40	315.74	-337.47

It is felt that the best scheme for determining the best pointing for the use of the PRISM mode is to average the positions of the two apertures, thus minimizing the miscentering problems for both data streams, instead of having good centering for one aperture and very poor centering for the other. Accordingly the average positions for the three assemblies, and the corresponding delta V2,V3 positions are as follows, with the deltas being defined as (finding aperture - prism aperture):

Detector	V2(av)	V3(av)	dV2(delta)	dV3(delta)
UV1	136.12	-444.51	43.010	-48.702
UV2	428.36	-163.21	64.913	5.158
VIS	315.61	-337.40	60.153	-24.575

What remains is to combine the delta positions in V2,V3 of the apertures with the current V2,V3 positions of the finding apertures as defined in the PDB. This will yield the new V2,V3 of the prism apertures. For reference the old V2,V3 of the prism apertures is given along with the old delta positions of the prism apertures WRT the finding aperture. The old and new delta's can be compared to look for systematic effects which might explain the unusually bad predicted positions of the prism apertures. The final table

Detector	V2(old)	V3(old)	V2(TAQ ap)	V3(TAQ ap)
UV1	135.850	-444.1201	179.6417	-492.3280
UV2	428.7297	-163.4393	493.5936	-157.6331
VIS	315.4012	-338.2685	375.8750	-362.4401

Detector	dV2(old)	dV3(old)	dV2(new)	dV3(new)	Change V2	Change V3
UV1	43.7912	-48.2079	43.010	-48.702	-0.7812	-0.4941
UV2	64.8639	5.8062	64.913	5.158	0.0491	-0.6482
VIS	60.4738	-24.1716	60.153	-24.575	-0.3208	-0.4034

lastly subtract the new deltas from the PDB V2,v3 of the finding aperture to yield the new V2,V3 of the prism apertures:

Aperture	New V2	New V3
VF135U1_A	+136.63170	-443.62600
VF248U1_A	+136.63170	-443.62600
VF145U2_A	+428.68060	-162.79110
VF262U2_A	+428.68060	-162.79110
VF240V_A	+315.72200	-337.86510
VF551V_A	+315.72200	-337.86510

3985 - Instrumental Polarization Test (revised)

This test is intended to characterize the capability of the HSP to determine polarization. It is based on the earlier tests, 1386 and 3377, but includes more than one target.

1086 - Pluto Rings

This GTO observation is indended to search for rings around Pluto using the PMT during an occultation.

1098 - Supernova Remnants

The 1987A supernova remnant is the target for this observation.

4.4 Data Analysis and Results

The major SV data analysis efforts were the short term photometric tests (Crab Pulsar observations), the Color Transformation tests, and the determination of aperture positions as a function of both deflection and V2/V3 coordinates, especially for the PRISM mode apertures.

4.4.1 Short Term Photometric Stability

The 1389 Short Term Photometric Stability test results showed two unexpected effects: a 92 minute oscillation and a "ramp". The cause of these effects has not been determined but so far no convincing correlation has been found with any HSP engineering data. HSP interior temperatures tend to be stable and the orbital variations of exterior (skin) temperatures are not in phase with the 1389 variations. The following chart (Fig 4.4.1 - 1) shows the 1389 HSP data, each point representing the average of 1000 data samples, plotted with one of the FGS #3 temperature monitors, E457. Note that the two plots are in phase. Fig 4.4.1-2 shows the rebinned data by itself. The HSP team has proposed a test to determine if there are apparent motions of the target relative the HSP detectors.

4.4.2 Color Transformation

Summary: The purpose of this test was to determine the color transformation coefficients from the HSP instrumental systems to that of standard stars for various filter-aperture combinations using the UV1, UV2 and VIS detectors. Three photometric standard stars were observed with UV1 and UV2 and four photometric standard stars were observed with the VIS tube. Each star had a different B-V value in order to span a wide-range of stellar colors. In each case, 100 one-second integrations were obtained through various filter-aperture combinations and 200 one-second integrations were scheduled with the PRISM mode.

Results: Data were successfully obtained with UV1 and UV2. Table 1 lists the mean count rate (counts per second) together with the standard deviation for each object. Fast Fourier Transforms of the UV1 and UV2 data were calculated. These FFTs showed numerous statistically significant features, many of which were near, in frequency, to the well-known 0.1, 0.4, and 0.6 Hz variations associated with the HST/solar arrays. The FGS switched from high gain to low gain just before the data using the VIS detector were obtained. Hence, the data were of poor quality and consequently, are not shown here. In addition, the position of the PRISM mode apertures were not well-known at the time of execution of this test, and hence, these data were also of poor quality. This portion of the color transformation test will be postponed until accurate calibration of the PRISM mode is obtained.

Plans: Reschedule the observations with the VIS tube and repeat the observations on AGK+81D266 using the UV1 detector in order to ascertain the repeatability of the photometry.

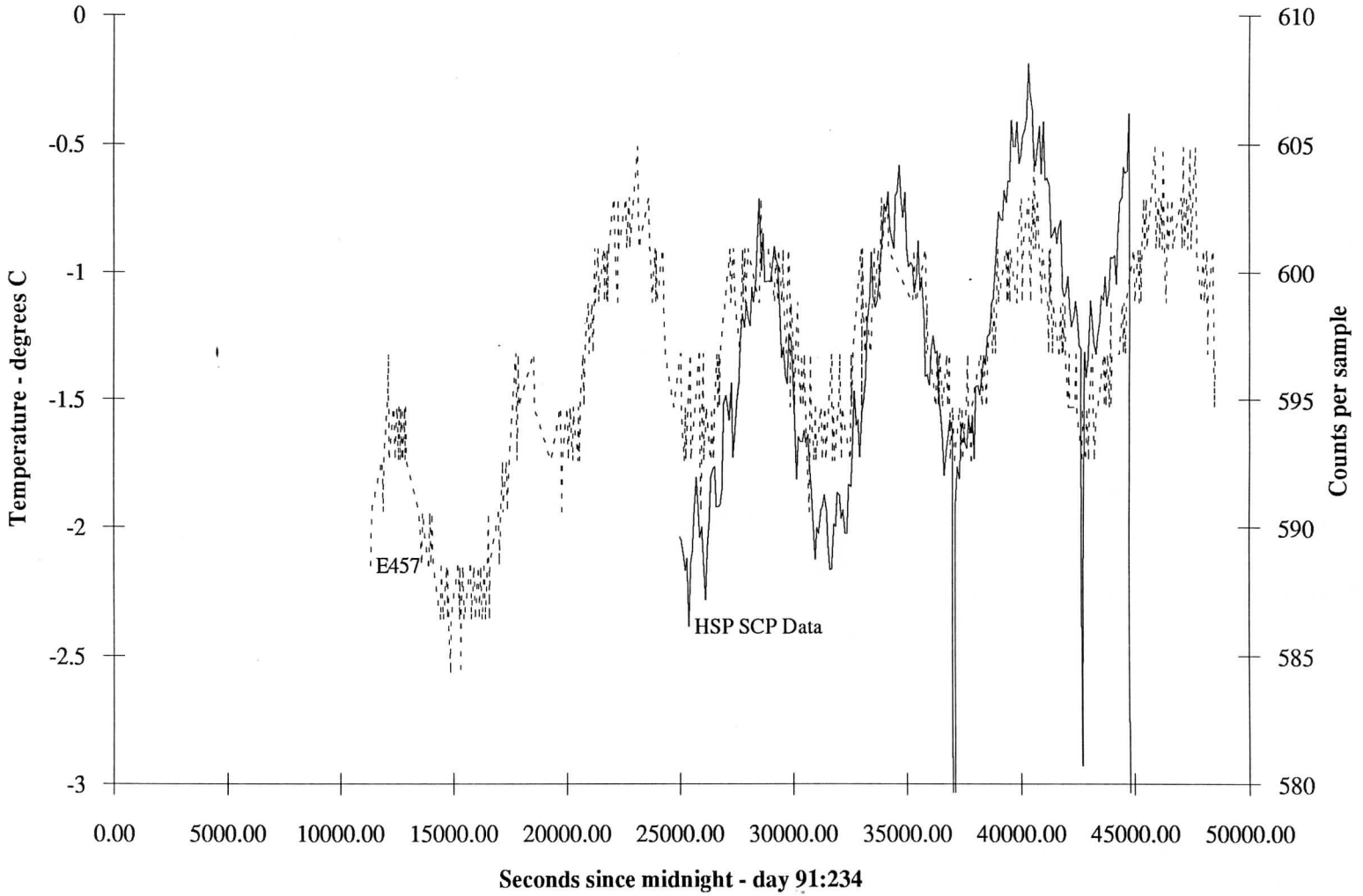
E457 - FGS #3 Temperature & 1389 SCP Data
Temperature - degrees C
0
-0.5
-1
-1.5
-2
-2.5
-3
Counts per sample
610
605
600
595
590
585
580
E457
HSP SCP Data
0.00
5000.00
10000.00
15000.00
20000.00
25000.00
30000.00
35000.00
40000.00
45000.00
50000.00
Seconds since midnight - day 91:234

Fig 4.4.1-1

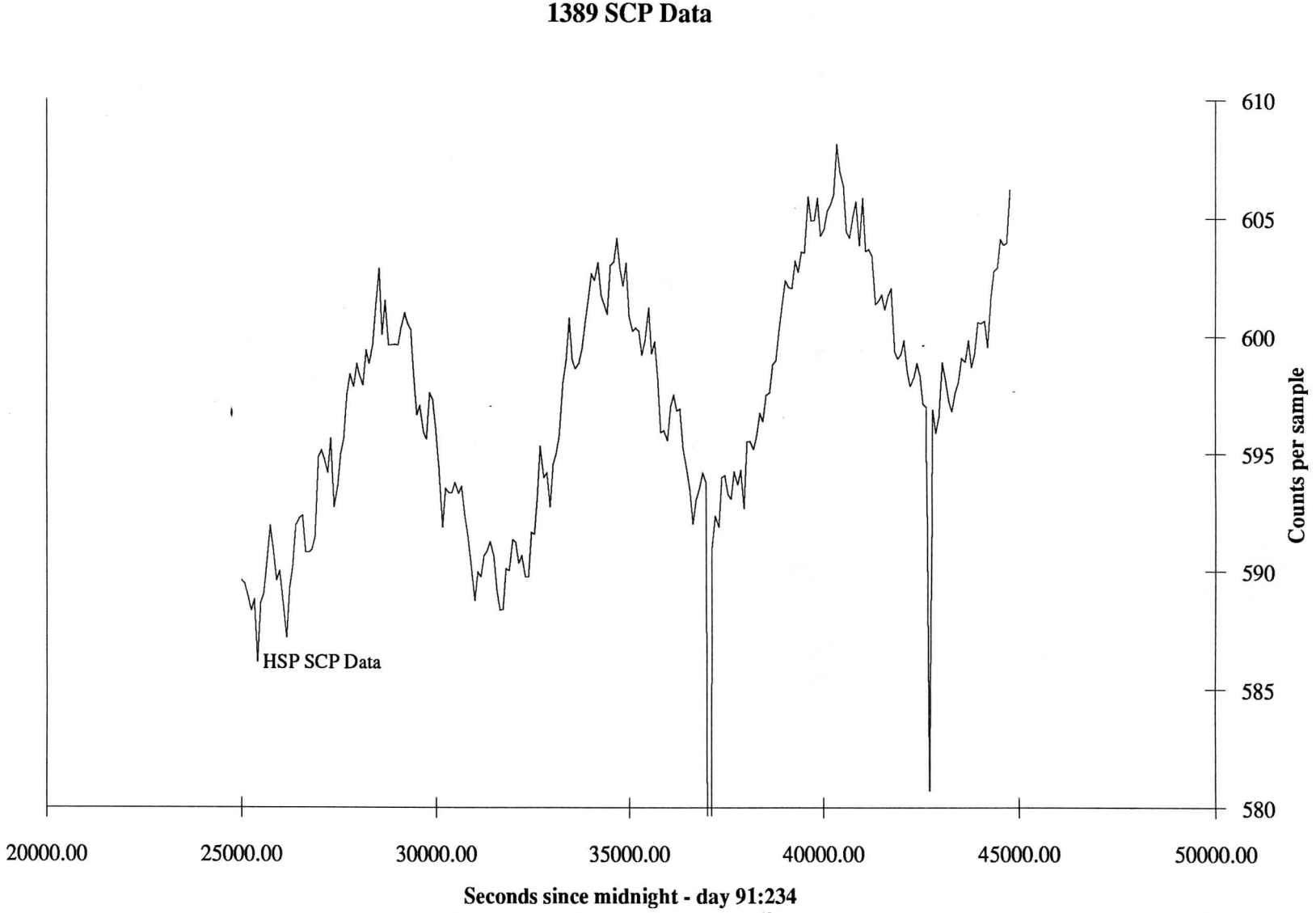
1389 SCP Data
610
605
600
595
590
585
580
Counts per sample
HSP SCP Data
20000.00
25000.00
30000.00
35000.00
40000.00
45000.00
50000.00
Seconds since midnight - day 91:234

Fig 4.4.1-2

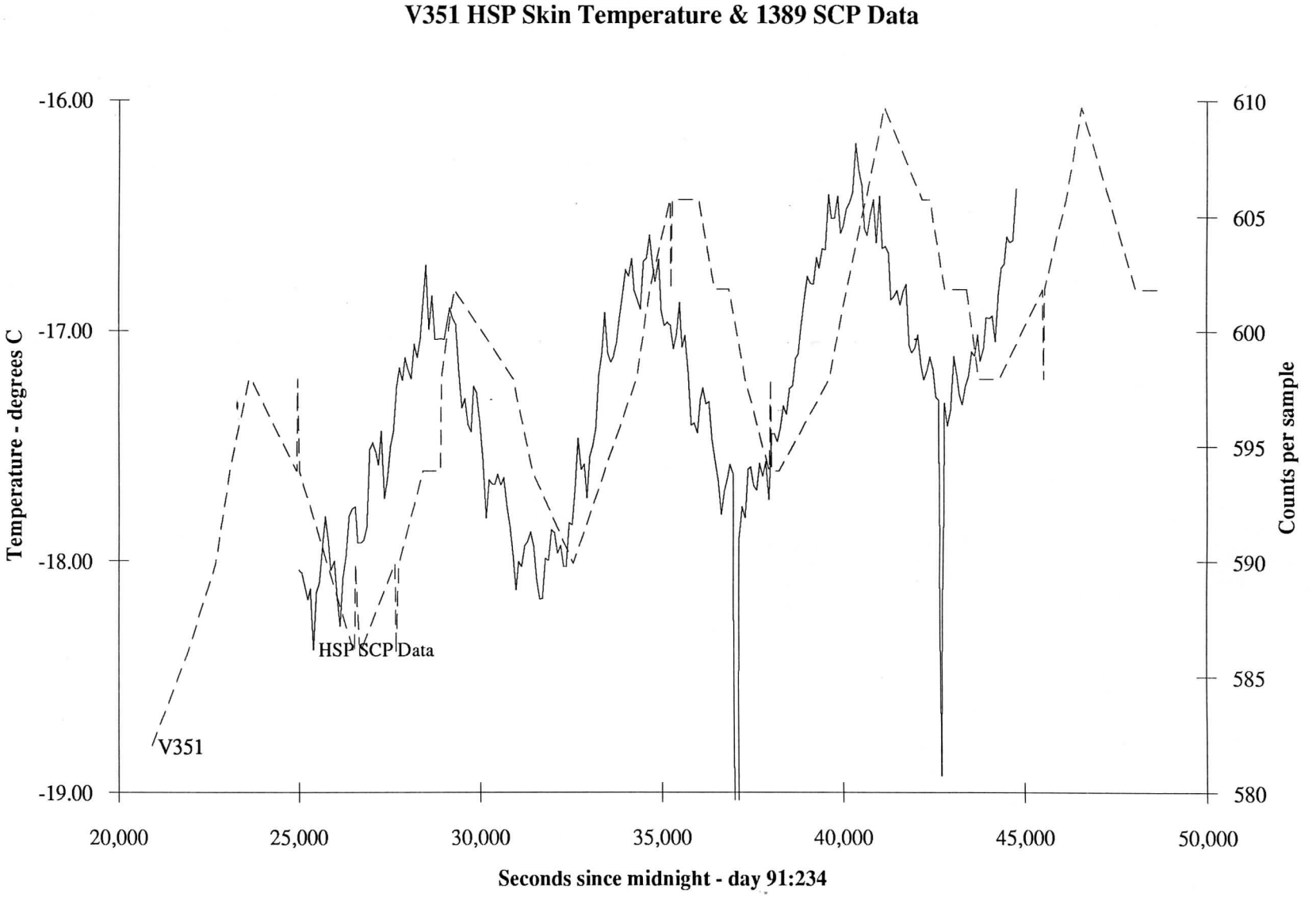
V351 HSP Skin Temperature & 1389 SCP Data
-16.00
-17.00
-18.00
-19.00
Temperature - degrees C
610
605
600
595
590
585
580
Counts per sample
HSP SCP Data
V351
20,000
25,000
30,000
35,000
40,000
45,000
50,000
Seconds since midnight - day 91:234

Fig. 4.4.1-3

Table I
Photometric Data for Color Transformation - UV1 & UV2

Filter-Aperture	AGK+81D266 (B-V=-0.34) Mean	σ	SA113-260 (B-V=+0.51) Mean	σ	SA113-339 (B-V=+0.57) Mean	σ
F135U1_C	1985.7500	40.3146	0.4700	0.7544	0.4400	0.6135
F145U1_A	1250.4700	38.7684	0.3000	0.5000	0.1200	0.3250
F152U1_A	1204.9900	39.2182	0.3800	0.6129	0.1850	0.4132
F184U1_A	11650.9100	116.2706	10.3400	3.0634	10.0250	3.1455
F218U1_A	6961.6300	82.9726	14.2800	4.1883	16.9750	3.9095
F220U1_A	11951.3700	116.0862	26.7000	5.2182	33.3200	5.7626
F248U1_C	9291.0100	100.7439	49.2300	7.4241	65.0150	8.1508
F278U1_A	1576.5900	35.4071	29.9200	5.5221	35.7200	5.8259
F145U2_C	1641.9000	42.4852	0.3700	0.6581	0.2950	0.5550
F152U2_A	1771.0400	53.4993	0.5700	0.7517	0.3400	0.5783
F160U2_A	101365.4700	321.1438	470.3900	25.7383	580.5550	24.2686
F179U2_A	7720.4900	85.5282	10.8300	3.2590	12.1450	3.3427
F184U2_A	10627.1900	117.4213	10.7500	3.3716	11.0550	3.3124
F248U2_A	11023.7500	119.5493	57.3200	7.8369	69.7950	8.4666
F278U2_A	1752.3800	41.8564	32.5800	6.0086	40.2750	6.0753
F284U2_A	6814.0000	76.9227	94.9100	9.5646	112.5650	11.1187

The data for the repeated observation of AGK+81D266 (taken 116 days later) using UV1 are shown in Table II. Each of these observations has a count rate which is consistently smaller by 4-12% than that given in Table I. Observations of a star in NGC 188 during this time with UV1 show no such variability. There is no indication of anything peculair with HSP. Hence, though AGK+81D266 is an HST photometric standard, there is a real possibility that it is in fact variable. The FFTs of the data show statistically significant features which are at slightly different frequencies than those for the previous observations, but which still fall within the jitter spectrum.

Table II
Photometric Data for Repeated Observation of
AGK+81D266 - UV1
(B-V=-0.34)

Filter-Aperture	Mean	σ
F135U1_C	1803.8500	45.0303
F145U1_A	1105.4000	41.2440
F152U1_A	1098.1000	32.4792
F184U1_A	10923.0400	120.8685
F218U1_A	6401.5100	95.5433
F220U1_A	11127.9900	140.3659
F248U1_C	8859.7200	90.7986
F278U1_A	1520.3500	42.1441

This test was originally designed to observe all three of the stars observed with the UV detectors in addition to two very red stars. However, this portion of the color transformation test was not implemented correctly

and a total of four stars (none of which were observed with the UV tubes) were observed with the VIS detector. Table III lists the data.

Table III
Photometric Data for Color Transformation - VIS

	BD+28D4211 (B-V=-0.34)		SA95-132 (B-V=+0.44)		SA95-302 (B-V=+0.84)		SA95-301 (B-V=+1.24)	
Filter-Aperture	Mean	σ	Mean	σ	Mean	σ	Mean	σ
F184V_A	42245.960	332.401	33.930	6.392	2.815	1.501	2.380	1.476
F240V_C	82328.830	458.458	234.490	17.284	52.265	7.263	14.480	3.611
F262V_A	31372.360	205.417	137.850	11.643	29.205	4.976	6.120	2.645
F355V_A	13482.350	111.711	377.790	18.469	244.665	15.854	118.010	10.899
F400V_A	627564.970	3741.140	27003.450	183.741	23488.915	176.213	30911.350	320.748
F419V_A	5432.000	75.236	593.630	25.162	324.160	17.995	257.230	16.504
F450V_A	83784.350	345.823	9506.290	109.844	6622.890	81.583	6911.210	86.921
F551V_A	248.081	17.103	55.646	7.508	42.894	7.477	190.576	21.941
F551V_C	4981.370	77.765	837.400	32.073	716.800	28.598	1019.190	31.242
F620V_A	12452.770	126.492	4678.080	65.914	5488.255	75.056		

4.4.3 Aperture Positions

Aperture positions of the POL tube were updated in SV as follows:

Aperture	V2	V3
VF327P0	+197.71360	-228.09910
VF327P90	+205.18890	-220.39410
VF327P45	+220.31870	-205.06420
VF327P135	+212.74860	-212.69940
VF277P0	+190.14860	-220.66440
VF277P90	+197.59360	-212.96970
VF277P45	+212.71360	-197.60960
VF277P135	+205.14390	-205.30950
VF237P0	+182.34880	-213.03980
VF237P90	+189.87840	-205.34950
VF237P45	+204.97360	-190.07920
VF237P135	+197.43330	-197.71480
VF216P0	+174.62800	-205.48440
VF216P90	+182.17830	-197.74950
VF216P45	+197.30380	-182.53990
VF216P135	+189.74880	-190.14910

The other apertures appeared to be stable throughout SV and the database positions were not changed. Except for the prism apertures, there is no indication that there will be a need to update these positions soon.

4.4.4 VIS Detector Sensitivity

NGC188-998 has been used for tests of all four image dissector tube over an extended period. If one integrates all the flux from the acquisition image in the finding aperture, the results are less subject to pointing errors than in the smaller apertures. The results are:

Detector	Date	Total Flux	Temperature
POL:	4/21/91	593010	-2.33
	6/03/91	591478	-1.69
	9/15/91	598079	-3.60
UV1:	3/15/91	145603	-0.74
	5/19/91	147879	-0.42
	7/14/91	144393	-4.55
UV2:	3/11/91	185081	-3.60
	5/18/91	183681	-1.37
	7/08/91	184095	-3.28
VIS:	4/21/91	534004	0.22
	6/08/91	497848	-1.69
	7/20/91	477161	-2.96

Note the VIS detector is the only one of the four to show a significant change over the period. The sensitivity loss of the VIS detector over the period of time covered by this data set is 10.7%.

The first two sets of HSP calibrations, 2912, performed in early March and late April 1992, did not show any indication of additional loss in VIS detector sensitivity. The change was small but in the positive direction.

Observation	# Pixels	Mean
v0vz0301t.d0h	400	8.20
v0vz0302t.d0h	400	7.62
v0vz0303t.d0h	1152	71.47
v0vz0304t.d0h	600	8161.00
v0vz0305t.d0h	14	794.40
v0vz0f01t.d0h	400	8.46
v0vz0f02t.d0h	400	8.17
v0vz0f03t.d0h	1152	72.55
v0vz0f04t.d0h	600	8519.00
v0vz0f05t.d0h	14	564.50

Differences

Filter	Mode	Δ Mean
F160LP/10.0	ACQ	0.26
F160LP/10.0	ACQ	0.55
F551W/1.0	Single	1.08
F160LP/1.0	Single	358.00
F551W/1.0	Prism	-229.90

		% Δ Mean
F160LP/10.0	ACQ	3.17%
F160LP/10.0	ACQ	7.16%
F551W/1.0	Single	1.51%
F160LP/1.0	Single	4.39%
F551W/1.0	Prism	-28.94%

4.4.5 Phase One Calibrations - 2912 Analysis

2912 is a photometric calibration program which was meant to run repeatedly (every 2 months) on the HSP to measure and monitor filter bandpasses. The test has run twice on dates 03-Mar-1992 and 29-Apr-1992, and this report is for these two runs. The test measures the throughput of the HSP for the object BD+75D325 which is an O subdwarf star. The bandpasses measured are:

UV1:	F135W, F218M, F220W, and the PRISM bandpasses F248M and F135W.
UV2:	F145M, F184W, F218M, F248M, F278N, F284M, F140LP and the PRISM bandpasses F262M and F145M.
VIS:	F551W, F160LP, F320N, and the PRISM bandpasses F551W and F240W.
POL:	F327M, F277M, F237M, F216M in all polarizer orientations.

In addition the flux from the target was measured through the finding aperture which is insensitive to effects from pointing or the PSF of the telescope. The bandpasses are F140LP for the UV detectors and F160LP for the VIS and POL detectors.

The measured count rates were compared between runs as well as against prelaunch calibration curves through a simulator. First was a comparison of the flux rate between the two runs. The count rates as seen in the finding apertures are as follows:

Detector	First(Temp)	Second(Temp)	ratio(dT)
UV1:	956.52(-5.06)	995.35(-7.70)	1.04(-2.64)
UV2:	1172.97(-4.39)	1189.84(-6.66)	1.01(-2.27)
VIS:	970.53(-1.21)	1039.92(-3.44)	1.07(-2.23)
POL:	2142.86(-1.83)	1979.25(-4.07)	0.92(-2.24)

As mentioned about, these data are insensitive to both pointing effects and PSF effects. Therefore the fluxes can be compared directly and related to either changes in target flux or detector sensitivity. The change in count rates between the two runs is difficult to interpret but would seem to be due to the target. The change in temperature is not enough to explain the differences. In other similar data for a different target (NGC188-998), hints of temperature dependancies are at a much lower level, corresponding to about 1% for 2.25 degrees for the POL and VIS cathodes, and about 1/3 that for the UV detectors. This change is more significant. Also the fact that the count rates rise for the later observations (except for POL) indicates that the change is not from contamination or degredation of the HSP/HST optics.

Why POL is different from the other detectors is of concern, although earlier data showed that the VIS detector was losing sensitivity slowly with time. These data show that the response of the VIS detector is stable, indicating that the sensitivity losses have stoped or slowed down. However, this may indicate a general problem with the type of detector used in the VIS and POL IDT's. Carefull monitoring of these detectors is definitely called for. The relatively larger change in the VIS count rates compared to the UV detectors could be explained by a change in the magnitude or temperature of the target star and the larger bandpass of the VIS detector compared to the UV detectors.

Comparison with models: Ratios are predicted/observed count rates

det	First(Ratio)	Second(Ratio)
UV1:	956.52(1.427)	995.35(1.371)
UV2:	1172.97(1.164)	1189.84(1.147)
VIS:	970.53(2.171)	1039.92(2.026)
POL:	2142.86(0.983)	1979.25(1.065)

The difference in count rates for the same object and the two UV detectors has been noticed before and is relatively stable. The ratio of count rates of ~1.23 has seen in earlier data from the 3152/3233/3362 tests. This ratio is maintained in these data sets with ratios of 1.23 for the first data set and 1.20 for the second one. The prediction of count rates for the POL detector is quite good at nearly unity, and the factor of two difference between it and the VIS detector with the same bandpass is the result of the earlier loss in VIS detector sensitivity.

Other Bandpasses

Filter	wavel	set #	Observed Counts/S	Predicted Counts/S	Ratio Pre/Obs	Ratio 1st/2nd
VF135U1_C	1513	01 03	10829.3091	18293.1	1.68922	
VF135U1_C	1513	0D 03	9826.7686	18293.1	1.86156	1.102
VF218U1_A	2172	01 04	48385.7645	87267.7	1.80358	
VF218U1_A	2172	0D 04	44365.3097	87267.7	1.96703	1.091
VF220U1_A	2181	01 05	86782.1555	170300.0	1.96238	
VF220U1_A	2181	0D 05	82953.4151	170300.0	2.05296	1.046
VF145U2_C	1545	02 03	8830.3469	17009.2	1.92622	
VF145U2_C	1545	0E 03	8604.9909	17009.2	1.97667	1.026
VF184U2_A	1905	02 04	72350.0000	175900.0	2.43124	
VF184U2_A	1905	0E 04	72217.6883	175900.0	2.43569	1.002
VF218U2_A	2172	02 05	52441.2281	87267.7	1.66410	
VF218U2_A	2172	0E 05	49893.2174	87267.7	1.74909	1.051
VF248U2_A	2448	02 06	87134.1463	128220.0	1.47152	
VF248U2_A	2448	0E 06	85853.2174	128220.0	1.49348	1.015
VF278U2_A	2762	02 07	14047.5046	14160.5	1.00804	
VF278U2_A	2762	0E 07	13684.8366	14160.5	1.03476	1.027
VF284U2_A	2709	02 08	54303.1646	63086.5	1.16175	
VF284U2_A	2709	0E 08	54668.0832	63086.5	1.15399	0.993
VCLRU2_A	2150	02 09	678048.1293	1365100.0	2.01328	
VCLRU2_A	2150	0E 09	675994.1480	1365100.0	2.01940	1.003
VF551V_C	5675	03 03	7134.4233	34226.4	4.79736	
VF551V_C	5675	0F 03	7263.8413	34226.4	4.71189	0.982
VCLRV_A	2194	03 04	816057.1675	2107200.0	2.58217	
VCLRV_A	2194	0F 04	851905.9337	2107200.0	2.47351	0.958
VF216P0	2239	04 03	3444.0977	4787.2	1.38997	
VF216P0	2239	0G 03	3211.8611	4787.2	1.49048	1.072
VF216P45	2239	04 04	3658.4040	4787.2	1.30855	
VF216P45	2239	0G 04	3387.4737	4787.2	1.41321	1.080
VF216P90	2239	04 05	3667.8884	4787.2	1.30517	
VF216P90	2239	0G 05	3478.1204	4787.2	1.37638	1.054
VF216P135	2239	04 06	3498.6035	4787.2	1.36832	
VF216P135	2239	0G 06	3337.0292	4787.2	1.43457	1.048
VF237P0	2431	04 07	8952.8829	7420.8	0.82887	
VF237P0	2431	0G 07	8591.4369	7420.8	0.86374	1.042
VF237P45	2431	04 08	9264.4042	7420.8	0.80100	
VF237P45	2431	0G 08	8781.7265	7420.8	0.84502	1.055
VF237P90	2431	04 09	8829.7694	7420.8	0.84043	
VF237P90	2431	0G 09	8748.1754	7420.8	0.84826	1.009
VF237P135	2431	04 0A	8886.1789	7420.8	0.83509	
VF237P135	2431	0G 0A	8500.8866	7420.8	0.87294	1.045
VF277P0	2856	04 0B	16115.6693	12383.9	0.76843	
VF277P0	2856	0G 0B	14938.0742	12383.9	0.82901	1.079
VF277P45	2856	04 0C	14762.9244	12383.9	0.83885	
VF277P45	2856	0G 0C	14210.6505	12383.9	0.87145	1.039
VF277P90	2856	04 0D	16462.6031	12383.9	0.75224	
VF277P90	2856	0G 0D	15209.2691	12383.9	0.81423	1.082
VF277P135	2856	04 0E	16936.5998	12383.9	0.73119	
VF277P135	2856	0G 0E	15376.0525	12383.9	0.80540	1.101
VF327P0	2945	04 0F	18588.1818	8828.2	0.47493	
VF327P0	2945	0G 0F	18289.3062	8828.2	0.48269	1.016
VF327P45	2945	04 0G	17412.7451	8828.2	0.50699	

VF327P45	2945	0G 0G	16535.0265	8828.2	0.53390	1.053
VF327P90	2945	04 0H	17709.5002	8828.2	0.49850	
VF327P90	2945	0G 0H	15743.6970	8828.2	0.56074	1.125
VF327P135	2945	04 0I	18486.5939	8828.2	0.47754	
VF327P135	2945	0G 0I	15477.3438	8828.2	0.57039	1.194

Items of note:

First, and of most interest, is that there seems to be a relationship between effective wavelength and correction factor, that peaks at between 1600 and 2000 Angstroms. It is not know what the origin of this problem is at this point, but indications are that the curve is fairly stable, and may reflect differences between the pre-launch calibration curves and actual filter bandpasses for HSP filters.

The second item of note is the differences between the predicted and observed count rates with the POL detector. The observed count rates are higher that predicted. In addition the effect seems to be strongly correlated with wavelength. This effect is unique and the only substantive difference between the models for the POL and UV detectors is the addition of the Polacoat calibration curve, which may well be the source of the differences.

Lastly, the measurements for the PRISM filters have not been included in this report. The PRISM apertures did not have good positions before the test was run, which resulted in very low count rates for these filters. Since this was a known problem with unknown effect on the data, those results were excluded. New positions have been updated to the PDB since, and the next run of this proposal should provide a good calibration of those filters.

4.4.6 Saturn Occultation

"Observer Report" for 1081: Saturn Ring Dynamics - Occultation of GSC6323-01396 by Saturn and its Rings by Amanda Bosh, Maren Cooke, and Jim Elliot (MIT), November 18, 1991

Background: On October 2, 3, 6, 7, and 8 1991, Saturn occulted GSC6323-01396 (see Bosh and McDonald, AJ in press for predicted circumstances of this event). This occultation was discovered in a search of the HST Guide Star Catalog for Saturn occultations. The GSC reports a photographic B magnitude of 12.5 for this star; recent photometry (Sybert et al., AJ submitted) indicates that it is V=11.9, B-V=0.7, and V-R=0.5. This was an important event for several reasons, most notably in that it occurred near the time when Saturn reversed its motion in its retrograde loop, so the sky plane velocities are very low (< 1 km/sec), yielding very high spatial resolution and low noise despite the star's moderate brightness.

4.4.6.1 Proposed Observations

A. The sequence of observations was to be as follows:

1. Dark measurement

2. Background scan of Saturn and rings (single line continuous scan): The spacecraft tracks relative to Saturn (a moving object) and scans across the planet, roughly along the track that will pass in front of the star during the occultation.

3. Background scan of Saturn and rings (quintuple-line continuous scan): a zigzag path intended to map out the strong (rings by far dominate the stellar signal) and possibly azimuthally varying ring background signal.

4. Background scan of Saturn and rings (identical to I.A.2)

5. Onboard acquisition of offset target (GSC6327-00161).
This is automatically done twice. An offset target was used because the occultation star is within the ring system and the large background gradients there make direct acquisition impossible.

6. Occultation observations: Starting when the star is in the C ring and following it through the F ring. Close approach to the planet center was at 2 Oct 1991 04:57 UT. These observations cover only egress. The observation sequence is broken into sections covering visibility windows for each orbit.

7. Background scan of Saturn and rings (identical to I.A.2)

8. Background scan of Saturn and rings (identical to I.A.3)

9. Background scan of Saturn and rings (identical to I.A.2)

B. Preparation for the observations

1. It was known ahead of time that items I.A.3 and I.A.8 would not execute correctly because the transformation software was not yet able to handle multiple-line scans in SINGLE-EXP mode for moving targets (a limitation of the MOSS software which would not have presented a problem if it had been made clear). We were not permitted to modify the proposal to remove the SINGLE-EXP specification and re-run the transformation software.

2. An inconsistency in the definition of position angle (used in our background scans, which are done relative to the center of Saturn) was discovered during the execution of SV2771 was declared fixed prior to the transformation of this 1081 proposal; a bug in the JPL software was altered to agree with both proposal instructions and PA convention.

3. Relative positions of offset target (GSC6327-00161) and occultation target (GSC6323-01396) were updated near the occultation date to reflect recent ground-based measurements of their positions.

4. Contemporaneous ground-based observations of this occultation event were made at the IRTF by Amanda Bosh, Leslie Young, and Jim Elliot, for possible later comparison.

4.4.6.2 Observations

Maren Cooke covered the observations from STScI (OSS). Data were taken with the photomultiplier tube (PMT; 7500 Angstroms) and visible (VIS; 3200 Angstroms) detectors during all of our observations. The desired simultaneous dual-wavelength observations were effected using the HSP's "star-sky" mode of operation. This mode currently has no allowance for separate gain settings for the analog signal, making the second (VIS) detector's analog data nearly unusable. (Jim Younger initiated an HSTAR on this, implemented a new command sequence in April 1992 for future use.)

A. Dark-sky measurement (I.A.1 above)

PMT digital signal varied around ~52 counts (noise mostly within +/-20 counts).

B. Backscans (I.A.2,3,4,7,8,9)

Guiding mode for the telescope during the background scans was Coarse Track.

1. Multiple-line scans

As expected (see I.B.3), the quintuple-line scans did not execute as originally intended; the entire time of the exposure was spent scanning the occultation track.

2. Single-line scans

Although the position angle problem noted above (I.B.4) was ostensibly fixed, there may remain some problem with the MOSS positioning of the S/C relative to Saturn; all four single-line

scans (I.A.2,4,7,9) should have been basically identical but instead seemed to scan different radial regions of the rings, each pair only partially overlapping (the pairs 2&4 and 7&9 were identical). This could conceivably also be due to some unexpected state of the guiding software after the failed multi-line scans. Jim Younger has been consulted about the position history during the observations, but has reported no great illuminations as yet. A short spate of telescope jitter is evident near the end of the first scan, about four minutes into orbital night. The period of the (prominent!) oscillations is about 1.8s (not atypical for solar panel wobble, according to Pierre Bely).

C. Offset Star Acquisitions

As with SV2771, this crucial step was performed flawlessly. Two successive on-board acquisitions were performed, and the faint offset star appeared nearly dead-center even in the first of the frames. On this occasion, the guide stars used were bright enough to attain (and hold, most of the time) Fine Lock. A great relief, given the significant telescope jitter that polluted the SV2771 data. Lock was lost between the two acquisitions, again ~4 minutes into orbital night; fine lock regained after a couple of minutes.

D. Stellar Occultation Observations

Fifteen segments of the slow occultation event were observed during thirteen successive orbits of the HST (observation was discontinued frequently due to Earth occultation and/or SAA passage). Transitions to orbital night were generally accompanied at least by serious jitter and often by temporary loss of lock, but at other times the signal was quite clean in the PMT (red) and somewhat noisier in the VIS (UV) detector. Variations in the stellar signal caused by features in the rings are superposed on the broad, smeared image of Saturn and its rings as seen by the 1 arcsec. aperture. Recognizable ring structure was immediately spotted in many of the segments, and while coverage is not complete, some regions are covered in more than one segment because of spacecraft parallax.

4.4.6.3 Data Reduction and Analysis

A. Data Obtained

1. Plots made on-site indicate that data are of relatively high S/N: (unocculted star)/(random noise) ~20 for a one second average

2. Two tapes of calibrated data were obtained by Maren Cooke, and installed on our local computer. Data from a third tape FTP'd from Wisconsin with the help of Jeff Percival.

3. All data are now in local format.

4. Definitive ephemerides obtained and translated into ascii.

B. Reductions

1. Transform X,Y,Z,Xdot,Ydot,Zdot of definitive ephemerides into observer latitudes and longitudes for use in local (MIT) software.

2. With observer positions, star and planet ephemerides, and times sampled, determine ring plane radii for each data point. Because Saturn was moving very slowly during this event, parallax caused by the HST's orbital motion is a major factor, and the apparent path of the star was a series of "curlicues" through the ring system. Further analysis depends on first being able to determine accurate ring plane radii.

C. Possible Analyses

Comparison of the HSP radial profile with past occultation data may show changes in the ring system over time; previous data sets include the Voyager encounters in 1980 and 1981 (a radio occultation in the X (3.6cm) and S (13 cm) bands by Voyager 1, and ultraviolet observations (2700 and 1100 angstroms) of a

stellar occultation by Voyager 2), and extensive Earth-based observations of the very bright star 28 Sgr being occulted by Saturn in 1989. The multiple tracks traced out in certain regions of the rings (because of spacecraft parallax) may help to constrain the kinematic behavior of known non-circular features, discover new noncircularities, and, along with the additional temporal coverage, provide important leverage in ring orbit models currently being refined. Simultaneous dual-wavelength observations may allow us to investigate the distribution of very fine particles in the rings by studying any color dependence in feature appearance, to the extent that we can subtract the ring background (hampered by the incorrect backscan coverage, as noted in I.B.3. and II.B) and given the relatively poor noise characteristics of the UV signal.

4.5 Database Updates

There were only two database updates in the period covered by this report:

The SIAF file defining the POL tube aperture positions was updated in January 1992 using the results of the 3377 POL fine alignment test. The new positions are shown in section 4.4.3.

The SIAF file defining the PRISM mode apertures was updated in May 1992. The new positions are discussed in section 4.3 in the description of test 3996.

The current SIAF and SICF database values are listed in appendices G and H.

4.6 SV Anomalies

The major anomalies of the SV period (those not covered in the OV report) are:

1. The "ramp" and ninety two minute period sinusoid in the 1389 observation. There has been no correlation found to any HSP engineering telemetry. The HSP ODS radiator skin temperture exhibits a similar orbital period but it is not in phase. Some of the FGS temperature variations are in phase with the HSP 1389 SCP data.

2. The missing packets in the 1383 Crab Pulsar data were eventually corrected. The problem was somewhere in the ground processing of the large files involved in this test. There were no missing packets in the UV observation of the Crab Pulsar in HSP GTO 1101.

HSP HSTAR status is detailed in Appendix C

4.7 End of SV Status and Liens

All basic HSP functions have been verified and all are working properly as of the end of the SV period. Fine alignment of the HSP prism apertures (3396) and the instrumental polarization test (1386) remain to be completed and analyzed.

No reasonable mechanism is available for dumping the HSP memory and getting the resulting science data in electronic form. The bus directory memory pages require special procedures to dump. The single event upset events (two so far in the OV period) have demonstrated the continuing need to have a straightforward means to dump and check the HSP memory including the bus director memory. As of the end of SV, an effort is underway to create standard procedures to perform this operation and to provide FITS files of the resulting data.

The commanding change to provide for resetting the frame count during a data collection is needed to restore full HSP capability. At this time our understanding is that it will be done, but it has low priority, and cannot be expected any sooner than late summer 1992.

The Crab Pulsar (1383 and 1101) observations produced such large amounts of data that the normal PODPS processing was overwhelmed. Raw data were provided (.pkx files) and proved to be straightforward to read and reduce.

4.8 Contract End Item (CEI) Specifications Verification Status

The following are the HSP CEI specifications and their current verification status:

4.8.1 Wavelength Range

Total instrument quantum efficiency excluding the photomultiplier tube will exceed 1% over the entire range 120 to 660 nm and will reach a maximum of no less than 9% at 400nm. Total instrument quantum efficiency of the photomultiplier tube will exceed 1% over the entire range 600 to 870 nm. Useful sensitivity for polarimetry will be achieved over the interval 210 to 300 nm.

The most conservative interpretation of the results from test 2912 leads to the overall quantum eficiency for the HSP shown in the following table

filter	Peak filter transmission	HSP QE %
f135w	.126	0.04
f218n	.354	0.71
f220w	.354	0.60
f145m	.134	0.05
f184w	.316	0.43
f248m	.354	0.69
f278n	.170	0.37
f284m	.316	0.53
f551w	.355	0.17

HSP does not meet this specification for several reasons: about half of the stellar flux is lost at the one arcsecond apertures because of the HST aberrated images; the VIS detector sensitivity dropped since prelaunch calibrations; and probably other (unknown) causes.

4.8.2 Spectral Resolution

The HSP spectral resolution of the image dissector tubes shall be that of the wavelength filters selected, and these filters shall have bandpasses covering the wavelength interval 120 to 660 nm. One filter with a bandpass selected between 800 and 900 nm shall be used on the photomultiplier tube.

This requirement was satisfied in the design of the HSP and required no specific verification.

4.8.3 Angular Field of view and resolution

The apertures available on each dissector shall be nominally 0.4, 1.0 and 10 arc sec. The apertures on the photomultiplier tube shall be as necessary to allow useful observations of stellar occultations.

The apertures are determined by the aperture plates which were verified in the design and fabrication phases.

4.8.4 Dynamic Range

The HSP shall be able to measure the intensity of astronomical point sources over a range of intensity of 10^8 with a departure from linearity of response as specified in 4.8.7.

Several stars were observed in 1385, 1474, and 3382 with the V filter and established the linearity of the HSP. The range in brightnesses in these observations was 1000 (the range of V was 5.28 to 12.79) and the linearity calculated to be 0.62% or about 6 mMag. The errors are probably dominated by effects external to the instrument, in particular pointing errors and jitter. These combned with the large HST images have made it impossible to do the high precision photometry we had intended with the HSP.

4.8.5 Signal to Noise Ratio

The HSP shall have a signal to noise ratio > 10 which shall be attainable for a visual band observation of a point source of visual apparent magnitude equal to 24 after a 2000 second integration time.

The signal to noise ratio was calculated with the HSP simulator for a 2000 second observation of a 24th magnitude A0 star in all HSP filters using a one arc second aperture. The resulting signal to noise ratio exceeds the requirement for most filters. The accuracy of the HSP simulator has been verified using OV and SV observations.

Target: A0 (T=9900, B-V=0.0491489) M(5556)=24 E(B-V)=0 z=0 LAMBDA FLUX

det	filt	aper	tstar	tsky	nstar	nsky	ndark	CVC(nA)	SNR
POL	F160LP	0.65-C	2.00e+03	0.00e+00	1.37e+03	2.30e+03	1.00e+02	2.93e-04	61.36
POL	F216M	POL0	2.00e+03	0.00e+00	1.67e+00	1.50e-01	1.00e+02	1.46e-07	10.09
POL	F237M	POL0	2.00e+03	0.00e+00	3.64e+00	3.92e-01	1.00e+02	3.22e-07	10.20
POL	F277M	POL0	2.00e+03	0.00e+00	1.19e+01	3.20e+00	1.00e+02	1.21e-06	10.73
POL	F327M	POL0	2.00e+03	0.00e+00	1.30e+01	6.89e+00	1.00e+02	1.59e-06	10.95
UV1	F122M	1.0-A	2.00e+03	0.00e+00	2.66e-01	1.01e-02	1.00e+04	2.21e-08	100.00
UV1	F135W	1.0-A	2.00e+03	0.00e+00	4.07e-01	1.04e-02	1.00e+04	3.34e-08	100.00
UV1	F140LP	1.0-C	2.00e+03	0.00e+00	2.43e+02	3.23e+01	1.00e+04	2.20e-05	101.37
UV1	F145M	1.0-A	2.00e+03	0.00e+00	2.91e-01	2.29e-03	1.00e+04	2.35e-08	100.00
UV1	F152M	1.0-A	2.00e+03	0.00e+00	6.17e-01	6.52e-03	1.00e+04	4.99e-08	100.00
UV1	F184W	1.0-A	2.00e+03	0.00e+00	1.39e+01	3.83e-01	1.00e+04	1.14e-06	100.07
UV1	F218M	1.0-A	2.00e+03	0.00e+00	1.36e+01	6.67e-01	1.00e+04	1.14e-06	100.07
UV1	F220W	1.0-A	2.00e+03	0.00e+00	2.74e+01	1.61e+00	1.00e+04	2.32e-06	100.15
UV1	F240W	1.0-A	2.00e+03	0.00e+00	6.57e+01	6.74e+00	1.00e+04	5.80e-06	100.36
UV1	F248M	1.0-A	2.00e+03	0.00e+00	3.55e+01	4.19e+00	1.00e+04	3.17e-06	100.20
UV1	F278N	1.0-A	2.00e+03	0.00e+00	6.58e+00	1.35e+00	1.00e+04	6.34e-07	100.04
UV1	F284M	1.0-A	2.00e+03	0.00e+00	2.74e+01	5.76e+00	1.00e+04	2.65e-06	100.17
VIS	F160LP	1.0-A	2.00e+03	0.00e+00	1.54e+03	2.62e+03	6.00e+01	3.33e-04	64.98
VIS	F184W	1.0-A	2.00e+03	0.00e+00	1.39e+01	3.97e-01	6.00e+01	1.14e-06	8.62
VIS	F240W	1.0-A	2.00e+03	0.00e+00	7.48e+01	8.91e+00	6.00e+01	6.70e-06	11.99
VIS	F262M	1.0-A	2.00e+03	0.00e+00	3.60e+01	6.07e+00	6.00e+01	3.37e-06	10.10
VIS	F320N	1.0-A	2.00e+03	0.00e+00	2.51e+01	1.79e+01	6.00e+01	3.44e-06	10.15
VIS	F355M	1.0-A	2.00e+03	0.00e+00	2.82e+01	2.12e+01	6.00e+01	3.96e-06	10.46
VIS	F400LP	1.0-A	2.00e+03	0.00e+00	7.84e+02	2.12e+03	6.00e+01	2.32e-04	54.43
VIS	F419N	1.0-A	2.00e+03	0.00e+00	3.77e+01	5.10e+01	6.00e+01	7.09e-06	12.19
VIS	F450W	1.0-A	2.00e+03	0.00e+00	4.36e+02	7.08e+02	6.00e+01	9.15e-05	34.70
VIS	F551W	1.0-A	2.00e+03	0.00e+00	1.03e+02	3.11e+02	6.00e+01	3.31e-05	21.78
VIS	F620W	1.0-A	2.00e+03	0.00e+00	1.24e+02	6.23e+02	6.00e+01	5.98e-05	28.42
UV2	F122M	1.0-A	2.00e+03	0.00e+00	2.66e-01	1.01e-02	2.00e+03	2.21e-08	44.72
UV2	F140LP	1.0-C	2.00e+03	0.00e+00	2.43e+02	3.23e+01	2.00e+03	2.20e-05	47.70
UV2	F145M	1.0-A	2.00e+03	0.00e+00	2.91e-01	2.29e-03	2.00e+03	2.35e-08	44.72
UV2	F152M	1.0-A	2.00e+03	0.00e+00	6.17e-01	6.52e-03	2.00e+03	4.99e-08	44.73
UV2	F160LP	1.0-A	2.00e+03	0.00e+00	2.39e+02	3.21e+01	2.00e+03	2.17e-05	47.66
UV2	F179M	1.0-A	2.00e+03	0.00e+00	7.28e+00	4.80e-01	2.00e+03	6.21e-07	44.81
UV2	F184W	1.0-A	2.00e+03	0.00e+00	1.39e+01	3.83e-01	2.00e+03	1.14e-06	44.88
UV2	F218M	1.0-A	2.00e+03	0.00e+00	1.36e+01	6.67e-01	2.00e+03	1.14e-06	44.88
UV2	F248M	1.0-A	2.00e+03	0.00e+00	3.55e+01	4.19e+00	2.00e+03	3.17e-06	45.16
UV2	F262M	1.0-C	2.00e+03	0.00e+00	6.45e+00	1.03e+00	2.00e+03	5.98e-07	44.80
UV2	F278N	1.0-A	2.00e+03	0.00e+00	6.58e+00	1.35e+00	2.00e+03	6.34e-07	44.81
UV2	F284M	1.0-A	2.00e+03	0.00e+00	2.74e+01	5.76e+00	2.00e+03	2.65e-06	45.09
PMT	F750W	1.0-A	2.00e+03	0.00e+00	1.97e+02	1.18e+03	8.00e+05	1.10e-04	895.20

4.8.6 Maximum signal to noise ratio

The maximum signal to noise ratio attainable in a single exposure shall be at least 4000.

There are no observations to date that demonstrate this requirement. The longest observation so far, 1389, was 5.5 hours and acheived a signal to noise ratio of 163. Correcting for the pointing and orbital effects, one can show a signal to noise ratio of 1372. This requirement would be difficult to demonstrate given the present jitter and pointing performance and no specific test is planned to collect the required data.

4.8.7 Relative Photometric Accuracy

The brightness ratio of any two signals within the first six decades of the dynamic range, at a given wavelength will be accurate to 0.2% or to 30% of the combined statistical photon noise, whichever is larger.

We do not have data with which to test this specification, but it is unlikely that given the present cirumstances the accuracy could be any better than the 0.6% given in 4.8.4.

4.8.8 Time Resolution

Time resolution shall be as fast as one millisecond, with integration times selectable to a resolution of one microsecond.

This requirement was satisfied in the design and has been verified repeatedly in operations.

4.8.9 In Flight Calibration

The HSP in flight calibration shall rely on internal or astronomical sources as necessary to produce required photometric accuracy.

There are internal test lamps in the HSP intended for ground tests only. All in flight calibrations rely on actual targets.

4.8.10 Thermal Control

The HSP thermal control system will insure the HSP remains within the acceptable operations temperature limits for all portions of the mission.

The HSP thermal control system has operated as expected since launch and has maintained the desired limits.

4.8.11 Engineering Data and Safing Provisions

The HSP instrumentation shall provide the necessary engineering data to enable monitoring and evaluation of the status of the instrument. The instrument must provide continuous on board, real time monitoring of critical elements, and the ability to switch the instrument to a safe condition without real time ground commands should hazardous conditions exist.

The HSP engineering data provides the required information. The difficulty in using the engineering data is that the ground system was not designed to maintain engineering data. Other than real time displays, the engineering data is not well maintained and archiving is chaotic.

5. Modifications and Recommendations

There were no major modifications to operations procedures arising from HSP SV results. The time required for HST step and dwell scans is now understood as a result of the 3377 experience. Data processing has been updated so that the packets missing in original 1383 data have been restored.

5.1 Trend Monitoring Recommendations

There are no trend monitoring procedures for the HSP engineering data. However, any significant or sudden unexplained change in temperatures, voltages, or other parameters should be investigated. Any limit exceeded also should be investigated. Detector parameters are monitored as part of the on-going HSP calibration plan.

It is important to characterize and monitor the sensitivity of all HSP detectors. The planned periodic calibration tests will provide the required data to quantify the loss of sensitivity and monitor any future changes.

The table below shows the HSP total number of on and off cycles and times and the average number of minutes on per cycle for the HSP detectors (HVPS) and support electronics. The Science Tape Recorder is also listed. Note the high number of cycles and low time per cycle of the tape recorder compared to HSP detectors. The data represents the totals from all SMSs from launch through the 92139 SMS. The individual SMS statistics are listed in Appendix F.

Item	#on	#off	on time	minutes/cycle
STR	23040	23040	133687.9	5.8
Det1	53	53	15496.4	292.4
Det2	91	91	23728.4	260.8
Det3	86	86	28918.3	336.3
Det4	68	68	18221.2	268.0
Det5	28	28	5883.9	210.1
HV1	50	50	14735.5	294.7
HV2	90	90	22481.0	249.8
HV3	85	85	27724.7	326.2
HV4	68	68	16719.4	245.9
HV5	28	28	4522.9	161.5

5.2 Instrument Operational Recommendations

There are several issues unresolved as of the end of the OV period that still remain so as of this writing. The following actions should be taken before the close of the SV/GTO period:

1. The capability to reset the frame counter should be implemented to allow the HSP to function with the 32 kb link to the tape recorder.

2. The remaining capabilities of the HSP thermal control system should be exercised. Should there be need to make changes in standard operating procedures, for example to conserve power, the change could be made quickly and with low risk.

3. The capability to dump HSP memory, including the bus director memory, and to provide FITS files of the resulting dump data should be implemented as soon as possible. If there are future single event upsets, or other anomalies, it will be important to have this capability to enable timely analysis of the problem.

4. The characterization tests of the POL tube needs to be completed so that the HSP capability for polarization measurements can be established.

5. FGS performance still has unexplained characteristics. The acquisitions for 1092 where the same target was acquired once or twice per week for over four months shows some interesting patterns. These data need to be further analyzed and communicated.

8. The sensitivity of the VIS tube needs to be closely monitored.

5.3 Conclusions & Lessons Learned

Perhaps the most significant lesson learned in the SV period was the importance of communicating information between the various HST project elements and participants. As this is written, it is not clear what caused the anomalies in the HSP 1389 data, taken in August 1991. Some of the possible causes have major impact beyond the HSP and yet there still does not seem to be a project-wide mechanism for dealing with the problem. A philosophy similar to that used in the GIDEP (Government-Industry Data Exchange Program) ALERT program would seem to have application in the HST project. In a project so large, it is difficult to determine just who may be affected by a problem and who may have relevant informtion to help solve it. In that case, it would seem logical to try to disseminate as much information as possible. Yet, we find that even within relatively small groups there seems to be a reluctance to communicate such information. The price for this could be huge. Consider the potential implications for follow-on instruments or COSTAR if the cause of the 1389 anomaly is SI motion greater than presently thought possible.

Other significant lessons learned, previously cited, include:

The OV/SV program has demonstrated that the ground system lacks the flexibility and capability to respond reasonably to normal verification activities.

The pre-launch test design and schedule were too success oriented. Tests had to be broken into smaller units to prevent large losses of spacecraft time in the event of problems. Tests were scheduled on the assumption that needed spacecraft support capabilities would exist by the time the test was executed. Often these assumptions were incorrect and led to additional test failures, loss of spacecraft time, and additional delays in implementing improved tests.

The OV/SV program has shown that efficient operations depend on being able to adjust operations procedures to meet the conditions actually encountered that may be different than anticipated before launch.

Appendices

A. HSP OV, SV, & GTO Proposal Numbers and Names
The HSP proposal numbers and names are listed and cross-referenced where proposals are continuations or modifications of earlier proposals

B. HST Flight SMS sequence
The SMS numbers and revision letters of the flight sms's actually executed are listed

C. HSP HSTARS
The numbers, names, and disposition summary of HSP related HSTARs are listed

D. HSP Data Collection Timing
The papers written by Mark Werner describing the HSP data collection timing considerations are included in this appendix.

E. Filter, Aperture, Proposal, Target, and Date Index
This appendix lists all HSP observations of stellar targets sorted by filter, aperture, target, proposal, and date.

F. HSP & STR Operating Times & Cycles
The number of on and off cycles, the total on time, and average on time in minutes is listed for the HSP detectors, detector electronics, and the science tape recorder.

G. HSP 1092 Acquisition Data
The acquisition positions of the target of 1092, Z Chamaeleontis, are discussed, listed, and charted.

H. SIAF Values
The HSP V2/V3 aperture positions in the PDB in arc seconds.

I. SICF Values
The HSP aperture locations in HSP detector deflection coordinates

J. SMS Activity Timelines
The parser timeline charts of selected HST & HSP activities for each SMS is included in this appendix.

K. HSP Detector Maps
Charts of all HSP filters and apertures with various other useful information

L. HSP Pulsar Timing and Light Curve Reduction
The paper by Jeff Percival describing the 1383 observations of the Crab Pulsar, data reduction, and analysis.

Appendix A - HSP OV, SV, & GTO proposal numbers and names

OV, SV, SV-delta, and GTO HSP proposals by proposal number:
version 1.23 4/7/92

"pgm" classes:

GO	Guest Observer
GTO	Guaranteed Time Observation
GTO+	Guaranteed Time Observation (Augmentation time)
OV	Orbital Verification
SAO	Science Assessment Observation
SV	Science Verification
SVD	Science Verification (Delta plan)
/X	Cancelled

prop	pgm	name
1079	GTO	Opportunity occultations by small bodies (3319,4015)
1080	GTO	The size and composition of planetary ring particles(3373)
1081	GTO	Saturn ring dynamics (3371, 3375)
1082	GTO	Helium abundances in Jovian planet upper atmospheres (3354)
1083	GTO	Dynamics of planetary upper atmospheres (3376)
1084	GTO	Lunar occultations with the HST
1085	GTO/X	Rotation periods of cometary nuclei
1086	GTO	Do Neptune and Pluto have rings? (4076)
1087	GTO/X	Eclipses and occultations by Pluto and Charon
1088	GTO	Small satellites in the Uranian system
1089	GTO	Captured satellites of the Jovian planets
1090	GTO	Periodic variations in DQ Herculis stars (3257)
1091	GTO	UV pulsations from X-ray pulsars
1092	GTO	Eclipses of cataclysmic variable stars (3238)
1093	GTO	Observations of ZZ Ceti stars
1094	GTO	Search for optical variability assoc. with black holes (3255)
1095	GTO	Variability of high luminosity stars (3252,3926)
1096	GTO	Gravitational lenses I (3250,4034)
1097	GTO	X-ray binaries (2952,2958,3234,3249,3256,4036)
1098	GTO	Remnant stars in SNRs (2953,3251,4037,4083)
1099	GTO	Active galactic nuclei (3248)
1100	GTO/X	Evolution of the nuclei of planetary nebulae
1101	GTO	Optical and UV observations of radio pulsars (3253)
1102	GTO	UV light and polar. variations in Beta Cephei stars
1103	GTO	Vis/UV light curves of short period RR-Lyrae stars (3254)
1104	GTO	High speed photometry of GBS 0526-66
1379	OV	Detector dark count test
1380	OV	MSC Focus and aperture mapping I (1526,3093,3119,3120)
1381	SV	Target acquisition test (3071-3074)
1382	OV	Pulse height distribution test
1383	SV	Time resolved photometry
1384	SV	Color transformation test (2769,2770,3378,3425)
1385	SV	Photometric performance test (3382)
1386	SV	Instrumental polarization test
1387	SV	Stokes parameter test
1389	SV	Short-term photometric stability
1391	GTO	Gravitational lenses II (4034)
1474	SV	Photometric performance test
1499	OV	Command response test

1500	OV	Detector data test
1501	OV	Data integrity test
1502	OV	High voltage turn-on test
1503	OV	MSC coarse FGS/HSP alignment II
1504	OV	MSC fine FGS/HSP alignment III (1524,2948-51,3140)
1524	SV	MSC fine FGS/HSP alignment III (1504,2948-51,3140)
1526	SV	MSC aperture mapping I (UV) (1380,3093,3119,3120)
2113	OV	Memory dump
2201	OV	Safe-to-oldhold
2608	GO	Constraints on continuum models of active nuclei
2749	SV	RIU polling on/off test
2768	SVD	Pulse height distribution test
2769	SV	Color transformation test (1384,2770,3378,3425)
2770	SVD	Color transformation test (1384,2769,3378,3425)
2771	SV	Stellar occultation by planetary rings
2772	SVD	Stellar occultation by dark lunar limb
2773	SVD	Stellar occultation by planetary atmospheres
2912	SV	Photometric calibration
2948	SV	MSC fine FGS/HSP alignment III UV2 (1504,2949,2950,2951,3140)
2949	SV	MSC fine FGS/HSP alignment III UV1 (1504,2948,2950,2951,3140)
2950	SV	MSC fine FGS/HSP alignment III VIS (1504,2948,2949,2951,3140)
2951	SV	MSC fine FGS/HSP alignment III POL (1504,2948,2949,2950,3140)
2952	GTO	X-ray binaries (1097,2958,3234,3249,3256,4036)
2953	GTO/X	Remnant stars in SNRs (1098,3251,4037,4083)
2958	GTO	X-ray binaries (1097,2952,3234,3249,3256,4036)
3006	SAO	Effect of centering errors on HSP photometry
3007	SAO	Effect of jitter on HSP photometry
3069	OV	10.2/Bright earth test
3071	SV	Target acquisition test POL (1381)
3072	SV	Target acquisition test UV1 (1381)
3073	SV	Target acquisition test UV2 (1381)
3074	SV	Target acquisition test VIS (1381)
3093	SV	MSC aperture mapping I VIS (1380,1526,3119,3120)
3119	SV	MSC aperture mapping I VIS visit 2 (1380,1526,3093,3120)
3120	SV	MSC aperture mapping I VIS visit 3 (1380,1526,3093,3119)
3135	SV	The Secret Stanley Test
3140	SV	MSC fine FGS/HSP alignment III (nelson plan) (1504,1524,2948-51)
3152	OV	MSC aperture mapping II/III (jwp plan) (3233,3362,3363)
3233	OV	MSC aperture mapping II/III (jwp plan) (3152,3362,3363)
3234	GTO	X-ray binaries (1097,2952,2958,3249,3256,4036)
3238	GTO	Eclipses of cataclysmic variable stars (1092)
3248	GTO	Active galactic nuclei (1099)
3249	GTO	X-ray binaries (1097,2952,2958,3234,3256,4036)
3250	GTO	Gravitational lenses I (1096,4034)
3251	GTO	Remnant stars in SNRs (1098,2953,4037,4083)
3252	GTO	Variability of high luminosity stars (1095,3926)
3253	GTO	Optical and UV observations of radio pulsars (1101)
3254	GTO	Vis/UV light curves of short period RR-Lyrae stars (1103)
3255	GTO	Search for optical variability assoc. with black holes (1094)
3256	GTO	X-ray binaries (1097,2952,2958,3234,3249,4036)
3257	GTO	Periodic variations in DQ Herculis stars (1090)
3319	GTO	Opportunity occultations by small bodies (1079,4015)
3321	GTO	Gravitational Lenses II (1391)
3354	GTO	Helium abundances in Jovian planet upper atmospheres (1082)
3362	OV	MSC aperture mapping II/III (jwp plan) visit 2 (3152,3233,3363)
3363	OV	MSC aperture mapping II/III (jwp plan) visit 3 (3152,3233,3362)
3371	GTO	Saturn ring dynamics (later cycles, 1081, 3375)
3373	GTO	The size and composition of planetary ring particles (1080)

3375	GTO	Saturn ring dynamics (cycle 1, 1081, 3373)
3376	GTO	Dynamics of planetary upper atmospheres (1083)
3377	SV	Pol detector test
3378	SV	Color transformation test II (1384,2769,2770,3425)
3382	SV	Photometric performance test (faint end) (1385)
3383	OLT	The STScI jitter test
3425	SV	Color transformation test VIS (1384,2769,2770,3378)
3926	GTO	Variability of high luminosity stars, retake 0 (1095,3252)
3985	SV	Instrumental polarization test (revised)
3996	SV	Prism mode test
4015	GTO	Opportunity occultations by small bodies (1079,3319)
4034	GTO+	Gravitational lenses I & II (1096,3250,1391)
4036	GTO+	X-ray binaries (1097,2952,2958,3234,3249,3256)
4037	GTO+	Remnant stars in SNRs (1098,2953,3251,4083)
4076	GTO	Do Neptune and Pluto have rings? (1086)
4083	GTO	Remnant stars in SNRs (1098,2953,3251,4037)

Appendix B - HST Flight SMS sequence

The flight SMS sequence is listed below for the period May 6, 1991 through July 19, 1992. Interruptions in the "in continuity with", usually associated with safemode recoveries, are indicated by ******.

******

911276a2r
911337c8
911407ah
911477c3
911547d3
911617ca
911687bg
911757b1
911827af
911897al
911967d4
912037acr
912107b3
912177d5r
912247c7
912317e2
912387c1
912457d5
912527e5
912597b1
912667c4
912737c6
912807ai
912877d1
912947b4
913017b5
913087d4
913157aa
913227c4
913297b7
913367e3
913437cd

****

913434b8r
913507dg
913577b2
913647e7
920067c7
920137d2
920207aa
920277ab
920347b5
920417b6
920487ah
920557e1
920627c2
920697ci
920767b4
920837b9
920907bar
920977f6r
921047d2
921117b6
921187e4
921257e4
921327c4
921397d1
921467d9
921537a5
921607c1
921677bf
921747bc

****

921811d4
921826f1
921887d1
921957c2

Appendix C - HSTAR STATUS

HSP HSTAR dispositions as of 01-13-92:

HSTAR #	Description	Disposition	Due	ORG
010	HSP Structure Temp VTPMTPB	CLOSED	04-29-90	
205	HSP 2113 Mem. Dump Miscompares 1097	STGS DR 07-19-90	HSP	
207	HSP High Volt Out of Limit	CLOSED	06-19-90	HSP
232	DCF Missing Data Packet for HSP 1500	CLOSED	06-07-90	LMSC
242	HSP 2113 Mem. Dump Miscompares 1097	STGS DR 07-19-90	PORTS	
298	HSP High Volt Mon Out of Limit	CLOSED	06-19-90	MOC
369	HSP UDL and SHPs Missing	CLOSED	06-07-90	LMSC
401	STR P/B of HSP Data Missing SHPS and UDLS	CLOSED	08-07-90	LMSC
529	HSP Data Missing from STR Dump	CLOSED	06-12-90	LMSC
530	HSP Data Missing from STR Dump	CLOSED	06-12-90	LMSC
574	Unexpected PMT Behavior in 1502 CLOSED	10-05-90	HSP	
578	HSP Data from STR Missing SHP/UDL	CLOSED	06-14-90	STPG
579	HSP Data Missing from STR Dump	CLOSED	07-24-90	STPG
581	HSP Data Missing from STR Dump	CLOSED	07-24-90	MOC
672	Missing Calibration Files 1500	CLOSED	07-19-90	HSP
836	HSP Safed by BOP in 1380 Det 3	CLOSED	09-20-90	HSP
958	HSP Safing Recovery STBF Error	CLOSED	08-28-90	STSCI
998	AN Crossing Times Missing	CLOSED	08-17-90	STSCI
999	OSS Not Able to Print Tab Listing	CLOSED	08-17-90	OSS
1072	HSP Safed by BOP During 1379 PMT	CLOSED	09-20-90	HSP
1112	VTPAFB1/VTPAFB2 Low Lim Violation	CLOSED	09-20-90	MOC
1115	VTPNP2C Low Lim Violation	CLOSED	09-20-90	MOC
1120	ESS Time Tag Error	CLOSED	ESS	
1145	HSP 1380 T Errors	CLOSED	09-26-90	HSP
1186	Third Dump of HSP STR Data Missing	CLOSED	09-14-90	

1267	OSS Data doesn't Match PODPS Data for HSP 1503 Det 4	CLOSED	01-17-91	STSCI
1358	HSP Clock Overflow Error	CLOSED	10-22-90	HSP
1476	HSP Data Contains Inversion	CLOSED	11-07-90	LMSC
1514	HSP Data Contains Multiple Inversions	CLOSED	11-21-90	LMSC
1537	Missed Target HSP	CLOSED	11-21-90	STPG
1555	Data Inversion In HSP Data	CLOSED	01-08-91	CD500
1662	HSP 1526 Failed Observations	OPEN	02-04-91	STSCI
1957	HSP TLM Error	CLOSED	02-20-91	MOC
1959	HSP 3140 Pointing Error Exceeds 2"	CLOSED	02-20-91	PCS
1967	VTERROR out of limits	CLOSED	02-20-91	HSP
2094	Incorrect Stmts in PSTOLS HSPSBYHD & HSPHDSBY	CLOSED	MOC	
2169	Missing Bright Earth in HSP 3152	CLOSED	03-27-91	STScI
2208	HSP FITS Header Discrepancies	OPEN	04-09-91	STScI
2235	PDB Update Identified Post Final Mode	CLOSED	04-10-91	HSP
2274	Missing HSP Observations in 2948/2949	OPEN	05-03-91	STScI
2307	HSP SCP Collection Star Not Seen in Aperture	CLOSED	04-30-91	STPG
2317	Missing Obs in HSP 3152 POL	CLOSED	05-02-91	STPG
2329	Missing Obs in HSP 3007	CLOSED	05-07-91	STPG
2334	HSP Bus Dir Memory Not Dumped	OPEN	05-08-91	STScI
2343	HSP Error Frag	OPEN	05-09-91	MOC
2371	HSP Memdump Compare Needs Modification	OPEN	05-17-91	MOC
2408	BE of HSP Microprocessor Dump	REJ.	05-28-91	MOC
2420	HSP Obs Not Written to FITS FMT Tape	OPEN	05-30-91	STScI
2471	No Target for HSP Program 1385	CLOSED	06-12-91	STScI
2484	Pointing Error >2" following Baseline GS Acq.	CLOSED	07-01-91	STScI
2485	Targets Not Seen In HSP 1385	CLOSED	06-14-91	STScI
2635	Missing Bright Earth HSP 3362	CLOSED	08-16-91	PCS

2659	Bad HSP 2769 VIS Data Due to S/C Jitter	CLOSED	08-19-91	PCS
2660	Inconclusive HSP 2769 Data Using AGK+81DZ66	CLOSED	08-19-91	STScI
2661	Missing Bright Earth in HSP 3119	CLOSED	08-19-91	STScI
2681	HSP FITS HEADER KEYWORD PTSROFLG CALLED-	OPEN	08-22-91	STSCI
2697	HSP DATA LOSS DUE TO STR TAPE TRACK CHANGE	OPEN	09-03-91	STSCI
2733	HSP 1389 DATA DEGRADATION	OPEN	09-13-91	PCS
2796	UNEXPLAINED PERIODIC EFFECT IN HSP 1389 SCI-	OPEN	10-01-91	SESD
2868	HSP DATA LOG AFTER OUTPUT CEASE	OPEN	10-25-91	STSCI
2869	OSS DISCARDED DATA FROM HSP OBSERVATION	OPEN	10-25-91	STSCI
2935	NO COMMANDING TO ENABLE HSP SCIENCE DATA IINTERFACE	CLOSED	01-15-92	STScI
2999	RANDOM SPIKES IN STR DUMP OF HSP DATA	OPEN	01-10-92	DOC
3041	BAD DATA PACKETS IN HSP 1383	OPEN	01-06-92	MOC

HSTAR Closures Submitted Since 11-20-91:

HSTAR#	Closure Title	Current Status	Assignee	Due	Submitted
1959	HSP 3140 Pointing Error Exceeds 2"	Close	PCS	02-20-91	12-09-91
2274	Missing HSP Observations in 2948/2949	Open	STScI	05-03-91	11-20-91
2471	No Target for HSP Program 1385	Close	STScI	06-12-91	12-09-91
2484	Pointing Error >2" following Baseline GS Acq.	Close	STScI	07-01-91	12-09-91
2485	Targets Not Seen In HSP 1385	Close	STScI	06-14-91	12-09-91
2697	HSP DATA LOSS DUE TO STR TAPE TRACK CHANGE	Open	STSCI	09-03-91	12-19-91

OPEN HSP HSTARs as of 01-09-92:

HSTAR#	Closure Title	Status	Assignee	Due	Submitted
1662	HSP 1526 failed observations	Open	STScI	02-4-91	

2208	HSP FITS Header Discrepancies	Open	STScI	04-09-91	
2274	Missing HSP Observations in 2948/2949	Open	STScI	05-03-91	11-20-91
2334	HSP Bus Dir Memory Not Dumped	Open	STScI	05-08-91	
2343	HSP Error Flag	Open	MOC	05-09-91	
2371	HSP Memdump Compare Needs Modification	Open	MOC	05-17-91	
2420	HSP Obs Not Written to FITS FMT Tape	Open	STScI	05-30-91	
2681	HSP FITS HEADER KEYWORD PTSROFLG CALLED-	Open	STSCI	08-22-91	
2697	HSP DATA LOSS DUE TO STR TAPE TRACK CHANGE	Open	STSCI	09-03-91	12-19-91
2733	HSP 1389 DATA DEGRADATION	Open	PCS	09-13-91	
2796	UNEXPLAINED PERIODIC EFFECT IN HSP 1389 SCI data	Open	SESD	10-01-91	
2868	HSP DATA LOG AFTER OUTPUT CEASE	Open	STSCI	10-25-91	
2869	OSS DISCARDED DATA FROM HSP OBSERVATION	Open	STSCI	10-25-91	
2999	RANDOM SPIKES IN STR DUMP OF	Open HSP DATA	DOC	01-10-92	
3041	Bad Data Packets In HSP 1383	Open	MOC	01-06-92	

Appendix D - HSP Data Collection Timing

(A discussion of HSP data collection timing considerations by Mark Werner, December 1991)

The following is a complete discussion on Data Collection Timing for the HSP. This document will give the necessary information to allow you to calculate,

1) the data collection period,

2) the total time needed for a data collection,

3) the Words/Line (WPL), Lines/Frame (LPF), and Frames/Observation (FPO) for an observation.

The data collection period is a function of the mode, data format, integration time and delay time. The collection period is given as the amount of time needed to collect one sample of data. A sample of data may be one or more bytes of data. The total time for a data collection is a function of many variables. For this discussion, I will only give the user the basic information. This information will allow you to calculate the time with an accuracy of a few tenths of a second. Examples are given for each type of observation.

The total time needed for a data collection will be broken down for each type of observation.

1) Mode 1 - Single Color Photometry (SCP)

2) Mode 2 - Star Sky Photometry (SSP)

3) Mode 3 - Area Scan (ARS)

The other parameters needed for an observation (WPL,LPF,FPO) are derived from the rules and a chart found in Appendix D-2. Appendix D-2 contains the pertinent information about choosing these parameters based on the tape recorder speed. There is also new information about the method to allow data collections to have more than 255 frames. Appendix C contains some extra information about the various set up times.

Mode 1 - Single Color Photometry (SCP)

The total time for an observation (i.e. collect the data) is given by:

$$t_{SCP\text{-}TOT} = t_A + t_B + t_C + t_D + (t_{FS/LS} * FPO) + (N_{TOT} * T_C)$$

Where:

t_A = setup time A , 28.5 - 34.5 ms

t_B = setup time B , 11.2 - 49.6 ms if [BAT(BDEXF)]= 1
0 if [BAT(BDEXF)]= 0 (i.e. special bus director programs)

t_C = setup time C , 1.0 - 2.0 ms

t_D = setup time D , 0 if [BAT(REQDET])=[BAT(SKYDET)], 24.0 ms if not equal.

$t_{FS/LS}$ = frame start to line start delay, 1-2 ms/frame **

T_C = data collection period (time/sample) (see Appendix D-1)

N_{TOT} = total number of samples/observation

= (WPL * LPF * FPO * 2 bytes/word) / X (bytes/sample)
= (words/line*lines/frame*frames/obs.* 2 bytes/word)/(bytes/sample)

X is a function of the data format chosen.

Data Format	X
1	1
2	2
3	3
4	2
7	5

The CU/SDF should be ready to receive data after the mode command is sent to the system controller for the minimum times for $t_A + t_B + t_C + t_{FS/LS}$ plus the time needed to collect one line. The time to the first byte is given by (assuming t_D=0);

$$t_{tfb} = t_{Amin} + t_{Bmin} + t_{Cmin} + t_{FS/LSmin} + (WPL*2/X * T_C)$$

The CU/SDF should remain enabled until the time given by the maximum times for $t_A + t_B + t_C +$ ($t_{FS/LS}$ * FPO) plus (N_{TOT} * T_C) plus the time needed to output the last line (i.e. WPL * 16.5 usec/word **). The time to the last byte is given by (assuming t_D=0);

$$t_{tlb} = t_{Amax}+t_{Bmax}+t_{Cmax}+(t_{FS/LSmax}*FPO)+(N_{TOT}*T_C)+WPL*16.5 \text{ usec}$$

** See Timing notes is appendix D-3

Example:

An observation using data format 3 (longword) with an actual integration time of 53.71 usec (55 T_{bd}) and an actual delay of 22.46 usec (23 T_{bd}) is needed for 1800 seconds.

Questions

1) What WPL,LPF,FPO should be used ?
2) What are the programmed integration and delay times ?
3) When can you expect the first data ?
4) When can you expect the last data ?

The first item to consider is the programmed integration and delay times that will give you the correct times. Using Appendix A you obtain the equations for SCP. The data collection period is given by;

$$T_C = INT_{tot} + DEL$$

Where: INT_{tot} = [BAT(INTTIMx)] + IOT, IOT from the table = 35

DEL = [BAT(DELINTx)] + $1T_{bd}$

T_C = (20+35) + (22+1)
= 78 T_{bd}
= 78 * 976.5625 ns
= 76.17 usec

You need to normalize to Ticks/byte to use the table in Appendix D-2.

78 T_{bd} / 3 bytes = 26 T_{bd} / byte

This implies WPL = 227 (from Appendix D-2), but (227*2)/3 is not an integer. The next smaller value of WPL that satisfies an integral number of samples in a line is 225.

One line of data is collected in;

Time/line = (225 * 2)/3 * T_C sec. = 11.4255 ms.

The total collection time desired is 1800 sec.

1800 sec = 11.4255 ms * Y
Y = 157,542.34

Using the rules from Appendix D-2, we choose,

LPF = 52,514
FPO = 3

The first data can be expected at;

Time to 1st byte = 28.5 ms + 11.2 ms + 1 ms + 1 ms + 11.42 ms = 53.12 ms.

The last data can be expected at;

Time to last byte = 34.5 ms + 49.6 ms + 2.0ms + (3 * 2.0) ms
+ (225*52,514*3*2)/3 * 76.17 usec + (225* 16.5 usec) = 1800.0919 sec

Answers:

1) 225 WPL, 52,514 LPF, 3 FPO,

2) [BAT(INTTIMx)] = 20, [BAT(DELINTx)] = 22

3) First byte at 53.12 ms.

4) Last byte at 1800.092 seconds.

Mode 2 - Star Sky Photometry (SSP)

The total time for an observation (i.e. collect the data) is given by:

$$t_{SSP\text{-}TOT} = t_A + t_B + t_C + t_D + (t_{FS/LS} * FPO) + (N_{TOT} * T_C)$$

Where:

t_A = setup time A , 28.5 - 34.5 ms

t_B = setup time B , 20.2 - 72.8 ms if [BAT(BDEXF)]= 1

0 if [BAT(BDEXF)]= 0 (i.e. special bus director programs)

t_C = setup time C , 1.0 - 2.0 ms

t_D = setup time D , 0 if [BAT(REQDET])=[BAT(SKYDET)]
(i.e. 1 detector star sky)
24.0 ms for 2 detector star sky.

$t_{FS/LS}$ = frame start to line start delay, 1-2 ms/frame **

T_C = data collection period (time/sample) (see Appendix A)

N_{TOT} = total number of samples/observation = (WPL * LPF * FPO * 2 bytes/word) / 2X (bytes/sample)

Note: 2X is needed in the above equation for SSP. An equal amount of data is collected from each detector. T_C takes into account the timing difference between 1 and 2 detector SSP. X is a function of the data format chosen.

Data Format	X
1	1
2	2
3	3
4	2
7	5

The CU/SDF should be ready to receive data after the mode command is sent to the system controller for the minimum times for $t_A + t_B + t_C + t_{FS/LS}$ plus the time needed to collect one line [i.e. (WPL*2)/X * T_C]. The time to the first byte is given by (assuming 1 detector SSP);

$$t_{tfb} = t_{Amin} + t_{Bmin} + t_{Cmin} + t_{FS/LSmin} + (WPL*2/2X * T_C)$$

If 2 detector SSP is used, insert t_D (of 24.0 ms) in the above equation.

The CU/SDF should remain enabled until the time given by the maximum times for $t_A + t_B + t_C + (t_{FS/LS} * FPO)$ plus $(N_{TOT} * T_C)$ plus the time needed to output the last line (i.e. WPL * 16.5 usec/word **). The time to the last byte is given by(assuming 1 detector SSP);

$$t_{tlb} = t_{Amax}+t_{Bmax}+t_{Cmax}+(t_{FS/LSmax}*FPO)+(N_{TOT}*T_C)+WPL*16.5 \text{ usec}$$

If 2 detector SSP is used, insert t_D (of 24.0 ms) in the above equation.

** See Timing notes is appendix D-3

Example:

An observation using data format 4 (alog) with a time between analog samples of 209 T_{bd} is needed for a 600 seconds, using 2 detectors.

Questions

1) What WPL,LPF,FPO should be used ?
2) What are the programmed integration and delay times ?
3) When can you expect the first data ?
4) When can you expect the last data ?

The first item to consider is the programmed integration time. Using Appendix D-1 you obtain the equations for SSP, 2 detector . The data collection period is given by;

$$T_C = INT_{tot} + DEL$$

Where: INT_{tot} = [BAT(INTTIMx)] + IOT , IOT from the table = 156
DEL = 0, for data format 4. (See Note 1, appendix D-1)

$$T_C = (156+53) = 209\ T_{bd} = 209 * 976.5625 \text{ ns} = 204.1 \text{ usec}$$

You need to normalize to Ticks/byte to use the table in Appendix D-2.

$$209\ T_{bd} /(2 \text{ Det.} * 2 \text{ bytes/Det.}) = 52.25\ T_{bd} / \text{byte}$$

The conservative approach rounds up to the next integer value (i.e. 53). This implies WPL = 91 (from Appendix B).
But, 91 WPL does not give an integer number of samples/line. The next smaller value divisable by four is 90. This implies WPL = 90. One line of data is collected in;

$$\text{Time/line} = (90 \text{ WPL}*2 \text{ bytes/word})/(2*2 \text{ bytes/sample.})*T_C = 45 \text{ samples/line} * T_C \text{ sec/sample}$$
$$= 9.1845 \text{ ms/line}$$

The total collection time desired is 600 sec.

$$600 \text{ sec} = 9.1845 \text{ ms} * Y$$
$$Y = 65{,}327$$

Using the rules from Appendix D-2, we choose,

LPF = 65,327
FPO = 1

The first data can be expected at;

Time to 1st byte = 28.5 ms + 20.2 ms + 1.0 ms + 24.0 ms + 1.0 ms + 9.1845 ms = 83.88 ms.

The last data can be expected at;

Time to last byte = 34.5 ms + 72.8 ms + 2.0 ms + 24.0 ms + 4.0 ms
+ (90 * 65,327 * 1 * 2)/2 * 204.1 usec + (90 * 16.5 usec) = 600.132 sec

Answers:

1) 90 WPL, 65,327 LPF, 1 FPO,

Note: Half the data will be from the Star detector and half will be from the Sky detector

2) [BAT(INTTIMx)] = 53, [BAT(INTIMS)] = Don't care (i.e. only the requested detector integration time is used.

3) First byte at 83.88 ms.

4) Last byte at 600.132 seconds.

Mode 3 - Area Scan Photometry (ARS)

The nominal total time for an observation is given by:

$$t_{ARS\text{-}TOT} = t_A + t_B + t_{FS/LS} + (H_{pts} * V_{pts})\,(t_{PDA} + t_{dpp} + t_{mv}) + (H_{pts} * V_{pts})\,(NIPP * T_C)$$

Where:

t_A = setup time A , 5.7 - 12 ms

t_B = setup time B , 11.2 - 49.6 ms if [BAT(BDEXF)]= 1
0 if [BAT(BDEXF)]= 0 (i.e. special bus director programs)

$t_{FS/LS}$ = frame start to line start delay, 1-2 ms **

H_{pts} = [BAT(HPOINTS)]

V_{pts} = [BAT(VPOINTS)]

t_{PDA} = 24.0 ms (See point 3 on the next page.)

t_{dpp} = [BAT(DELAYPT)] in ms

t_{mv} = BYTPS * 100 usec/byte/XY point + 1.1 ms

T_C = data collection period (time/sample) (see Appendix D-1)

NIPP = [BAT(NOINTPT)] = number of integrations/ XY point

BYTPS = NIPP * BPI (bytes/integration) gives bytes/XY point

The bytes/integration are a function of the data format chosen.

Data Format	X
1	1
2	2
3	3
4	2
7	5

Other restraints and important details;

1) One must also satisfy the relationship: $H_{pts} * V_{pts} * NIPP * BPI \leq 1920$

2) For ARS data collections you **MUST use only 1 LPF and 1 FPO**.

3) If [BAT(REQDET)] does not equal [BAT(SKYDET)], insert $2*t_{PDA}$ for t_{PDA} in the above (i.e. $t_{ARS-TOT}$ =) equation.

4) The bus director is started for each XY point and runs long enough to collect BYTPS bytes of data. Think of ARS data collections as a number of SCP data collections strung together in rapid succession.

5) All the data for the area scan is collected before it is sent to the CU/SDF. Remember, only 1 LPF and 1 FPO is used. This also implies that an extra data ready is impossible for ARS.

6) The term $(t_{PDA} + t_{dpp} + t_{mv})$ can be considered as the total delay between points.
(i.e. $t_{del\_tot} = t_{PDA} + t_{dpp} + t_{mv}$)

7) The CU/SDF should be ready for data at time;

$$t_{tfb} = t_{Amin}+t_{Bmin}+t_{FS/LSmin}+(H_{pts} * V_{pts})(t_{PDA} + t_{dpp} +t_{mv}) + (H_{pts} * V_{pts}) (NIPP * T_C) - (H_{pts} * V_{pts}) * 2 \text{ ms}$$

The last term in the above equation is due to the unknown exact times for t_{PDA} and t_{dpp}. and stay enabled for a time: $t_{tlb} = (t_{Amax}+t_{Bmax}+t_{FS/LSmax}+(H_{pts}*V_{pts})(t_{PDA}+t_{dpp}+t_{mv} +(H_{pts}*V_{pts})(NIPP*T_C)$
$+(WPL*16.5 \text{ usec}) - t_{tfb} = (t_{Amax}-t_{Amin})+(t_{Bmax}-t_{Bmin}) + (t_{FS/LSmax}-t_{FS/LSmin})$
$+(H_{pts}*V_{pts})*2 \text{ ms} + (WPL*16.5 \text{ usec})$

8) The time order sequence of events for an ARS collection are;

a) transfer detector controller parameters (term t_{PDA})
b) delay for N ms (term t_{dpp})
c) collect data for current XY point (term NIPP * T_C)
d) move data from temporary buffer to output buffer (and other code) (term t_{mv})
e) GOTO step a (if haven't taken all data)

f) output line of data

Example:

An area scan observation using;

1) data format 7 (all),
2) 10 horizontal points, 10 vertical points,
3) 2 integrations per point,
4) a desired integration time 1,024 T_{bd} (1 ms),
5) a delay between integrations of 256 T_{bd} (.25 ms),
6) a nominal delay between points of 50 ms
7) [BAT(REQDET)] = [BAT(SKYDET)] is required.

Questions:

1) What WPL,LPF,FPO should be used ?
2) What are the programmed integration and delay times ?
3) What is the programmed delay between points ?
4) What is the nominal time for the observation
5) When can you expect the first data ?
6) When can you expect the last data ?

The first item to consider is the programmed integration and delay times. Using Appendix D-1 you obtain the equations for ARS. The data collection period is given by;

$$T_C = INT_{tot} + DEL$$

Where: INT_{tot} = [BAT(INTTIMx)] + IOT, IOT from the table = 159
DEL = [BAT(DELINTx)] + $1T_{bd}$

$$T_C = (865 + 159) + (255 + 1) = 1280\ T_{bd} = 1280 * 976.5625 \text{ ns} = 1.25 \text{ ms}$$

The next item to consider is the WPL. The total number of points is: Total points = $H_{pts} * V_{pts} = 10 * 10 = 100$

The integrations per XY point is 2 and the data format is 7.

BYTPS = NIPP * BPI (bytes/integration) = 2 * 5 = 10 bytes/ XY point

This gives the total number of bytes to be;

Total bytes = Total points * BYTPS = 100 * 10 = 1000 bytes

WPL = 1000 bytes * 1 word/2 bytes = 500 words

The nominal delay between points desired is 50 ms. It is given by the equation;

$$t_{del\_tot} = t_{PDA} + t_{dpp} + t_{mv}$$

we know t_{PDA} = 24.0 ms, and

t_{mv} = (2 * 5 * 100 usec) + 1.1 ms = 2.1 ms

50 ms = 24.0 + 2.1 + x
x = 23.9 ms

Rounding up we get x = 24.0

Note: You may round off in either direction.

The nominal time for an observation is;

$t_{ARS\text{-}TOT}$ = 12.0 ms + 49.6 ms + 2.0 ms + (100 * (24.0 + 24.0 + 2.1) ms + 100 (2* 1.25) ms
= 5.3236 sec

The first data can be expected at: Time to 1st byte = 5.7 ms + 11.2 ms + 1.0 ms + (100 * 50.1) ms + 100 (2 * 1.25) ms = 5.2779 sec.

The CU/SDF should stay enabled for;

CU/SDF enable time = 6.3 ms + 38.4 ms + 1.0 ms + (100 * 2) ms + (500 * 16.5 usec) = 253.95 ms

Answers:

1) 500 WPL, 1 LPF, 1 FPO.
2) [BAT(INTTIMx)] = 865, [BAT(DELINTx] = 255.
3) [BAT(DELAYPT] = 24.
4) The nominal data collection time = 5.3236 sec.
5) 1st byte at 5.2779 sec.
6) CU/SDF enable time is 254 ms.

Appendix D-1 - Timing Parameters

Data collection periods (T_C) as a function of:

1) data collection mode (MODE),
2) data format (DFMT),
3) integration time (INT),
4) delay (DEL)

for bus director (BD) programs assembled by the system controller (SC).

Notes:

1) The delay (DEL) (in multiples of T_{bd}) in the following equations is given by:

A) Data formats 1,2,3,7.
DEL = 0, for [BAT(DELINTx)] = 0
DEL = [BAT(DELINTx)] + $1T_{bd}$, for [BAT(DELINTx)] > 0
x = [BAT(REQDET)]

B) Data format 4.
DEL is always = 0 , (even if you set [BAT(DELINTx)] > 0)

The integration time serves only as a means to inject time between the A/D samples. The actual sample and hold time is a constant and has been chosen to give LSB accuracy for a full swing of the input voltage.

2) The Integration Offset Time (IOT) (in multiples of T_{bd}) in the following equations varies by data format and data collection mode. The smallest T_C for a system controller assembled BD program is given by the IOTs in the table on page A3. Any data collections requiring a smaller T_C than those in the table must use a special BD program.

3) The smallest T_C allowed in a special BD is 11 T_{bd}/byte (10.74 us).

4) The period of the bus director (T_{bd}) is 976.5625 ns.

Data Collection Mode:

1) Single Color Photometry (SCP)

$T_C = INT_{tot} + DEL$
Where: INT_{tot} = [BAT(INTTIMx)] + IOT

2.1) Star/Sky Photometry -- 2 Detector

Note: x is the value for [BAT(REQDET)] for the integration and delay times for both Star and Sky collections.

A) Data formats 1,2,3.

$T_C = INT_{tot} + DEL$, for all data collections after 2.
Where: INT_{tot} = [BAT(INTTIMx)] + IOT

The time for 1st data collection is INT_{tot}. The 2nd collection starts DEL after the end of the first. The 3rd and subsequent collections start INT_{tot} + DEL after the previous ones.

B) Data formats 4,7

$T_C = INT_{tot} + DEL$

Where: INT_{tot} = [BAT(INTTIMx)] + IOT

2.2) Star/Sky Photometry -- 1 Detector

A) For all data formats.

$T_C = INT_{tot\_REQ} + DEL_{REQ} + INT_{tot\_Sky} + DEL_{Sky} + N$

Where:

INT_{tot_REQ} = [BAT(INTTIMx)] + IOT x = [BAT(REQDET)]

INT_{tot_Sky} = [BAT(INTIMS)] + IOT

DEL_{Sky} = 0, for [BAT(DELINTS)] = 0

DEL_{Sky} = [BAT(DELINTS)] + $1T_{bd}$, for [BAT(DELINTS)] > 0

B) N varies by format.

Data Format	N (T_{bd})
1	20075
2	20099
3	20119
4	20300
7	20157

3) Area Scan Photometry (ARS)

$T_C = INT_{tot} + DEL$

Where: INT_{tot} = [BAT(INTTIMx)] + IOT

Integration Offset Times

Data Format	SCP	ARS	Star/Sky (1 det)	Star/Sky (2 det)
1	13	13	1	29
2	25	25	1	53
3	35	35	1	73
4	128	128	0	156
7	159	159	105	217

Note: The cause for the DEL = DEL + 1 for DEL > 0 has to do with the bus director instruction for controlling the counters. For the case of DEL = 0, one counter control instruction is used to stop one counter and to start the other.

For the case of DEL > 0, one counter instruction is used to stop the counter. The programmed DEL (delay) takes place next. Another counter control instruction is used to start the other counter. Since this second control instruction takes 1 T_{bd}, the effective delay is DEL + 1. Hint: The counter starts on the next rising edge of the system clock (i.e. at the start of the decoding for the next instruction).

Appendix D-2 - Choosing WPL, LFP, FPO

These guidelines pertain only to mode 1 (SCP) and 2 (SSP) data collections. For mode 3 (ARS) data collections see the other restraints and important details for ARS on pages 8 & 9.

There are many factors to consider when choosing the number of words per line (WPL), lines per frame (LPF) and frames per observation (FPO). The dominant ones to take into consideration are the programmed integration time and the total data collection time. When all the appropriate functions are considered, the following chart is realized.

Fast tape speed = 1.024 E06 bps
Slow tape speed = 32.0 E03 bps

For the following sample times, use the rules and the chart later in this appendix to obtain the correct WPL.

Data Format	Sample Time	Maximum Tape Tape Speed	Recorder Time/Side
1 (byte)	< 0.2844 ms/byte	fast	10 minutes
2 (word)	< 0.5688 ms/word	fast	10 minutes
3 (lngwd)	< 0.8533 ms/lngwd	fast	10 minutes
4 (alog)	0.5688 ms/word	fast	10 minutes
7 (all)	< 1.4222 ms/5 bytes	fast	10 minutes

For the following sample times, choose any WPL $\geq$ 7, 1 LPF and any FPO to achieve the desired total data collection time. If the desired total data collection time is longer than you can achieve with 960 WPL, 1 LPF and 255 FPO, then you MUST choose the new method of "The HSP Commanding Fix for Long Observations" to obtain the desired data collection time. See a more complete discussion about this new method below.

Data Format	Sample Time	Maximum Tape Tape Speed	Recorder Time/Side
1 (byte)	$\geq$ 0.2844 ms/byte	slow	5.2 Hours
2 (word)	$\geq$ 0.5688 ms/word	slow	5.2 Hours
3 (lngwd)	$\geq$ 0.8533 ms/lngwd	slow	5.2 Hours
4 (alog)	$\geq$ 0.5688 ms/word	slow	5.2 Hours
7 (all)	$\geq$ 1.4222 ms/5 bytes	slow	5.2 Hours

Note: The table above assumes 960 WPL. The ultimate time constraint is the rate to the tape recorder.

The following discussion concerns the choice of WPL for the fast data rate to the tape recorder (i.e. 1.024 E06 bps). There are many choices of WPL for short integration times that do not exceed the maximum rate to the tape recorder (i.e. 1.07 ms/ 64 word segment). However, if a user were to choose a number that only

satisfies this maximum rate to the tape recorder, the HSP may send data at the wrong time to the CU/SDF. This miss timed data will cause an "extra data ready error". A complete definition of the extra data ready error can be found in the SI to SI C&DH ICD (ST ICD-08) section 3.9.3.5 "Science Data Transfer".

The HSP uses input DMA to collect data and output DMA to send data out. If these 2 DMAs finish close to each other, there is a possibility of getting an extra data ready error. In order to guarantee the HSP will not cause an extra data ready, we choose the WPL parameter so an input DMA channel will not finish when the output DMA channel finishes. In other words, the time to output a line should be less than the time to input a line.

There are three other factors to consider. The first factor we need to take into account is the frame start to line start delay. This delay will vary and will effectively add more to the time to output a line. The second factor to consider is the variable delay in the time needed by the HSP to actually start sending out data once it has collected a line of data. This delay will also add more to the time to output a line. The third factor to consider is the maximum delay allowed between lines of data. This maximum delay is 10 milliseconds. We choose the WPL to be the maximum WPL that:

1) Will not cause the input DMA to finish when the output DMA finishes AND

2) still not cause a 10 ms line to line time-out error.

Rules to Assure NO Extra Data Ready

1) Always choose the WPL from the chart for the selected data collection rate (in clock ticks /byte). See Note below and point 4.

2) Increment the LPF (up to a max. of 65,535) using 1 FPO to achieve the selected total data collection time.

3) If 1 FPO does not achieve the desired total data collection time, increment FPO as necessary.

4) When integration times are greater than 291 ticks/byte choose N WPL, (Where N=7-960), 1 LPF and the appropriate number of FPO to achieve the desired total data collection time.

5) When the WPL from the chart is not an integer multiple of the bytes chosen (i.e. due to data format), always choose the next **LOWEST** integer multiple. (e.g. for 330 T/byte, DFMT=7, choose 10 WPL; for 1000 T/byte, DFMT=7, choose 960 WPL, 1 LPF, and relevant FPO).

Note: The numbers for the chart were calculated by using the following equations.

Input time = WPL * Ticks/byte * 2 byte/word * 0.97656 us/tick + 2 ms
Output time = WPL * 15.625 usec/word
Input time - Output time < 10 msec
OR WPL = INTEGER (4096/(i-8)) Where i = ticks/byte , $i \geq 12$
For i = 11 use 960 WPL

The 2 msec in the Input time equation is necessary due to fluctuations in firmware timing to enable the output DMA channel.

Ticks/Byte Vs WPL

Ticks/byte = 11 WPL = 960	Ticks/byte = 64 WPL = 73	Ticks/byte = 117 WPL = 37
Ticks/byte = 12 WPL = 960	Ticks/byte = 65 WPL = 71	Ticks/byte = 118 WPL = 37
Ticks/byte = 13 WPL = 819	Ticks/byte = 66 WPL = 70	Ticks/byte = 119 WPL = 36
Ticks/byte = 14 WPL = 682	Ticks/byte = 67 WPL = 69	Ticks/byte = 120 WPL = 36
Ticks/byte = 15 WPL = 585	Ticks/byte = 68 WPL = 68	Ticks/byte = 121 WPL = 36
Ticks/byte = 16 WPL = 512	Ticks/byte = 69 WPL = 67	Ticks/byte = 122 WPL = 35
Ticks/byte = 17 WPL = 455	Ticks/byte = 70 WPL = 66	Ticks/byte = 123 WPL = 35
Ticks/byte = 18 WPL = 409	Ticks/byte = 71 WPL = 65	Ticks/byte = 124 WPL = 35
Ticks/byte = 19 WPL = 372	Ticks/byte = 72 WPL = 64	Ticks/byte = 125 WPL = 35
Ticks/byte = 20 WPL = 341	Ticks/byte = 73 WPL = 63	Ticks/byte = 126 WPL = 34
Ticks/byte = 21 WPL = 315	Ticks/byte = 74 WPL = 62	Ticks/byte = 127 WPL = 34
Ticks/byte = 22 WPL = 292	Ticks/byte = 75 WPL = 61	Ticks/byte = 128 WPL = 34
Ticks/byte = 23 WPL = 273	Ticks/byte = 76 WPL = 60	Ticks/byte = 129 WPL = 33
Ticks/byte = 24 WPL = 256	Ticks/byte = 77 WPL = 59	Ticks/byte = 130 WPL = 33
Ticks/byte = 25 WPL = 240	Ticks/byte = 78 WPL = 58	Ticks/byte = 131 WPL = 33
Ticks/byte = 26 WPL = 227	Ticks/byte = 79 WPL = 57	Ticks/byte = 132 WPL = 33
Ticks/byte = 27 WPL = 215	Ticks/byte = 80 WPL = 56	Ticks/byte = 133 WPL = 32
Ticks/byte = 28 WPL = 204	Ticks/byte = 81 WPL = 56	Ticks/byte = 134 WPL = 32
Ticks/byte = 29 WPL = 195	Ticks/byte = 82 WPL = 55	Ticks/byte = 135 WPL = 32
Ticks/byte = 30 WPL = 186	Ticks/byte = 83 WPL = 54	Ticks/byte = 136 WPL = 32
Ticks/byte = 31 WPL = 178	Ticks/byte = 84 WPL = 53	
Ticks/byte = 32 WPL = 170	Ticks/byte = 85 WPL = 53	Ticks/byte = 137-140 WPL = 31
Ticks/byte = 33 WPL = 163	Ticks/byte = 86 WPL = 52	Ticks/byte = 141-144 WPL = 30
Ticks/byte = 34 WPL = 157	Ticks/byte = 87 WPL = 51	Ticks/byte = 145-149 WPL = 29
Ticks/byte = 35 WPL = 151	Ticks/byte = 88 WPL = 51	Ticks/byte = 150-154 WPL = 28
Ticks/byte = 36 WPL = 146	Ticks/byte = 89 WPL = 50	Ticks/byte = 155-159 WPL = 27
Ticks/byte = 37 WPL = 141	Ticks/byte = 90 WPL = 49	Ticks/byte = 160-165 WPL = 26
Ticks/byte = 38 WPL = 136	Ticks/byte = 91 WPL = 49	Ticks/byte = 166-171 WPL = 25
Ticks/byte = 39 WPL = 132	Ticks/byte = 92 WPL = 48	Ticks/byte = 172-178 WPL = 24
Ticks/byte = 40 WPL = 128	Ticks/byte = 93 WPL = 48	Ticks/byte = 179-186 WPL = 23
Ticks/byte = 41 WPL = 124	Ticks/byte = 94 WPL = 47	Ticks/byte = 187-194 WPL = 22
Ticks/byte = 42 WPL = 120	Ticks/byte = 95 WPL = 47	Ticks/byte = 195-203 WPL = 21
Ticks/byte = 43 WPL = 117	Ticks/byte = 96 WPL = 46	Ticks/byte = 204-212 WPL = 20
Ticks/byte = 44 WPL = 113	Ticks/byte = 97 WPL = 46	Ticks/byte = 213-223 WPL = 19
Ticks/byte = 45 WPL = 110	Ticks/byte = 98 WPL = 45	Ticks/byte = 224-235 WPL = 18
Ticks/byte = 46 WPL = 107	Ticks/byte = 99 WPL = 45	Ticks/byte = 236-248 WPL = 17
Ticks/byte = 47 WPL = 105	Ticks/byte = 100 WPL = 44	Ticks/byte = 249-264 WPL = 16
Ticks/byte = 48 WPL = 102	Ticks/byte = 101 WPL = 44	Ticks/byte = 265-281 WPL = 15
Ticks/byte = 49 WPL = 99	Ticks/byte = 102 WPL = 43	Ticks/byte = 282-291 WPL = 14
Ticks/byte = 50 WPL = 97	Ticks/byte = 103 WPL = 43	
Ticks/byte = 51 WPL = 95	Ticks/byte = 104 WPL = 42	For ticks/byte > 291 you may use
Ticks/byte = 52 WPL = 93	Ticks/byte = 105 WPL = 42	the slow rate to the tape recorder.
Ticks/byte = 53 WPL = 91	Ticks/byte = 106 WPL = 41	The time/line must not exceed the
Ticks/byte = 54 WPL = 89	Ticks/byte = 107 WPL = 41	rate to the tape recorder. See page
Ticks/byte = 55 WPL = 87	Ticks/byte = 108 WPL = 40	B5.
Ticks/byte = 56 WPL = 85	Ticks/byte = 109 WPL = 40	
Ticks/byte = 57 WPL = 83	Ticks/byte = 110 WPL = 40	
Ticks/byte = 58 WPL = 81	Ticks/byte = 111 WPL = 39	**DO NOT USE 1,2,3,4,5,or 6 WPL.**
Ticks/byte = 59 WPL = 80	Ticks/byte = 112 WPL = 39	
Ticks/byte = 60 WPL = 78	Ticks/byte = 113 WPL = 39	
Ticks/byte = 61 WPL = 77	Ticks/byte = 114 WPL = 38	
Ticks/byte = 62 WPL = 75	Ticks/byte = 115 WPL = 38	
Ticks/byte = 63 WPL = 74	Ticks/byte = 116 WPL = 37	

Data Rates

The data are written on the tape recorder in 64 word (1024 bit) segments. Each segment contains some header information as well as science data. For each line, the first segment contains 50 words of science data and 14 header words. All subsequent segments contain 61 words of science data and 3 header words. Fill data are inserted in the last segment if it contains fewer than 61 words of science data. Every 15th segment is used for overhead (e.g. error correction bits). This overhead segment gives an effective data rate of 14/15 of the true data rate. For the fast tape recorder rate (1.024 M bps) this means it takes

15/14 * 1.0 ms/segment = 1.0714 ms/segment or 933.333 segments/sec

The table on the previous page will always fabricate data with a time much more than 1.0714 ms/segment.

For the slow tape recorder rate (32 K bps) this means it takes 15/14 * 32 ms/segment = 34.2857 ms/segment or 29.1666 segments/sec

This is the fastest one may try to send data to the CU/SDF. Using this knowledge one may always choose the WPL to guarantee a data rate slower than the tape recorder rate. This WPL is given by the following equation.

time/line = (15/14) * 32ms

words/line * 2 bytes/word * time/sample * sample/N bytes > M segments/line * 15/14 * 32ms/segment

OR

words/line > M segments/line * 15/14 * 32ms/segment * word/2bytes * sample/time * N bytes/sample

M = 1 + INT ((WPL-50)/61) + [1 (If MOD (WPL-50,61) > 0)]

The HSP Commanding Fix for Long Observations

If you are not able to attain the desired total data collection time by using 960 WPL, 1 LPF and 255 FPO, you will have to use the HSP commanding fix for long observations . The commanding fix allows for data collections with an infinite number of frames. The only limit is the tape recorder total record time. For a complete discussion about the commanding fix see the article "Reformulation of the HSP commanding fix for long observations", Space Astronomy Lab, University of Wisconsin, 22 October, 1991.

Brief Description

The HSP has an 8 bit software variable which keeps track of the number of frames it has sent to the CU/SDF. When this variable reaches the programmed number of FPO (i.e. VFPOBS command, VFRAOBS telemetry) the HSP stops collecting data and returns to the idle state. The commanding fix allows you to set this software variable to zero during the data collection. The commanding fix sets the software variable to zero the appropriate number of times. After the variable has been set to zero for the last time, the HSP collects and sends 255 more frames of data and returns to the idle state.

Appendix D-3 - Definition of Setup Times

There are several setup times for the three data collection modes. The first two (t_A,t_B) are common to all three modes.

1) t_A is defined as the time it takes from the sending of the serial magnitude command (VMODE), to the point where the assembly of a bus director program will begin.

2) t_B is defined as the time it takes to assemble a bus director program. This time varies with the type of data collection, data format, integration time and delay time.

The other two setup times (t_C,t_D) are common only to SCP and SSP modes.

1) t_C is defined as the time variance possible from the setting of the bit to start the bus director and the actual starting of the bus director. This is due to the firmware.

2) t_D is defined as the time needed to process detector controller parameters for the sky detector.

Timing Notes:

1) The frame start to line start delay ($t_{FL/LS}$) value listed does not exactly conform to ST ICD-08 Figure 3-17. The time given was obtained from C&DH guru Art Rankin. It assumes only one instrument at a time will send data to the CU/SDF. If, in the future, more than one instrument at a time may send data to the CU/SDF, a new value should be used (once it is defined).

2) The time given to output a word of data is from HSP is an average time. A word of science data is actually clocked out at the time given in ST ICD-08.

For large integration times, HSP will have a word of data available immediately after the previous word was sent out. The time to output a word of data can be said to be 15.625 usec.

For small integration times, HSP will not have a word of data available immediately after the previous word was sent out. The time to output a word of data can go as high as 16.50 usec. This extra time is due to input and output DMA interactions.

The value I have chosen takes this extra time into account. It was also chosen so as to guarantee the CU/SDF interface will remain enabled long enough to collect all the data from the HSP.

Appendix E - Filter, Aperture, Proposal, Target, & Date Index

The HSP observations for which there was a steller target are listed below, sorted by filter/aperture.

Filter/Aperture	Proposal/Tape	Date	Target
vclru1_a	2949t01	11-apr-1991	f14vid998
vclru1_a	2949t02	11-apr-1991	f14vid998
vclru1_a	1504t01	22-oct-1990	ngc188-998
vclru1_a	1504t02	22-oct-1990	ngc188-998
vclru1_a	1504t02	23-oct-1990	ngc188-998
vclru1_a	1504t03	23-oct-1990	ngc188-998
vclru1_a	3140t03	13-feb-1991	ngc188-998
vclru1_a	3233t02	19-may-1991	vid998
vclru1_a	3233t03	19-may-1991	vid998
vclru1_a	3006t01	05-jul-1991	vid998
vclru1_a	3362t02	14-jul-1991	vid998
vclru1_t	2949t01	10-apr-1991	f14vid998
vclru1_t	2949t01	11-apr-1991	f14vid998
vclru1_t	2949t02	11-apr-1991	f14vid998
vclru2_a	2948t01	10-apr-1991	f14vid998
vclru2_a	2948t02	10-apr-1991	f14vid998
vclru2_a	1504t06	14-nov-1990	ngc188-998
vclru2_t	2948t01	10-apr-1991	f14vid998
vclru2_t	2948t02	10-apr-1991	f14vid998
vclru2_t	2948t03	10-apr-1991	f14vid998
vclru2_t	3383t02	13-oct-1991	hd49798
vf135u1_c	2769t01	17-jun-1991	agk+81d266
vf135u1_c	2769t06	11-oct-1991	agk+81d266
vf135u1_c	2769t02	17-jun-1991	sa113-260
vf135u1_c	2769t02	17-jun-1991	sa113-339
vf135u1_c	1092t01	31-jan-1992	z-cha
vf135u1_c	1092t02	01-feb-1992	z-cha
vf135u1_c	1092t03	05-feb-1992	z-cha
vf135u1_c	1092t04	09-feb-1992	z-cha
vf135u1_c	1092t06	12-feb-1992	z-cha
vf135u1_c	1092t06	13-feb-1992	z-cha
vf135u1_c	1097t07	17-feb-1992	z-cha
vf135u1_c	1092t08	21-feb-1992	z-cha
vf135u1_c	1092t09	24-feb-1992	z-cha
vf135u1_c	1092t10	25-feb-1992	z-cha
vf135u1_c	1092t11	01-mar-1992	z-cha
vf135u1_c	1092t12	05-mar-1992	z-cha
vf135u1_c	1092t13	08-mar-1992	z-cha
vf135u1_c	1092t14	09-mar-1992	z-cha
vf135u1_c	1092t15	13-mar-1992	z-cha
vf135u1_c	1092t16	17-mar-1992	z-cha
vf135u1_c	1092t17	20-mar-1992	z-cha
vf135u1_c	1092t18	21-mar-1992	z-cha
vf135u1_c	1092t19	25-mar-1992	z-cha
vf135u1_c	1092t20	29-mar-1992	z-cha
vf145u1_a	2769t01	17-jun-1991	agk+81d266
vf145u1_a	2769t07	11-oct-1991	agk+81d266
vf145u1_a	2769t02	17-jun-1991	sa113-260
vf145u1_a	2769t02	17-jun-1991	sa113-339
vf145u2_c	2769t01	17-jun-1991	agk+81d266
vf145u2_c	2769t02	18-jun-1991	sa113-260
vf145u2_c	2769t02	18-jun-1991	sa113-339
vf152u1_a	2769t01	17-jun-1991	agk+81d266
vf152u1_a	2769t06	11-oct-1991	agk+81d266
vf152u1_a	2769t02	17-jun-1991	sa113-260
vf152u1_a	2769t02	17-jun-1991	sa113-339
vf152u2_a	2769t01	17-jun-1991	agk+81d266
vf152u2_a	1095t01	13-sep-1991	hd193237
vf152u2_a	1095t02	19-sep-1991	hd193237
vf152u2_a	1095t03	22-sep-1991	hd193237
vf152u2_a	2769t02	18-jun-1991	sa113-260
vf152u2_a	2769t02	18-jun-1991	sa113-339
vf160u2_a	2769t01	17-jun-1991	agk+81d266
vf160u2_a	2948t01	10-apr-1991	f14vid998
vf160u2_a	2948t02	10-apr-1991	f14vid998
vf160u2_a	2948t03	10-apr-1991	f14vid998
vf160u2_a	1504t06	14-nov-1990	ngc188-998
vf160u2_a	1504t08	14-nov-1990	ngc188-998
vf160u2_a	3140t01	13-feb-1991	ngc188-998
vf160u2_a	2769t02	18-jun-1991	sa113-260
vf160u2_a	2769t02	18-jun-1991	sa113-339
vf160u2_c	3152t01	11-mar-1991	vid998
vf160u2_c	3233t01	18-may-1991	vid998
vf160u2_c	3362t01	08-jul-1991	vid998
vf179u2_a	2769t01	17-jun-1991	agk+81d266
vf179u2_a	2769t02	18-jun-1991	sa113-260
vf179u2_a	2769t02	18-jun-1991	sa113-339
vf184u1_a	2769t01	17-jun-1991	agk+81d266
vf184u1_a	2769t06	11-oct-1991	agk+81d266
vf184u1_a	2769t02	17-jun-1991	sa113-260
vf184u1_a	2769t02	17-jun-1991	sa113-339
vf184u1_c	3152t02	15-mar-1991	vid998
vf184u2_a	2769t01	17-jun-1991	agk+81d266
vf184u2_a	2769t02	18-jun-1991	sa113-260
vf184u2_a	2769t02	18-jun-1991	sa113-339
vf184v_a	2769t04	24-jun-1991	agk+81d266
vf184v_a	3425t01	22-oct-1991	bd+28d4211
vf184v_a	2769t05	24-jun-1991	sa101-207
vf184v_a	2769t05	24-jun-1991	sa101-429
vf184v_a	2769t05	24-jun-1991	sa113-260
vf184v_a	3425t01	23-oct-1991	sa95-132
vf184v_a	3425t02	19-dec-1991	sa95-301
vf184v_a	3425t02	19-dec-1991	sa95-302
vf184v_a	3378t01	11-nov-1991	sao27635
vf216p0	1386t01	24-sep-1991	hd11408
vf216p0	1386t02	26-sep-1991	hd11408
vf216p0	3985t01	15-mar-1992	hd115271
vf216p0	3377t04	31-aug-1991	sao6392
vf216p0	3377t06	30-nov-1991	sao6392
vf216p135	1386t01	24-sep-1991	hd11408
vf216p135	1386t02	26-sep-1991	hd11408
vf216p135	3985t01	15-mar-1992	hd115271
vf216p135	3377t04	31-aug-1991	sao6392
vf216p135	3377t06	30-nov-1991	sao6392
vf216p45	1386t01	24-sep-1991	hd11408
vf216p45	1386t02	26-sep-1991	hd11408
vf216p45	3985t01	15-mar-1992	hd115271
vf216p45	3377t04	31-aug-1991	sao6392
vf216p45	3377t06	30-nov-1991	sao6392
vf216p90	1386t01	24-sep-1991	hd11408
vf216p90	1386t02	26-sep-1991	hd11408
vf216p90	3985t01	15-mar-1992	hd115271
vf216p90	3377t04	31-aug-1991	sao6392
vf216p90	3377t06	30-nov-1991	sao6392
vf218u1_a	2769t01	17-jun-1991	agk+81d266
vf218u1_a	2769t07	11-oct-1991	agk+81d266
vf218u1_a	2769t02	17-jun-1991	sa113-260
vf218u1_a	2769t02	17-jun-1991	sa113-339
vf220u1_a	2769t01	17-jun-1991	agk+81d266
vf220u1_a	2769t07	11-oct-1991	agk+81d266
vf220u1_a	2769t02	17-jun-1991	sa113-260
vf220u1_a	2769t02	17-jun-1991	sa113-339
vf237p0	1386t01	24-sep-1991	hd11408
vf237p0	1386t02	26-sep-1991	hd11408
vf237p0	3985t01	15-mar-1992	hd115271
vf237p0	3377t03	30-aug-1991	sao6392
vf237p0	3377t06	30-nov-1991	sao6392
vf237p135	2912t01	03-mar-1992	bd+75d325
vf237p135	1386t01	24-sep-1991	hd11408
vf237p135	1386t02	26-sep-1991	hd11408
vf237p135	3985t01	15-mar-1992	hd115271
vf237p135	3377t04	31-aug-1991	sao6392
vf237p135	3377t06	30-nov-1991	sao6392
vf237p135	3152t04	21-apr-1991	vid998
vf237p135	3233t04	03-jun-1991	vid998
vf237p135	3362t04	15-sep-1991	vid998
vf237p45	2912t01	03-mar-1992	bd+75d325
vf237p45	1386t01	24-sep-1991	hd11408
vf237p45	1386t02	26-sep-1991	hd11408
vf237p45	3985t01	15-mar-1992	hd115271
vf237p45	3377t03	31-aug-1991	sao6392
vf237p45	3377t04	31-aug-1991	sao6392

vf237p45	3377t06	30-nov-1991	sao6392
vf237p90	2912t01	03-mar-1992	bd+75d325
vf237p90	1386t01	24-sep-1991	hd11408
vf237p90	1386t02	26-sep-1991	hd11408
vf237p90	3985t01	15-mar-1992	hd115271
vf237p90	3377t03	30-aug-1991	sao6392
vf237p90	3377t06	30-nov-1991	sao6392
vf240u1_a	2949t01	11-apr-1991	f14vid998
vf240u1_a	2949t02	11-apr-1991	f14vid998
vf240u1_a	1389t02	22-aug-1991	hd60435
vf240u1_a	1504t02	23-oct-1990	ngc188-998
vf240u1_a	3006t01	05-jul-1991	vid998
vf240u1_c	3152t02	15-mar-1991	vid998
vf240u1_c	3233t02	19-may-1991	vid998
vf240u1_c	3233t03	19-may-1991	vid998
vf240u1_c	3362t02	14-jul-1991	vid998
vf240v_a	3378t01	11-nov-1991	sao27635
vf240v_c	2769t04	24-jun-1991	agk+81d266
vf240v_c	3425t01	22-oct-1991	bd+28d4211
vf240v_c	2769t05	24-jun-1991	sa101-207
vf240v_c	2769t05	24-jun-1991	sa101-429
vf240v_c	2769t05	24-jun-1991	sa113-260
vf240v_c	3425t01	23-oct-1991	sa95-132
vf240v_c	3425t02	19-dec-1991	sa95-301
vf240v_c	3425t02	19-dec-1991	sa95-302
vf240v_c	3378t01	11-nov-1991	sao27635
vf240v_e	3152t05	21-apr-1991	vid998
vf240v_e	3233t05	08-jun-1991	vid998
vf240v_e	3362t03	20-jul-1991	vid998
vf248u1_a	2769t03	17-jun-1991	agk+81d266
vf248u1_a	2769t07	11-oct-1991	agk+81d266
vf248u1_a	2769t03	17-jun-1991	sa113-260
vf248u1_a	2769t03	17-jun-1991	sa113-339
vf248u1_c	2769t01	17-jun-1991	agk+81d266
vf248u1_c	2769t06	11-oct-1991	agk+81d266
vf248u1_c	2769t02	17-jun-1991	sa113-260
vf248u1_c	2769t02	17-jun-1991	sa113-339
vf248u1_e	2949t02	11-apr-1991	f14vid998
vf248u1_e	1504t03	23-oct-1990	ngc188-998
vf248u1_e	3152t02	15-mar-1991	vid998
vf248u1_e	3233t02	19-may-1991	vid998
vf248u1_e	3233t03	19-may-1991	vid998
vf248u1_e	3362t02	14-jul-1991	vid998
vf248u2_a	2769t01	17-jun-1991	agk+81d266
vf248u2_a	2769t02	18-jun-1991	sa113-260
vf248u2_a	2769t02	18-jun-1991	sa113-339
vf248u2_c	2948t02	10-apr-1991	f14vid998
vf248u2_c	2948t03	10-apr-1991	f14vid998
vf248u2_c	1504t08	14-nov-1990	ngc188-998
vf248u2_c	3152t01	11-mar-1991	vid998
vf248u2_c	3233t01	18-may-1991	vid998
vf248u2_c	3362t01	08-jul-1991	vid998
vf262u2_a	2769t03	17-jun-1991	agk+81d266
vf262u2_a	2769t03	18-jun-1991	sa113-260
vf262u2_a	2769t03	18-jun-1991	sa113-339
vf262v_a	2769t04	24-jun-1991	agk+81d266
vf262v_a	3425t01	23-oct-1991	bd+28d4211
vf262v_a	2769t05	24-jun-1991	sa101-207
vf262v_a	2769t05	24-jun-1991	sa101-429
vf262v_a	2769t05	24-jun-1991	sa113-260
vf262v_a	3425t01	23-oct-1991	sa95-132
vf262v_a	3425t02	19-dec-1991	sa95-301
vf262v_a	3425t02	19-dec-1991	sa95-302
vf262v_a	3378t01	11-nov-1991	sao27635
vf277p0	2912t01	03-mar-1992	bd+75d325
vf277p0	1386t01	24-sep-1991	hd11408
vf277p0	1386t02	25-sep-1991	hd11408
vf277p0	1386t02	26-sep-1991	hd11408
vf277p0	3985t01	14-mar-1992	hd115271
vf277p0	3377t03	30-aug-1991	sao6392
vf277p0	3377t06	29-nov-1991	sao6392
vf277p135	2912t01	03-mar-1992	bd+75d325
vf277p135	1386t01	24-sep-1991	hd11408
vf277p135	1386t02	26-sep-1991	hd11408
vf277p135	3985t01	15-mar-1992	hd115271
vf277p135	3377t03	30-aug-1991	sao6392
vf277p135	3377t06	29-nov-1991	sao6392
vf277p135	3377t06	30-nov-1991	sao6392
vf277p45	2912t01	03-mar-1992	bd+75d325
vf277p45	1386t01	24-sep-1991	hd11408
vf277p45	1386t02	26-sep-1991	hd11408
vf277p45	3985t01	14-mar-1992	hd115271
vf277p45	3377t03	30-aug-1991	sao6392
vf277p45	3377t06	29-nov-1991	sao6392
vf277p90	2912t01	03-mar-1992	bd+75d325
vf277p90	1386t01	24-sep-1991	hd11408
vf277p90	1386t02	26-sep-1991	hd11408
vf277p90	3985t01	14-mar-1992	hd115271
vf277p90	3377t03	30-aug-1991	sao6392
vf277p90	3377t06	29-nov-1991	sao6392
vf278u1_a	2769t01	17-jun-1991	agk+81d266
vf278u1_a	2769t06	11-oct-1991	agk+81d266
vf278u1_a	2769t02	17-jun-1991	sa113-260
vf278u1_a	2769t02	17-jun-1991	sa113-339
vf278u2_a	2769t01	17-jun-1991	agk+81d266
vf278u2_a	2769t02	18-jun-1991	sa113-260
vf278u2_a	2769t02	18-jun-1991	sa113-339
vf284u2_a	2769t01	17-jun-1991	agk+81d266
vf284u2_a	2769t02	18-jun-1991	sa113-260
vf284u2_a	2769t02	18-jun-1991	sa113-339
vf284u2_c	3152t01	11-mar-1991	vid998
vf284u2_c	3233t01	18-may-1991	vid998
vf284u2_c	3362t01	08-jul-1991	vid998
vf327p0	2912t01	03-mar-1992	bd+75d325
vf327p0	1386t01	24-sep-1991	hd11408
vf327p0	1386t02	25-sep-1991	hd11408
vf327p0	1386t02	26-sep-1991	hd11408
vf327p0	3985t01	14-mar-1992	hd115271
vf327p0	3377t03	30-aug-1991	sao6392
vf327p0	3377t06	29-nov-1991	sao6392
vf327p0	3152t04	21-apr-1991	vid998
vf327p0	3233t04	03-jun-1991	vid998
vf327p0	3006t01	05-jul-1991	vid998
vf327p0	3362t04	15-sep-1991	vid998
vf327p135	2912t01	04-mar-1992	bd+75d325
vf327p135	1386t01	24-sep-1991	hd11408
vf327p135	1386t02	25-sep-1991	hd11408
vf327p135	1386t02	26-sep-1991	hd11408
vf327p135	3985t01	14-mar-1992	hd115271
vf327p135	3377t03	30-aug-1991	sao6392
vf327p135	3377t06	29-nov-1991	sao6392
vf327p45	2912t01	03-mar-1992	bd+75d325
vf327p45	1386t01	24-sep-1991	hd11408
vf327p45	1386t02	25-sep-1991	hd11408
vf327p45	1386t02	26-sep-1991	hd11408
vf327p45	3985t01	14-mar-1992	hd115271
vf327p45	3377t03	30-aug-1991	sao6392
vf327p45	3377t06	29-nov-1991	sao6392
vf327p45	3152t04	21-apr-1991	vid998
vf327p45	3233t04	03-jun-1991	vid998
vf327p45	3362t04	15-sep-1991	vid998
vf327p90	2912t01	04-mar-1992	bd+75d325
vf327p90	1386t01	24-sep-1991	hd11408
vf327p90	1386t02	25-sep-1991	hd11408
vf327p90	1386t02	26-sep-1991	hd11408
vf327p90	3985t01	14-mar-1992	hd115271
vf327p90	3377t03	30-aug-1991	sao6392
vf327p90	3377t06	29-nov-1991	sao6392
vf355v_a	2769t04	24-jun-1991	agk+81d266
vf355v_a	3425t01	22-oct-1991	bd+28d4211
vf355v_a	2769t05	24-jun-1991	sa101-207
vf355v_a	2769t05	24-jun-1991	sa101-429
vf355v_a	2769t05	24-jun-1991	sa113-260
vf355v_a	3425t01	23-oct-1991	sa95-132
vf355v_a	3425t02	19-dec-1991	sa95-301
vf355v_a	3425t02	19-dec-1991	sa95-302
vf355v_a	3378t01	11-nov-1991	sao27635
vf400v_a	2769t04	24-jun-1991	agk+81d266
vf400v_a	3425t01	23-oct-1991	bd+28d4211
vf400v_a	2769t05	24-jun-1991	sa101-207
vf400v_a	2769t05	24-jun-1991	sa101-429
vf400v_a	2769t05	24-jun-1991	sa113-260
vf400v_a	3425t01	23-oct-1991	sa95-132
vf400v_a	3425t02	19-dec-1991	sa95-301
vf400v_a	3425t02	19-dec-1991	sa95-302
vf400v_a	3378t01	11-nov-1991	sao27635
vf419v_a	2769t04	24-jun-1991	agk+81d266
vf419v_a	3425t01	22-oct-1991	bd+28d4211
vf419v_a	2769t05	24-jun-1991	sa101-207
vf419v_a	2769t05	24-jun-1991	sa101-429
vf419v_a	2769t05	24-jun-1991	sa113-260
vf419v_a	3425t01	23-oct-1991	sa95-132

vf419v_a	3425t02	19-dec-1991	sa95-301
vf419v_a	3425t02	19-dec-1991	sa95-302
vf419v_a	3378t01	11-nov-1991	sao27635
vf419v_c	3152t05	21-apr-1991	vid998
vf419v_c	3233t05	08-jun-1991	vid998
vf419v_c	3362t03	20-jul-1991	vid998
vf450v_a	2769t04	24-jun-1991	agk+81d266
vf450v_a	3425t01	22-oct-1991	bd+28d4211
vf450v_a	2769t05	24-jun-1991	sa101-207
vf450v_a	2769t05	24-jun-1991	sa101-429
vf450v_a	2769t05	24-jun-1991	sa113-260
vf450v_a	3425t01	23-oct-1991	sa95-132
vf450v_a	3425t02	19-dec-1991	sa95-301
vf450v_a	3425t02	19-dec-1991	sa95-302
vf450v_a	3378t01	11-nov-1991	sao27635
vf551v_a	2769t04	24-jun-1991	agk+81d266
vf551v_a	3425t01	23-oct-1991	bd+28d4211
vf551v_a	2769t05	24-jun-1991	sa101-207
vf551v_a	2769t05	25-jun-1991	sa101-429
vf551v_a	2769t05	24-jun-1991	sa113-260
vf551v_a	3425t01	23-oct-1991	sa95-132
vf551v_a	3425t02	19-dec-1991	sa95-301
vf551v_a	3425t02	19-dec-1991	sa95-302
vf551v_c	2769t04	24-jun-1991	agk+81d266
vf551v_c	3425t01	22-oct-1991	bd+28d4211
vf551v_c	1385t01	05-jun-1991	e7-u
vf551v_c	3382t02	27-sep-1991	giclas153-41
vf551v_c	1474t03	24-aug-1991	hd102232
vf551v_c	1474t01	19-aug-1991	hd102703
vf551v_c	1385t02	05-jun-1991	hd105498
vf551v_c	1385t01	05-jun-1991	hd156623
vf551v_c	1385t01	05-jun-1991	hd157243
vf551v_c	2769t04	24-jun-1991	sa101-207
vf551v_c	1385t02	05-jun-1991	sa101-330
vf551v_c	2769t05	24-jun-1991	sa101-429
vf551v_c	1385t03	06-jun-1991	sa107-351
vf551v_c	1385t02	05-jun-1991	sa107-452
vf551v_c	1385t02	05-jun-1991	sa107-990
vf551v_c	1474t02	21-aug-1991	sa113-241
vf551v_c	2769t05	24-jun-1991	sa113-260
vf551v_c	3425t01	23-oct-1991	sa95-132
vf551v_c	3425t02	19-dec-1991	sa95-301
vf551v_c	3425t02	19-dec-1991	sa95-302
vf551v_c	3382t01	23-sep-1991	sa95-42
vf551v_c	1474t01	20-aug-1991	sa95-52
vf551v_c	1474t01	20-aug-1991	sa95-68
vf551v_c	3378t01	11-nov-1991	sao27635
vf551v_e	3378t01	11-nov-1991	sao27635
vf620v_a	2769t04	24-jun-1991	agk+81d266
vf620v_a	3425t01	22-oct-1991	bd+28d4211
vf620v_a	2769t04	24-jun-1991	sa101-207
vf620v_a	2769t05	24-jun-1991	sa101-429
vf620v_a	2769t05	24-jun-1991	sa113-260
vf620v_a	3425t01	23-oct-1991	sa95-132
vf620v_a	3425t02	19-dec-1991	sa95-301
vf620v_a	3425t02	19-dec-1991	sa95-302
vf620v_a	3378t01	11-nov-1991	sao27635
vf620v_c	3152t05	21-apr-1991	vid998
vf620v_c	3233t05	08-jun-1991	vid998
vf620v_c	3362t03	20-jul-1991	vid998
vf750_f320	2769t04	24-jun-1991	agk+81d266
vf750_f320	3425t01	23-oct-1991	bd+28d4211
vf750_f320	1081t02	02-oct-1991	gsc6323-0139
vf750_f320	1081t02	03-oct-1991	gsc6323-0139
vf750_f320	2771t01	05-sep-1991	gsc6323-0146
vf750_f320	2771t02	05-sep-1991	gsc6323-0146
vf750_f320	2771t01	06-sep-1991	gsc6323-0146
vf750_f320	2771t02	06-sep-1991	gsc6323-0146
vf750_f320	2769t05	24-jun-1991	sa101-207
vf750_f320	2769t05	24-jun-1991	sa101-429
vf750_f320	2769t05	24-jun-1991	sa113-260
vf750_f320	3425t01	23-oct-1991	sa95-132
vf750_f320	3425t02	19-dec-1991	sa95-301
vf750_f320	3425t02	19-dec-1991	sa95-302
vf750_f320	3378t02	11-nov-1991	sao27635

Appendix F - HSP and STR Operating Cycles & Times, by SMS and Total

Note: For SMSs with no HSP activity, HSP items have been deleted

SMS	Item	#on	#off	on time	min/cycle
901051c3	STR	0	0	0.0	0.0
901067b6	STR	7	7	25.5	3.6
901067b6	Det1	1	1	2.0	2.0
901067b6	Det2	1	1	2.0	2.0
901067b6	Det3	1	1	2.0	2.0
901067b6	Det4	1	1	2.0	2.0
901067b6	Det5	1	1	1.9	1.9
901067b6	HV1	0	0	0.0	0.0
901067b6	HV2	0	0	0.0	0.0
901067b6	HV3	0	0	0.0	0.0
901067b6	HV4	0	0	0.0	0.0
901067b6	HV5	0	0	0.0	0.0
901137a6	STR	5	5	35.8	7.2
901137a6	Det1	1	1	9.8	9.8
901137a6	Det2	1	1	9.8	9.8
901137a6	Det3	1	1	9.8	9.8
901137a6	Det4	1	1	9.8	9.8
901137a6	Det5	1	1	10.2	10.2
901137a6	HV1	0	0	0.0	0.0
901137a6	HV2	0	0	0.0	0.0
901137a6	HV3	0	0	0.0	0.0
901137a6	HV4	0	0	0.0	0.0
901137a6	HV5	0	0	0.0	0.0
901172f3	STR	0	0	0.0	0.0
901182f2	STR	1	1	4.5	4.5
SMS 901191b2 not found					
901207d5	STR	6	6	21.0	3.5
901207d5	Det1	1	1	2.0	2.0
901207d5	Det2	1	1	2.0	2.0
901207d5	Det3	1	1	2.0	2.0
901207d5	Det4	1	1	2.0	2.0
901207d5	Det5	1	1	1.9	1.9
901207d5	HV1	0	0	0.0	0.0
901207d5	HV2	0	0	0.0	0.0
901207d5	HV3	0	0	0.0	0.0
901207d5	HV4	0	0	0.0	0.0
901207d5	HV5	0	0	0.0	0.0
901225a7	STR	55	55	116.9	2.1
901225a7	Det1	3	3	38.0	12.7
901225a7	Det2	2	2	25.3	12.6
901225a7	Det3	2	2	25.3	12.6
901225a7	Det4	2	2	25.3	12.6
901225a7	Det5	2	2	25.3	12.6
901225a7	HV1	3	3	1.9	0.3
901225a7	HV2	2	2	1.3	0.3
901225a7	HV3	2	2	1.3	0.3
901225a7	HV4	2	2	1.3	0.3
901225a7	HV5	2	2	1.3	0.3
901252k1	STR	0	0	0.0	0.0
901252k1	Det1	1	1	2.0	2.0
901252k1	Det2	1	1	2.0	2.0
901252k1	Det3	1	1	2.0	2.0
901252k1	Det4	1	1	2.0	2.0
901252k1	Det5	1	1	1.9	1.9
901252k1	HV1	0	0	0.0	0.0
901252k1	HV2	0	0	0.0	0.0
901252k1	HV3	0	0	0.0	0.0
901252k1	HV4	0	0	0.0	0.0
901252k1	HV5	0	0	0.0	0.0
901277d5	STR	5	5	35.8	7.2
901277d5	Det1	1	1	9.8	9.8
901277d5	Det2	1	1	9.8	9.8
901277d5	Det3	1	1	9.8	9.8

901277d5	Det4	1	1	9.8	9.8
901277d5	Det5	1	1	10.2	10.2
901277d5	HV1	0	0	0.0	0.0
901277d5	HV2	0	0	0.0	0.0
901277d5	HV3	0	0	0.0	0.0
901277d5	HV4	0	0	0.0	0.0
901277d5	HV5	0	0	0.0	0.0
901283m3	STR	8	8	75.8	9.5
901312m4	STR	0	0	0.0	0.0
901323m6	STR	10	10	135.9	13.6
901347a6	STR	77	77	219.9	2.9
901352m2	STR	1	1	4.3	4.3
901352m2	Det1	1	1	12.7	12.7
901352m2	Det2	0	0	0.0	0.0
901352m2	Det3	0	0	0.0	0.0
901352m2	Det4	0	0	0.0	0.0
901352m2	Det5	0	0	0.0	0.0
901352m2	HV1	1	1	0.6	0.3
901352m2	HV2	0	0	0.0	0.0
901352m2	HV3	0	0	0.0	0.0
901352m2	HV4	0	0	0.0	0.0
901352m2	HV5	0	0	0.0	0.0
901363m1	STR	42	42	152.6	3.6
901382m3	STR	0	0	0.0	0.0
901392m3	STR	0	0	0.0	0.0
901402m8	STR	7	7	15.8	2.3
901417ac	STR	231	231	921.2	4.0
901417ac	Det1	2	2	218.4	109.2
901417ac	Det2	2	2	133.9	66.9
901417ac	Det3	5	5	2054.2	410.8
901417ac	Det4	2	2	122.9	61.4
901417ac	Det5	0	0	0.0	0.0
901417ac	HV1	2	2	212.4	53.1
901417ac	HV2	2	2	127.8	31.9
901417ac	HV3	5	5	2039.0	203.9
901417ac	HV4	2	2	116.8	29.2
901417ac	HV5	0	0	0.0	0.0
901432m5	STR	0	0	0.0	0.0
901452m8	STR	8	8	32.5	4.1
901452m8	Det1	1	1	12.7	12.7
901452m8	Det2	1	1	12.6	12.6
901452m8	Det3	1	1	12.7	12.7
901452m8	Det4	1	1	12.6	12.6
901452m8	Det5	1	1	12.6	12.6
901452m8	HV1	1	1	0.6	0.3
901452m8	HV2	1	1	0.6	0.3
901452m8	HV3	1	1	0.6	0.3
901452m8	HV4	1	1	0.6	0.3
901452m8	HV5	1	1	0.6	0.3
901463m4	STR	7	7	8.8	1.3
901492n2	STR	0	0	0.0	0.0
901503n2	STR	4	4	5.0	1.3
901522n4	STR	2	2	45.1	22.6
901562p4	STR	43	43	214.2	5.0
901562p4	Det1	0	0	0.0	0.0
901562p4	Det2	1	1	68.8	68.8
901562p4	Det3	1	1	81.6	81.6
901562p4	Det4	0	0	0.0	0.0
901562p4	Det5	0	0	0.0	0.0
901562p4	HV1	0	0	0.0	0.0
901562p4	HV2	1	1	58.4	29.2
901562p4	HV3	1	1	57.2	28.6
901562p4	HV4	0	0	0.0	0.0
901562p4	HV5	0	0	0.0	0.0

901584a8	STR	4	4	5.0	1.2
901613a3	STR	8	8	49.2	6.1
901613a3	Det1	1	1	66.3	66.3
901613a3	Det2	0	0	0.0	0.0
901613a3	Det3	0	0	0.0	0.0
901613a3	Det4	1	1	63.3	63.3
901613a3	Det5	0	0	0.0	0.0
901613a3	HV1	1	1	55.9	28.0
901613a3	HV2	0	0	0.0	0.0
901613a3	HV3	0	0	0.0	0.0
901613a3	HV4	1	1	52.9	26.4
901613a3	HV5	0	0	0.0	0.0
901627b2	STR	329	329	1438.6	4.4
901627b2	Det1	1	1	250.2	250.2
901627b2	Det2	1	1	250.2	250.2
901627b2	Det3	2	2	525.3	262.7
901627b2	Det4	1	1	248.4	248.4
901627b2	Det5	1	1	308.5	308.5
901627b2	HV1	1	1	240.4	120.2
901627b2	HV2	1	1	245.4	122.7
901627b2	HV3	2	2	516.3	129.1
901627b2	HV4	1	1	237.3	118.7
901627b2	HV5	1	1	304.8	152.4
901634aa	STR	14	14	17.5	1.3
901662b3	STR	23	23	270.3	11.8
901673b2	STR	33	33	207.9	6.3
901694a4	STR	12	12	15.0	1.3
901713b2	STR	12	12	15.0	1.2
901733b3	STR	12	12	15.0	1.2
901753b2	STR	12	12	15.0	1.3
901773b3	STR	24	24	137.1	5.7
901773b3	Det1	0	0	0.0	0.0
901773b3	Det2	0	0	0.0	0.0
901773b3	Det3	0	0	0.0	0.0
901773b3	Det4	0	0	0.0	0.0
901773b3	Det5	1	1	12.7	12.7
901773b3	HV1	0	0	0.0	0.0
901773b3	HV2	0	0	0.0	0.0
901773b3	HV3	0	0	0.0	0.0
901773b3	HV4	0	0	0.0	0.0
901773b3	HV5	1	1	0.2	0.1
901823a4	STR	19	19	145.6	7.7
901823a4	Det1	0	0	0.0	0.0
901823a4	Det2	0	0	0.0	0.0
901823a4	Det3	0	0	0.0	0.0
901823a4	Det4	0	0	0.0	0.0
901823a4	Det5	1	1	12.7	12.7
901823a4	HV1	0	0	0.0	0.0
901823a4	HV2	0	0	0.0	0.0
901823a4	HV3	0	0	0.0	0.0
901823a4	HV4	0	0	0.0	0.0
901823a4	HV5	1	1	0.3	0.1
901844a9	STR	47	47	300.5	6.4
901844a9	Det1	0	0	0.0	0.0
901844a9	Det2	0	0	0.0	0.0
901844a9	Det3	0	0	0.0	0.0
901844a9	Det4	0	0	0.0	0.0
901844a9	Det5	1	1	12.7	12.7
901844a9	HV1	0	0	0.0	0.0
901844a9	HV2	0	0	0.0	0.0
901844a9	HV3	0	0	0.0	0.0
901844a9	HV4	0	0	0.0	0.0
901844a9	HV5	1	1	0.2	0.1
901882a3	STR	0	0	0.0	0.0
901893c1	STR	28	28	53.8	1.9

901915a4	STR	42	42	80.7	1.9
901953a6	STR	17	17	37.8	2.2
901974a3	STR	260	260	1117.6	4.3
901974a3	Det1	3	3	561.1	187.0
901974a3	Det2	3	3	766.5	255.5
901974a3	Det3	4	4	1372.5	343.1
901974a3	Det4	3	3	668.5	222.8
901974a3	Det5	0	0	0.0	0.0
901974a3	HV1	4	4	291.8	36.5
901974a3	HV2	4	4	490.2	61.3
901974a3	HV3	4	4	1360.3	170.0
901974a3	HV4	4	4	405.0	50.6
901974a3	HV5	0	0	0.0	0.0
902005c8	STR	127	127	581.2	4.6
902045a9	STR	140	140	754.2	5.4
902085ab	STR	94	94	488.6	5.2
902125e4	STR	137	137	442.7	3.2
902165b5	STR	77	77	510.2	6.6
902165b5	Det1	0	0	0.0	0.0
902165b5	Det2	0	0	0.0	0.0
902165b5	Det3	0	0	0.0	0.0
902165b5	Det4	0	0	0.0	0.0
902165b5	Det5	1	1	13.0	13.0
902165b5	HV1	0	0	0.0	0.0
902165b5	HV2	0	0	0.0	0.0
902165b5	HV3	0	0	0.0	0.0
902165b5	HV4	0	0	0.0	0.0
902165b5	HV5	1	1	0.6	0.3
902205a7	STR	95	95	502.1	5.3
902245c1	STR	78	78	165.2	2.1

SMS 902287a1 not found

902314a4	STR	150	150	453.4	3.0
902314a4	Det1	0	0	0.0	0.0
902314a4	Det2	0	0	0.0	0.0
902314a4	Det3	0	0	0.0	0.0
902314a4	Det4	0	0	0.0	0.0
902314a4	Det5	1	1	84.8	84.8
902314a4	HV1	0	0	0.0	0.0
902314a4	HV2	0	0	0.0	0.0
902314a4	HV3	0	0	0.0	0.0
902314a4	HV4	0	0	0.0	0.0
902314a4	HV5	1	1	73.7	36.9

SMS 902333a1 not found

902344a7	STR	78	78	166.2	2.1
902384a6	STR	131	131	265.9	2.0
902384a6	Det1	0	0	0.0	0.0
902384a6	Det2	2	2	518.1	259.0
902384a6	Det3	0	0	0.0	0.0
902384a6	Det4	0	0	0.0	0.0
902384a6	Det5	0	0	0.0	0.0
902384a6	HV1	0	0	0.0	0.0
902384a6	HV2	2	2	512.0	128.0
902384a6	HV3	0	0	0.0	0.0
902384a6	HV4	0	0	0.0	0.0
902384a6	HV5	0	0	0.0	0.0
902494a6	STR	116	116	253.7	2.2
902494a6	Det1	0	0	0.0	0.0
902494a6	Det2	0	0	0.0	0.0
902494a6	Det3	0	0	0.0	0.0
902494a6	Det4	3	3	461.3	153.8
902494a6	Det5	0	0	0.0	0.0
902494a6	HV1	0	0	0.0	0.0
902494a6	HV2	0	0	0.0	0.0
902494a6	HV3	0	0	0.0	0.0
902494a6	HV4	3	3	452.1	75.3
902494a6	HV5	0	0	0.0	0.0

902537ab	STR	117	117	650.4	5.6
902537ab	Det1	0	0	0.0	0.0
902537ab	Det2	1	1	85.3	85.3
902537ab	Det3	0	0	0.0	0.0
902537ab	Det4	0	0	0.0	0.0
902537ab	Det5	0	0	0.0	0.0
902537ab	HV1	0	0	0.0	0.0
902537ab	HV2	1	1	82.2	41.1
902537ab	HV3	0	0	0.0	0.0
902537ab	HV4	0	0	0.0	0.0
902537ab	HV5	0	0	0.0	0.0
902607d2	STR	253	253	1158.0	4.6
902607d2	Det1	0	0	0.0	0.0
902607d2	Det2	0	0	0.0	0.0
902607d2	Det3	0	0	0.0	0.0
902607d2	Det4	1	1	79.8	79.8
902607d2	Det5	0	0	0.0	0.0
902607d2	HV1	0	0	0.0	0.0
902607d2	HV2	0	0	0.0	0.0
902607d2	HV3	0	0	0.0	0.0
902607d2	HV4	1	1	76.7	38.4
902607d2	HV5	0	0	0.0	0.0
SMS 902677ab not found					
902747bf	STR	242	242	862.6	3.6
902817b8	STR	308	308	1111.9	3.6
902817b8	Det1	0	0	0.0	0.0
902817b8	Det2	1	1	353.7	353.7
902817b8	Det3	0	0	0.0	0.0
902817b8	Det4	1	1	351.8	351.8
902817b8	Det5	0	0	0.0	0.0
902817b8	HV1	0	0	0.0	0.0
902817b8	HV2	1	1	348.8	174.4
902817b8	HV3	0	0	0.0	0.0
902817b8	HV4	1	1	340.8	170.4
902817b8	HV5	0	0	0.0	0.0
902885a3	STR	29	29	688.8	23.8
902932aa	STR	94	94	290.9	3.1
902957a9	STR	282	282	1040.4	3.7
902957a9	Det1	0	0	0.0	0.0
902957a9	Det2	1	1	1199.7	1199.7
902957a9	Det3	0	0	0.0	0.0
902957a9	Det4	0	0	0.0	0.0
902957a9	Det5	0	0	0.0	0.0
902957a9	HV1	0	0	0.0	0.0
902957a9	HV2	1	1	1196.7	598.3
902957a9	HV3	0	0	0.0	0.0
902957a9	HV4	0	0	0.0	0.0
902957a9	HV5	0	0	0.0	0.0
903027ac	STR	328	328	1106.9	3.4
903027ac	Det1	0	0	0.0	0.0
903027ac	Det2	2	2	1074.9	537.4
903027ac	Det3	0	0	0.0	0.0
903027ac	Det4	2	2	276.2	138.1
903027ac	Det5	0	0	0.0	0.0
903027ac	HV1	0	0	0.0	0.0
903027ac	HV2	3	3	824.4	137.4
903027ac	HV3	0	0	0.0	0.0
903027ac	HV4	2	2	270.1	67.5
903027ac	HV5	0	0	0.0	0.0
903097e1	STR	305	305	1214.9	4.0
903097e1	Det1	1	1	259.9	259.9
903097e1	Det2	3	3	1427.0	475.7
903097e1	Det3	1	1	262.5	262.5
903097e1	Det4	5	5	1628.7	325.7
903097e1	Det5	1	1	265.2	265.2
903097e1	HV1	1	1	257.0	128.5
903097e1	HV2	3	3	1417.9	236.3
903097e1	HV3	1	1	257.0	128.5
903097e1	HV4	6	6	1357.2	113.1
903097e1	HV5	1	1	257.0	128.5
903104a2	STR	132	132	690.3	5.2

903104a2	Det1	1	1	259.9	259.9
903104a2	Det2	1	1	59.8	59.8
903104a2	Det3	1	1	262.5	262.5
903104a2	Det4	1	1	54.3	54.3
903104a2	Det5	1	1	265.2	265.2
903104a2	HV1	1	1	257.0	128.5
903104a2	HV2	1	1	56.8	28.4
903104a2	HV3	1	1	257.0	128.5
903104a2	HV4	1	1	51.3	25.6
903104a2	HV5	1	1	257.0	128.5
903133b2	STR	128	128	398.3	3.1
903133b2	Det1	0	0	0.0	0.0
903133b2	Det2	3	3	1425.7	475.2
903133b2	Det3	0	0	0.0	0.0
903133b2	Det4	3	3	938.8	312.9
903133b2	Det5	0	0	0.0	0.0
903133b2	HV1	0	0	0.0	0.0
903133b2	HV2	3	3	1416.6	236.1
903133b2	HV3	0	0	0.0	0.0
903133b2	HV4	4	4	673.3	84.2
903133b2	HV5	0	0	0.0	0.0
903167b3	STR	572	572	1474.1	2.6
903167b3	Det1	0	0	0.0	0.0
903167b3	Det2	3	3	475.7	158.6
903167b3	Det3	0	0	0.0	0.0
903167b3	Det4	3	3	2192.2	730.7
903167b3	Det5	0	0	0.0	0.0
903167b3	HV1	0	0	0.0	0.0
903167b3	HV2	3	3	466.6	77.8
903167b3	HV3	0	0	0.0	0.0
903167b3	HV4	4	4	1943.8	243.0
903167b3	HV5	0	0	0.0	0.0
903237cb	STR	152	152	1124.7	7.4
903237cb	Det1	0	0	0.0	0.0
903237cb	Det2	0	0	0.0	0.0
903237cb	Det3	0	0	0.0	0.0
903237cb	Det4	2	2	302.2	151.1
903237cb	Det5	0	0	0.0	0.0
903237cb	HV1	0	0	0.0	0.0
903237cb	HV2	0	0	0.0	0.0
903237cb	HV3	0	0	0.0	0.0
903237cb	HV4	2	2	296.1	74.0
903237cb	HV5	0	0	0.0	0.0
903307bgr	STR	400	400	2178.7	5.4
903307bgr	Det1	0	0	0.0	0.0
903307bgr	Det2	0	0	0.0	0.0
903307bgr	Det3	0	0	0.0	0.0
903307bgr	Det4	3	3	723.8	241.3
903307bgr	Det5	0	0	0.0	0.0
903307bgr	HV1	0	0	0.0	0.0
903307bgr	HV2	0	0	0.0	0.0
903307bgr	HV3	0	0	0.0	0.0
903307bgr	HV4	3	3	714.6	119.1
903307bgr	HV5	0	0	0.0	0.0
903377d6	STR	395	395	2131.4	5.4
903422a3r	STR	4	4	5.0	1.3
903447b9	STR	513	513	1481.5	2.9
903447b9	Det1	0	0	0.0	0.0
903447b9	Det2	0	0	0.0	0.0
903447b9	Det3	0	0	0.0	0.0
903447b9	Det4	3	3	163.0	54.3
903447b9	Det5	0	0	0.0	0.0
903447b9	HV1	0	0	0.0	0.0
903447b9	HV2	0	0	0.0	0.0
903447b9	HV3	0	0	0.0	0.0
903447b9	HV4	3	3	153.9	25.7
903447b9	HV5	0	0	0.0	0.0
903517e8	STR	251	251	933.7	3.7
903517e8	Det1	0	0	0.0	0.0
903517e8	Det2	2	2	2235.4	1117.7
903517e8	Det3	0	0	0.0	0.0
903517e8	Det4	5	5	1404.0	280.8
903517e8	Det5	0	0	0.0	0.0

903517e8	HV1	0	0	0.0	0.0
903517e8	HV2	3	3	1999.0	333.2
903517e8	HV3	0	0	0.0	0.0
903517e8	HV4	5	5	1388.8	138.9
903517e8	HV5	0	0	0.0	0.0
910022a1r	STR	38	38	103.1	2.7
910034a1r	STR	96	96	595.7	6.2
910077c9	STR	261	261	2136.8	8.2
910147e4	STR	158	158	1527.8	9.7
910217bd	STR	220	220	1804.4	8.2
910217bd	Det1	0	0	0.0	0.0
910217bd	Det2	1	1	85.3	85.3
910217bd	Det3	0	0	0.0	0.0
910217bd	Det4	1	1	79.8	79.8
910217bd	Det5	0	0	0.0	0.0
910217bd	HV1	0	0	0.0	0.0
910217bd	HV2	1	1	82.2	41.1
910217bd	HV3	0	0	0.0	0.0
910217bd	HV4	1	1	76.7	38.4
910217bd	HV5	0	0	0.0	0.0
910287d2	STR	238	238	1217.4	5.1
910357e7	STR	255	255	1582.1	6.2
910427d6	STR	509	509	2179.4	4.3
910427d6	Det1	0	0	0.0	0.0
910427d6	Det2	1	1	557.9	557.9
910427d6	Det3	0	0	0.0	0.0
910427d6	Det4	1	1	535.5	535.5
910427d6	Det5	0	0	0.0	0.0
910427d6	HV1	0	0	0.0	0.0
910427d6	HV2	1	1	554.8	277.4
910427d6	HV3	0	0	0.0	0.0
910427d6	HV4	1	1	532.4	266.2
910427d6	HV5	0	0	0.0	0.0
910497e7	STR	233	233	1265.2	5.4
910567g1	STR	189	189	1049.3	5.6
910637c2	STR	381	381	2014.8	5.3
910707c6	STR	300	300	1512.1	5.0
910707c6	Det1	3	3	526.1	175.4
910707c6	Det2	1	1	461.5	461.5
910707c6	Det3	7	7	1751.8	250.3
910707c6	Det4	1	1	474.4	474.4
910707c6	Det5	0	0	0.0	0.0
910707c6	HV1	3	3	516.4	86.1
910707c6	HV2	1	1	458.4	229.2
910707c6	HV3	7	7	1729.1	123.5
910707c6	HV4	1	1	471.3	235.7
910707c6	HV5	0	0	0.0	0.0
910777d4	STR	224	224	1848.3	8.3
910777d4	Det1	3	3	273.8	91.3
910777d4	Det2	0	0	0.0	0.0
910777d4	Det3	6	6	3747.5	624.6
910777d4	Det4	0	0	0.0	0.0
910777d4	Det5	0	0	0.0	0.0
910777d4	HV1	3	3	264.0	44.0
910777d4	HV2	0	0	0.0	0.0
910777d4	HV3	7	7	3499.4	250.0
910777d4	HV4	0	0	0.0	0.0
910777d4	HV5	0	0	0.0	0.0
910847f2	STR	229	229	1351.3	5.9
910847f2	Det1	3	3	937.0	312.3
910847f2	Det2	0	0	0.0	0.0
910847f2	Det3	6	6	1041.4	173.6
910847f2	Det4	0	0	0.0	0.0
910847f2	Det5	0	0	0.0	0.0
910847f2	HV1	3	3	927.2	154.5
910847f2	HV2	0	0	0.0	0.0
910847f2	HV3	7	7	812.8	58.1

910847f2	HV4	0	0	0.0	0.0
910847f2	HV5	0	0	0.0	0.0
910917bc	STR	408	408	1753.1	4.3
910917bc	Det1	1	1	176.1	176.1
910917bc	Det2	1	1	551.0	551.0
910917bc	Det3	2	2	140.6	70.3
910917bc	Det4	1	1	326.8	326.8
910917bc	Det5	0	0	0.0	0.0
910917bc	HV1	1	1	172.8	86.4
910917bc	HV2	1	1	547.9	274.0
910917bc	HV3	2	2	134.1	33.5
910917bc	HV4	1	1	323.7	161.9
910917bc	HV5	0	0	0.0	0.0
910987c9	STR	268	268	1867.6	7.0
910987c9	Det1	0	0	0.0	0.0
910987c9	Det2	1	1	1224.1	1224.1
910987c9	Det3	0	0	0.0	0.0
910987c9	Det4	1	1	1199.7	1199.7
910987c9	Det5	0	0	0.0	0.0
910987c9	HV1	0	0	0.0	0.0
910987c9	HV2	1	1	1221.1	610.5
910987c9	HV3	0	0	0.0	0.0
910987c9	HV4	1	1	1196.7	598.3
910987c9	HV5	0	0	0.0	0.0
911057d5	STR	113	113	1562.5	13.8
911057d5	Det1	1	1	552.8	552.8
911057d5	Det2	0	0	0.0	0.0
911057d5	Det3	1	1	550.7	550.7
911057d5	Det4	0	0	0.0	0.0
911057d5	Det5	0	0	0.0	0.0
911057d5	HV1	1	1	549.6	274.8
911057d5	HV2	0	0	0.0	0.0
911057d5	HV3	1	1	547.5	273.7
911057d5	HV4	0	0	0.0	0.0
911057d5	HV5	0	0	0.0	0.0
911127e4	STR	209	209	1641.6	7.9
911197b8	STR	286	286	1519.5	5.3
911197b8	Det1	0	0	0.0	0.0
911197b8	Det2	1	1	282.8	282.8
911197b8	Det3	0	0	0.0	0.0
911197b8	Det4	0	0	0.0	0.0
911197b8	Det5	0	0	0.0	0.0
911197b8	HV1	0	0	0.0	0.0
911197b8	HV2	1	1	279.8	139.9
911197b8	HV3	0	0	0.0	0.0
911197b8	HV4	0	0	0.0	0.0
911197b8	HV5	0	0	0.0	0.0
911267c1	STR	214	214	1498.9	7.0
911267c1	Det1	2	2	1024.3	512.1
911267c1	Det2	2	2	749.5	374.7
911267c1	Det3	2	2	1012.2	506.1
911267c1	Det4	1	1	551.5	551.5
911267c1	Det5	0	0	0.0	0.0
911267c1	HV1	2	2	1017.8	254.4
911267c1	HV2	2	2	743.3	185.8
911267c1	HV3	2	2	1005.7	251.4
911267c1	HV4	1	1	548.5	274.2
911267c1	HV5	0	0	0.0	0.0
911276a2r	STR	129	129	1004.6	7.8
911276a2r	Det1	1	1	283.7	283.7
911276a2r	Det2	0	0	0.0	0.0
911276a2r	Det3	1	1	271.4	271.4
911276a2r	Det4	0	0	0.0	0.0
911276a2r	Det5	0	0	0.0	0.0
911276a2r	HV1	1	1	280.5	140.2
911276a2r	HV2	0	0	0.0	0.0
911276a2r	HV3	1	1	268.1	134.1
911276a2r	HV4	0	0	0.0	0.0
911276a2r	HV5	0	0	0.0	0.0
911337c8	STR	126	126	1155.8	9.2
911337c8	Det1	0	0	0.0	0.0
911337c8	Det2	1	1	548.4	548.4
911337c8	Det3	0	0	0.0	0.0

911337c8	Det4	1	1	506.3	506.3
911337c8	Det5	0	0	0.0	0.0
911337c8	HV1	0	0	0.0	0.0
911337c8	HV2	1	1	545.4	272.7
911337c8	HV3	0	0	0.0	0.0
911337c8	HV4	1	1	503.3	251.6
911337c8	HV5	0	0	0.0	0.0
911407ah	STR	278	278	1587.1	5.7
911477c3	STR	140	140	1161.2	8.3
911547d3	STR	196	196	1524.2	7.8
911547d3	Det1	1	1	750.7	750.7
911547d3	Det2	0	0	0.0	0.0
911547d3	Det3	3	3	1817.7	605.9
911547d3	Det4	0	0	0.0	0.0
911547d3	Det5	0	0	0.0	0.0
911547d3	HV1	1	1	747.4	373.7
911547d3	HV2	0	0	0.0	0.0
911547d3	HV3	3	3	1808.0	301.3
911547d3	HV4	0	0	0.0	0.0
911547d3	HV5	0	0	0.0	0.0
911617ca	STR	271	271	1898.1	7.0
911687bg	STR	227	227	1005.6	4.4
911687bg	Det1	0	0	0.0	0.0
911687bg	Det2	1	1	672.1	672.1
911687bg	Det3	0	0	0.0	0.0
911687bg	Det4	2	2	753.0	376.5
911687bg	Det5	0	0	0.0	0.0
911687bg	HV1	0	0	0.0	0.0
911687bg	HV2	2	2	489.3	122.3
911687bg	HV3	0	0	0.0	0.0
911687bg	HV4	2	2	746.9	186.7
911687bg	HV5	0	0	0.0	0.0
911757b1	STR	190	190	1719.8	9.1
911757b1	Det1	0	0	0.0	0.0
911757b1	Det2	0	0	0.0	0.0
911757b1	Det3	1	1	1376.0	1376.0
911757b1	Det4	0	0	0.0	0.0
911757b1	Det5	2	2	849.8	424.9
911757b1	HV1	0	0	0.0	0.0
911757b1	HV2	0	0	0.0	0.0
911757b1	HV3	1	1	1372.7	686.4
911757b1	HV4	0	0	0.0	0.0
911757b1	HV5	4	4	334.0	41.8
911827af	STR	153	153	1351.5	8.8
911827af	Det1	1	1	151.1	151.1
911827af	Det2	1	1	166.2	166.2
911827af	Det3	0	0	0.0	0.0
911827af	Det4	0	0	0.0	0.0
911827af	Det5	0	0	0.0	0.0
911827af	HV1	1	1	147.8	73.9
911827af	HV2	1	1	163.2	81.6
911827af	HV3	0	0	0.0	0.0
911827af	HV4	0	0	0.0	0.0
911827af	HV5	0	0	0.0	0.0
911897al	STR	168	168	1826.8	10.9
911897al	Det1	0	0	0.0	0.0
911897al	Det2	1	1	430.4	430.4
911897al	Det3	0	0	0.0	0.0
911897al	Det4	1	1	507.2	507.2
911897al	Det5	0	0	0.0	0.0
911897al	HV1	0	0	0.0	0.0
911897al	HV2	1	1	427.4	213.7
911897al	HV3	0	0	0.0	0.0
911897al	HV4	1	1	504.2	252.1
911897al	HV5	0	0	0.0	0.0
911967d4	STR	237	237	1376.6	5.8
911967d4	Det1	0	0	0.0	0.0
911967d4	Det2	0	0	0.0	0.0
911967d4	Det3	1	1	713.5	713.5
911967d4	Det4	0	0	0.0	0.0
911967d4	Det5	0	0	0.0	0.0
911967d4	HV1	0	0	0.0	0.0

911967d4	HV2	0	0	0.0	0.0
911967d4	HV3	1	1	710.3	355.1
911967d4	HV4	0	0	0.0	0.0
911967d4	HV5	0	0	0.0	0.0
912037acr	STR	207	207	1777.3	8.6
912107b3	STR	164	164	1295.6	7.9
912107b3	Det1	0	0	0.0	0.0
912107b3	Det2	0	0	0.0	0.0
912107b3	Det3	5	5	2282.7	456.5
912107b3	Det4	0	0	0.0	0.0
912107b3	Det5	0	0	0.0	0.0
912107b3	HV1	0	0	0.0	0.0
912107b3	HV2	0	0	0.0	0.0
912107b3	HV3	5	5	2266.5	226.6
912107b3	HV4	0	0	0.0	0.0
912107b3	HV5	0	0	0.0	0.0
912177d5r	STR	184	184	818.8	4.4
912177d5r	Det1	1	1	330.7	330.7
912177d5r	Det2	0	0	0.0	0.0
912177d5r	Det3	0	0	0.0	0.0
912177d5r	Det4	0	0	0.0	0.0
912177d5r	Det5	0	0	0.0	0.0
912177d5r	HV1	1	1	327.5	163.7
912177d5r	HV2	0	0	0.0	0.0
912177d5r	HV3	0	0	0.0	0.0
912177d5r	HV4	0	0	0.0	0.0
912177d5r	HV5	0	0	0.0	0.0
912247c7	STR	251	251	1233.3	4.9
912317e2	STR	161	161	1966.5	12.2
912317e2	Det1	0	0	0.0	0.0
912317e2	Det2	1	1	457.4	457.4
912317e2	Det3	3	3	657.1	219.0
912317e2	Det4	0	0	0.0	0.0
912317e2	Det5	0	0	0.0	0.0
912317e2	HV1	0	0	0.0	0.0
912317e2	HV2	1	1	454.4	227.2
912317e2	HV3	3	3	647.4	107.9
912317e2	HV4	0	0	0.0	0.0
912317e2	HV5	0	0	0.0	0.0
912387c1	STR	190	190	1335.5	7.0
912387c1	Det1	3	3	2015.2	671.7
912387c1	Det2	0	0	0.0	0.0
912387c1	Det3	0	0	0.0	0.0
912387c1	Det4	0	0	0.0	0.0
912387c1	Det5	0	0	0.0	0.0
912387c1	HV1	3	3	2005.4	334.2
912387c1	HV2	0	0	0.0	0.0
912387c1	HV3	0	0	0.0	0.0
912387c1	HV4	0	0	0.0	0.0
912387c1	HV5	0	0	0.0	0.0
912457d5	STR	174	174	2437.7	14.0
912457d5	Det1	0	0	0.0	0.0
912457d5	Det2	0	0	0.0	0.0
912457d5	Det3	8	8	3624.2	453.0
912457d5	Det4	0	0	0.0	0.0
912457d5	Det5	1	1	756.4	756.4
912457d5	HV1	0	0	0.0	0.0
912457d5	HV2	0	0	0.0	0.0
912457d5	HV3	9	9	3399.4	188.9
912457d5	HV4	0	0	0.0	0.0
912457d5	HV5	2	2	548.4	137.1
912527e5	STR	332	332	1167.0	3.5
912527e5	Det1	1	1	748.1	748.1
912527e5	Det2	0	0	0.0	0.0
912527e5	Det3	1	1	156.1	156.1
912527e5	Det4	1	1	147.3	147.3
912527e5	Det5	0	0	0.0	0.0
912527e5	HV1	1	1	744.8	372.4
912527e5	HV2	0	0	0.0	0.0
912527e5	HV3	1	1	152.8	76.4
912527e5	HV4	1	1	144.2	72.1
912527e5	HV5	0	0	0.0	0.0

912597b2	STR	209	209	824.3	3.9
912597b2	Det1	0	0	0.0	0.0
912597b2	Det2	0	0	0.0	0.0
912597b2	Det3	0	0	0.0	0.0
912597b2	Det4	2	2	294.5	147.3
912597b2	Det5	0	0	0.0	0.0
912597b2	HV1	0	0	0.0	0.0
912597b2	HV2	0	0	0.0	0.0
912597b2	HV3	0	0	0.0	0.0
912597b2	HV4	2	2	288.4	72.1
912597b2	HV5	0	0	0.0	0.0
912667c4	STR	375	375	1434.2	3.8
912667c4	Det1	4	4	2373.9	593.5
912667c4	Det2	1	1	253.1	253.1
912667c4	Det3	2	2	409.2	204.6
912667c4	Det4	1	1	617.3	617.3
912667c4	Det5	0	0	0.0	0.0
912667c4	HV1	5	5	2097.7	209.8
912667c4	HV2	1	1	250.1	125.0
912667c4	HV3	2	2	402.7	100.7
912667c4	HV4	2	2	386.7	96.7
912667c4	HV5	0	0	0.0	0.0
912737c6	STR	278	278	2101.5	7.6
912737c6	Det1	0	0	0.0	0.0
912737c6	Det2	0	0	0.0	0.0
912737c6	Det3	3	3	1678.7	559.6
912737c6	Det4	0	0	0.0	0.0
912737c6	Det5	3	3	1694.4	564.8
912737c6	HV1	0	0	0.0	0.0
912737c6	HV2	0	0	0.0	0.0
912737c6	HV3	3	3	1665.5	277.6
912737c6	HV4	0	0	0.0	0.0
912737c6	HV5	3	3	1682.4	280.4
912807ai	STR	337	337	1261.7	3.7
912807ai	Det1	0	0	0.0	0.0
912807ai	Det2	1	1	140.6	140.6
912807ai	Det3	0	0	0.0	0.0
912807ai	Det4	1	1	910.6	910.6
912807ai	Det5	0	0	0.0	0.0
912807ai	HV1	0	0	0.0	0.0
912807ai	HV2	1	1	137.5	68.7
912807ai	HV3	0	0	0.0	0.0
912807ai	HV4	1	1	907.5	453.8
912807ai	HV5	0	0	0.0	0.0
912877d1	STR	181	181	476.6	2.6
912877d1	Det1	0	0	0.0	0.0
912877d1	Det2	0	0	0.0	0.0
912877d1	Det3	4	4	512.4	128.1
912877d1	Det4	0	0	0.0	0.0
912877d1	Det5	0	0	0.0	0.0
912877d1	HV1	0	0	0.0	0.0
912877d1	HV2	0	0	0.0	0.0
912877d1	HV3	4	4	499.4	62.4
912877d1	HV4	0	0	0.0	0.0
912877d1	HV5	0	0	0.0	0.0
912947b4	STR	247	247	1218.8	4.9
912947b4	Det1	0	0	0.0	0.0
912947b4	Det2	0	0	0.0	0.0
912947b4	Det3	1	1	645.2	645.2
912947b4	Det4	0	0	0.0	0.0
912947b4	Det5	1	1	384.1	384.1
912947b4	HV1	0	0	0.0	0.0
912947b4	HV2	0	0	0.0	0.0
912947b4	HV3	1	1	641.9	321.0
912947b4	HV4	0	0	0.0	0.0
912947b4	HV5	2	2	168.0	42.0
913017b5	STR	221	221	1430.8	6.5
913087d4	STR	224	224	1070.5	4.8
913157aa	STR	171	171	546.2	3.2
913157aa	Det1	0	0	0.0	0.0
913157aa	Det2	0	0	0.0	0.0
913157aa	Det3	1	1	278.2	278.2
913157aa	Det4	0	0	0.0	0.0

913157aa	Det5	1	1	84.2	84.2
913157aa	HV1	0	0	0.0	0.0
913157aa	HV2	0	0	0.0	0.0
913157aa	HV3	1	1	274.9	137.5
913157aa	HV4	0	0	0.0	0.0
913157aa	HV5	1	1	80.7	40.3
913227c4	STR	205	205	756.1	3.7
913297b7	STR	213	213	1800.8	8.5
913297b7	Det1	1	1	1590.3	1590.3
913297b7	Det2	0	0	0.0	0.0
913297b7	Det3	0	0	0.0	0.0
913297b7	Det4	0	0	0.0	0.0
913297b7	Det5	0	0	0.0	0.0
913297b7	HV1	1	1	1587.1	793.5
913297b7	HV2	0	0	0.0	0.0
913297b7	HV3	0	0	0.0	0.0
913297b7	HV4	0	0	0.0	0.0
913297b7	HV5	0	0	0.0	0.0
913367e3	STR	255	255	1650.3	6.5
913507dg	STR	236	236	822.3	3.5
913507dg	Det1	0	0	0.0	0.0
913507dg	Det2	0	0	0.0	0.0
913507dg	Det3	1	1	422.8	422.8
913507dg	Det4	0	0	0.0	0.0
913507dg	Det5	1	1	219.7	219.7
913507dg	HV1	0	0	0.0	0.0
913507dg	HV2	0	0	0.0	0.0
913507dg	HV3	1	1	419.5	209.8
913507dg	HV4	0	0	0.0	0.0
913507dg	HV5	1	1	215.7	107.9
913577b2	STR	146	146	826.2	5.7
913647e7	STR	215	215	1130.3	5.3
920067c7	STR	213	213	1124.3	5.3
920137d2	STR	283	283	1696.2	6.0
920207b2r	STR	140	140	814.7	5.8
920207b2r	Det1	0	0	0.0	0.0
920207b2r	Det2	0	0	0.0	0.0
920207b2r	Det3	0	0	0.0	0.0
920207b2r	Det4	1	1	147.0	147.0
920207b2r	Det5	0	0	0.0	0.0
920207b2r	HV1	0	0	0.0	0.0
920207b2r	HV2	0	0	0.0	0.0
920207b2r	HV3	0	0	0.0	0.0
920207b2r	HV4	1	1	144.0	72.0
920207b2r	HV5	0	0	0.0	0.0
920277ac	STR	124	124	1278.9	10.3
920277ac	Det1	0	0	0.0	0.0
920277ac	Det2	2	2	336.3	168.1
920277ac	Det3	0	0	0.0	0.0
920277ac	Det4	1	1	974.2	974.2
920277ac	Det5	0	0	0.0	0.0
920277ac	HV1	0	0	0.0	0.0
920277ac	HV2	2	2	330.2	82.5
920277ac	HV3	0	0	0.0	0.0
920277ac	HV4	1	1	971.1	485.6
920277ac	HV5	0	0	0.0	0.0
920347c1	STR	210	210	671.2	3.2
920347c1	Det1	0	0	0.0	0.0
920347c1	Det2	2	2	347.9	173.9
920347c1	Det3	0	0	0.0	0.0
920347c1	Det4	0	0	0.0	0.0
920347c1	Det5	0	0	0.0	0.0
920347c1	HV1	0	0	0.0	0.0
920347c1	HV2	2	2	341.8	85.4
920347c1	HV3	0	0	0.0	0.0
920347c1	HV4	0	0	0.0	0.0
920347c1	HV5	0	0	0.0	0.0
920417b6	STR	130	130	1480.9	11.4
920417b6	Det1	0	0	0.0	0.0

920417b6	Det2	2	2	336.5	168.2
920417b6	Det3	0	0	0.0	0.0
920417b6	Det4	0	0	0.0	0.0
920417b6	Det5	0	0	0.0	0.0
920417b6	HV1	0	0	0.0	0.0
920417b6	HV2	2	2	330.4	82.6
920417b6	HV3	0	0	0.0	0.0
920417b6	HV4	0	0	0.0	0.0
920417b6	HV5	0	0	0.0	0.0
920487ah	STR	183	183	1468.2	8.0
920487ah	Det1	0	0	0.0	0.0
920487ah	Det2	2	2	329.9	164.9
920487ah	Det3	0	0	0.0	0.0
920487ah	Det4	0	0	0.0	0.0
920487ah	Det5	0	0	0.0	0.0
920487ah	HV1	0	0	0.0	0.0
920487ah	HV2	2	2	323.8	80.9
920487ah	HV3	0	0	0.0	0.0
920487ah	HV4	0	0	0.0	0.0
920487ah	HV5	0	0	0.0	0.0
920557f1	STR	149	149	911.7	6.1
920557f1	Det1	0	0	0.0	0.0
920557f1	Det2	3	3	499.3	166.4
920557f1	Det3	0	0	0.0	0.0
920557f1	Det4	0	0	0.0	0.0
920557f1	Det5	0	0	0.0	0.0
920557f1	HV1	0	0	0.0	0.0
920557f1	HV2	3	3	490.2	81.7
920557f1	HV3	0	0	0.0	0.0
920557f1	HV4	0	0	0.0	0.0
920557f1	HV5	0	0	0.0	0.0
920627c6	STR	373	373	1873.1	5.0
920627c6	Det1	1	1	203.2	203.2
920627c6	Det2	4	4	572.3	143.1
920627c6	Det3	2	2	253.3	126.7
920627c6	Det4	2	2	238.6	119.3
920627c6	Det5	1	1	82.5	82.5
920627c6	HV1	1	1	200.0	100.0
920627c6	HV2	4	4	560.0	70.0
920627c6	HV3	2	2	245.6	61.4
920627c6	HV4	2	2	232.5	58.1
920627c6	HV5	1	1	78.5	39.2
920697ci	STR	158	158	1368.1	8.7
920697ci	Det1	1	1	327.1	327.1
920697ci	Det2	2	2	333.0	166.5
920697ci	Det3	0	0	0.0	0.0
920697ci	Det4	0	0	0.0	0.0
920697ci	Det5	0	0	0.0	0.0
920697ci	HV1	1	1	323.8	161.9
920697ci	HV2	2	2	326.9	81.7
920697ci	HV3	0	0	0.0	0.0
920697ci	HV4	0	0	0.0	0.0
920697ci	HV5	0	0	0.0	0.0
920767b4	STR	206	206	1838.9	8.9
920767b4	Det1	1	1	264.7	264.7
920767b4	Det2	3	3	507.3	169.1
920767b4	Det3	0	0	0.0	0.0
920767b4	Det4	0	0	0.0	0.0
920767b4	Det5	0	0	0.0	0.0
920767b4	HV1	1	1	261.4	130.7
920767b4	HV2	3	3	498.1	83.0
920767b4	HV3	0	0	0.0	0.0
920767b4	HV4	0	0	0.0	0.0
920767b4	HV5	0	0	0.0	0.0
920837b9	STR	190	190	2514.1	13.2
920837b9	Det1	0	0	0.0	0.0
920837b9	Det2	2	2	336.1	168.0
920837b9	Det3	0	0	0.0	0.0
920837b9	Det4	0	0	0.0	0.0
920837b9	Det5	0	0	0.0	0.0
920837b9	HV1	0	0	0.0	0.0
920837b9	HV2	2	2	330.0	82.5
920837b9	HV3	0	0	0.0	0.0
920837b9	HV4	0	0	0.0	0.0
920837b9	HV5	0	0	0.0	0.0

920907bar	STR	163	163	1616.3	9.9
920907bar	Det1	0	0	0.0	0.0
920907bar	Det2	2	2	352.3	176.1
920907bar	Det3	0	0	0.0	0.0
920907bar	Det4	0	0	0.0	0.0
920907bar	Det5	0	0	0.0	0.0
920907bar	HV1	0	0	0.0	0.0
920907bar	HV2	2	2	346.2	86.5
920907bar	HV3	0	0	0.0	0.0
920907bar	HV4	0	0	0.0	0.0
920907bar	HV5	0	0	0.0	0.0
920977f6r	STR	182	182	1199.3	6.6
920977f6r	Det1	0	0	0.0	0.0
920977f6r	Det2	3	3	489.1	163.0
920977f6r	Det3	0	0	0.0	0.0
920977f6r	Det4	0	0	0.0	0.0
920977f6r	Det5	0	0	0.0	0.0
920977f6r	HV1	0	0	0.0	0.0
920977f6r	HV2	3	3	479.9	80.0
920977f6r	HV3	0	0	0.0	0.0
920977f6r	HV4	0	0	0.0	0.0
920977f6r	HV5	0	0	0.0	0.0
921047d2	STR	141	141	1699.3	12.1
921047d2	Det1	0	0	0.0	0.0
921047d2	Det2	2	2	527.1	263.5
921047d2	Det3	0	0	0.0	0.0
921047d2	Det4	0	0	0.0	0.0
921047d2	Det5	0	0	0.0	0.0
921047d2	HV1	0	0	0.0	0.0
921047d2	HV2	2	2	521.0	130.2
921047d2	HV3	0	0	0.0	0.0
921047d2	HV4	0	0	0.0	0.0
921047d2	HV5	0	0	0.0	0.0
921117b6	STR	192	192	2202.5	11.5
921117b6	Det1	0	0	0.0	0.0
921117b6	Det2	3	3	504.5	168.2
921117b6	Det3	0	0	0.0	0.0
921117b6	Det4	0	0	0.0	0.0
921117b6	Det5	0	0	0.0	0.0
921117b6	HV1	0	0	0.0	0.0
921117b6	HV2	3	3	495.3	82.6
921117b6	HV3	0	0	0.0	0.0
921117b6	HV4	0	0	0.0	0.0
921117b6	HV5	0	0	0.0	0.0
921187e6	STR	220	220	1298.0	5.9
921187e6	Det1	2	2	462.9	231.5
921187e6	Det2	3	3	379.0	126.3
921187e6	Det3	2	2	213.9	107.0
921187e6	Det4	2	2	214.8	107.4
921187e6	Det5	1	1	87.1	87.1
921187e6	HV1	2	2	456.5	114.1
921187e6	HV2	3	3	369.8	61.6
921187e6	HV3	2	2	206.3	51.6
921187e6	HV4	2	2	208.7	52.2
921187e6	HV5	1	1	83.0	41.5
921257e4	STR	174	174	1635.9	9.4
921257e4	Det1	3	3	799.9	266.6
921257e4	Det2	3	3	504.5	168.2
921257e4	Det3	0	0	0.0	0.0
921257e4	Det4	0	0	0.0	0.0
921257e4	Det5	0	0	0.0	0.0
921257e4	HV1	3	3	790.2	131.7
921257e4	HV2	3	3	495.3	82.6
921257e4	HV3	0	0	0.0	0.0
921257e4	HV4	0	0	0.0	0.0
921257e4	HV5	0	0	0.0	0.0
921327c4	STR	159	159	968.5	6.1
921327c4	Det1	0	0	0.0	0.0
921327c4	Det2	2	2	316.9	158.5
921327c4	Det3	0	0	0.0	0.0
921327c4	Det4	0	0	0.0	0.0
921327c4	Det5	0	0	0.0	0.0
921327c4	HV1	0	0	0.0	0.0
921327c4	HV2	2	2	310.8	77.7

921327c4	HV3	0	0	0.0	0.0
921327c4	HV4	0	0	0.0	0.0
921327c4	HV5	0	0	0.0	0.0
921397c7	STR	187	187	1885.2	10.1
921397c7	Det1	0	0	0.0	0.0
921397c7	Det2	2	2	337.9	168.9
921397c7	Det3	1	1	739.5	739.5
921397c7	Det4	0	0	0.0	0.0
921397c7	Det5	1	1	686.9	686.9
921397c7	HV1	0	0	0.0	0.0
921397c7	HV2	2	2	331.8	83.0
921397c7	HV3	2	2	526.4	131.6
921397c7	HV4	0	0	0.0	0.0
921397c7	HV5	2	2	436.5	109.1

Totals

Item	#on	#off	on time (minutes)	min/cycle
STR	23040	23040	133687.9	5.8
Det1	53	53	15496.4	292.4
Det2	91	91	23728.4	260.8
Det3	86	86	28918.3	336.3
Det4	68	68	18221.2	268.0
Det5	28	28	5883.9	210.1
HV1	50	50	14735.5	294.7
HV2	90	90	22481.0	249.8
HV3	85	85	27724.7	326.2
HV4	68	68	16719.4	245.9
HV5	28	28	4522.9	161.5

Appendix G - 1092 Acquisition Data

The HSP GTO 1092 program has acquired the same target, Z Chamaeleontis, 42 times, each time with two iterations for a total of 84 acquisition data sets. There was one unsuccessful acquisition, V0U80501 and V0U80502, where the target was not seen in either acquisition image. The reason for this failure is not known. Several acquisitions were made during eclipse so the acquisition was shown to work even at reduced light levels. These 84 data sets were taken with the same target but different FGS configurations over a long period of time, from late January to early June 1992.

An onboard acquisition is performed followed by an area scan of the image in the finding aperture of UV1. The acquisition and area scan are then repeated. These two iterations are referred to as "acquisition #1" and "acquisition #2" in the following discussion.

The FGS configuration is determined from the SMS and the assumption has been made in all cases that the primary guide star pair was used for all observations. The SMS designates the dominant and subdominant FGS for each guide star pair.

The image centroid in HSP detector deflection coordinates was determined from the IRAF - STSDAS program "Apercen" output. The centroid location is given in units of horizontal and vertical deflection steps; H,V.

The target location in V2, V3 coordinates was taken from the FGS telemetry report summary files for the particular observation. The units are arc seconds from V3. This data is not available for observations in which the telemetry format was "PN". The time of the observation was determined from PASS output.

The difference between these two locations was calculated by transforming the deflection coordinates (H/V) into focal plane (V2/V3) coordinates using the following parameters:

The current project database values for the center of the UV1 finding aperture are:

2476, 3263 in H,V(steps) and
179.64170, -492.3280 in V2, V3 (arc seconds)

There are 41.11 deflection steps per arc second in this region of UV1 and the angle between the V3 and H axes is 18.45 degrees.

The following are attached:

1. The data from each observation: For each observation number the tape number, acquisition number (1 or 2), FGS Configuration (dominant and subdominant FGS number), the image centroid in H,V, the target position in V2,V3, and the difference in V2, V3 between the image centroid and target position in arc seconds. The data are sorted by acquisition and FGS configuration.

2. A chart showing the image centroid positions. The points are plotted in H,V using different symbols for different FGS configurations as shown on the chart. The first acquisition symbols are plain and the second are filled on this and all following charts.

3. A chart as above but showing a smaller area for greater detail.

4. A chart showing the FGS reported positions.

5. A chart showing the difference in a one arc second region.

Several interesting patterns are evident:

1. As one would expect, the deflection positions are grouped "tighter" for the second acquisitions than the first.

2. First acquisitions with FGS #2 dominant have some large errors.

3. In both the deflection map and the V2,V3 map there are groupings by FGS configuration.

4. There are a large number of points on the difference chart apparently randomly distributed closely around zero suggesting agreement between the FGS and deflection data.

The data suggest different FGS configurations perform differently. The "tightest" clusters of points seem to be for the case when FGS #3 is dominant. In any case, this large number of acquisitions with a single target represents an opportunity to obtain unique FGS performance information.

The GSFC project has suggested that the data be examined further to see if there is any corelation between the position of the target and the position of the guide stars in the FGS pickle. This will be investigated.

Acknowledgement: Thanks to Colleen Townsley for calculating the image centroid positions using IRAF/SDAS and for determining the time of each observation from PASS files.

HSP 1092 Acquisition Data

		FGS Configuration			Deflection		FGS T/M		Difference	
Observation	Tape	Acq	Dom	Sub	H	V	V2	V3	Δv2	Δv3
V0U80501T	109204	1	1	2						
V0U80502T	109204	1	1	2						
V0U80J01T	109214	1	1	2	2440	3259	178.90	-492.46	0.12	0.05
V0U80L01T	109215	1	1	2	2437	3259	178.72	-492.31	0.03	0.01
V0U80N01T	109216	1	1	2	2433	3255	178.81	-492.49	0.20	0.07
V0U80P01T	109218	1	1	2	2432	3263	178.80	-492.57	0.17	0.11
V0U80X01T	109224	1	1	2	2449	3267	177.87	-493.05	-0.84	-0.93
V0U81701T	109231	1	1	2	2435	3249	178.59	-492.32	0.01	0.00
V0U81J01T	109239	1	1	2	2431	3270				
V0U81L01T	109240	1	1	2	2446	3272	178.79	-492.47	-0.08	-0.08
V0U81Z01T	109217	1	1	2	2432	3263	178.81	-492.55	0.18	0.12
V0U82301T	109226	1	1	2	2462	3256	179.45	-492.27	0.18	-0.08
V0U82501T	109230	1	1	2	2436	3252	178.55	-492.26	-0.10	0.00
V0U82901T	109238	1	1	2	2432	3265	179.45	-492.11	0.69	-0.37
V0U80101T	109202	1	1	3	2456	3255	179.33	-492.23	0.19	-0.07
V0U80701T	109206	1	1	3	2448	3244	179.05	-492.03	0.12	-0.11
V0U80B01T	109208	1	1	3	2463	3258	179.81	-492.20	-0.11	-0.07
V0U80D01T	109210	1	1	3	2463	3255	179.43	-492.30	0.15	-0.06
V0U80F01T	109211	1	1	3	2451	3257	179.94	-492.16	-0.22	-0.15
V0U80H01T	109212	1	1	3	2450	3259	179.31	-492.26	0.29	-0.01
V0U81R01T	109201	1	1	3	2456	3254	179.32	-492.19	0.16	-0.08
V0U81V01T	109209	1	1	3	2456	3256	179.37	-492.21	0.19	-0.10
V0U81X01T	109213	1	1	3	2447	3257	179.30	-492.30	0.38	0.01
V0U80901T	109207	1	2	1	2501	3251	179.49	-492.28	-0.47	-0.22
V0U80R01T	109219	1	2	1	2612	3289	181.44	-491.89	1.41	0.56
V0U80T01T	109220	1	2	1	2606	3275	181.42	-491.77	1.13	0.67
V0U80V01T	109222	1	2	1	2606	3269	181.42	-491.69	1.05	0.75
V0U81101T	109227	1	2	1	2602	3249	180.94	-491.61	0.95	1.30
V0U81301T	109228	1	2	1	2604	3240	181.28	-491.29	0.60	1.07
V0U81501T	109229	1	2	1	2468	3268				
V0U81901T	109232	1	2	1	2471	3322	179.88	-492.28	0.49	-1.09
V0U81B01T	109233	1	2	1	2467	3273	179.95	-492.25	0.00	-0.02
V0U81D01T	109235	1	2	1	2472	3279	180.04	-492.28	0.00	0.01
V0U81F01T	109236	1	2	1	2470	3275	179.96	-492.20	0.00	0.02
V0U81H01T	109237	1	2	1	2469	3281	180.00	-492.23	0.03	-0.10
V0U81T01T	109205	1	2	1	2503	3267				
V0U82101T	109221	1	2	1	2606	3276	181.43	-491.73	1.10	0.67
V0U82701M	109234	1	2	1	2470	3276	180.07	-492.34	0.01	0.08
V0U80301T	109203	1	3	1	2465	3277				
V0U80Z01T	109225	1	3	2	2475	3260	177.54	-495.47	-3.72	0.07
V0U81N01T	109241	1	3	2	2425	3298	178.45	-494.03	0.18	-0.54
V0U81P01T	109243	1	3	2	2444	3279				
V0U82B01T	109242	1	3	2	2419	3294	178.39	-494.11	0.12	-0.58
V0U80J02T	109214	2	1	2	2478	3259	179.78	-492.23	0.03	-0.05
V0U80L02T	109215	2	1	2	2478	3258	179.65	-492.07	0.13	-0.01
V0U80N02T	109216	2	1	2	2473	3259	179.78	-492.27	0.03	-0.01
V0U80P02T	109218	2	1	2	2486	3252	179.80	-492.22	-0.03	0.17

		FGS Configuration			Deflection		FGS T/M		Difference	
Observation	Tape	Acq	Dom	Sub	H	V	V2	V3	Δv2	Δv3
V0U80X02T	109224	2	1	2	2472	3265	178.41	-492.80	-0.45	-1.11
V0U81702T	109231	2	1	2	2466	3262	179.41	-492.12	-0.07	0.04
V0U81J02T	109239	2	1	2	2476	3267				
V0U81L02T	109240	2	1	2	2483	3271	179.55	-492.08	0.00	0.00
V0U81Z02T	109217	2	1	2	2477	3262	179.81	-492.24	0.04	-0.14
V0U82302T	109226	2	1	2	2480	3262	179.87	-492.23	-0.08	-0.13
V0U82502T	109230	2	1	2	2476	3274	179.59	-492.29	0.06	0.21
V0U82902T	109238	2	1	2	2477	3269	179.56	-492.07	-0.09	-0.08
V0U80102T	109202	2	1	3	2477	3260	179.85	-492.17	0.12	-0.13
V0U80702T	109206	2	1	3	2472	3265	179.98	-492.21	0.11	0.23
V0U80B02T	109208	2	1	3	2476	3255				
V0U80D02T	109210	2	1	3	2478	3260	179.85	-492.26	0.02	-0.14
V0U80F02T	109211	2	1	3	2478	3266	179.91	-492.13	-0.26	0.01
V0U80H02T	109212	2	1	3	2476	3274	179.98	-492.42	0.00	0.09
V0U81R02T	109201	2	1	3	2476	3259	179.82	-492.15	0.14	-0.06
V0U81V02T	109209	2	1	3	2479	3257	179.86	-492.16	0.06	-0.10
V0U81X02T	109213	2	1	3	2470	3262	179.87	-492.17	0.11	0.09
V0U80902T	109207	2	2	1	2473	3269	179.53	-492.17	-0.04	-0.02
V0U80R02T	109219	2	2	1	2483	3261	178.37	-492.30	0.88	0.64
V0U80T02T	109220	2	2	1	2472	3259	178.22	-492.45	-1.22	0.48
V0U80V02T	109222	2	2	1	2474	3264	178.30	-492.64	-0.70	-1.12
V0U81102T	109227	2	2	1	2482	3265	178.23	-492.94	1.26	0.54
V0U81302T	109228	2	2	1	2482	3260	178.57	-492.73	0.35	0.91
V0U81502T	109229	2	2	1	2473	3265				
V0U81902T	109232	2	2	1	2483	3230	180.05	-492.03	-0.21	0.23
V0U81B02T	109233	2	2	1	2474	3268	180.03	-492.08	-0.17	0.29
V0U81D02T	109235	2	2	1	2476	3258	179.99	-491.85	0.46	-0.13
V0U81F02T	109236	2	2	1	2474	3276	179.99	-492.07	-0.09	0.09
V0U81H02T	109237	2	2	1	2477	3262	179.95	-491.76	0.35	-0.51
V0U81T02T	109205	2	2	1	2483	3266	179.59	-492.24	-0.03	0.07
V0U82102T	109221	2	2	1	2479	3258	178.36	-492.35	0.30	1.09
V0U82702M	109234	2	2	1	2476	3264	180.01	-491.91	-0.53	0.02
V0U80302T	109203	2	3	1	2482	3255				
V0U80Z02T	109225	2	3	2	2473	3261	177.70	-495.33	-2.48	-2.45
V0U81N02T	109241	2	3	2	2477	3259	179.42	-492.75	-0.35	0.15
V0U81P02T	109243	2	3	2	2482	3258				
V0U82B02T	109242	2	3	2	2476	3269				

1092 Acquisitions

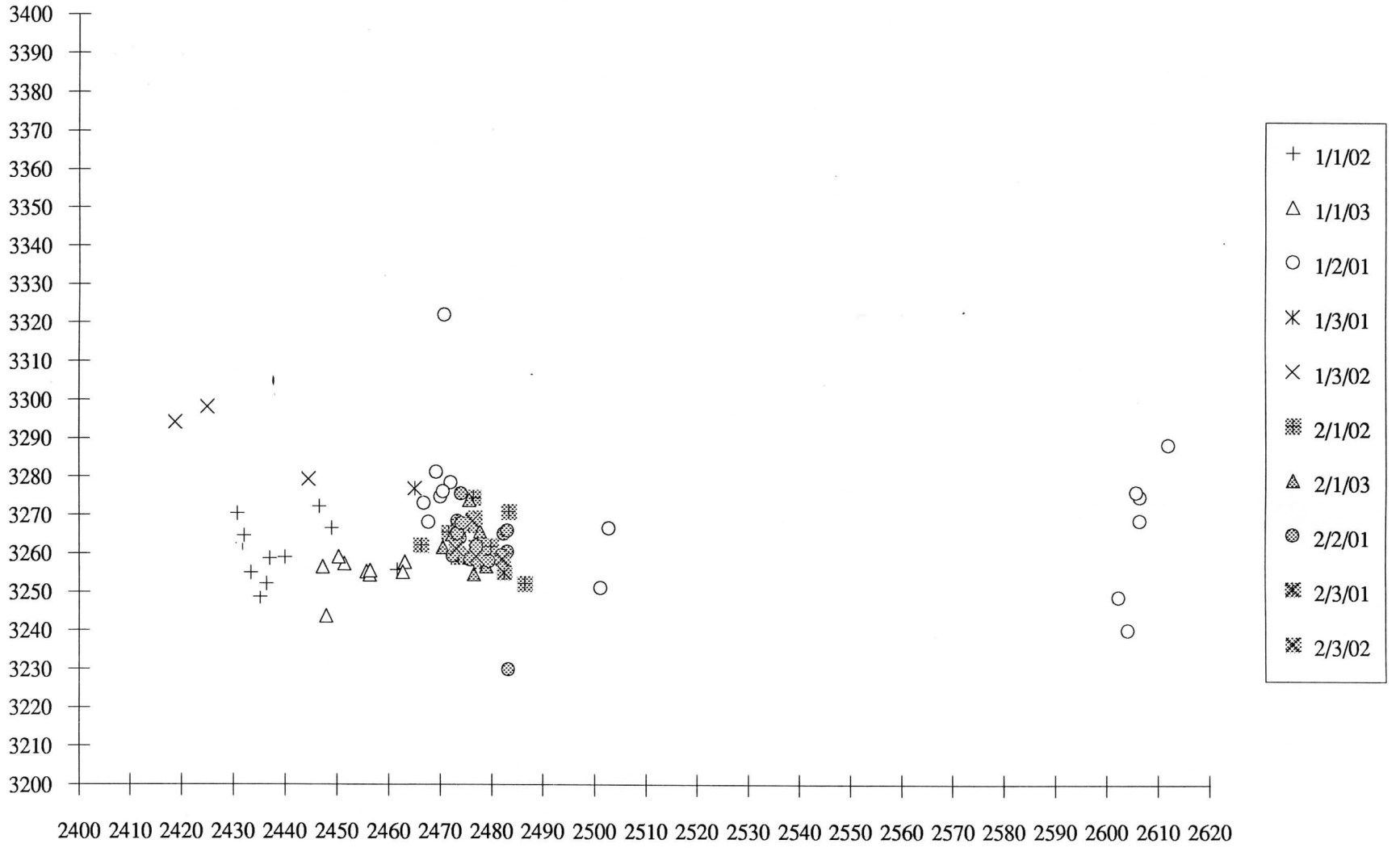

a/d/s - acquisition/dominant fgs/subdominant fgs

1092 Acquisitions

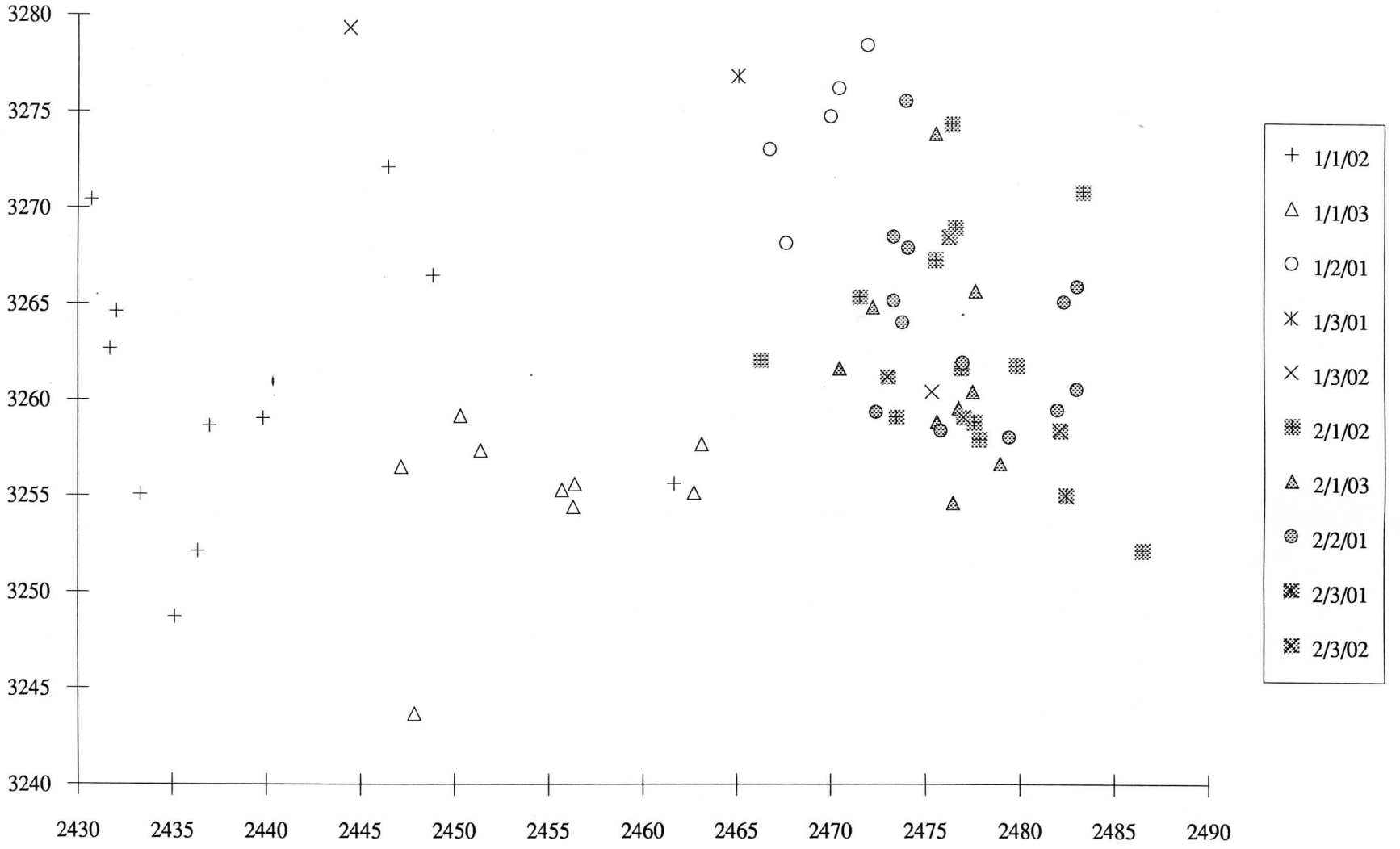

a/d/s - acquisition/dominant fgs/subdominant fgs

1092 FGS Telemetry

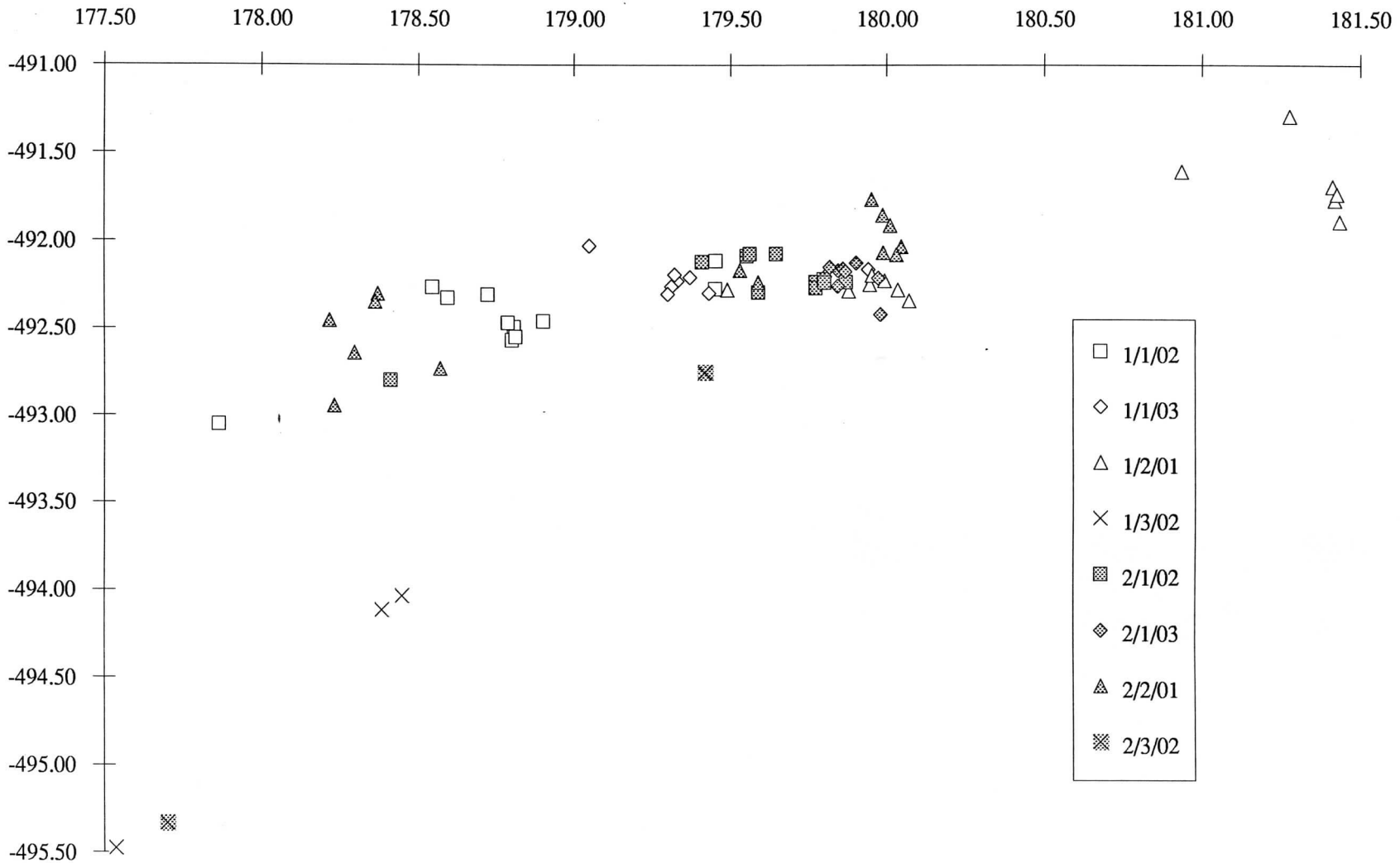

a/d/s - acquisition/dominant fgs/subdominant fgs

Deflection - FGS Difference - arc seconds

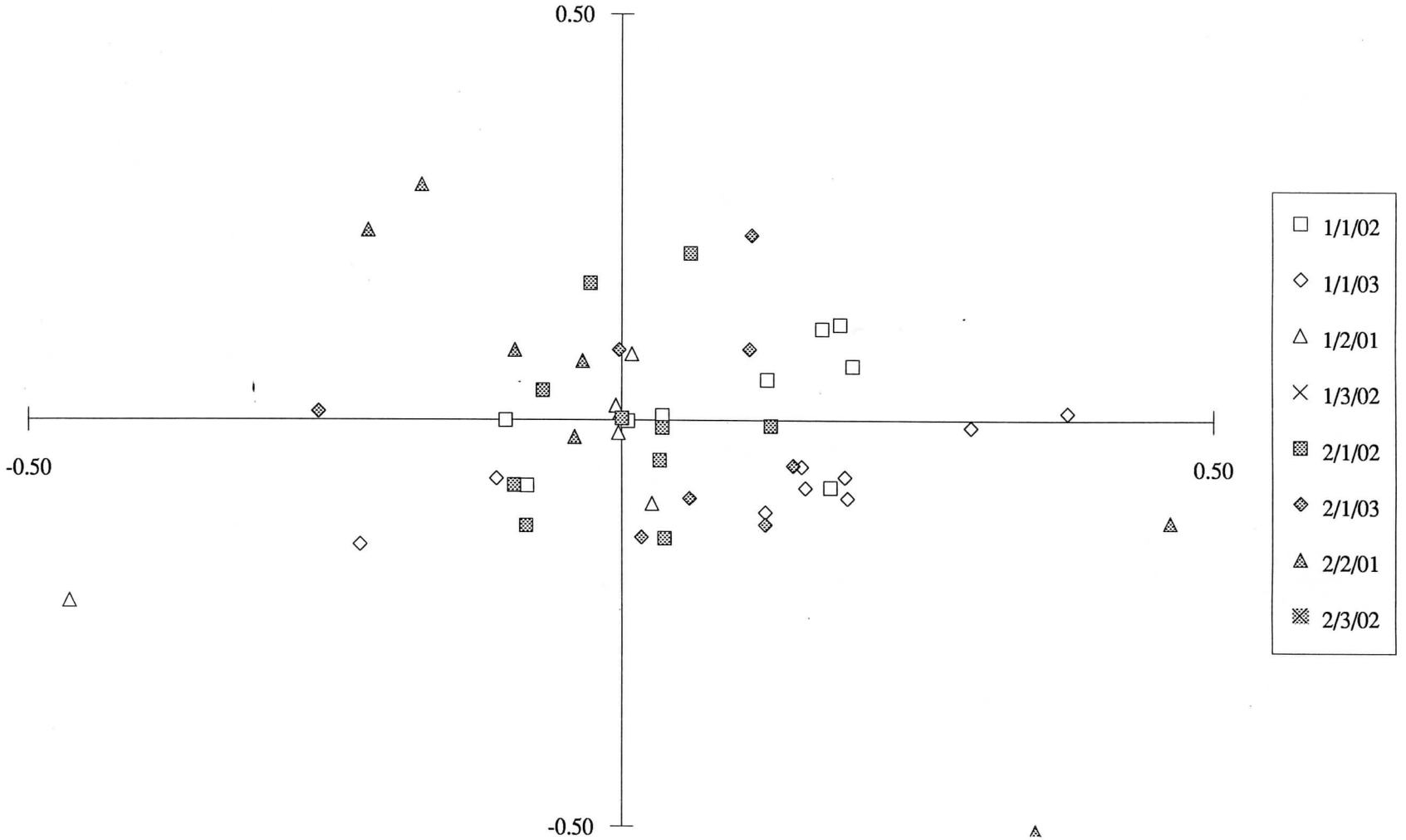

Appendix H - SIAF values - Aperture locations in HST V2, V3 coordinates (arc seconds)

Aperture	V2	V3
VPCENTER	+196.00000	-203.76230
VCLRP_A	+172.14820	-192.70940
VCLRP_T	+178.45590	-186.35250
VCLRP_S	+178.45590	-186.35250
VCLRP_C	+184.76370	-179.99580
VF327P0	+197.71360	-228.09910
VF327P90	+205.18890	-220.39410
VF327P45	+220.31870	-205.06420
VF327P135	+212.74860	-212.69940
VF277P0	+190.14860	-220.66440
VF277P90	+197.59360	-212.96970
VF277P45	+212.71360	-197.60960
VF277P135	+205.14390	-205.30950
VF237P0	+182.34880	-213.03980
VF237P90	+189.87840	-205.34950
VF237P45	+204.97360	-190.07920
VF237P135	+197.43330	-197.71480
VF216P0	+174.62800	-205.48440
VF216P90	+182.17830	-197.74950
VF216P45	+197.30380	-182.53990
VF216P135	+189.74880	-190.14910
VUV1CENTER	+156.95090	-470.34240
VF135U1_A	+136.63170	-443.62600
VF135U1_B	+121.59890	-448.99870
VF248U1_A	+136.63170	-443.62600
VF248U1_B	+171.82080	-431.81500
VF135U1_C	+142.31690	-453.05200
VF135U1_D	+135.19050	-455.49120
VF135U1_E	+128.06410	-457.93070
VF135U1_F	+120.93790	-460.37070
VF152U1_A	+157.92750	-447.71080
VF152U1_B	+165.05440	-445.27300
VF152U1_C	+172.18140	-442.83570
VF152U1_D	+179.30870	-440.39880
VF145U1_A	+145.73020	-463.03170
VF145U1_B	+138.60310	-465.47100
VF145U1_C	+131.47630	-467.91080
VF145U1_D	+124.34940	-470.35100
VF220U1_A	+161.34220	-457.68990
VF220U1_B	+168.46960	-455.25200
VF220U1_C	+175.59720	-452.81450
VF220U1_D	+182.72510	-450.37730
VF184U1_A	+149.14440	-473.01380
VF184U1_B	+142.01670	-475.45340
VF184U1_C	+134.88920	-477.89340
VF184U1_D	+127.76180	-480.33380
VF240U1_A	+164.75760	-467.67160
VF240U1_B	+171.88570	-465.23340
VF240U1_C	+179.01400	-462.79570
VF240U1_D	+186.14240	-460.35840
VF218U1_A	+152.55940	-482.99860
VF218U1_B	+145.43120	-485.43830
VF218U1_C	+138.30300	-487.87860

VF218U1_D	+131.17490	-490.31930
VF278U1_A	+168.17400	-477.65580
VF278U1_B	+175.30270	-475.21750
VF278U1_C	+182.43160	-472.77960
VF278U1_D	+189.56060	-470.34220
VF248U1_C	+155.97520	-492.98590
VF248U1_D	+148.84640	-495.42600
VF248U1_E	+141.71770	-497.86650
VF248U1_F	+134.58900	-500.30740
VCLRU1_A	+192.97990	-480.32850
VCLRU1_B	+185.85010	-482.76610
VCLRU1_D	+171.59130	-487.64270
VCLRU1_F	+192.32560	-491.71050
VCLRU1_T	+179.64170	-492.32800
VCLRU1_S	+179.64170	-492.32800
VF122U1_A	+156.33660	-504.02180
VF122U1_B	+149.20710	-506.46230
VF122U1_D	+142.07780	-508.90330
VUV2CENTER	+462.37020	-162.44890
VF145U2_A	+428.68060	-162.79110
VF145U2_B	+424.01480	-177.74540
VF262U2_A	+428.68060	-162.79110
VF262U2_B	+440.63610	-127.33600
VF179U2_A	+439.75320	-163.67660
VF179U2_B	+437.39530	-170.83010
VF179U2_C	+435.03780	-177.98370
VF179U2_D	+432.68060	-185.13770
VF184U2_A	+444.91970	-148.00760
VF184U2_B	+447.27890	-140.85460
VF184U2_C	+449.63860	-133.70170
VF184U2_D	+451.99880	-126.54890
VF160U2_A	+449.76870	-166.98030
VF160U2_B	+447.41070	-174.13430
VF160U2_C	+445.05300	-181.28870
VF160U2_D	+442.69570	-188.44310
VF218U2_A	+454.93570	-151.31000
VF218U2_B	+457.29510	-144.15640
VF218U2_C	+459.65500	-137.00290
VF218U2_D	+462.01540	-129.84950
VF278U2_A	+459.78680	-170.28480
VF278U2_B	+457.42850	-177.43950
VF278U2_C	+455.07070	-184.59440
VF278U2_D	+452.71330	-191.74960
VF248U2_A	+464.95410	-154.61330
VF248U2_B	+467.31380	-147.45900
VF248U2_C	+469.67390	-140.30490
VF248U2_D	+472.03460	-133.15100
VF284U2_A	+469.80750	-173.59030
VF284U2_B	+467.44900	-180.74550
VF284U2_C	+465.09100	-187.90110
VF284U2_D	+462.73340	-195.05680
VF152U2_A	+474.97520	-157.91730
VF152U2_B	+477.33510	-150.76240
VF152U2_C	+479.69540	-143.60780
VF152U2_D	+482.05630	-136.45310
VF145U2_C	+479.83080	-176.89660
VF145U2_D	+477.47210	-184.05260
VF145U2_E	+475.11390	-191.20870

VF145U2_F	+472.75610	-198.36500
VCLRU2_A	+492.08060	-139.75620
VCLRU2_B	+489.71960	-146.91140
VCLRU2_D	+484.99890	-161.22220
VCLRU2_F	+500.75850	-147.14920
VCLRU2_T	+493.59360	-157.63310
VCLRU2_S	+493.59360	-157.63310
VF122U2_A	+488.84570	-183.27090
VF122U2_B	+486.48710	-190.42760
VF122U2_D	+484.12890	-197.58460
VVCENTER	+345.85050	-352.60700
VF240V_A	+315.72200	-337.86510
VF240V_B	+304.72370	-348.89360
VF551V_A	+315.72200	-337.86510
VF551V_B	+342.35450	-311.45880
VF240V_C	+325.12480	-343.46810
VF240V_D	+319.78550	-348.78070
VF240V_E	+314.44620	-354.09380
VF240V_F	+309.10740	-359.40710
VF262V_A	+336.82180	-331.83220
VF262V_B	+342.16220	-326.52050
VF262V_C	+347.50290	-321.20920
VF262V_D	+352.84410	-315.89820
VF184V_A	+332.56210	-350.94620
VF184V_B	+327.22220	-356.25930
VF184V_C	+321.88270	-361.57270
VF184V_D	+316.54330	-366.88660
VCLRV_A	+344.26000	-339.30920
VCLRV_B	+349.60090	-333.99720
VCLRV_C	+354.94210	-328.68540
VCLRV_D	+360.28370	-323.37400
VF450V_A	+340.00130	-358.42620
VF450V_B	+334.66090	-363.73980
VF450V_C	+329.32090	-369.05370
VF450V_D	+323.98120	-374.36790
VF355V_A	+351.70010	-346.78820
VF355V_B	+357.04150	-341.47570
VF355V_C	+362.38310	-336.16360
VF355V_D	+367.72520	-330.85160
VF551V_C	+347.44220	-365.90810
VF551V_D	+342.10150	-371.22210
VF551V_E	+336.76100	-376.53660
VF551V_F	+331.42090	-381.85130
VF419V_A	+359.14220	-354.26910
VF419V_B	+364.48390	-348.95620
VF419V_C	+369.82620	-343.64350
VF419V_D	+375.16870	-338.33120
VF620V_A	+354.88530	-373.39200
VF620V_B	+349.54410	-378.70650
VF620V_C	+344.20320	-384.02140
VF620V_D	+338.86260	-389.33680
VCLRV_E	+382.61420	-345.81270
VCLRV_F	+377.27120	-351.12540
VCLRV_J	+387.00830	-356.33220
VCLRV_H	+366.58620	-361.75190
VCLRV_T	+375.87500	-362.44010
VCLRV_S	+375.87500	-362.44010
VF400V_A	+360.04090	-383.15570

VF400V_B	+354.69940	-388.47100
VF400V_D	+349.35810	-393.78660
VF750_F320	+373.14590	-380.04860
VPMTCENTER	+345.85050	-352.60700

Appendix I - SICF file values - HSP aperture locations in deflection coordinates (steps).

Aperture	H	V	Focus
CLRP_A	1557	3624	1500
CLRP_T	1816	3316	1500
CLRP_S	1976	3476	1500
CLRP_C	2694	3644	1500
F216P0	1117	2943	1500
F216P45	3147	2959	1500
F216P90	1800	2943	1500
F216P135	2474	2944	1500
F237P0	1131	2249	1500
F237P45	3148	2265	1500
F237P90	1806	2254	1500
F237P135	2477	2258	1500
F277P0	1140	1575	1500
F277P45	3157	1592	1500
F277P90	1812	1587	1500
F277P135	2483	1590	1500
F327P0	1141	890	1500
F327P45	3176	903	1500
F327P90	1820	904	1500
F327P135	2496	909	1500
CLRP_Z	2000	3000	1500
F216P_Z	2000	3000	1500
F237P_Z	2000	1900	1500
F277P_Z	2000	1900	1500
F327P_Z	3600	1900	1500
CLRP_X	2129	3635	1500
F216P_X	2135	2947	1500
F237P_X	2141	2257	1500
F277P_X	2148	1586	1500
F327P_X	2158	902	1500
CLRP_TX	2136	3636	1500
CLRU1_A	3151	2991	1500
CLRU1_B	2841	2981	1500
CLRU1_D	2231	2972	1500
CLRU1_F	2976	3424	1500
CLRU1_T	2156	2943	1500
CLRU1_S	2316	3103	1500
F122U1_A	1431	3410	1500
F122U1_B	1124	3412	1500
F122U1_D	812	3413	1500
F135U1_A	1450	812	1500
F135U1_B	827	793	1500
F135U1_C	1582	1257	1500
F135U1_D	1276	1253	1500
F135U1_E	967	1245	1500
F135U1_F	653	1233	1500
F145U1_A	1581	1690	1500
F145U1_B	1277	1688	1500
F145U1_C	969	1682	1500
F145U1_D	657	1673	1500
F152U1_A	2247	1257	1500
F152U1_B	2552	1256	1500

F152U1_C	2860	1256	1500
F152U1_D	3172	1256	1500
F184U1_A	1578	2118	1500
F184U1_B	1275	2117	1500
F184U1_C	968	2112	1500
F184U1_D	657	2106	1500
F218U1_A	1574	2544	1500
F218U1_B	1271	2544	1500
F218U1_C	964	2542	1500
F218U1_D	653	2538	1500
F220U1_A	2242	1690	1500
F220U1_B	2545	1690	1500
F220U1_C	2851	1692	1500
F220U1_D	3161	1694	1500
F240U1_A	2238	2117	1500
F240U1_B	2540	2118	1500
F240U1_C	2845	2121	1500
F240U1_D	3154	2126	1500
F248U1_A	2385	813	1500
F248U1_B	3006	810	1500
F248U1_C	1569	2973	1500
F248U1_D	1265	2974	1500
F248U1_E	957	2974	1500
F248U1_F	644	2973	1500
F278U1_A	2234	2543	1500
F278U1_B	2536	2545	1500
F278U1_C	2841	2550	1500
F278U1_D	3151	2557	1500
CLRU1_Z	2000	3000	1500
F122U1_Z	2000	3000	1500
F135U1_Z	2000	1900	1500
F145U1_Z	2000	1900	1500
F152U1_Z	3600	1900	1500
F184U1_Z	2000	1900	1500
F218U1_Z	2000	3000	1500
F220U1_Z	3600	1900	1500
F240U1_Z	3600	1900	1500
F248U1_Z	2000	1900	1500
F278U1_Z	2000	3000	1500
F248U1PZ	3600	1900	1500
F135U1PZ	2000	1900	1500
CLRU1_X	2735	3126	1500
F122U1_X	1122	3412	1500
F135U1PX	1139	803	1500
F145U1_X	1121	1683	1500
F152U1_X	2708	1256	1500
F184U1_X	1120	2113	1500
F218U1_X	1116	2542	1500
F220U1_X	2700	1692	1500
F240U1_X	2694	2121	1500
F248U1PX	2696	812	1500
F278U1_X	2691	2549	1500
F135U1_X	1120	1247	1500
F248U1_X	1109	2974	1500
CLRU1_TX	2476	3263	1500
CLRV_A	2340	1581	1500
CLRV_B	2633	1583	1500
CLRV_C	2929	1585	1500

CLRV_D	3232	1586	1500
CLRV_E	3207	2873	1500
CLRV_F	2902	2861	1500
CLRV_H	2308	2846	1500
CLRV_J	3033	3312	1500
CLRV_T	2223	2824	1500
CLRV_S	2383	2984	1500
F184V_A	1703	1572	1500
F184V_B	1408	1566	1500
F184V_C	1107	1560	1500
F184V_D	799	1552	1500
F240V_A	1589	704	1500
F240V_B	978	679	1500
F240V_C	1711	1146	1500
F240V_D	1414	1139	1500
F240V_E	1112	1129	1500
F240V_F	802	1117	1500
F262V_A	2353	1156	1500
F262V_B	2648	1157	1500
F262V_C	2947	1157	1500
F262V_D	3252	1154	1500
F355V_A	2329	2000	1500
F355V_B	2620	2004	1500
F355V_C	2916	2008	1500
F355V_D	3218	2012	1500
F400V_A	1517	3283	1500
F400V_B	1213	3287	1500
F400V_D	901	3295	1500
F419V_A	2318	2419	1500
F419V_B	2611	2424	1500
F419V_C	2907	2431	1500
F419V_D	3210	2438	1500
F450V_A	1692	1992	1500
F450V_B	1398	1988	1500
F450V_C	1098	1985	1500
F450V_D	790	1981	1500
F551V_A	2496	719	1500
F551V_B	3100	713	1500
F551V_C	1680	2412	1500
F551V_D	1384	2411	1500
F551V_E	1083	2410	1500
F551V_F	774	2411	1500
F620V_A	1664	2840	1500
F620V_B	1366	2841	1500
F620V_C	1062	2844	1500
F620V_D	750	2849	1500
F750F320	1964	3495	1500
CLRV_Z	3600	1900	1500
F184V_Z	2000	1900	1500
F240V_Z	2000	1900	1500
F262V_Z	3600	1900	1500
F355V_Z	3600	1900	1500
F400V_Z	2000	3000	1500
F419V_Z	2000	3000	1500
F450V_Z	2000	1900	1500
F551V_Z	2000	1900	1500
F620V_Z	2000	3000	1500
F551VPZ	3600	1900	1500

F240VPZ	2000	1900	1500
CLRV_X	2784	1584	1500
F184V_X	1254	1563	1500
F240VPX	1284	692	1500
F262V_X	2800	1156	1500
F355V_X	2771	2006	1500
F400V_X	1210	3288	1500
F419V_X	2762	2428	1500
F450V_X	1245	1987	1500
F551VPX	2798	716	1500
F620V_X	1211	2844	1500
F240V_X	1260	1133	1500
F551V_X	1230	2411	1500
CLRVT_X	2799	3007	1500
CLRV_TX	2543	3144	1500
CLRU2_A	3265	2951	1500
CLRU2_B	2952	2944	1500
CLRU2_D	2339	2934	1500
CLRU2_F	3089	3391	1500
CLRU2_T	2266	2911	1500
CLRU2_S	2426	3071	1500
F122U2_A	1539	3368	1500
F122U2_B	1233	3368	1500
F122U2_D	924	3370	1500
F145U2_A	1558	746	1500
F145U2_B	940	733	1500
F145U2_C	1675	2928	1500
F145U2_D	1371	2927	1500
F145U2_E	1065	2927	1500
F145U2_F	756	2928	1500
F152U2_A	2341	2500	1500
F152U2_B	2645	2503	1500
F152U2_C	2953	2507	1500
F152U2_D	3264	2511	1500
F160U2_A	1685	1631	1500
F160U2_B	1382	1627	1500
F160U2_C	1077	1623	1500
F160U2_D	768	1618	1500
F179U2_A	1688	1194	1500
F179U2_B	1383	1190	1500
F179U2_C	1076	1184	1500
F179U2_D	766	1177	1500
F184U2_A	2354	1198	1500
F184U2_B	2661	1198	1500
F184U2_C	2970	1196	1500
F184U2_D	3284	1193	1500
F218U2_A	2349	1636	1500
F218U2_B	2653	1636	1500
F218U2_C	2961	1637	1500
F218U2_D	3273	1636	1500
F248U2_A	2344	2068	1500
F248U2_B	2648	2071	1500
F248U2_C	2955	2072	1500
F248U2_D	3267	2074	1500
F262U2_A	2493	752	1500
F262U2_B	3117	745	1500
F278U2_A	1683	2063	1500
F278U2_B	1380	2061	1500

F278U2_C	1075	2058	1500
F278U2_D	767	2055	1500
F284U2_A	1679	2495	1500
F284U2_B	1376	2493	1500
F284U2_C	1071	2491	1500
F284U2_D	763	2490	1500
CLRU2_Z	2000	3000	1500
F122U2_Z	2000	3000	1500
F145U2_Z	2000	1900	1500
F152U2_Z	2000	3000	1500
F160U2_Z	2000	1900	1500
F179U2_Z	2000	1900	1500
F184U2_Z	3600	1900	1500
F218U2_Z	3600	1900	1500
F248U2_Z	3600	1900	1500
F262U2_Z	3600	1900	1500
F278U2_Z	2000	1900	1500
F284U2_Z	2000	3000	1500
F262U2PZ	3600	1900	1500
F145U2PZ	2000	1900	1500
CLRU2T_X	2846	3090	1500
F122U2_X	1232	3369	1500
F145U2PX	1249	740	1500
F152U2_X	2801	2505	1500
F160U2_X	1228	1625	1500
F179U2_X	1228	1186	1500
F184U2_X	2817	1196	1500
F218U2_X	2809	1636	1500
F248U2_X	2804	2071	1500
F262U2PX	2805	749	1500
F278U2_X	1226	2059	1500
F284U2_X	1222	2492	1500
F145U2_X	1217	2928	1500
CLRU2_TX	2586	3231	1500
DARK1P	2000	1900	1500
DARK1U1	2000	1900	1500
DARK1V	2000	1900	1500
DARK1U2	2000	1900	1500
DARK2P	3600	1900	1500
DARK2U1	3600	1900	1500
DARK2V	3600	1900	1500
DARK2U2	3600	1900	1500
DARK3P	2000	3000	1500
DARK3U1	2000	3000	1500
DARK3V	2000	3000	1500
DARK3U2	2000	3000	1500
ZERODEFL	0	0	1500
PROTECT1	2000	600	1500
PROTECT3	1000	900	1500

Appendix J - SMS Activity Timelines

The HSP parser produces various products, one of which is a graphic timeline showing various HSP, SI, and ST activities. The timeline covers the entire period of the SMS, ususally seven days.

913017b5

SMS Chart version 2.14 (11/10/91) by Jeffrey W Percival

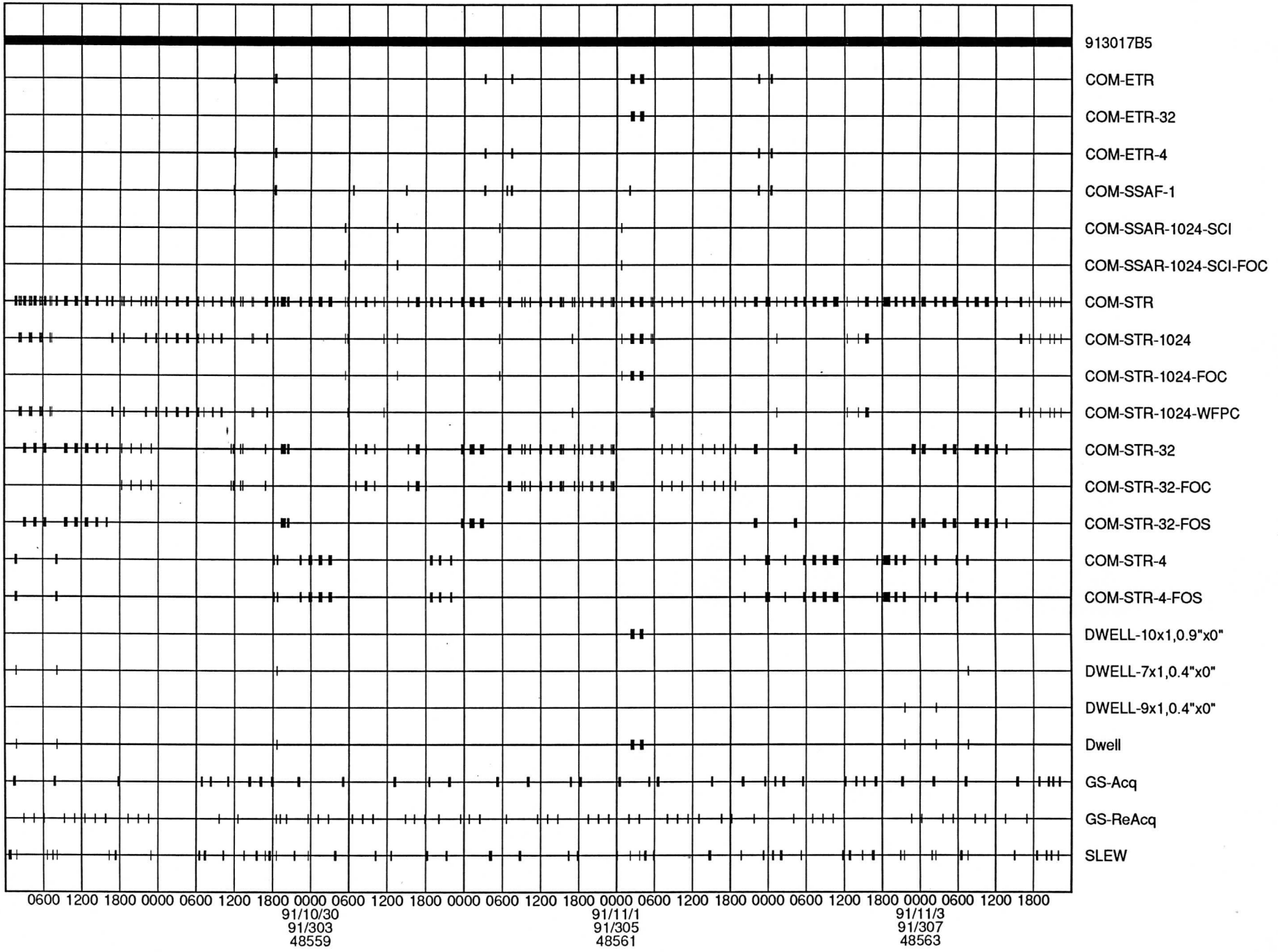

913087d4

SMS Chart version 2.14 (11/10/91) by Jeffrey W Percival

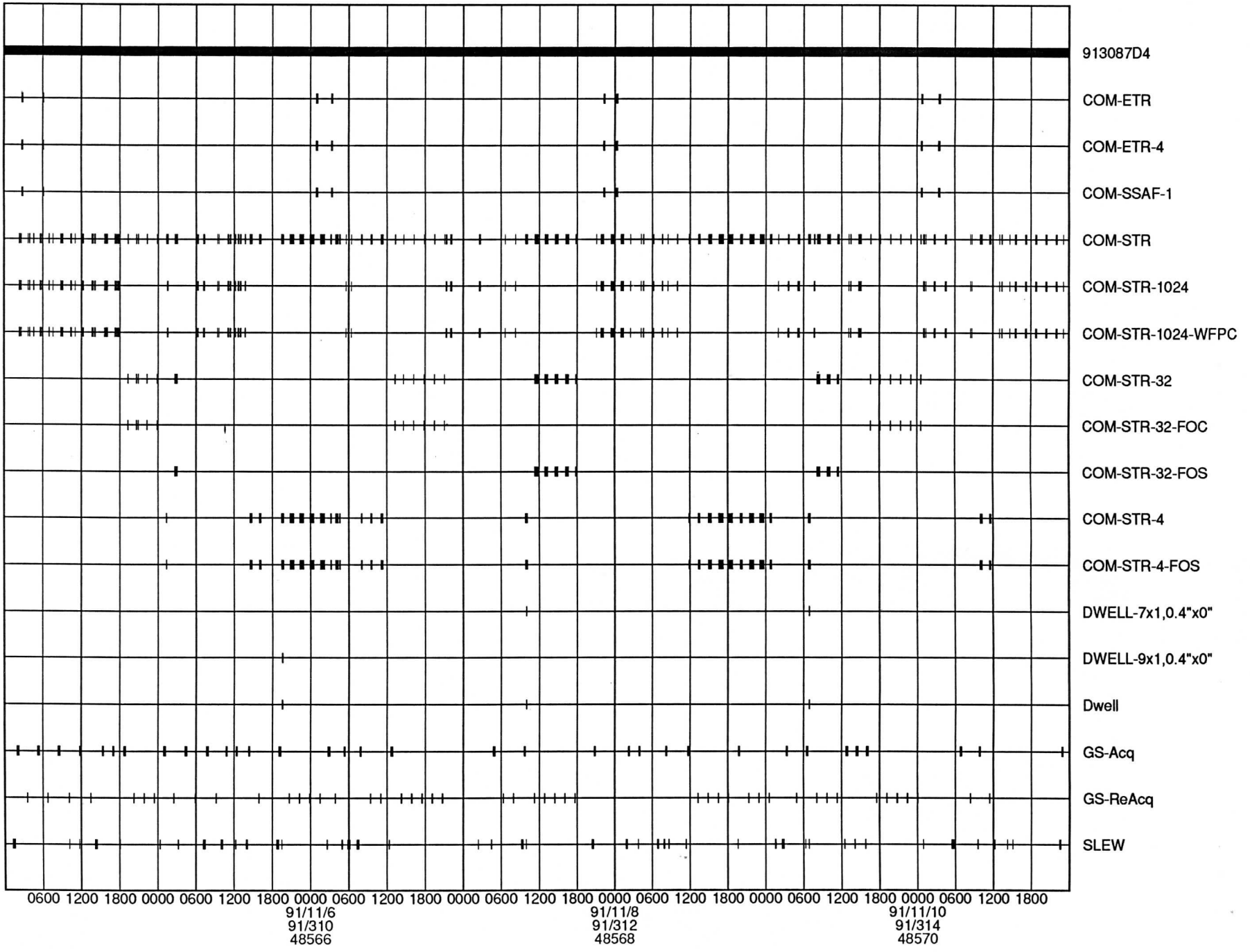

913157aa

SMS Chart version 2.14 (11/10/91) by Jeffrey W Percival

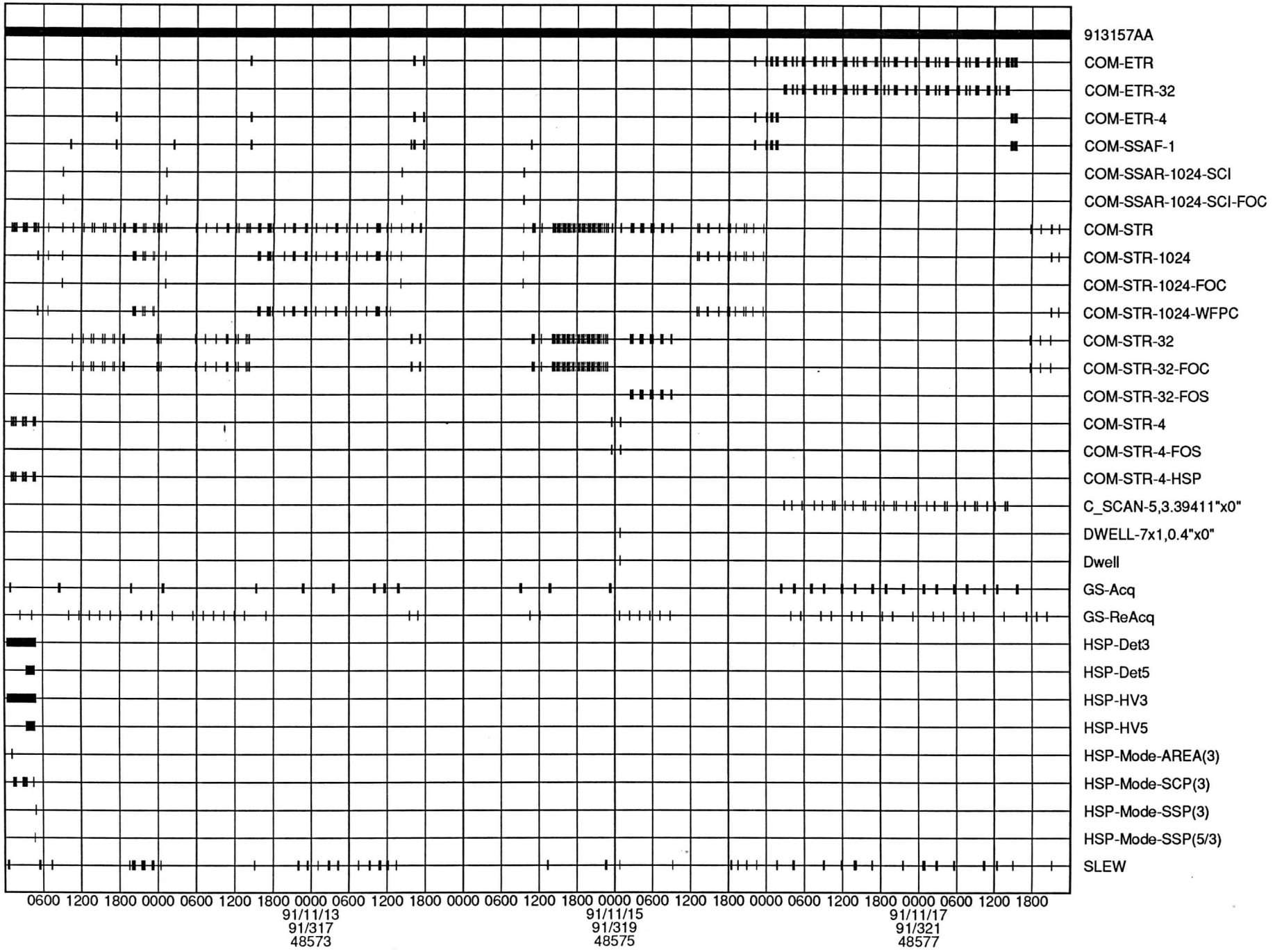

913227c4

SMS Chart version 2.14 (11/10/91) by Jeffrey W Percival

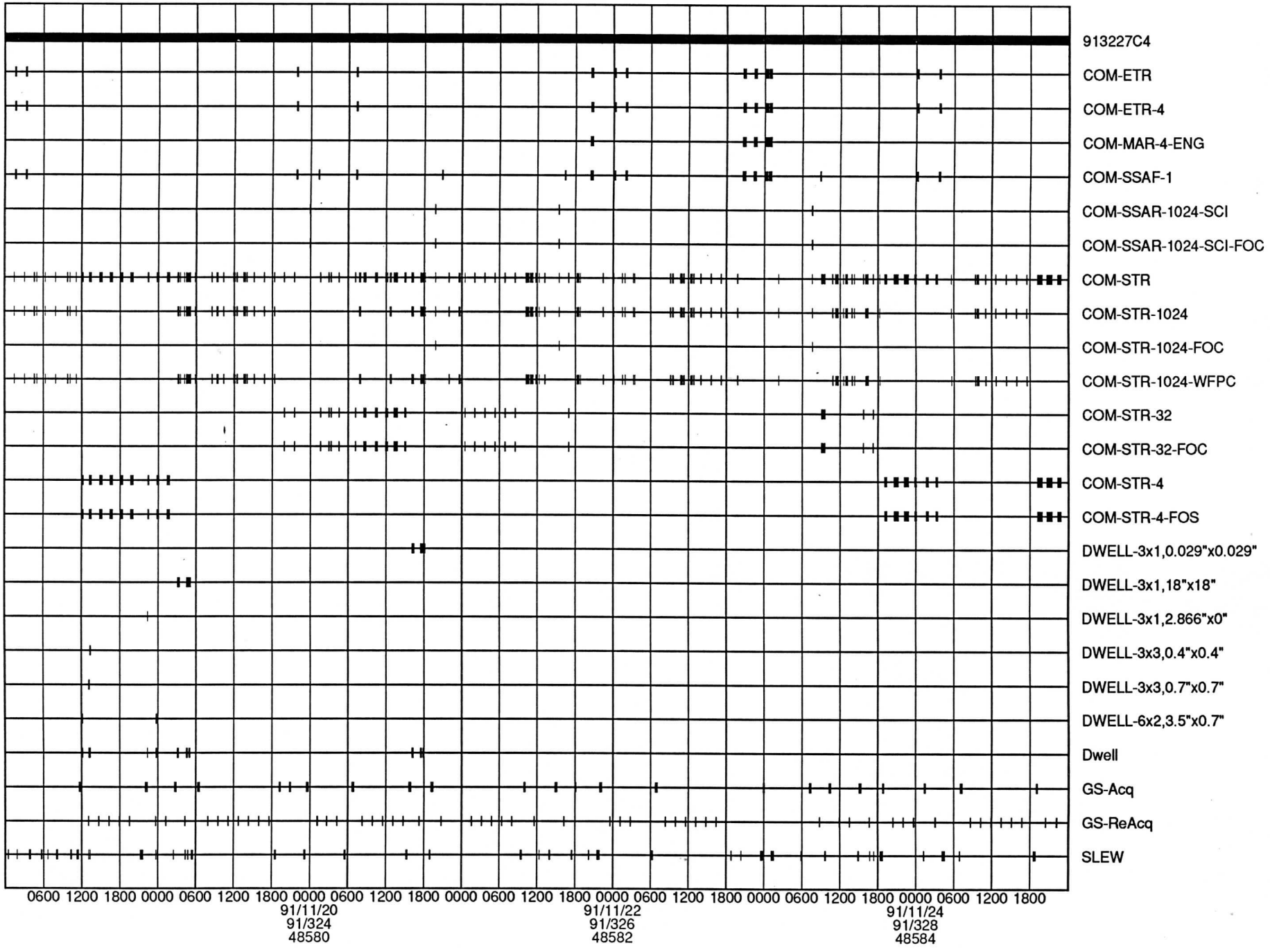

913297b7

SMS Chart version 2.14 (11/10/91) by Jeffrey W Percival

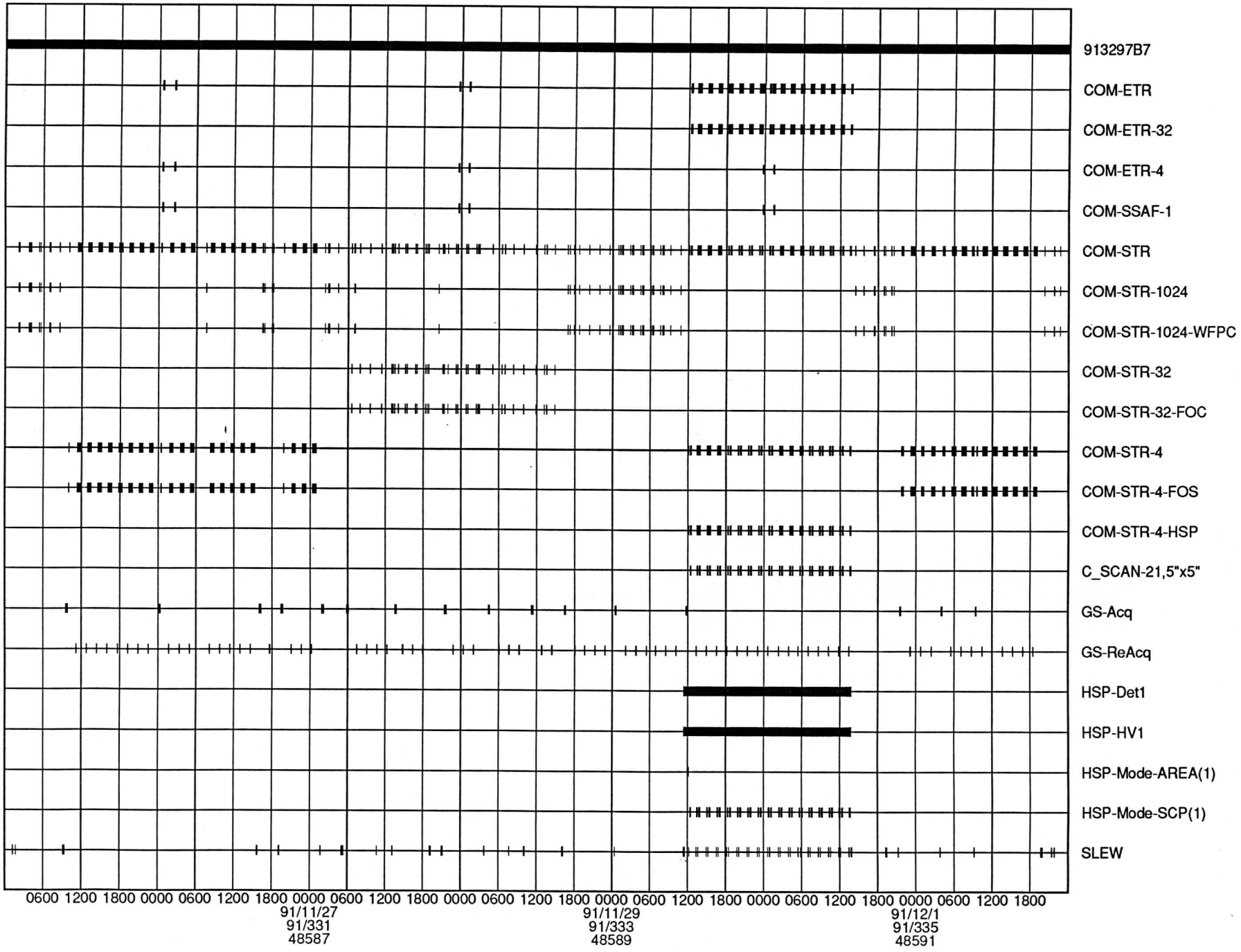

913367e3

SMS Chart version 2.14 (11/10/91) by Jeffrey W Percival

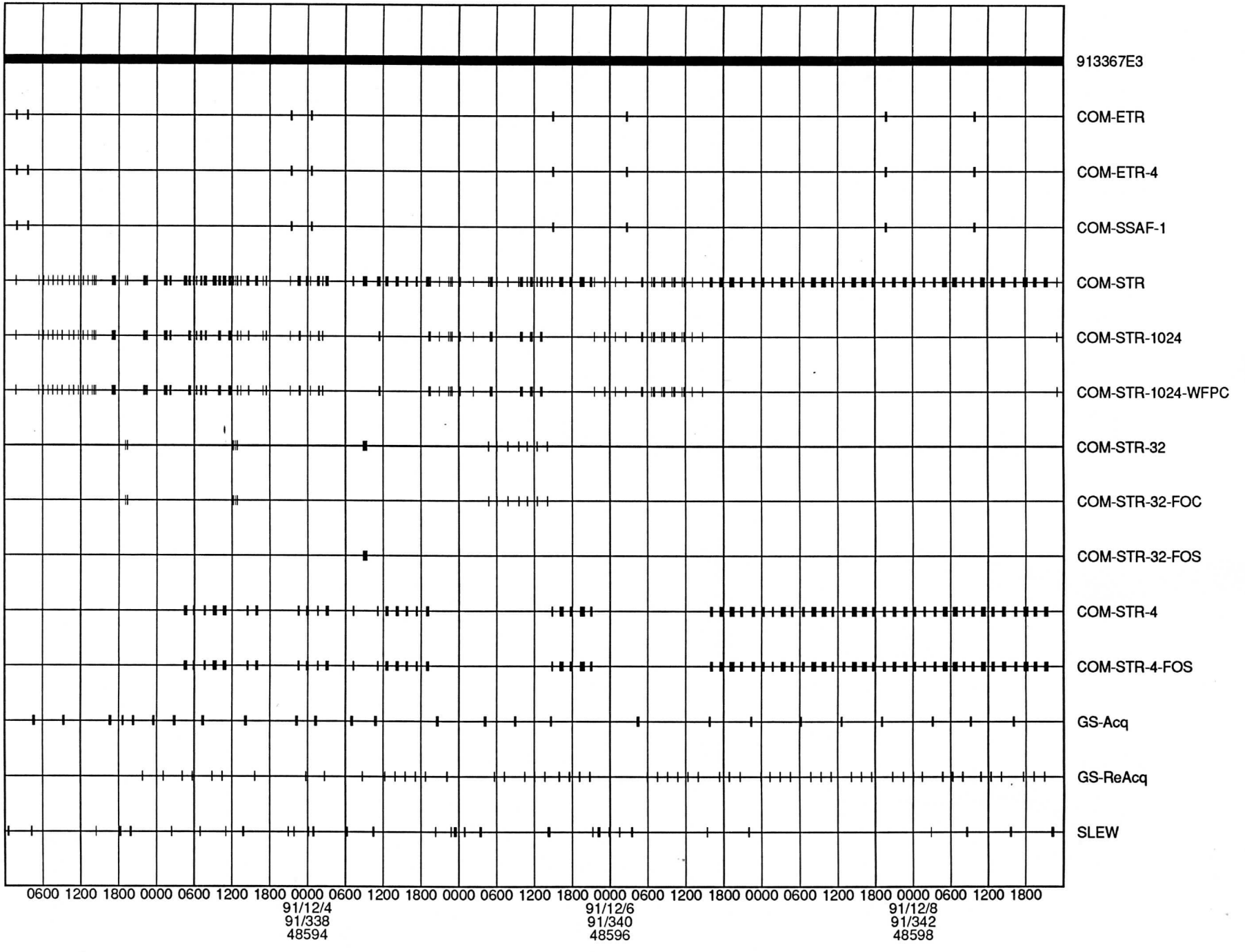

913507dg

SMS Chart version 2.14 (11/10/91) by Jeffrey W Percival

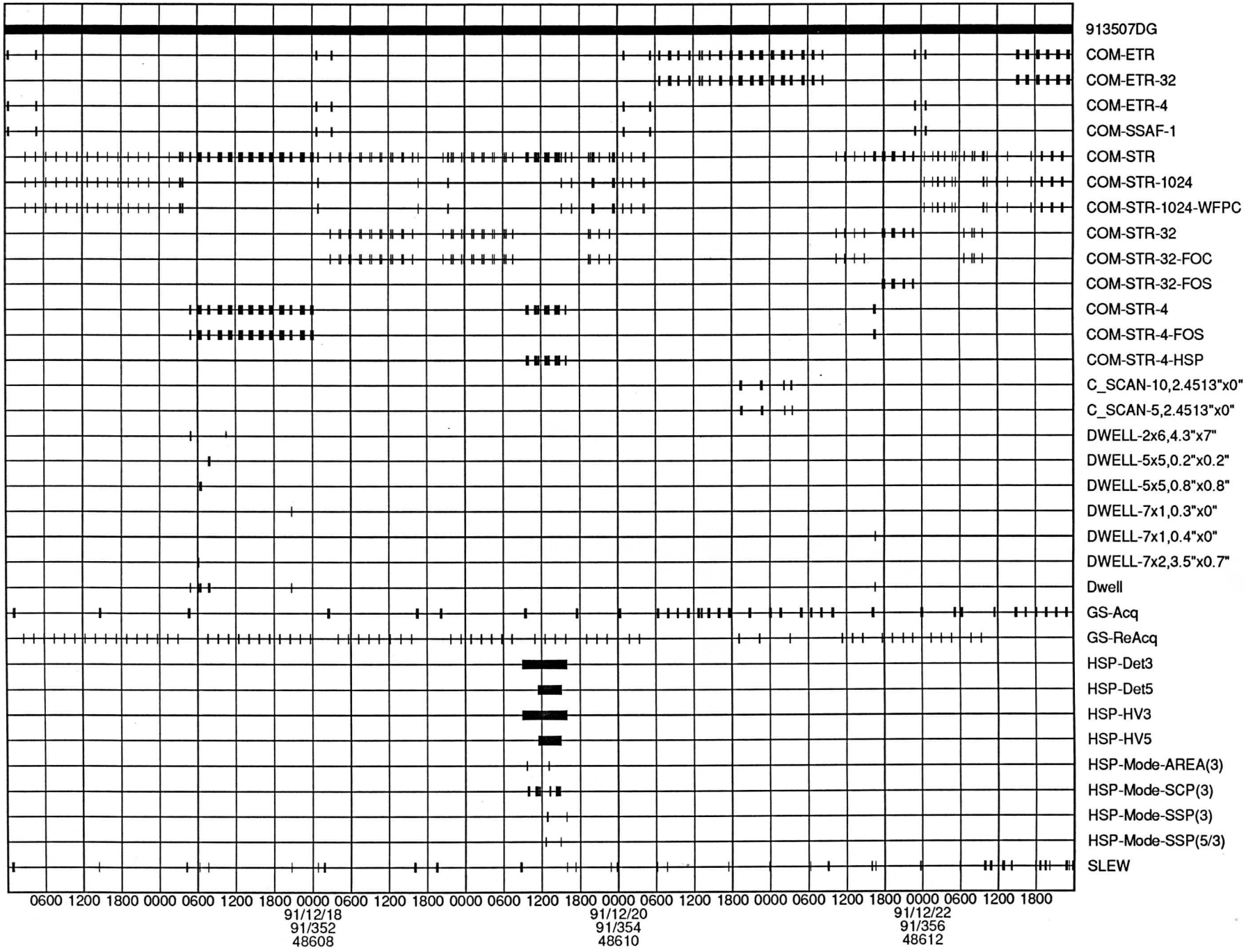

913577b2

SMS Chart version 2.14 (11/10/91) by Jeffrey W Percival

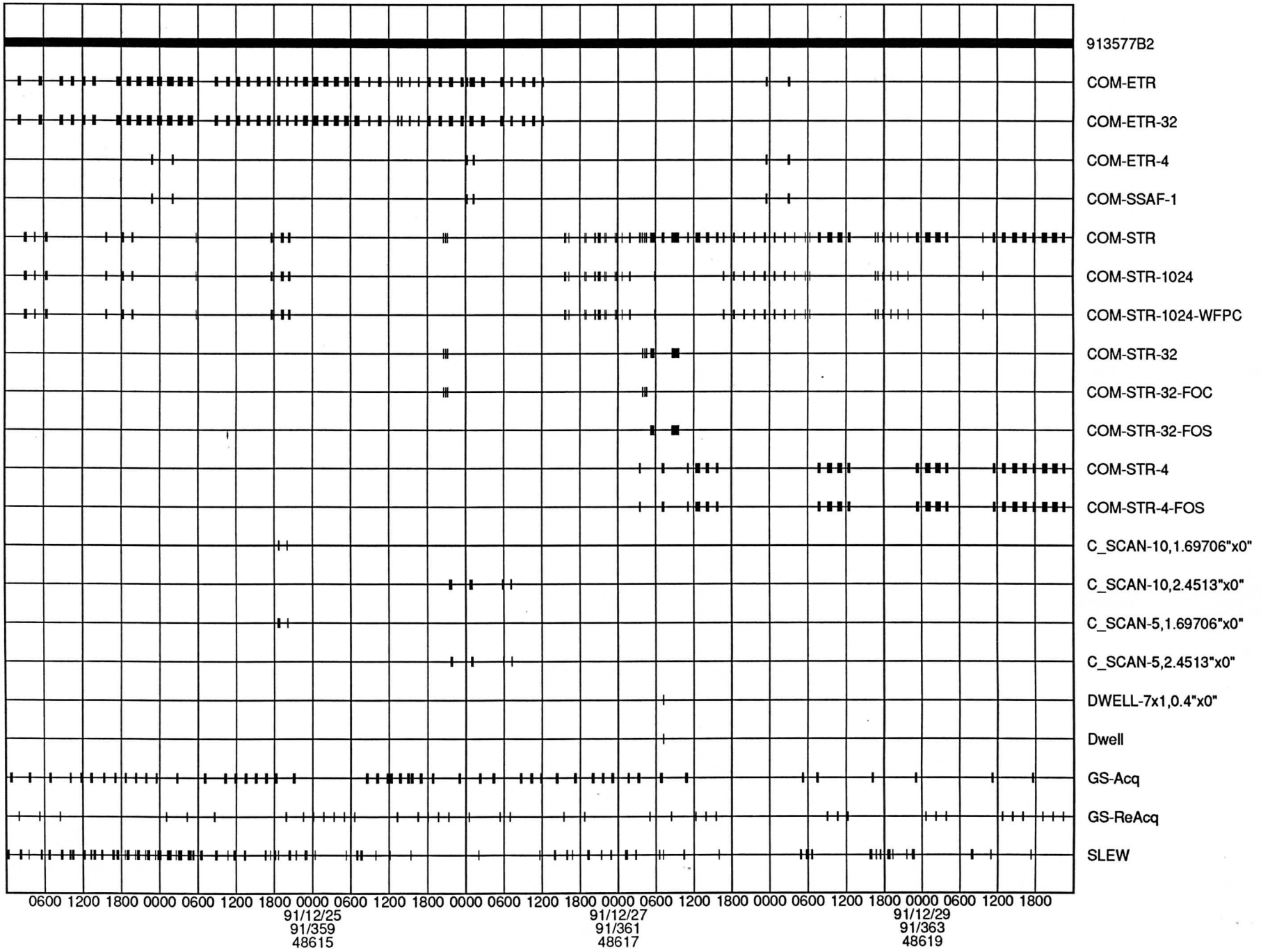

913647e7

SMS Chart version 2.15 (2/14/92) by Jeffrey W Percival

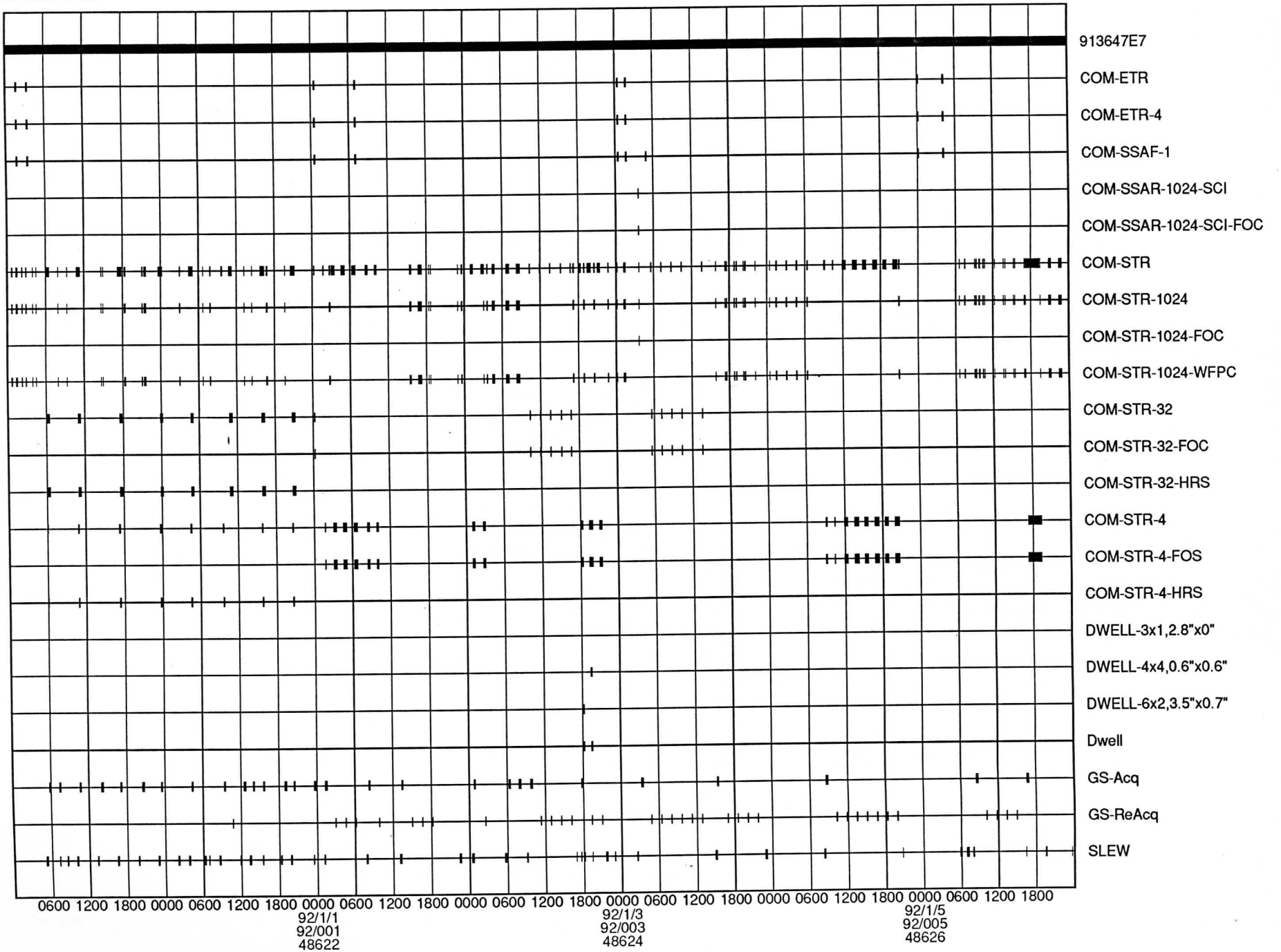

920067c7

SMS Chart version 2.14 (11/10/91) by Jeffrey W Percival

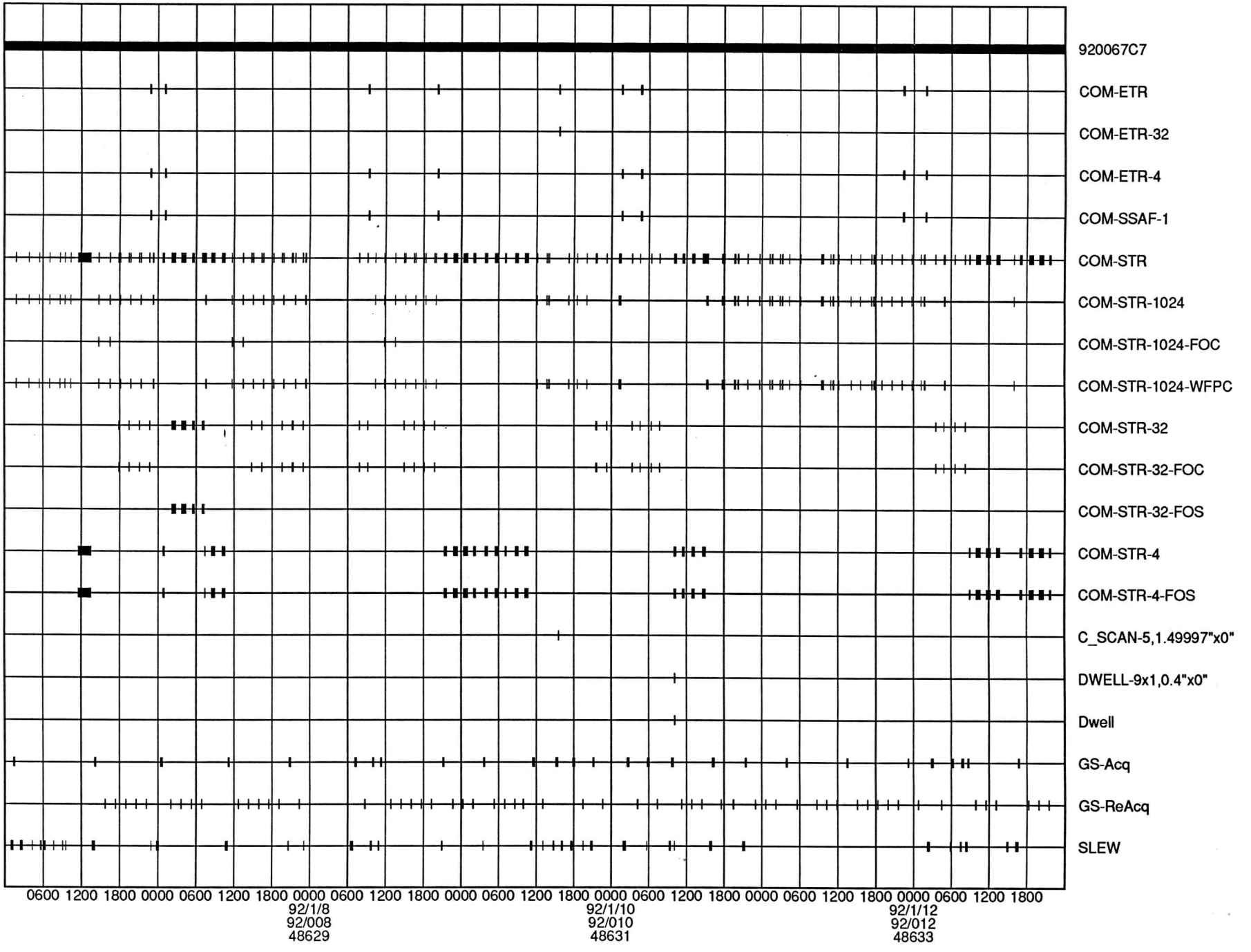

920137d2

SMS Chart version 2.14 (11/10/91) by Jeffrey W Percival

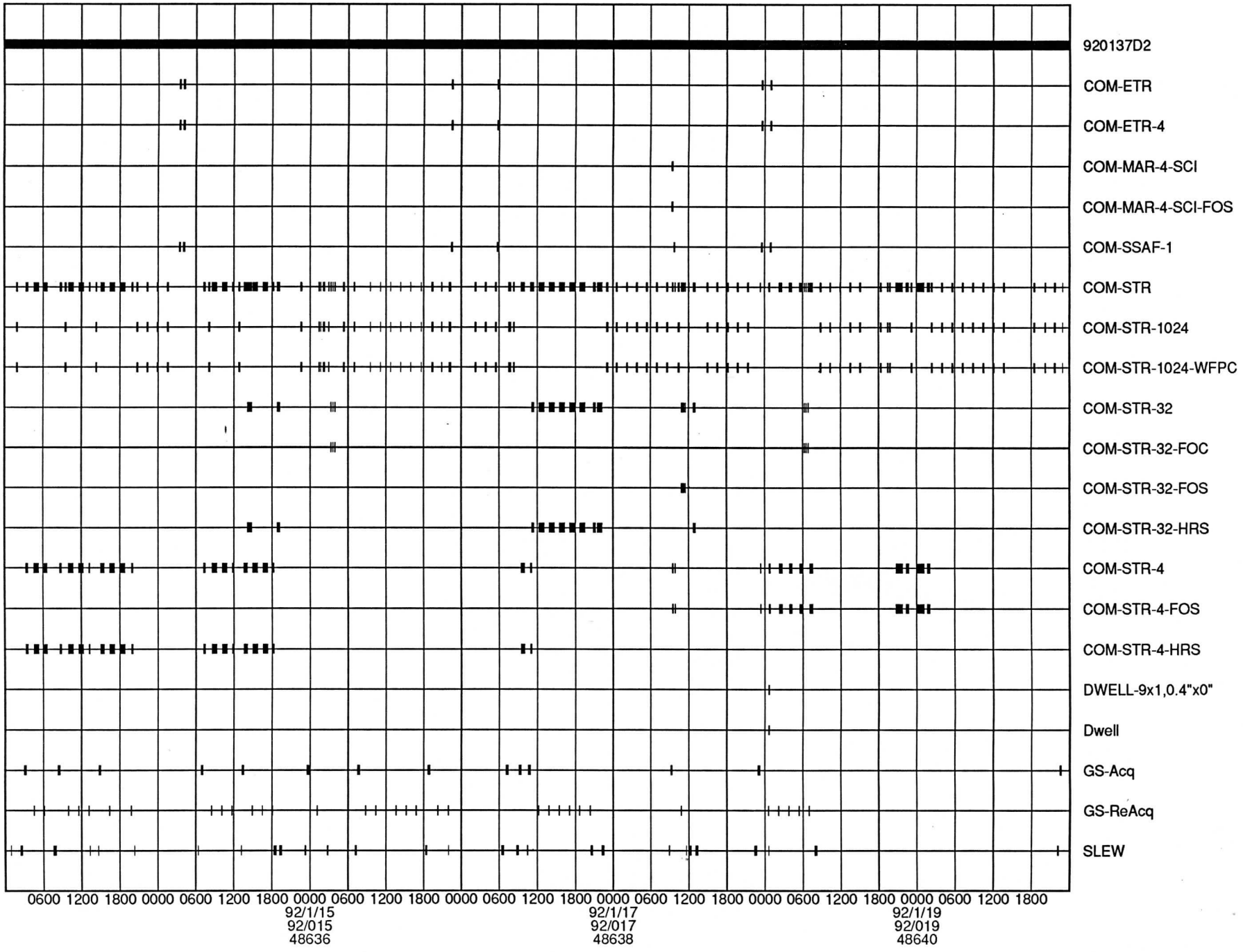

920207b2r

SMS Chart version 2.14 (11/10/91) by Jeffrey W Percival

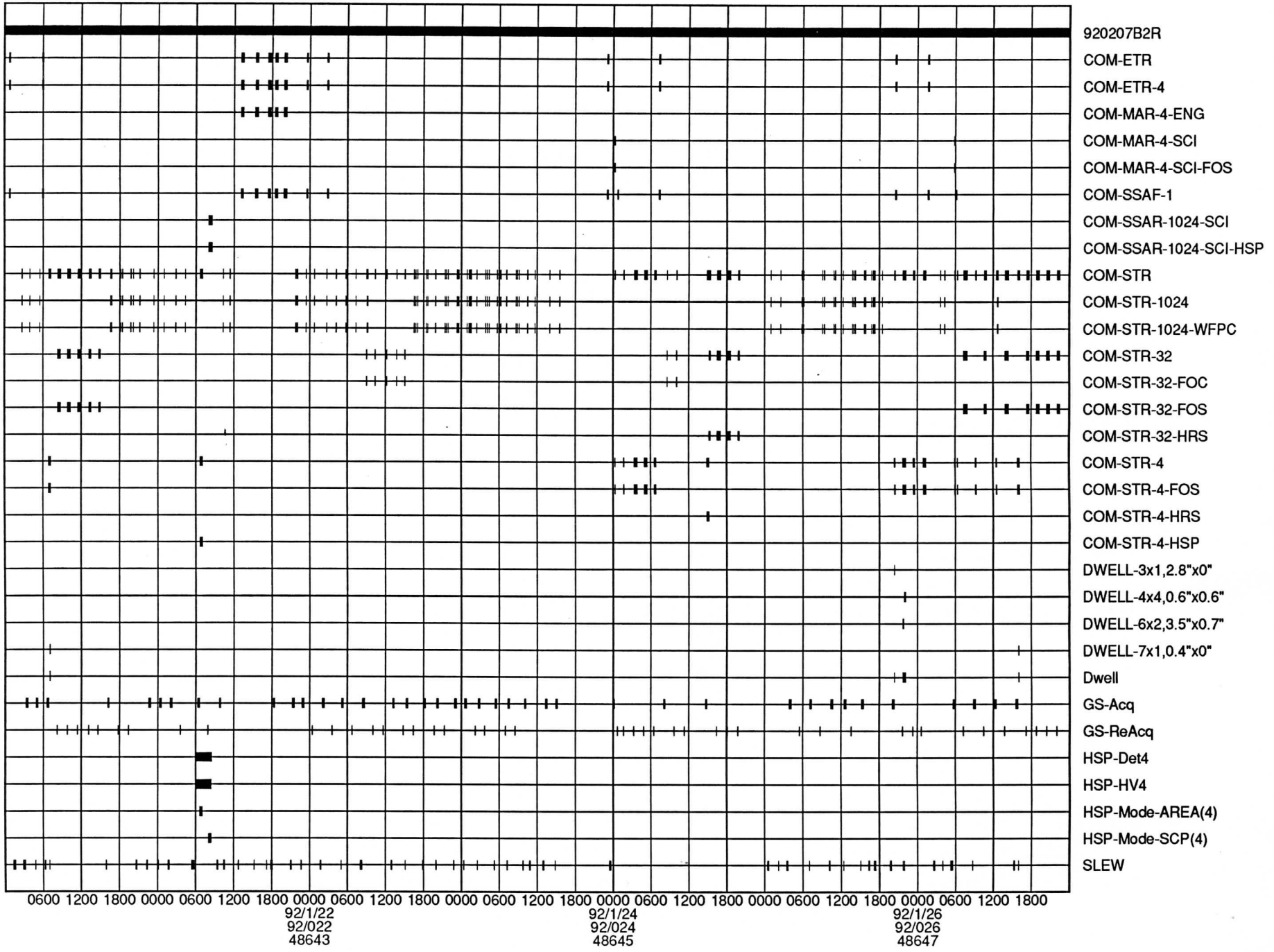

920277ac

SMS Chart version 2.14 (11/10/91) by Jeffrey W Percival

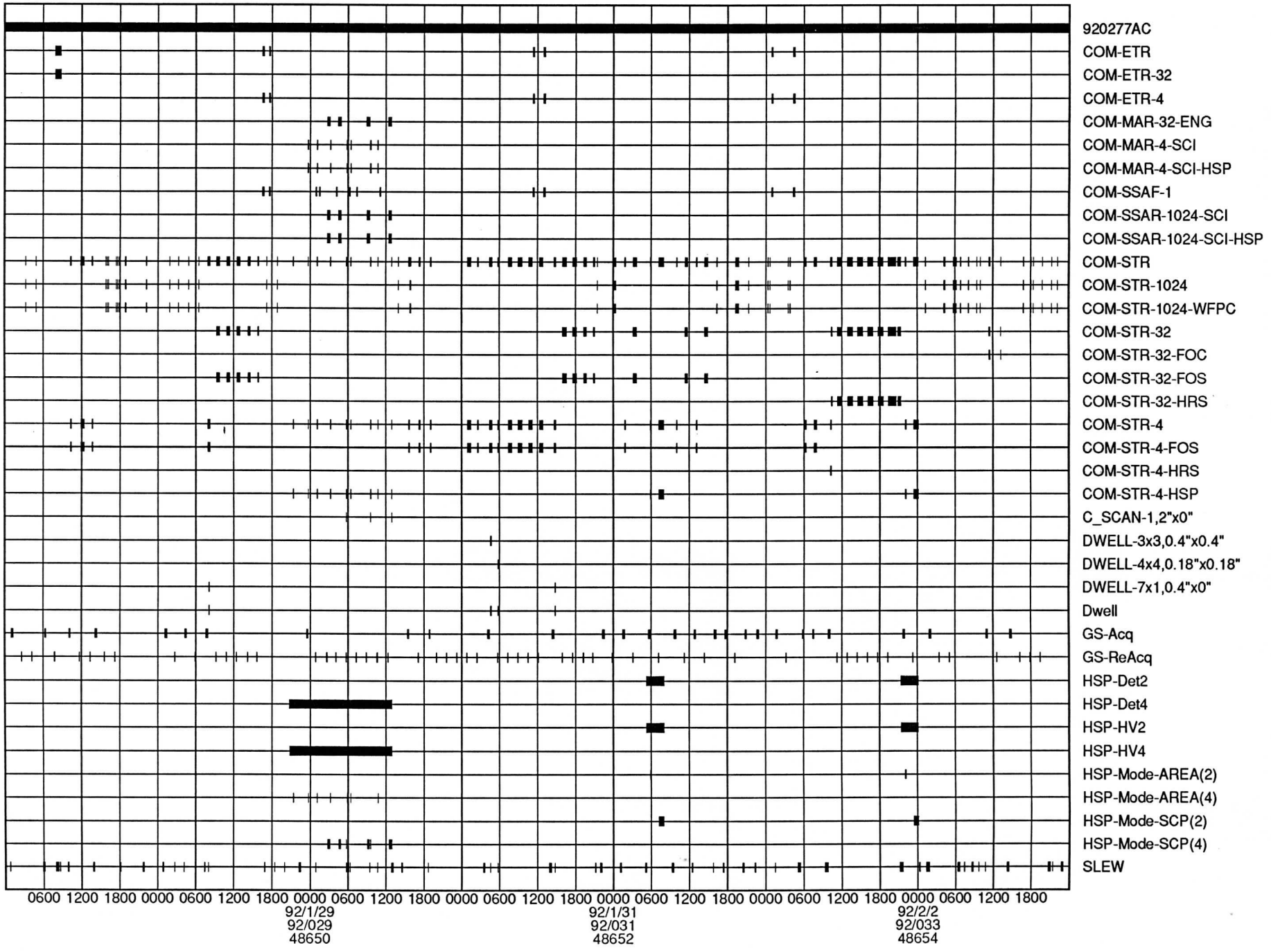

920347c1

SMS Chart version 2.14 (11/10/91) by Jeffrey W Percival

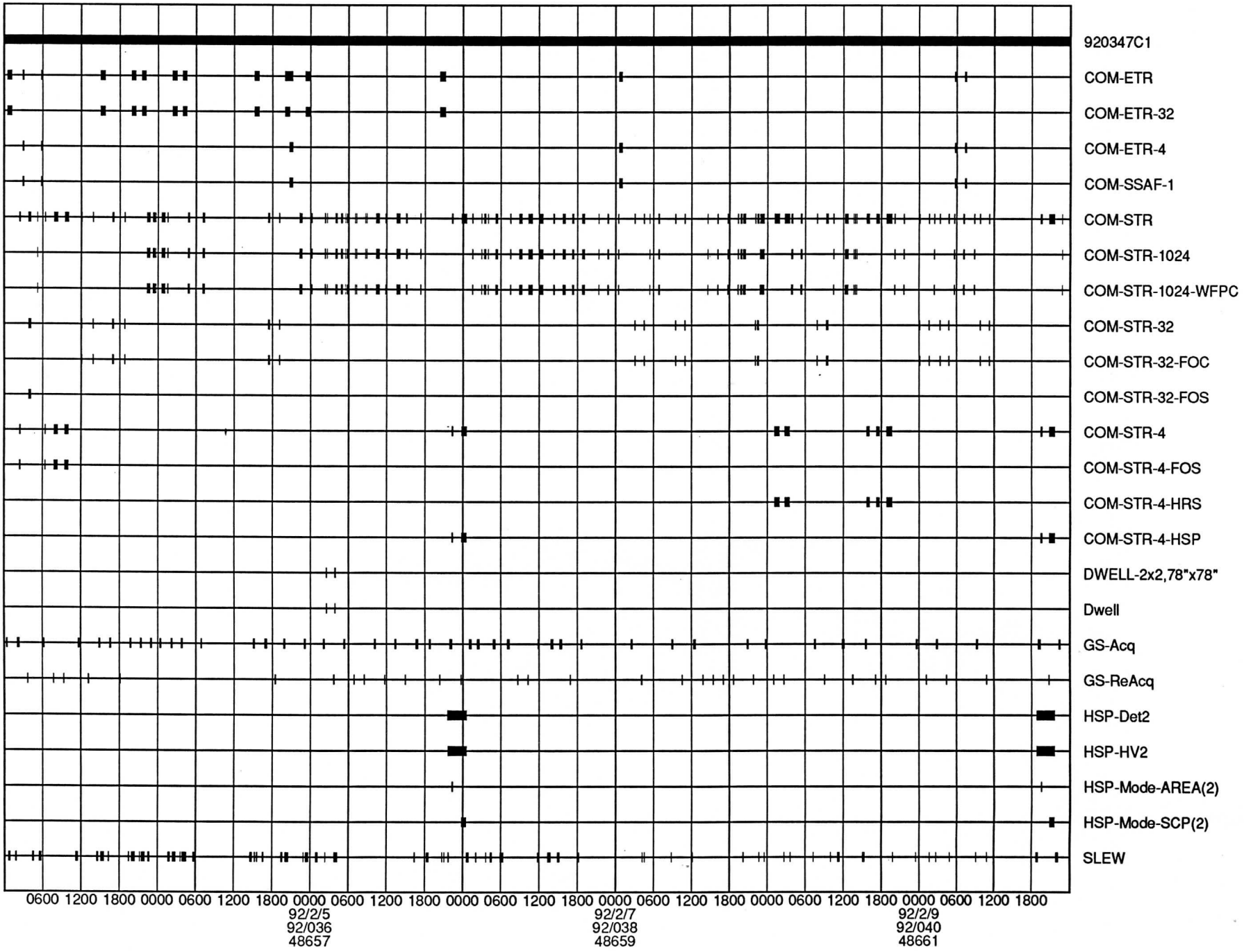

920417b6

SMS Chart version 2.14 (11/10/91) by Jeffrey W Percival

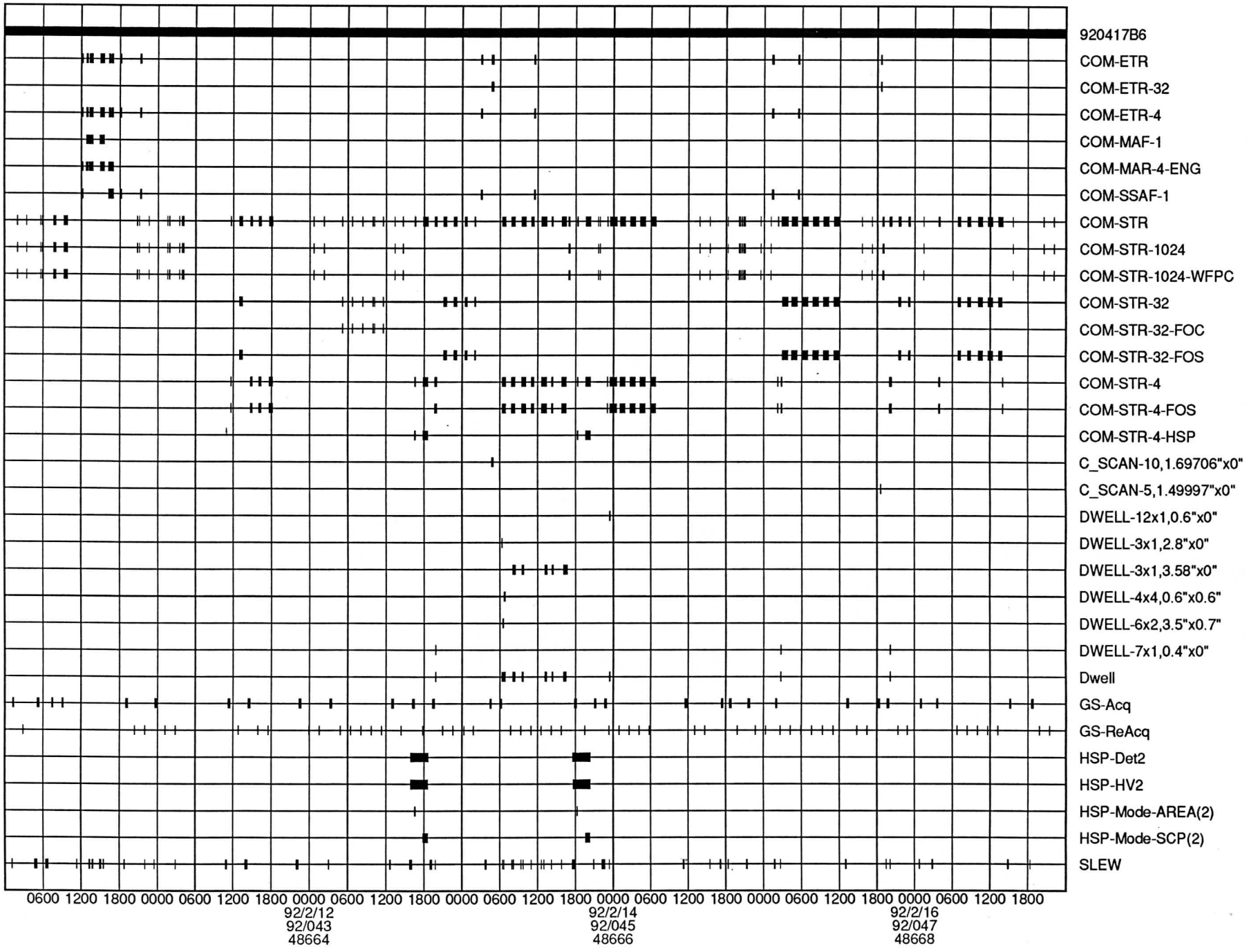

920487ah

SMS Chart version 2.14 (11/10/91) by Jeffrey W Percival

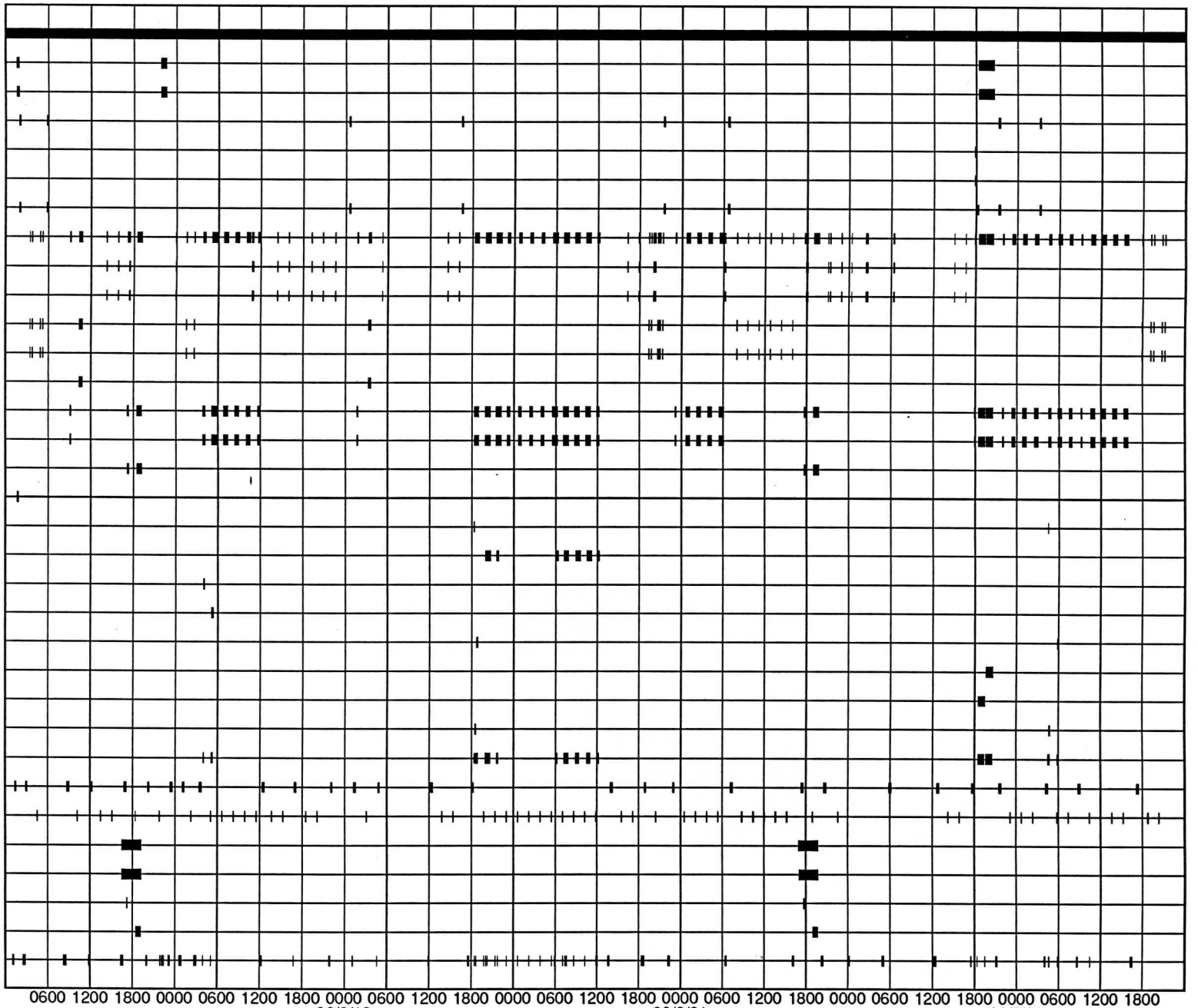

920557f1

SMS Chart version 2.15 (2/14/92) by Jeffrey W Percival

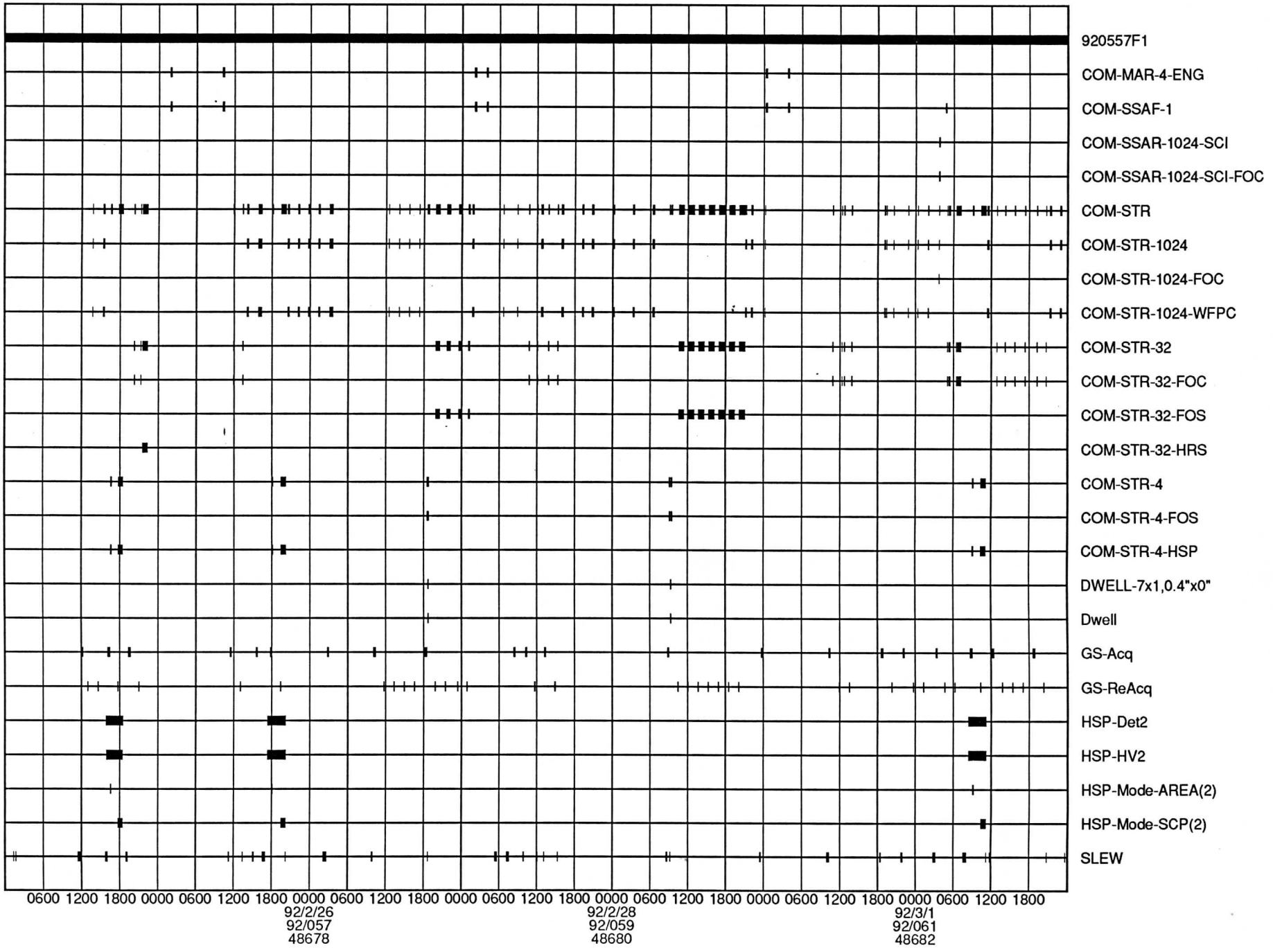

920627c6

SMS Chart version 2.15 (2/14/92) by Jeffrey W Percival

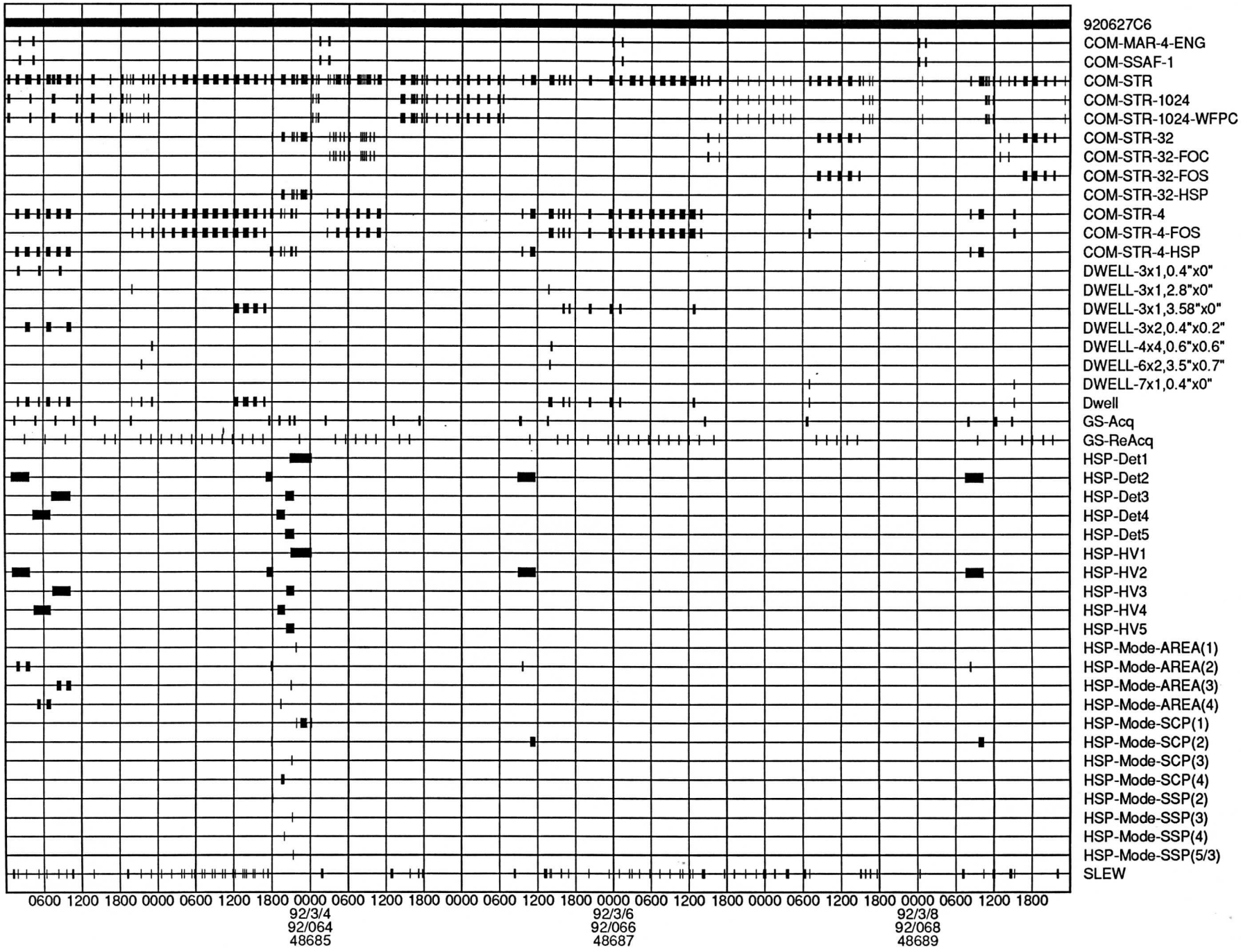

920697ci

SMS Chart version 2.15 (2/14/92) by Jeffrey W Percival

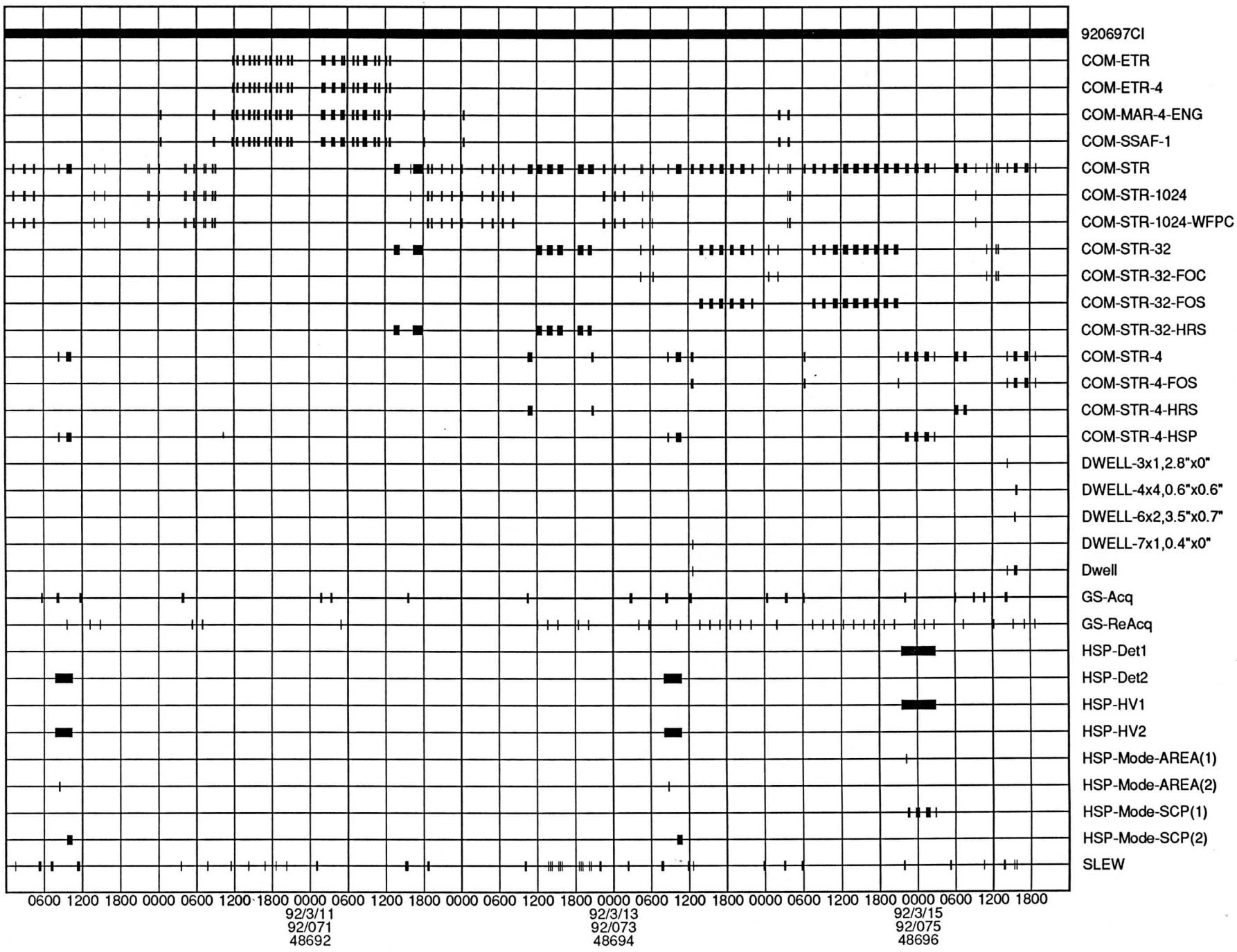

920767b4

SMS Chart version 2.15 (2/14/92) by Jeffrey W Percival

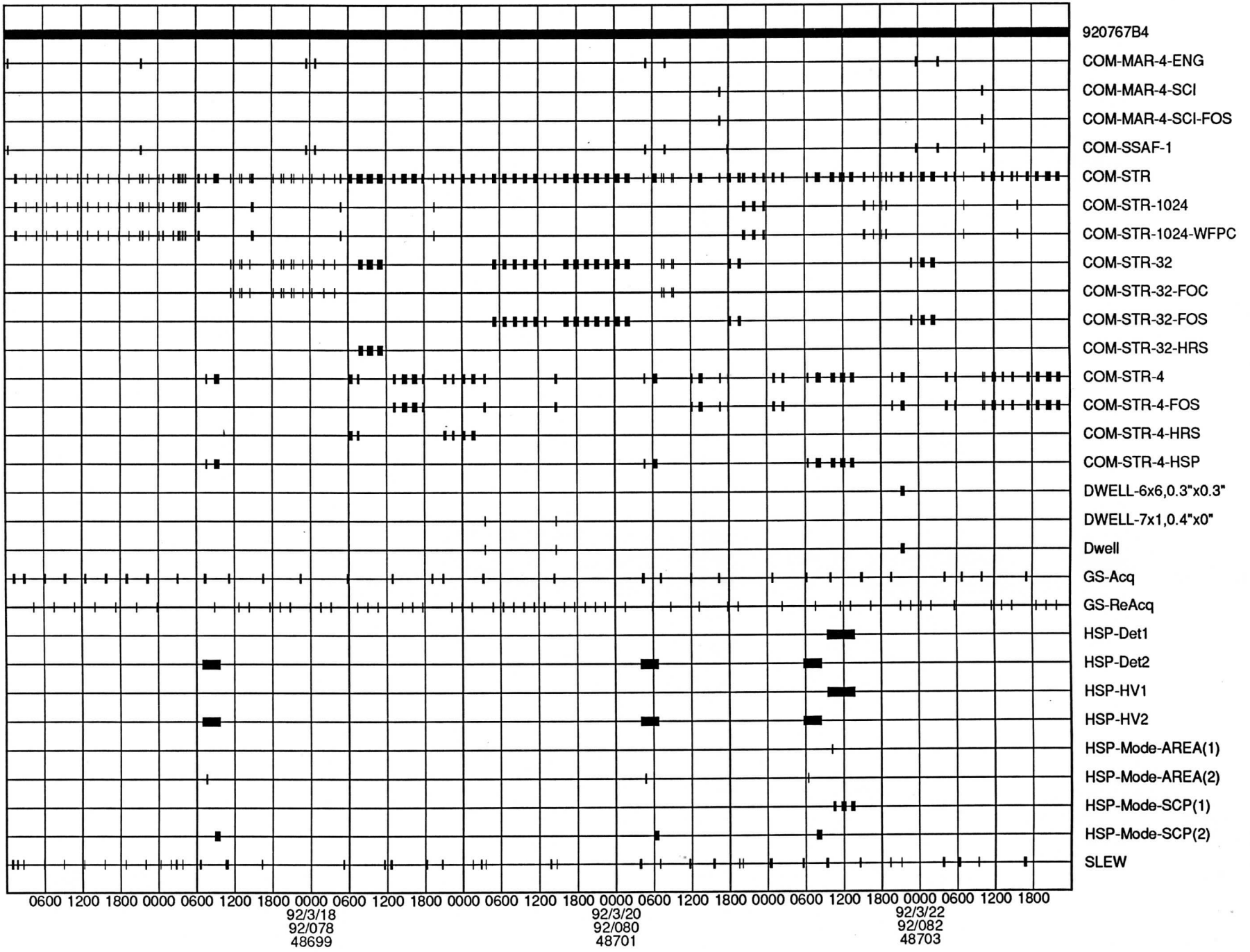

920837b9

SMS Chart version 2.15 (2/14/92) by Jeffrey W Percival

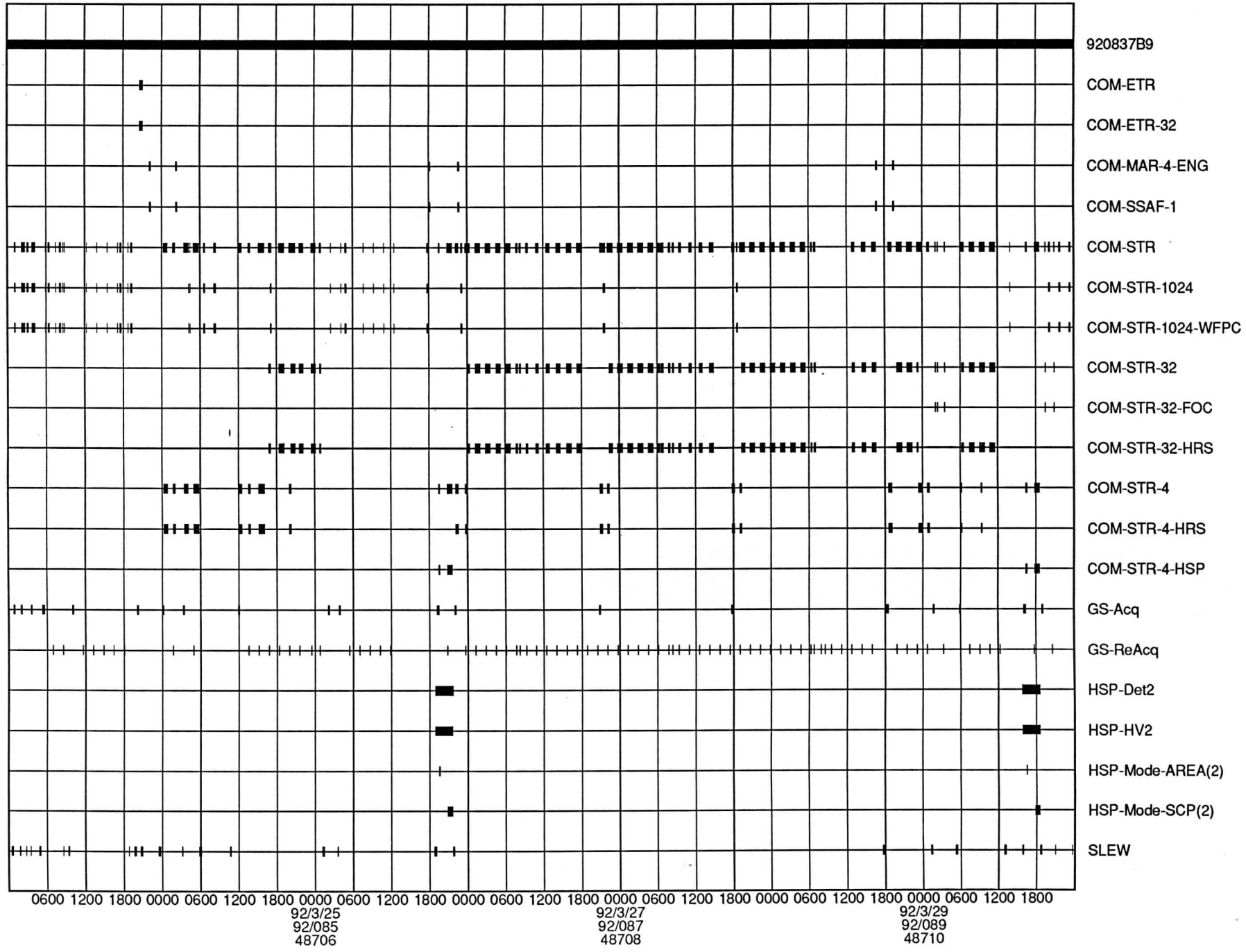

920907bar

SMS Chart version 2.15 (2/14/92) by Jeffrey W Percival

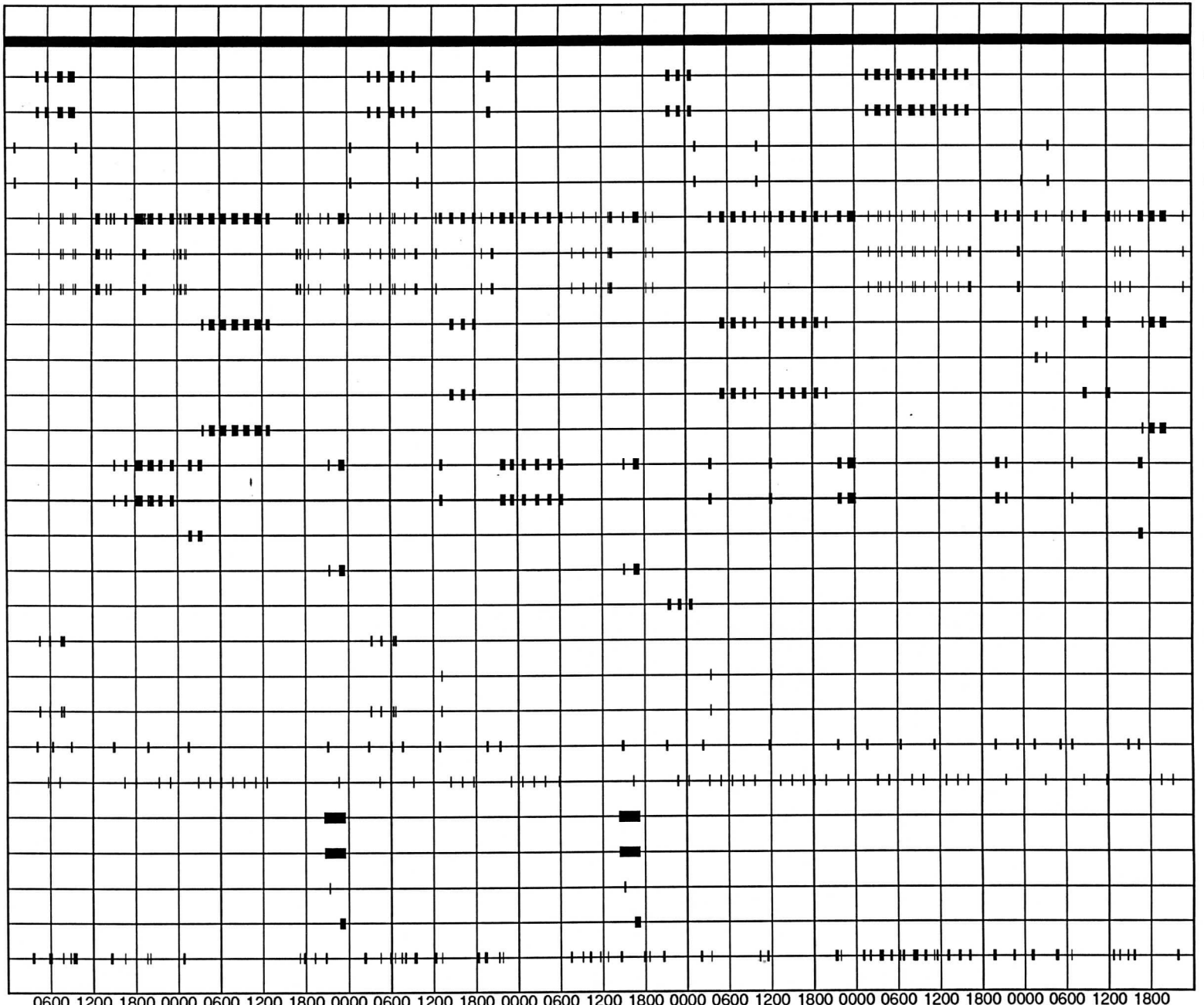

920977f6r

SMS Chart version 2.15 (2/14/92) by Jeffrey W Percival

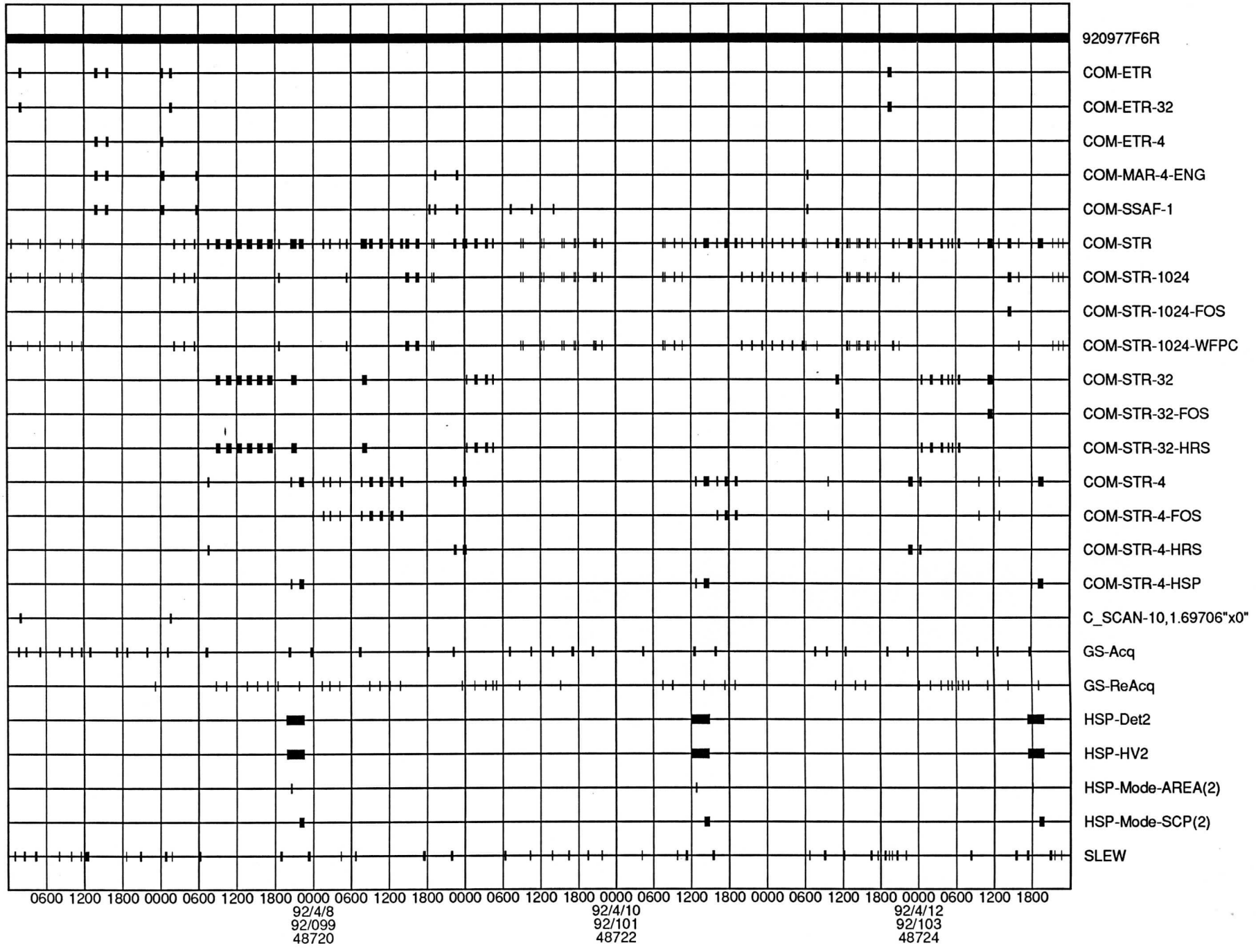

921047d2

SMS Chart version 2.15 (2/14/92) by Jeffrey W Percival

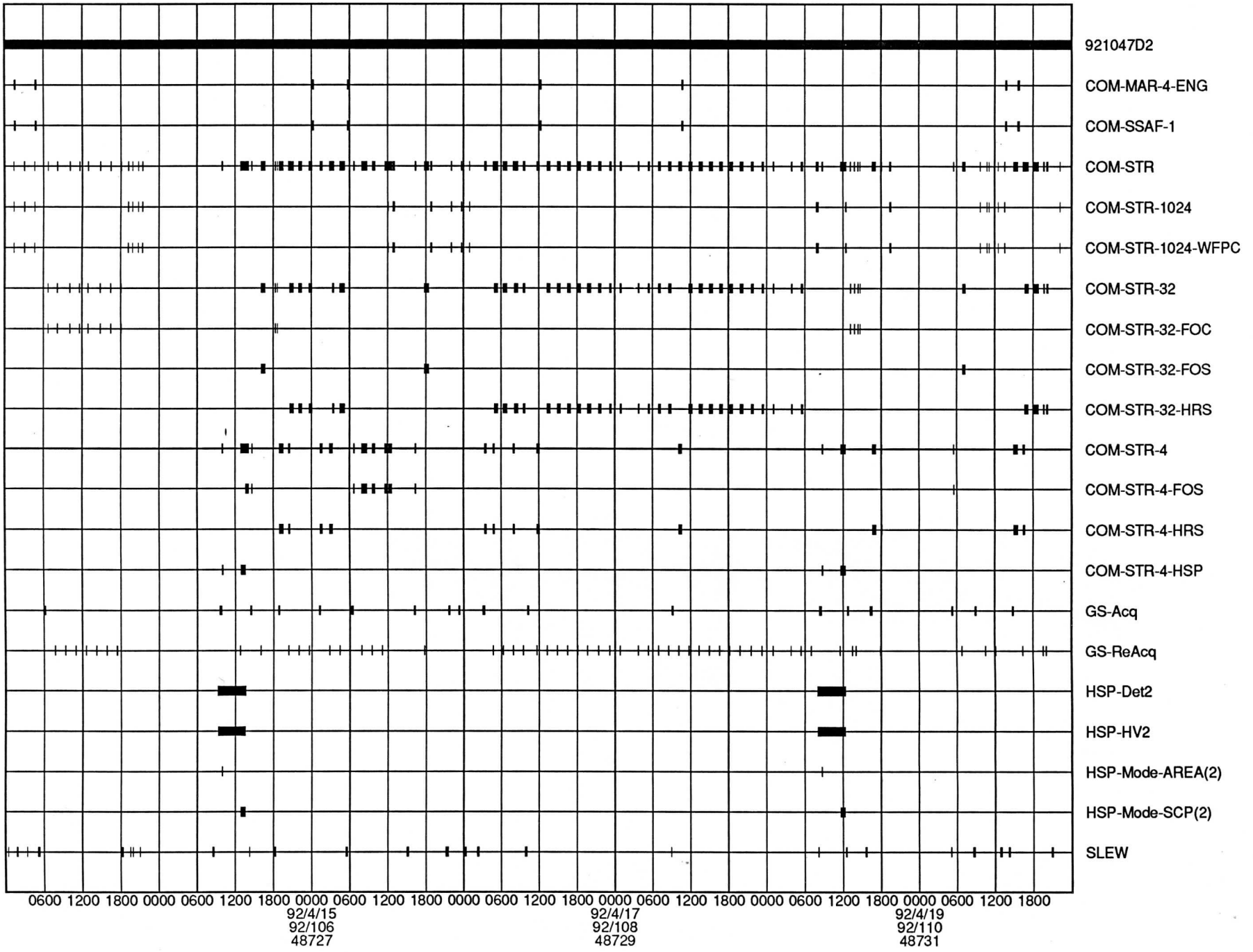

921117b6

SMS Chart version 2.15 (2/14/92) by Jeffrey W Percival

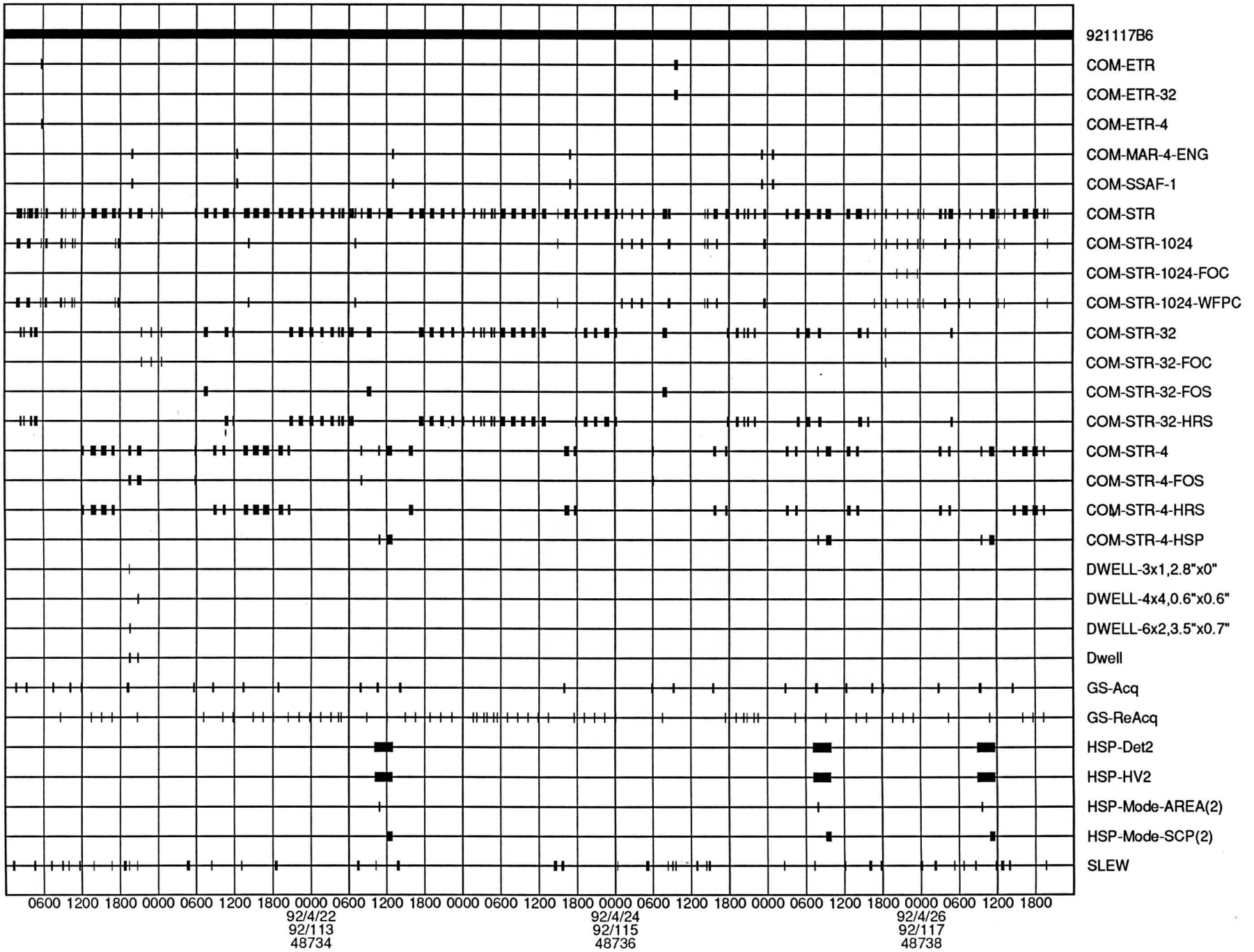

921187e6

SMS Chart version 2.15 (2/14/92) by Jeffrey W Percival

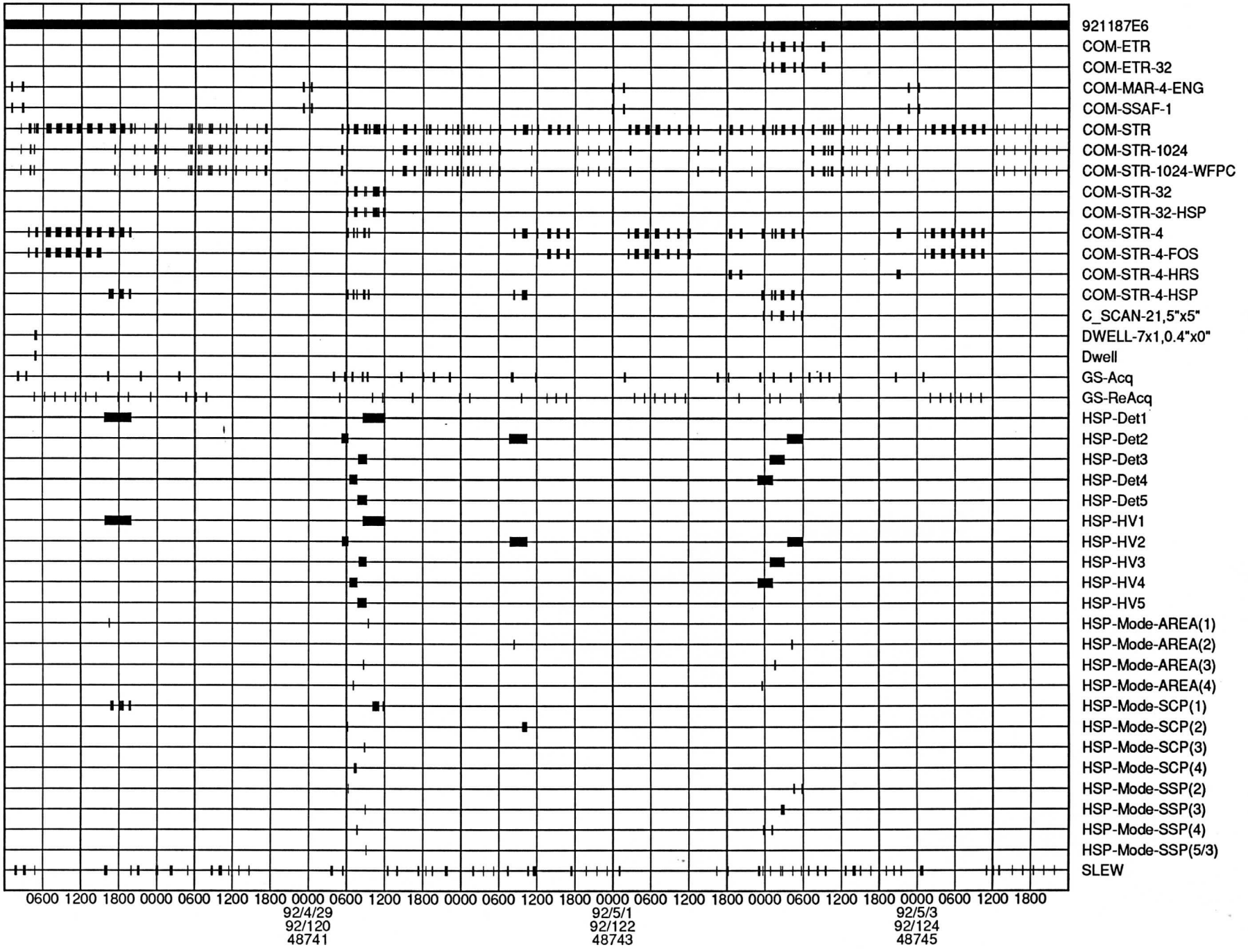

921257e4

SMS Chart version 2.15 (2/14/92) by Jeffrey W Percival

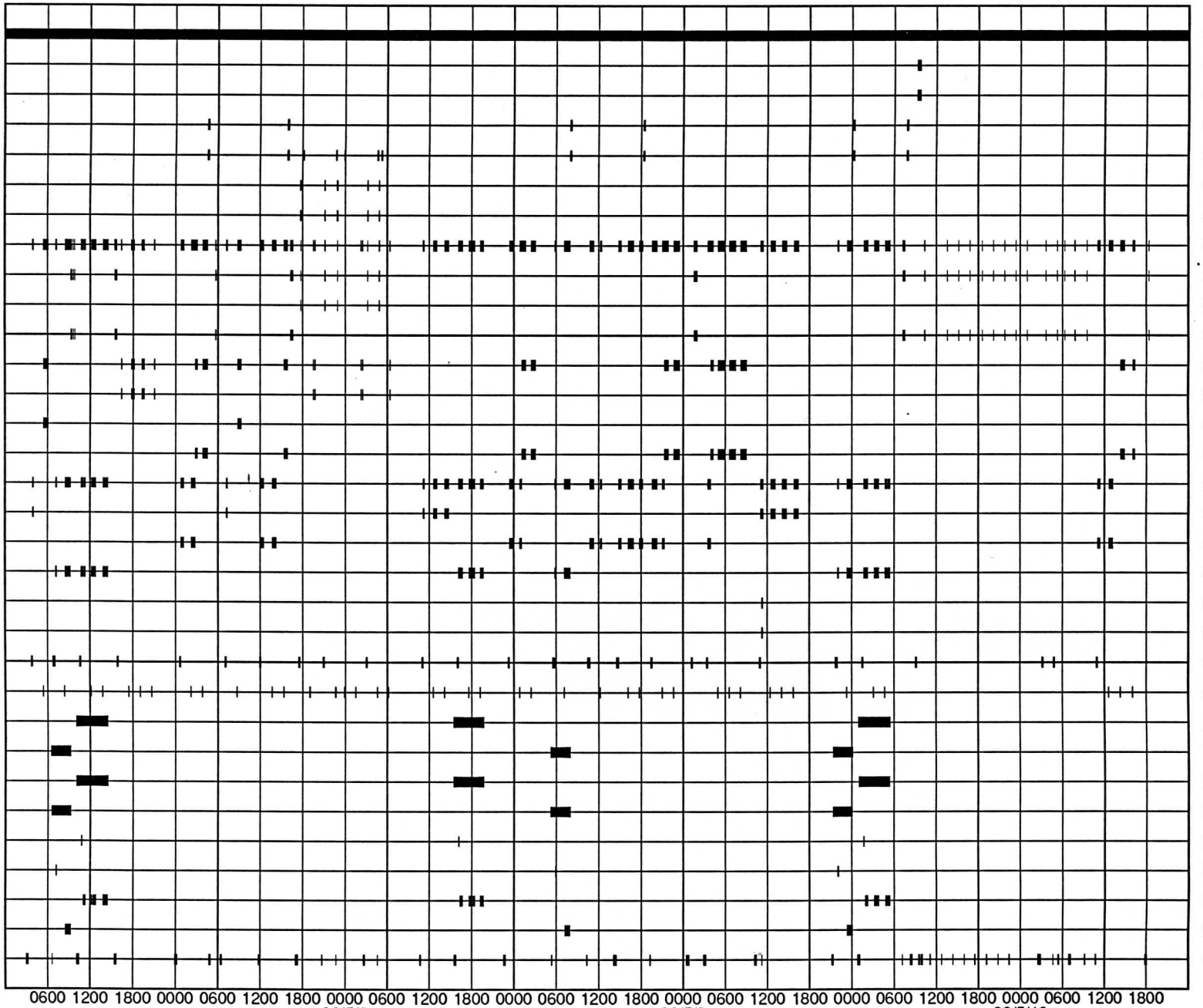

921327c4

SMS Chart version 2.15 (2/14/92) by Jeffrey W Percival

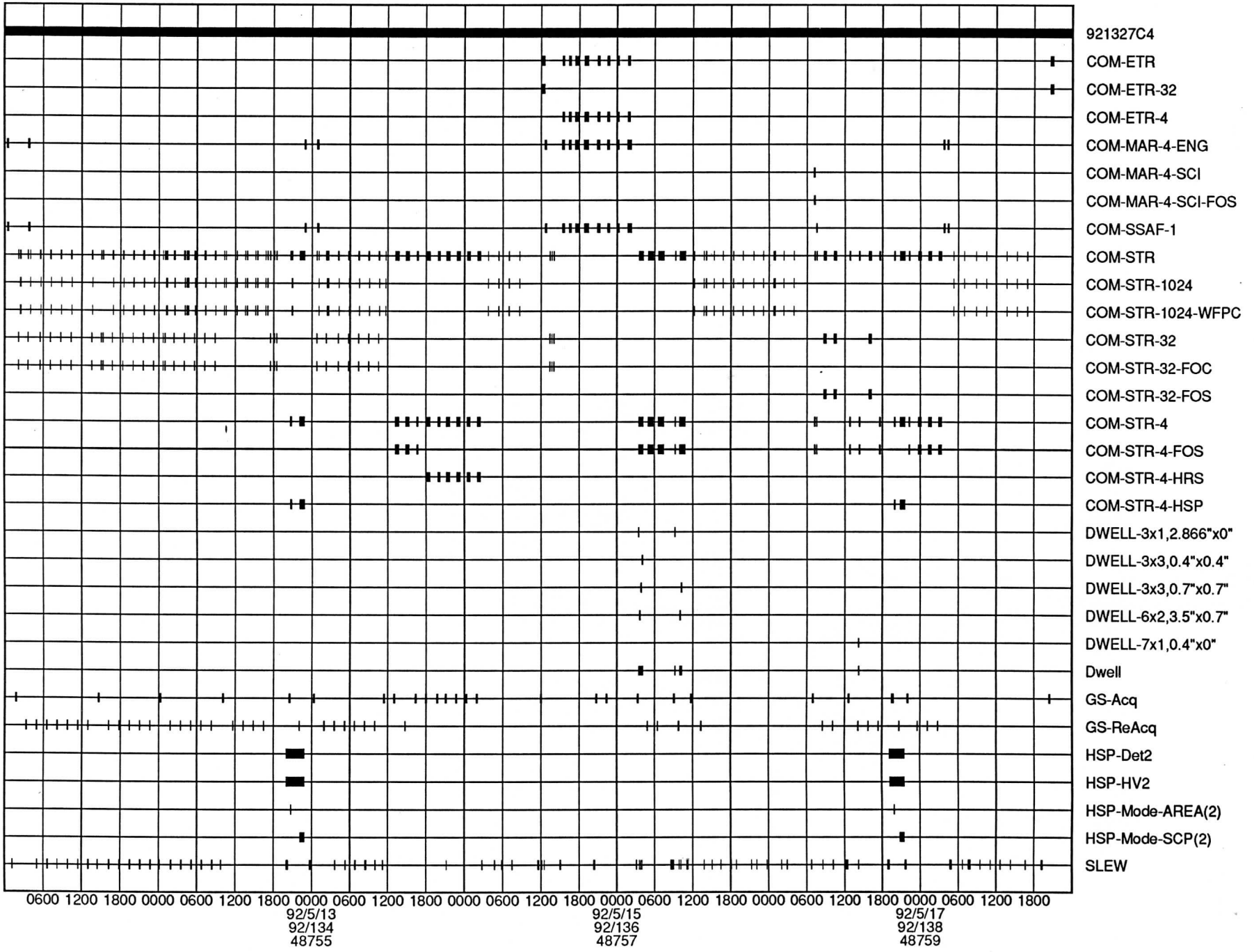

921397d1

SMS Chart version 2.15 (2/14/92) by Jeffrey W Percival

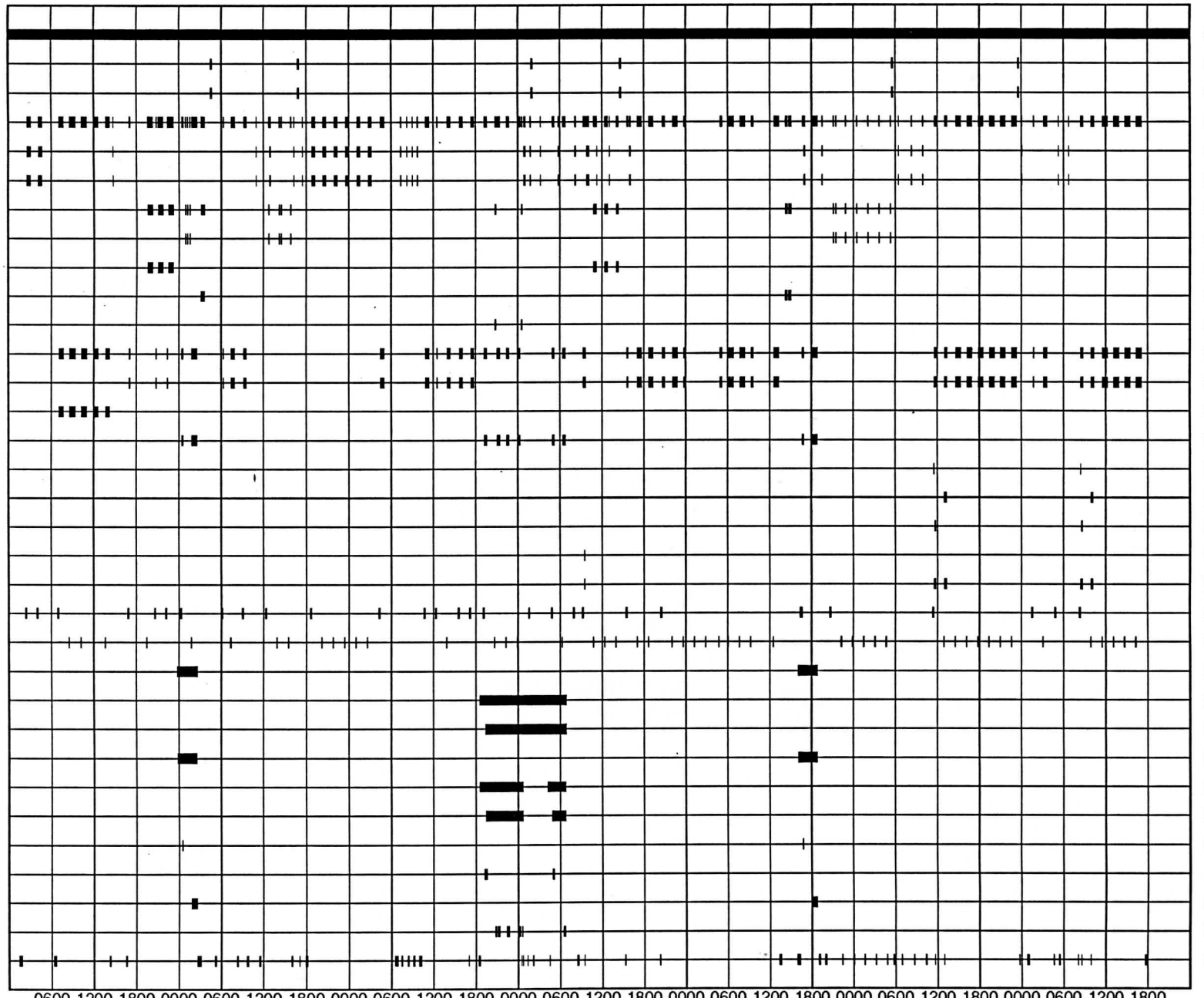

921467d6

SMS Chart version 2.15 (2/14/92) by Jeffrey W Percival

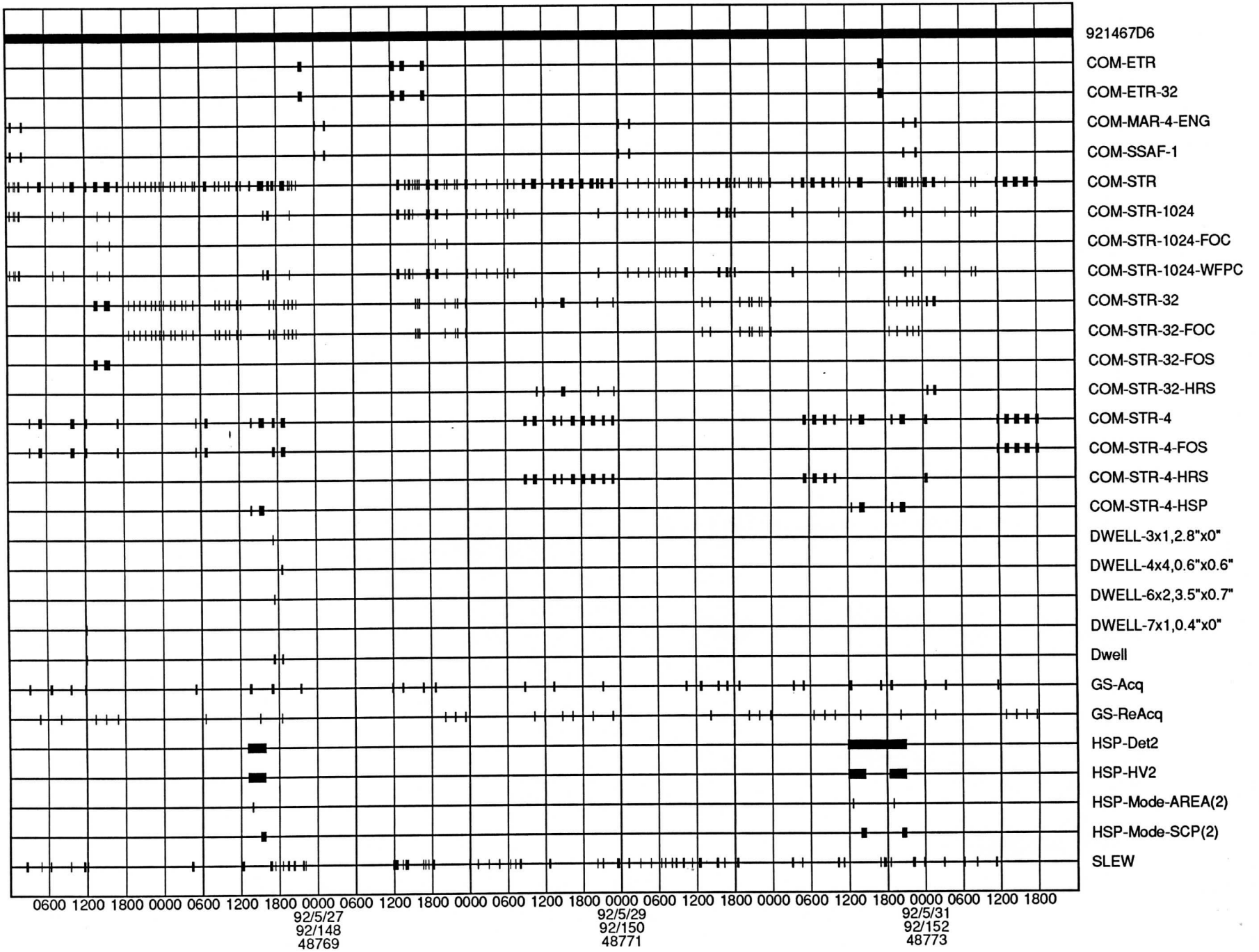

921537a5

SMS Chart version 2.15 (2/14/92) by Jeffrey W Percival

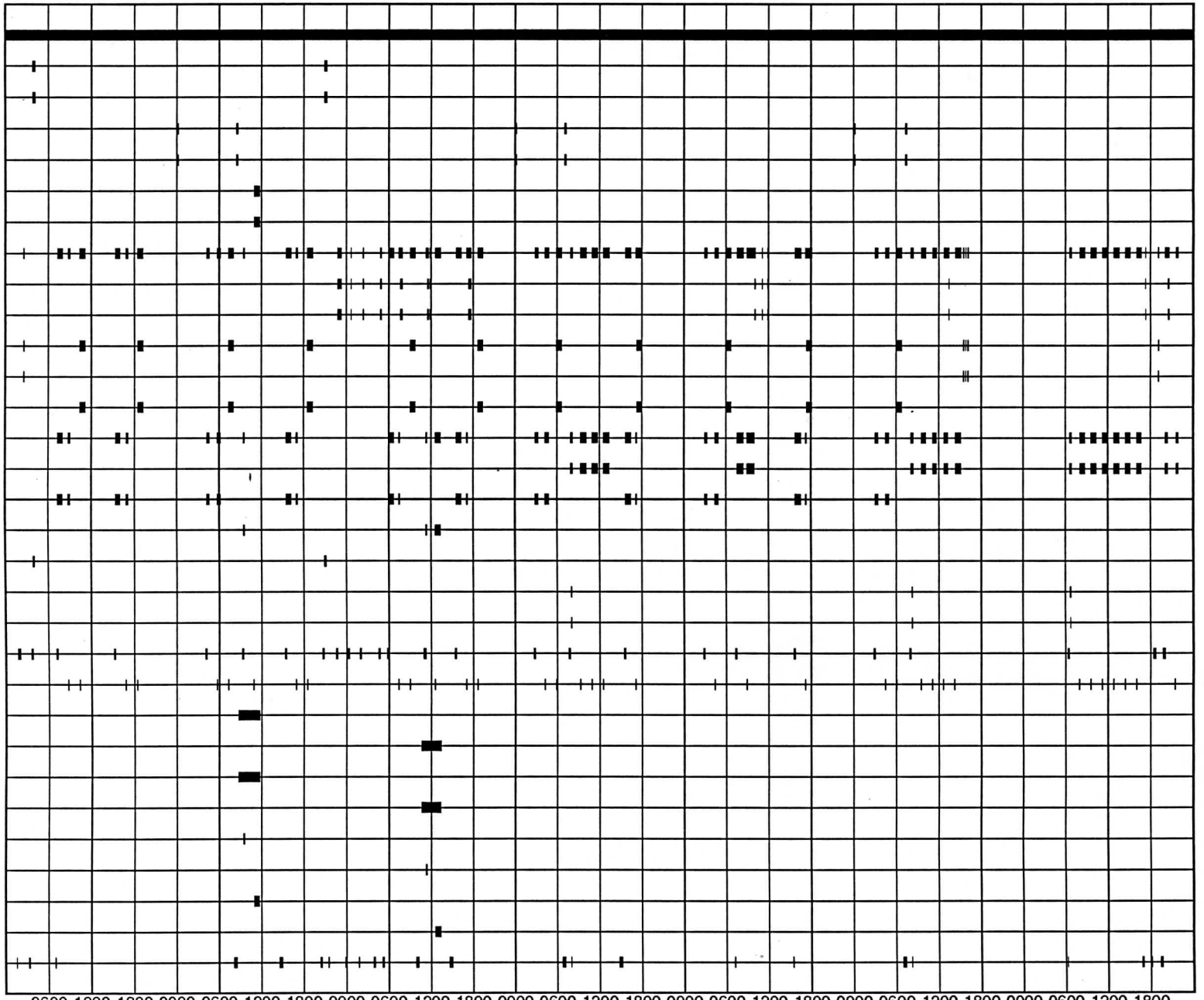

Appendix K - HSP Detector Maps

There are two sets of maps in this appendix: one shows the filter and aperture names in proposal syntax and the other in project database syntax. There are scales indicating deflection steps, physical dimensions in mm, and arc seconds. The orientation of the detector with respect to the V2 and V3 axes is also shown.

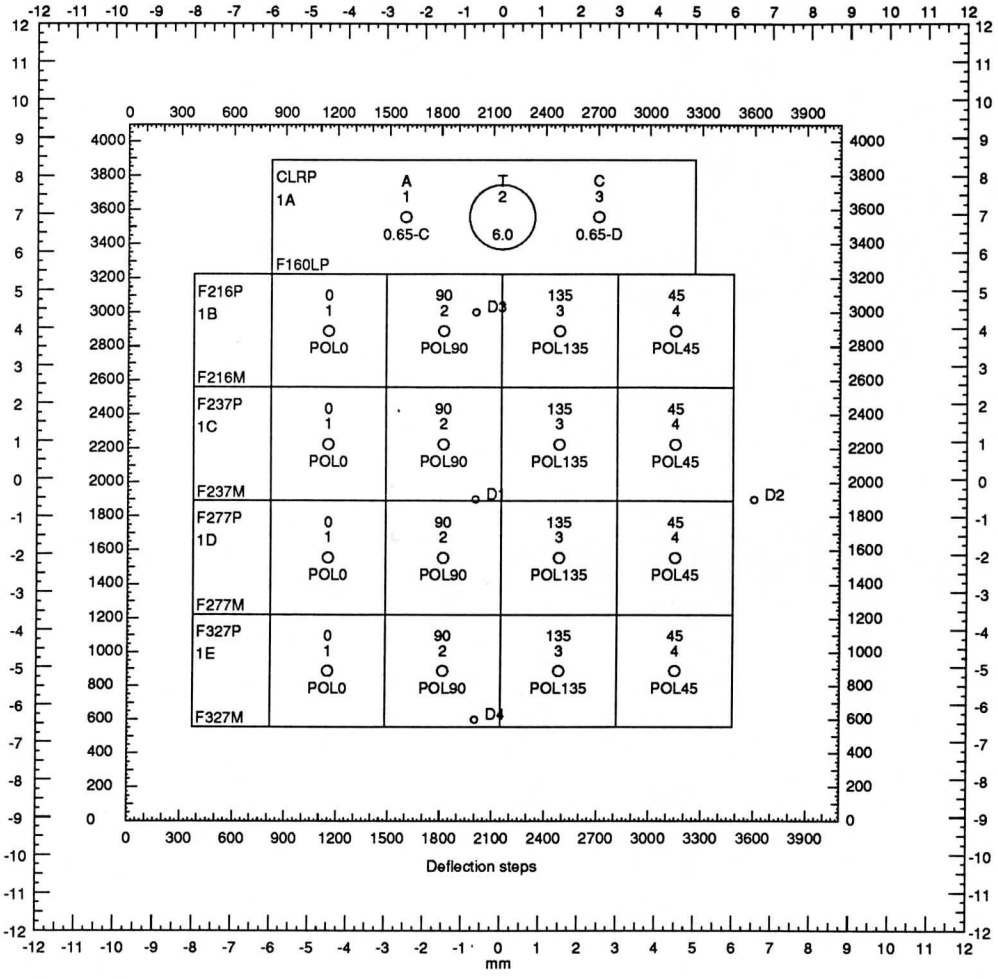

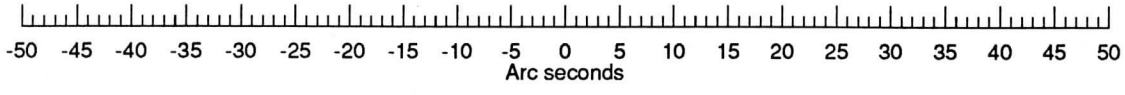

IDT1/POL

Proposal names

Chart version 1.6 (4/30/91)

Jeffrey W Percival

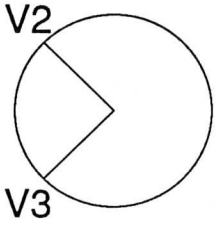

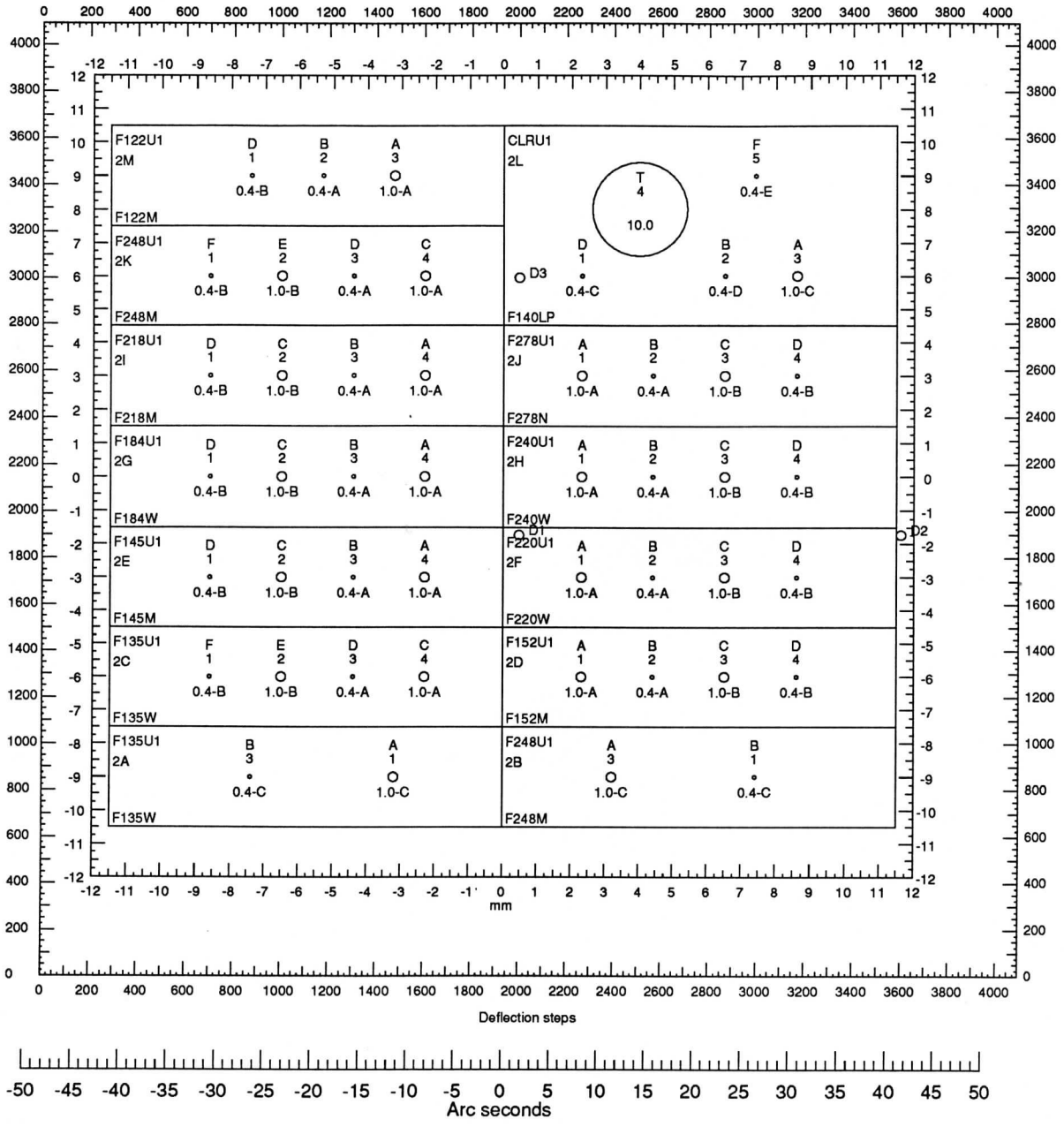

IDT2/UV1

Proposal names

Chart version 1.4 (11/10/90)

Jeffrey W Percival

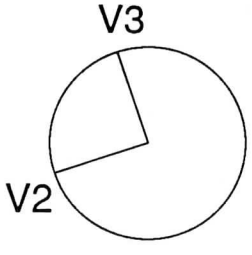

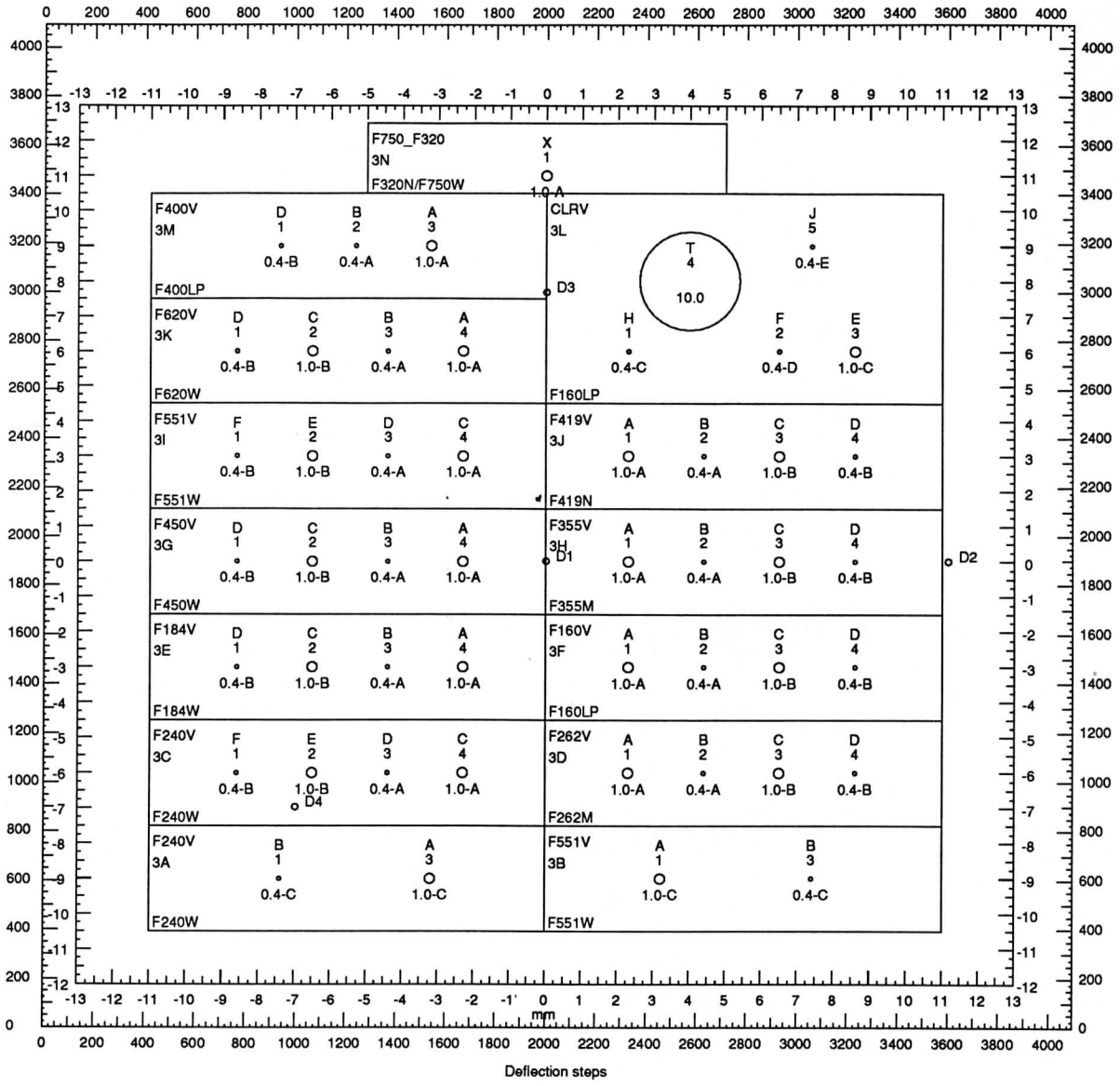

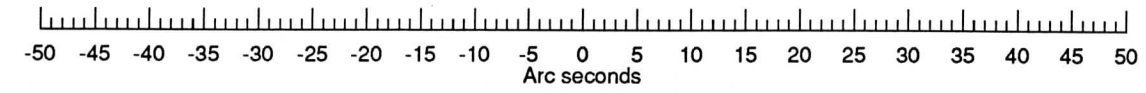

IDT3/VIS

Proposal names

Chart version 1.4 (11/10/90)

Jeffrey W Percival

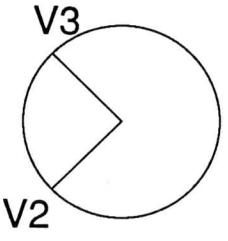

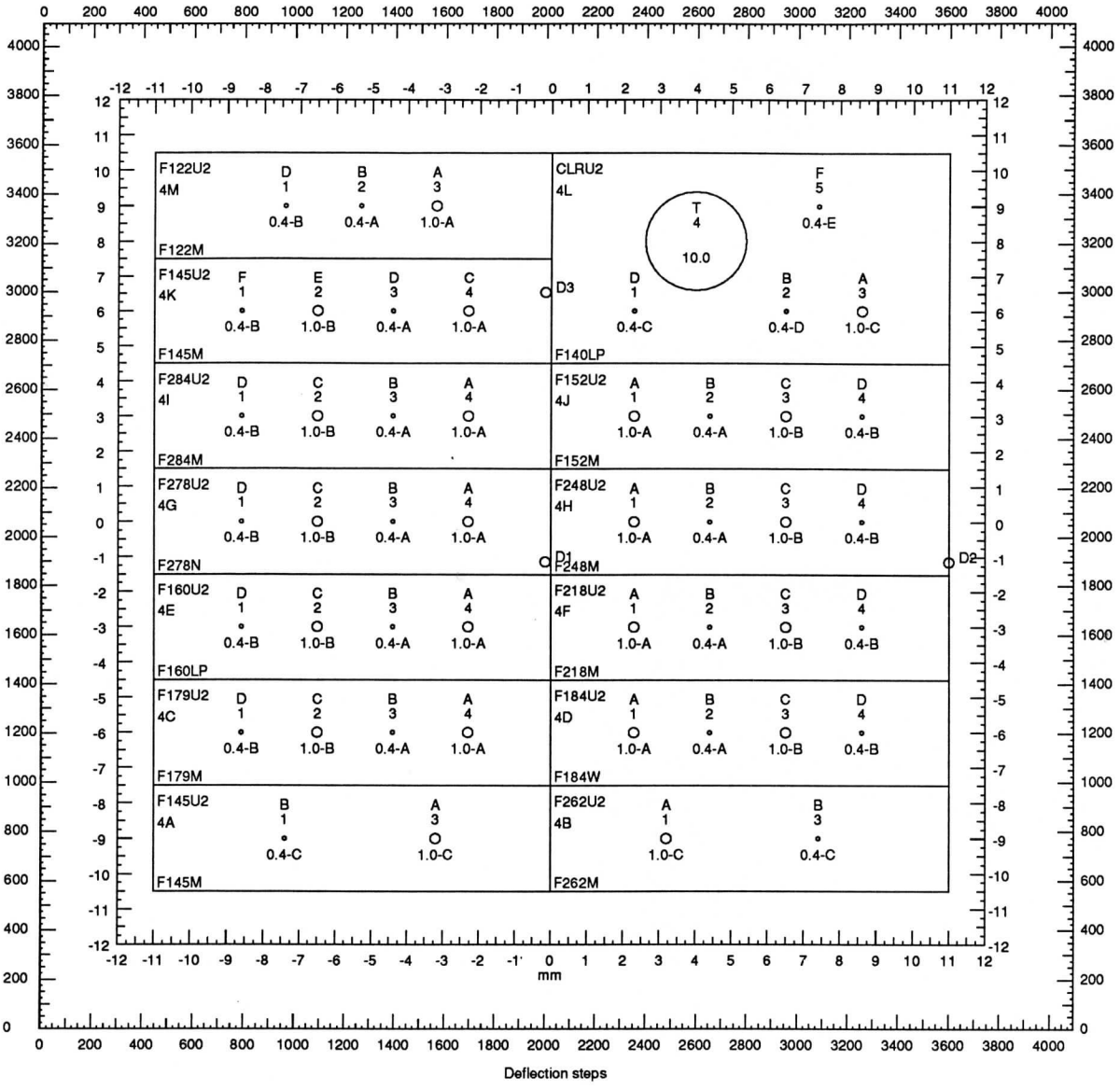

IDT4/UV2

Proposal names

Chart version 1.6 (11/10/90)

Jeffrey W Percival

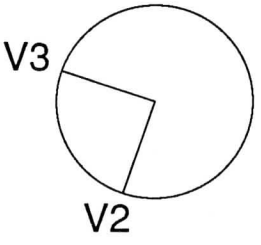

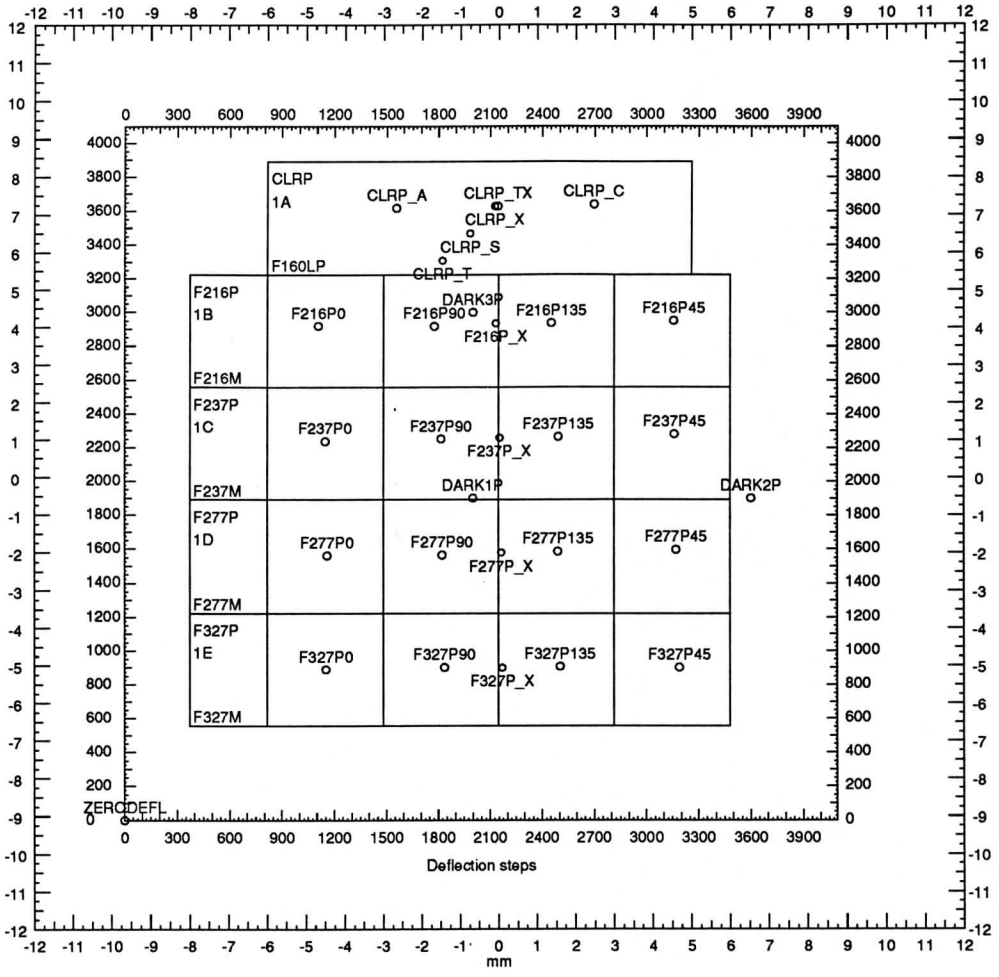

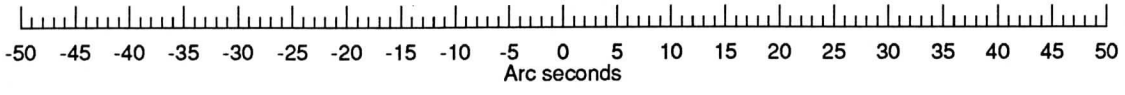

IDT1/POL

Data base names

Chart version 1.5 (4/30/91)

Jeffrey W Percival

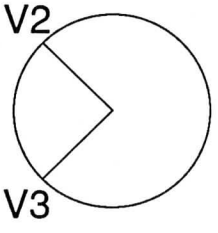

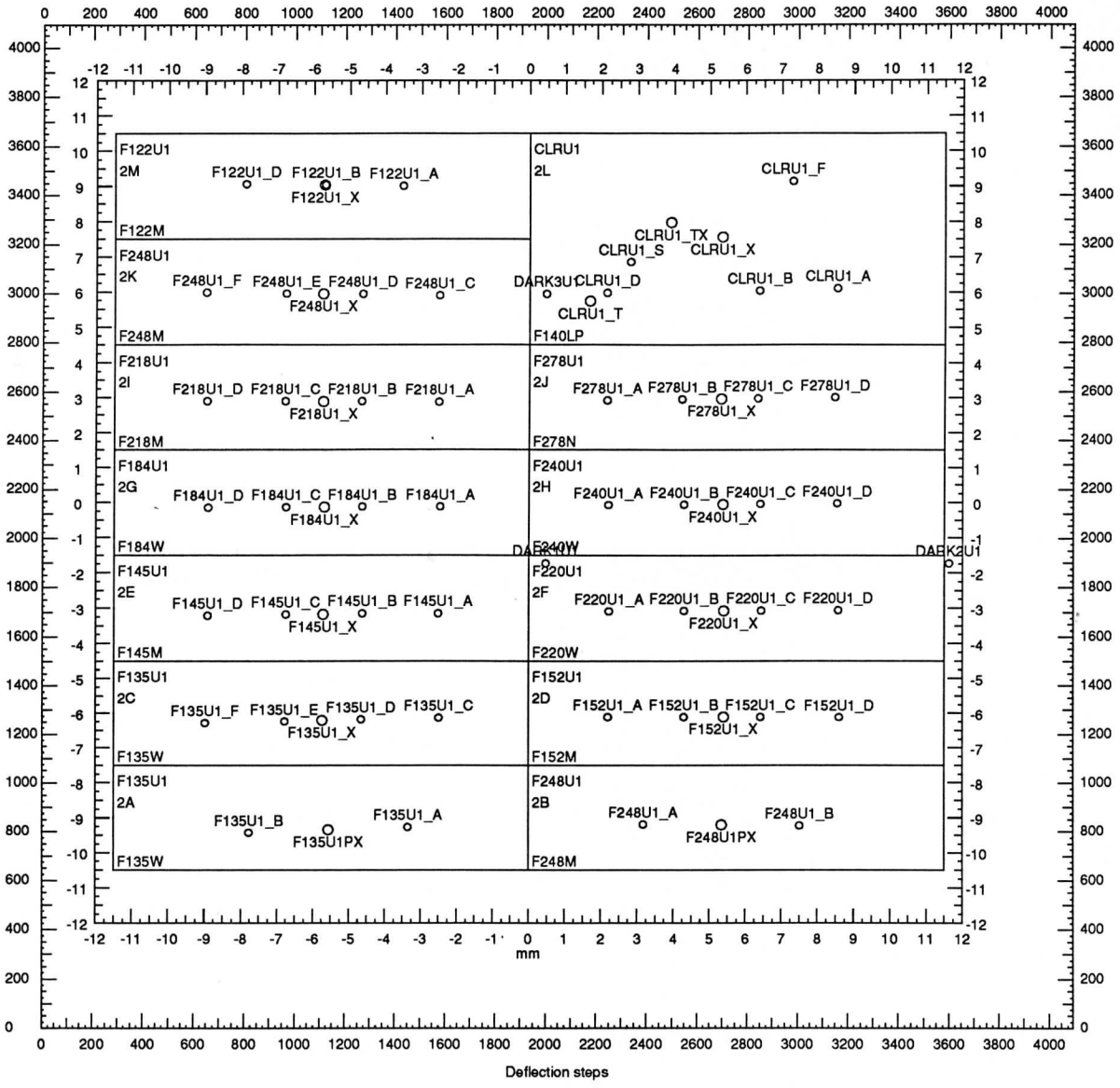

IDT2/UV1

Data base names

Chart version 1.4 (11/10/90)

Jeffrey W Percival

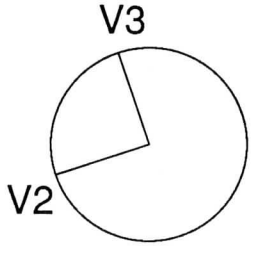

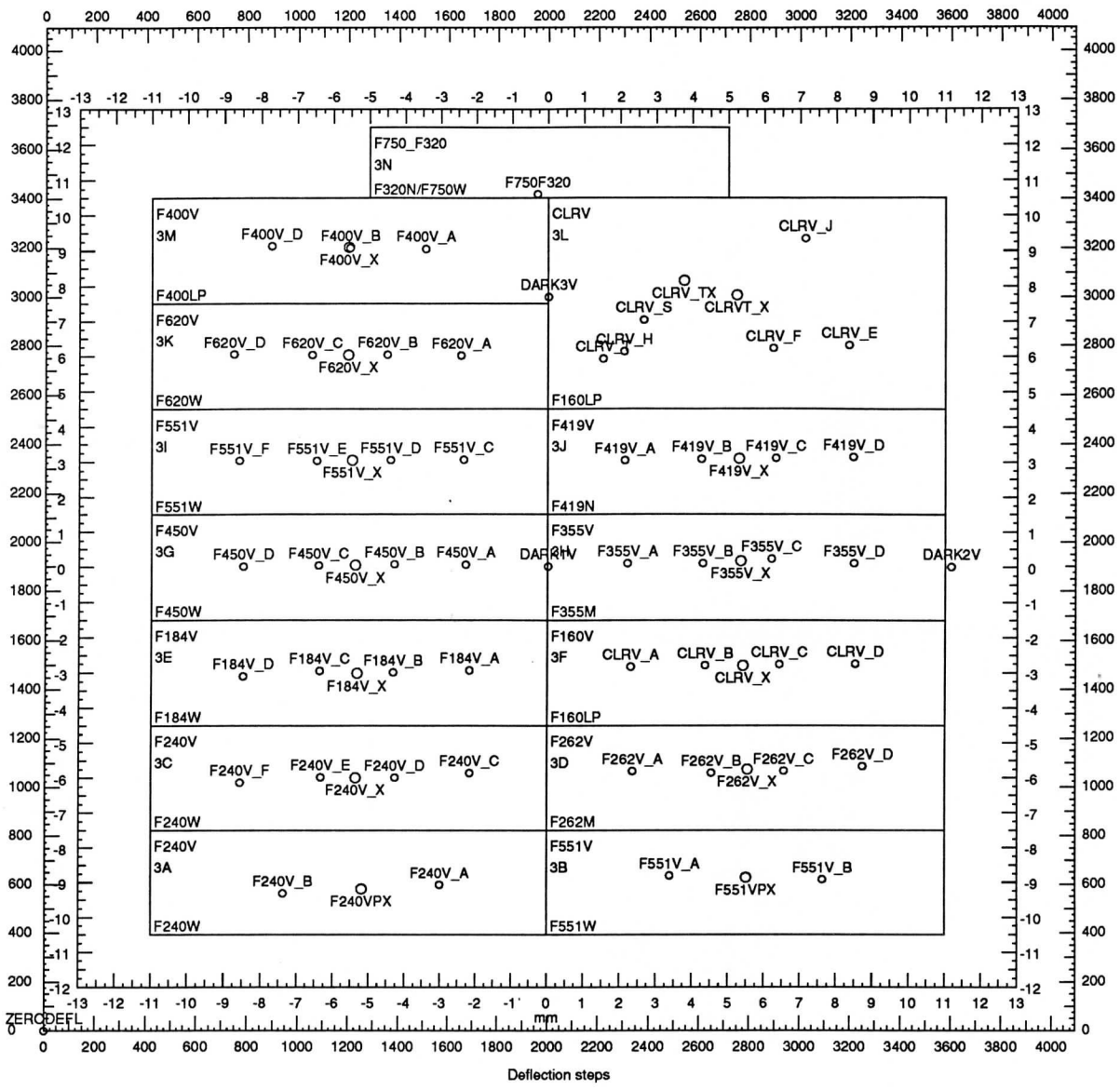

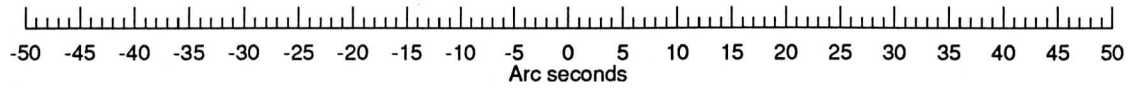

IDT3/VIS

Data base names

Chart version 1.4 (11/10/90)

Jeffrey W Percival

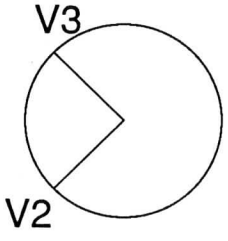

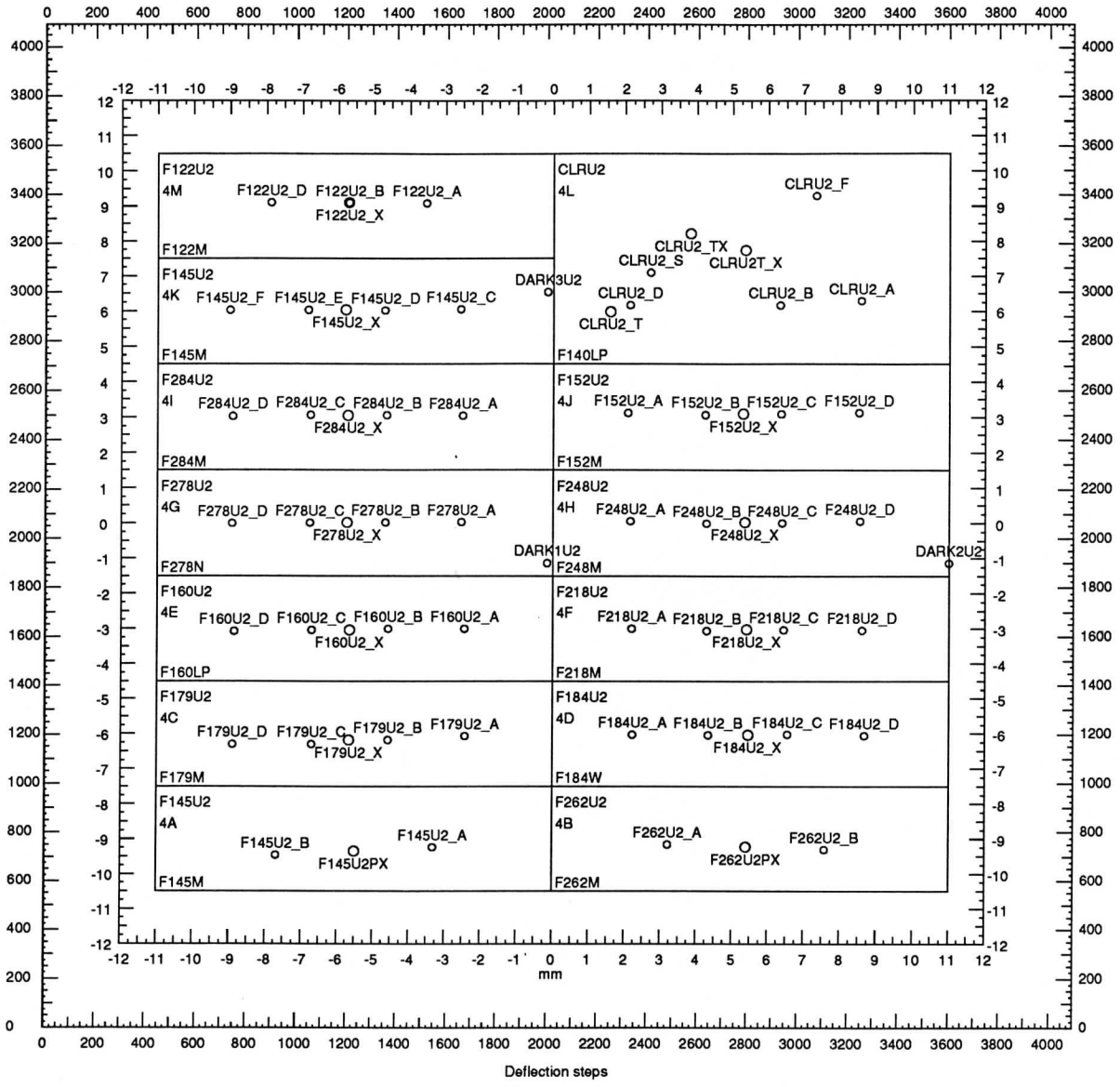

IDT4/UV2

Data base names

Chart version 1.5 (11/10/90)

Jeffrey W Percival

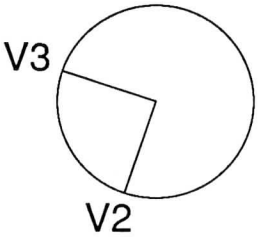

Grant Year FY2013

REQUEST FOR CONTINUED ASSISTANCE

COVER SHEET

1. STATEVIEW MEMBER-OF-RECORD:	2. STATE OR TERRITORY REPRESENTED:
University of Wisconsin-Madison	Wisconsin

3. PRINCIPAL INVESTIGATOR INFORMATION

3a. Name:	3b. Pi Business Address:
Samuel A. Batzli	Environmental Remote Sensing Center Space Science and Engineering Center University of Wisconsin-Madison 1225 W. Dayton St Madison, WI 53706
3c. PI Phone No.: (608)263-3126	3d. PI E-mail Address: sabatzli@wisc.edu

4. SPONSORED PROGRAMS OFFICE POINT-OF-CONTACT INFORMATION

4a. Name and Title:	4b. Phone and e-mail:	4c. Address:
David Ngo, Pre-award Manager Research and Sponsored Programs Office	(608) 262-3822 dvngo@rsp.wisc.edu	21 N. Park St., Ste 6401 Madison, WI 53715-1218

5. PROJECT INFORMATION

5a. Project Title:

"StateView Program Development and Operations for the State of ___Wisconsin____".

5b. AMOUNT REQUESTED (*Round to nearest whole dollar*):		5c. PROJECT PERIOD: Start: (*YY/MM/DD*)	End: (*YY/MM/DD*)	5c. Is the applicant delinquent on an existing AmericaView, Inc. award?
$23,672	.00	2013/12/1	2014/9/15	☐ Yes (If yes, attach an explanation) ☒ No

By signing and submitting this request for continued assistance, including supporting statement of work and budgetary information, the applicant certifies that the information contained herein is true and complete to the best of his/her knowledge. The applicant also acknowledges that in the event that continued assistance is awarded, the terms and conditions of the existing award will remain in effect for the duration of the project.

SIGNATURE OF PRINCIPAL INVESTIGATOR	DATE
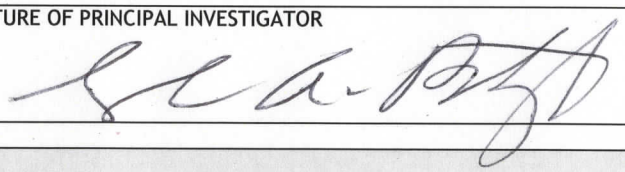	11/26/2013

AV USE ONLY

Received:
Reviewed:
Board Notification:
NOTES:

High Speed Photometer
Pulsar Timing and Light Curve Reduction

Jeffrey W Percival

Space Astronomy Laboratory,

University of Wisconsin,

Madison, WI 53706

May 19, 1992

Abstract

This memo describes in detail the reduction of the 5 High Speed Photometer observations of the Crab Pulsar. This analysis shows that the correlation of the Hubble Space Telescope clock with UTC is well within the design specification of 10 milliseconds, and may be within 1 millisecond.

1 Introduction

The Crab pulsar was observed on five separate occasions by the High Speed Photometer (HSP) on the Hubble Space Telescope (HST). In each case the sample time was $11/1.024 \times 10^6 \approx 10.74$ microseconds. Table 1 gives the circumstances of each observation. Table 2 gives the histograms of the raw data.

The light curves were produced with the following procedure. First, the definitive HST ephemeris was obtained from the Flight Dynamics Facility at Goddard Spaceflight Center. This ephemeris gives the 6-element HST barycentric J2000 state vector at one minute intervals, expressed as the Modified Julian Date in units of 100 nanoseconds. For each of these state vectors, the barycentric state vector of the earth was obtained from the JPL DE-200 Planetary Ephemeris. The sum of these vectors gives the barycentric state vector $\mathbf{v}$ of the HST, and the arrival time correction is then $\mathbf{v} \cdot \hat{\mathbf{p}}/c$ where $\hat{\mathbf{p}}$ is the unit vector in the direction of the Crab Pulsar and c is the speed of light. Cubic spline interpolation in the resulting table of corrections was used to arrive at barycentric corrections within each minute. The phase of each non-zero sample was calculated using the procedure outlined

in the Jodrell Bank Monthly Ephemeris (Lyne & Pritchard 1992). Figures 1- 5 show the resulting mean light curves.

The following sections describe each of these steps in detail.

2 Position of HST

The definitive HST ephemeris is given in files that ultimately originate in the Goddard Spaceflight Center's Flight Dynamics Facility. We obtained the appropriate files from the Science Institute's Data Management Facility. Table 3 gives the files used, and their time coverage in Modified Julian Dates. The accuracy of the HST state vector can be estimated from the data files. Consecutive files share one common time point. The last time point of the previous file is the same as the first time point of the next file. The state vectors for these time points, however, differ according to their respective regression solutions. Comparing pbag0000r.orx with pbai0000r.orx, we find two state vectors for MJD 48547.0: (6632.978, -1360.692, -1706.646) km and (6632.962, -1360.749, -1706.670) km. The difference is (-0.016, 0.057, 0.024) km, or a total displacement of 64 meters. The light travel time for this distance is less than 2% of our sample time, and is negligible for our purposes.

3 Time of day

Events on the HST are driven by the HST clock, a 32-bit counter with a resolution of 125 ms. Events inside the HSP are driven by a separate, internal, clock. The HSP clock is also a 32-bit counter, but the resolution is 1 ms. (HSP events are driven by an oscillator whose rate is $1.024 \times 10^6 s^{-1}$, but the system uses the 1 ms clock for timekeeping.) Assigning absolute times to the photometry samples collected by the HSP requires establishing a time correlation for each of these clocks. That is, one must calibrate the zero point and count rate in order to map clock value onto absolute time.

The HSP/HST clock correlation is established by logging the HST clock value at the instant that the HSP clock is set to zero. No calibration of the HSP clock rate has been performed, so we simply assume that the advertised resolution of 1 ms is correct. The pulsar

observations indicate that this is not too gross an assumption, and in any case the HSP clock only controls events on relatively short time scales, so deviations from the 1 ms resolution are not allowed to accumulate for very long.

The HST/UTC correlation is established by time tagging the receipt of certain telemetry signals at the White Sands ground station. The time tags are then corrected for signal propagation times from White Sands to the TDRS relay satellite in use, and from the TDRS to the HST. The largest remaining uncertainty is in the HST telemetry hardware. Depending on the telemetry format in use at the time of the calibration, the uncertainty can vary from 1 ms (format A) to 8 ms (format C). The calibration is performed daily, and a regression is performed against the accumulated data to extract the coefficients of a quadratic polynomial mapping the HST clock onto UTC. The clock rate (seconds / count) and clock drift (seconds / count^2) are important outputs of this regression.

We obtained the results of several regressions from Morlock and Kimmer (1992) We chose to use a solution whose epoch was close in time to the final Pulsar observation. The correlation we chose is:

T_0 = 1992.004 05:44:00.443 (epoch)
V_0 = 428038096
r_0 = 0.1250000009901 seconds/count (clock rate)
d_0 = 8.861552441864 $\times 10^{-19}$ seconds / count^2 (clock drift)

Using these coefficients, the time of day is given by

$$T = T_0 + (V_1 - V_0)r_0 + (V_1 - V_0)^2 d_0/2 \quad (1)$$

where T_0 is the absolute time corresponding to vehicle time V_0, and V_1 is the vehicle time of the desired event.

4 Time of observation

Now, with these two clock correlations, we can convert any given HST or HSP time to absolute time. The one remaining problem is assigning the correct HST time to the

first photometry sample. There are two ways to approach this, and in order to appreciate the distinction between them we must describe the sequence of events that leads up to the collection of science data with the HSP. In the photometry mode used for the Crab Pulsar, the HSP is programmed to start integrating the first sample at some prearranged HSP time. That is, when the HSP clock reaches some target value, then exactly 1 ms + 1 HSP clock tick later, the first sample begins (Werner, 1992). Although the HSP collects its samples in a continuous stream, the HST Science Data Formatter (SDF) quantizes the downlink into data packets. For the Crab observations, each packet contains 1920 1-byte photometry samples. When the HSP finishes the 1920th sample, it begins an interaction with the SDF to read out the packet. The HSP asserts a signal called Frame Start, and then sometime later, typically 1-2 ms, the SDF asserts a signal called Line Start. The data are then read out of the HSP. Before shipping the packet out to the downlink, the SDF inserts the HST clock value at which the Line Start was generated into the packet header (Rankin, 1992). Although the HST clock has a resolution of only 125 ms, the SDF adds an additional 10 bits of resolution, improving it to $125/2^{10}$ ms, or about $122\mu s$.

We can now estimate the HST time of the first photometry sample in two ways: adding the 1 ms + 1 HSP clock tick offset to the programmed start time, or by taking the time embedded in the first data packet and subtracting the time it took to collect the first packet's data, including all the known delays and overheads. We call these two methods the forward method and the backward method. The two principle overheads to account for in the backward method are the amount of time that elapses *after* the 1920th sample has been collected but *before* the HSP asserts the Frame Start, and the delay in the SDF before asserting the Line Start. The HSP delay has been estimated to be 1.068-2.61 ms (Werner, 1992), and the SDF delay is 1-2 ms. Table 4 shows the HST times for the Crab observations using each method. The packet time is the actual value recovered from the first data packet. The "backward time" column has 1920 sample times removed, *but not the HSP or SDF overheads.* The "forward time" column gives the programmed start time, *without the 1 ms + 1 HSP clock tick delay.* We see that the two methods are discrepant by 0.041703 ± 0.003340 HST clock ticks, or about 5.2 ± 0.4 ms. The sense is that the forward method times are *earlier* than the

backward method times. Some of the mean discrepancy is due to the neglect of the various delays and overheads. They would move the forward method later by about a millisecond, and would move the backward method earlier by about 3.3 ms (assuming average values for the ranges given above). There remains about 0.9 ms of unknown error.

5 Calculation of phase

The phase of each non-zero sample was calculated using the following procedure, given in Lyne & Pritchard (1992). Denoting the pulsar period with P, and letting ν_0 and $\dot{\nu}$ be the pulsar's frequency and frequency derivative at some epoch, we have

$$P = 1/\nu_0, \tag{2}$$

$$\dot{P} = -\dot{\nu}/\nu_0^2, \tag{3}$$

and

$$\ddot{\nu} = 2\dot{P}^2/P^3. \tag{4}$$

The phase at the instant of observation T is then

$$\Phi = \nu_0 T + \dot{\nu}T^2/2 + \ddot{\nu}T^3/6. \tag{5}$$

Table 5 gives the radio epoch, and the phase of the first sample of each observation.

6 Mean light curves

Figures 1-5 show each observation coadded into 3125 phase bins covering one pulsar period. 3125 was chosen to make each phase bin approximately as wide as the $10.74\mu s$ sample width. The backward method times in Table 4 were used to produce the light curves in these figures. Tables 6 and 7 give the phase error of the main peak and the phase drift during the observation. The phase error and phase drift ($\Delta P/P$) was estimated by dividing the observation into about 200 time slices, and coadding the light curve separately for each slice. The phase of the maximum value was found for each slice, and a least squares fit was performed using the resulting few hundred pairs of points. Figures 6-10 show the peak phase

as a function of pulse number, with the linear regression superimposed. The large variance in the data is primarily due to the crude estimate of the peak phase in each of the slices: we chose the phase bin containing the most counts, rather than using a more elaborate technique such as smoothing with curve fitting. Each time slice lasted for only about 10 seconds, and contained just a few hundred counts. The "maximum value" choice would be expected to suffer using the relatively noisy 10-second light curves, but should not do any systematic damage to the regression.

We take the y-intercept of the linear fit to be the phase error with respect to the radio ephemeris, and the slope to be the phase drift within a given observation. Using an average pulsar frequency of 29.94 Hz to convert the phase errors into time errors, we end up with -3.190 ± 0.02979 ms for the forward method, and 1.982 ± 0.3938 ms for the backward method. Now recall the neglected delays and overheads. The forward method should be increased by about a millisecond, to -2.2 ms, and the backward method should be decreased by about 3.3 ms, to -1.3 ms. The residual discrepancy of about 0.9 ms is what we expected, and is due to the unexplained discrepancy in the time of the first datum. Adding the backward method timing uncertainties in quadrature (using 0.771 ms for the HSP delay and 0.5 ms for the SDF delay) we get a total uncertainty in the calculated arrival times of 1.0 ms. The forward method delays of 1 ms + 1 HSP clock tick are exact, so the total uncertainty is just the dispersion of phase errors, or 0.02979 ms.

We see that each of these methods has an advantage. The forward method gives a larger phase error, but produces a very small variance. We believe that the phase error is due to some small, but highly deterministic, overhead in the HSP, perhaps occurring when the HSP resets its internal clock. In fact, a small phase shift between the HST and HSP clocks could introduce a millisecond delay in the reset (Werner, 1992), thereby shifting the HSP time axis by the amount required to eliminate the discrepancy. Note that the backward method times would not be affected by such a phase shift, because they are derived from the HST clock in the packet headers.

The backward method gives a better match to the radio ephemeris, but with a larger dispersion. We think the real phase error of the backward method may be smaller than the

-1.3 ms quoted above, because an average value of 1.5 ms was used for the SDF delay, but with only one active instrument, the SDF delay may be closer to the 1 ms lower limit, and this would bring the backward method phase error to within the 1 ms total uncertainty in the delays and overheads.

These small phase errors and dispersions are a little surprising, given the variability of the HST clock drift term d_0. A plot in Morlock and Kimmer (1992) shows d_0 plotted as a function of time in 1991, and shows rapid and frequent excursions of at least 3×10^{-18} seconds per count^2. Extrapolating such a change from the January solution back to the October Crab observations (90 days, at 8 HST ticks per second), we get a temporal uncertainty of about 6 ms. The January Crab observation fell much closer to the correlation epoch, and so is far less sensitive to the uncertainty in d_0. It is not clear to what extent our small errors and dispersions and due to good luck. A different d_0 would have thrown the October light curves further from the radio ephemeris, increasing the mean error, and further from the January light curve, increasing the dispersion of phase errors. In any case, the HST clock seems to be calibrated to within the 10 ms specification even after folding in all methods, errors, delays, and overheads.

The phase drift provides an estimate of the amount of smearing in the final light curve for each observation. The RMS phase drift of $\Delta P/P = -3 \times 10^{-8}$ over approximately half an hour implies a smearing of about $54\mu s$, or about 5 samples. Referring to Figures 6-10, it is clear that the measured drifts are much smaller than the variance of the data, and are therefore statistically negligible. Figures 11-15 show enlargements centered on the peaks. Note that the peak v0qy0401 shows a profile about as wide as the others, yet its drift measurement in Table 7 is 4 orders of magnitude lower than the others. This too indicates the statistical meaninglessness of the residual phase drift, and bolsters the feeling that the flat tops of the peaks are intrinsic to the pulsar and not an artifact of numerical smearing in the data reduction.

REFERENCES

Lyne, A. G. and Pritchard, R. S. 1992, *Jodrell N Bank Crab Pulsar Timing Results Monthly Ephemeris (March 10, 1992)*

Morlock, S. and Kimmer, E. 1992, *memo to J. Hodges dated January 27, 1992*

Rankin, A. 1992, *Private communication*

Werner, M. L. 1992, *Private communication*

Table 1

Observation	Date	Filter	Duration (s)
v0qy0102	1991 Oct 17 16:09:03.60	F400LP	2160
v0qy0201	1991 Oct 18 06:39:02.61	F400LP	1800
v0qy0301	1991 Oct 19 06:49:52.61	F400LP	1800
v0qy0401	1991 Oct 20 07:00:43.61	F400LP	1800
v0ui0103	1992 Jan 21 07:58:06.67	F160LP	1680

Table 1: Summary of HSP observations of the Crab pulsar

Table 2

	Counts per sample							
Observation	6	5	4	3	2	1	0	total
v0qy0102	0	0	12	329	13908	733379	200180372	200928000
v0qy0201	1	0	9	384	17002	844570	166577394	167439360
v0qy0301	0	0	5	254	11550	655336	166772215	167439360
v0qy0401	0	0	2	243	10321	601035	166827759	167439360
v0ui0103	0	0	0	0	164	72859	156203457	156276480

Table 2: Histograms of the raw data.

Table 3

Ephemeris file	Start (MJD)	Stop (MJD)
pbag0000r.orx	48545.0	48547.0
pbai0000r.orx	48547.0	48549.0
pbak0000r.orx	48549.0	48551.0
pc1k0000r.orx	48641.0	48643.0

Table 3: Definitive Ephemeris files used for HST position

Table 4

Observation	packet time	backward time	forward time	difference
v0qy0102	373733321.875977	373733321.710977	373733321.672008	0.038969
v0qy0201	374150913.881836	374150913.716836	374150913.672008	0.044828
v0qy0301	374847313.875977	374847313.710977	374847313.672008	0.038969
v0qy0401	375543721.876953	375543721.711953	375543721.672008	0.039945
v0ui0103	439852865.882813	439852865.717812	439852865.672008	0.045804
mean				0.041703
std. dev.				0.003340

Table 4: Timing data (values are in HST clock ticks, 125 ms)

Table 5

Observation	Radio Epoch	ν_0 (Hz)	$\dot{\nu}(10^{-10}/s^2)$
v0qy0102	48544 + 0.030786 s	29.9436079304	-3.7748018
v0qy0201	48544 + 0.030786 s	29.9436079304	-3.7748018
v0qy0301	48544 + 0.030786 s	29.9436079304	-3.7748018
v0qy0401	48544 + 0.030786 s	29.9436079304	-3.7748018
v0ui0103	48636 + 0.020498 s	29.9406077550	-3.7737775

Table 5: Radio ephemerides used in the data reduction

Table 6

Observation	Φ_0	Phase error	Phase drift ($\Delta P/P$)
v0qy0102	6922707.609	-9.66670e-02	-2.507667e-08
v0qy0201	8485862.431	-9.50542e-02	-4.144763e-08
v0qy0301	11092663.576	-9.56528e-02	5.811730e-09
v0qy0401	13699489.437	-9.42972e-02	-2.386960e-08
v0ui0103	16391899.795	-9.58908e-02	-3.832335e-08
mean		-9.55124e-02	-2.458110e-08
std. dev.		8.92000e-04	1.869362e-08
RMS			2.97286e-08

Table 6: Phase errors and drifts (Forward method).

Table 7

Observation	Φ_0	Phase error	Phase drift ($\Delta P/P$)
v0qy0102	6922707.755	4.823839e-02	-1.618972e-08
v0qy0201	8485862.599	7.154610e-02	-3.709999e-08
v0qy0301	11092663.722	5.051263e-02	-6.236897e-08
v0qy0401	13699489.587	5.380815e-02	4.463694e-12
v0ui0103	16391899.966	7.258340e-02	-4.114319e-09
mean		5.933773e-02	-2.395371e-08
std. dev.		1.179137e-02	2.586712e-08
RMS			3.33026e-08

Table 7: Phase errors and drifts (Backward method).

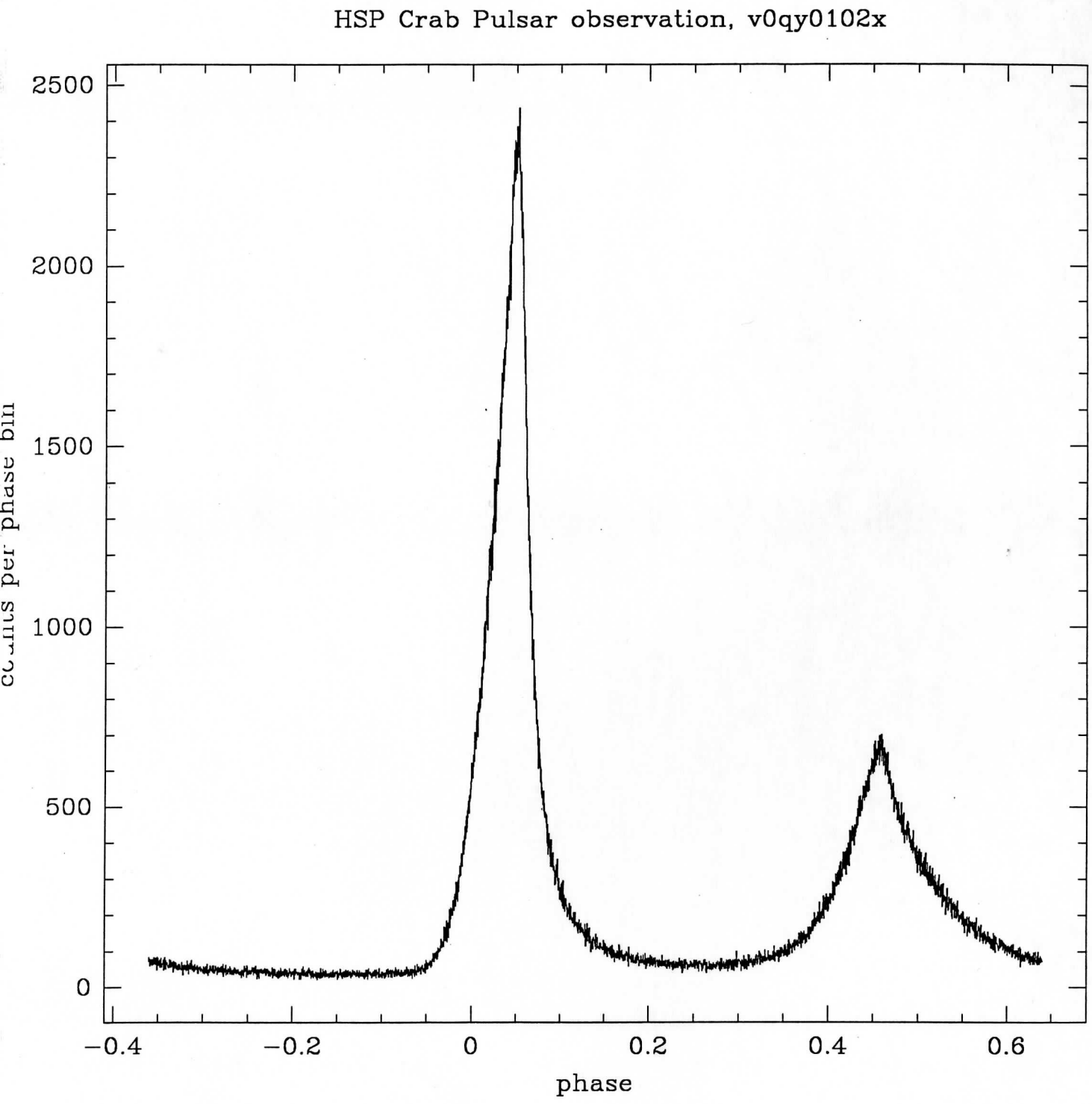

Figure 1: v0qy0102

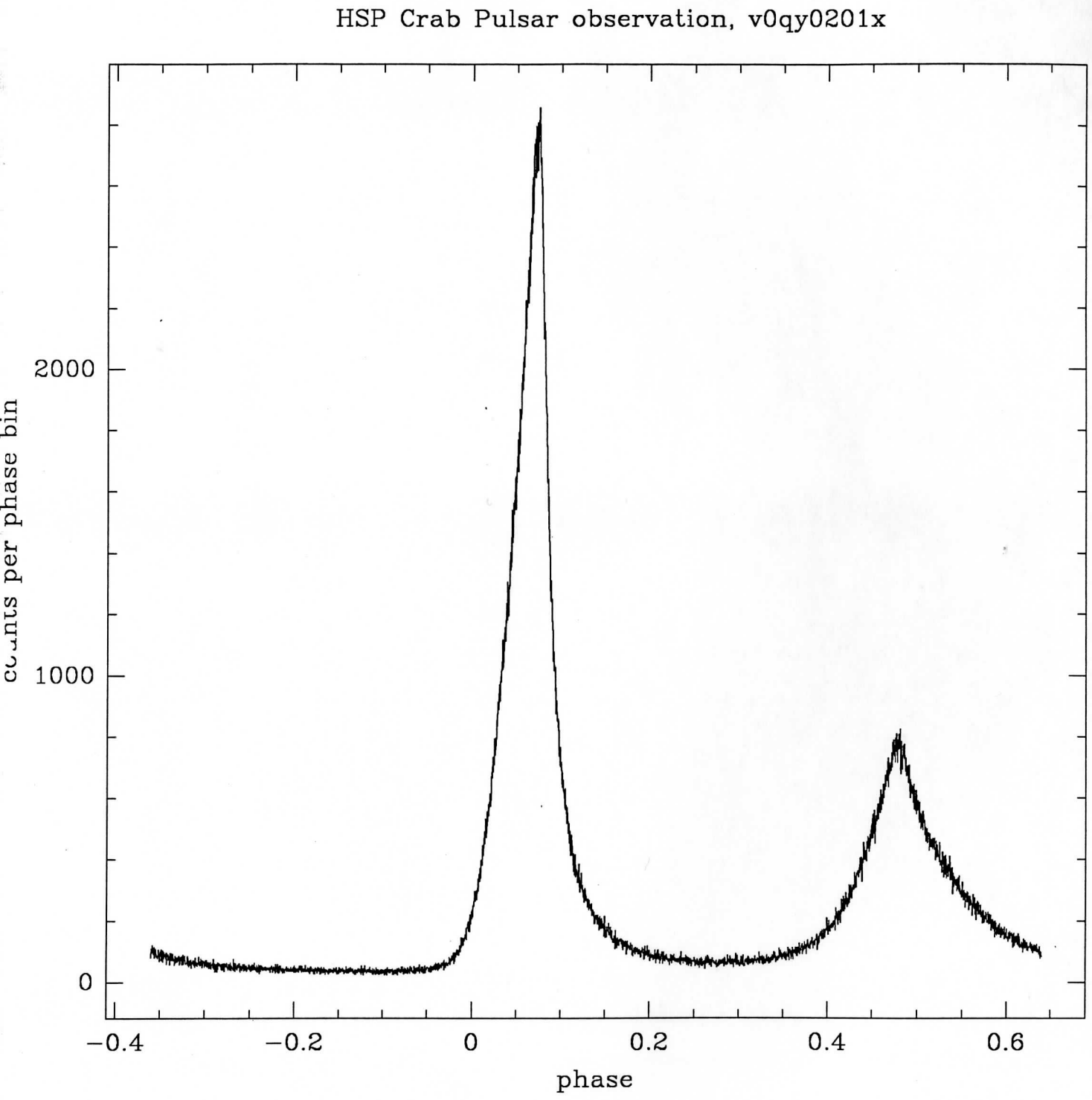

Figure 2: v0qy0201

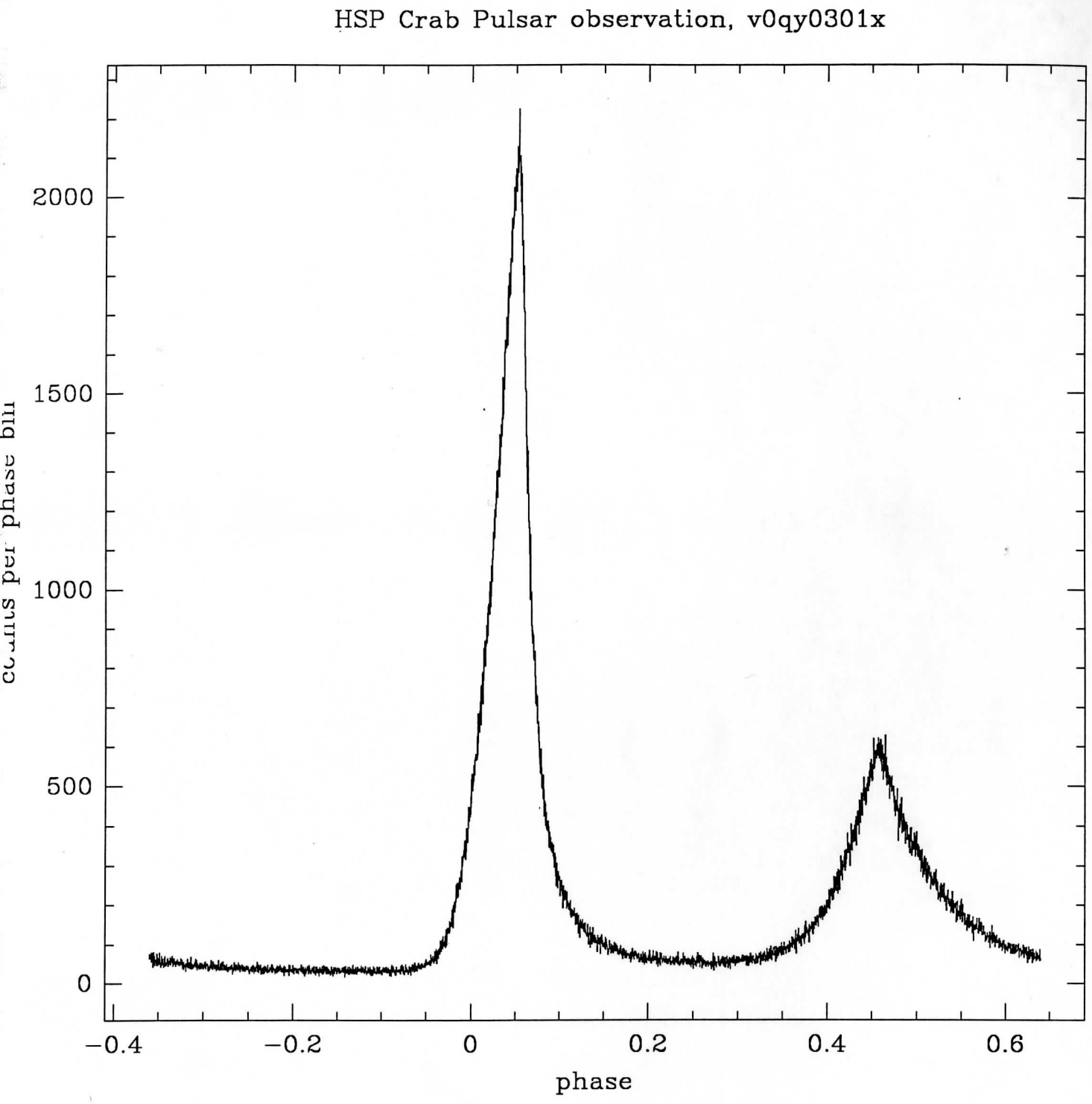

Figure 3: v0qy0301

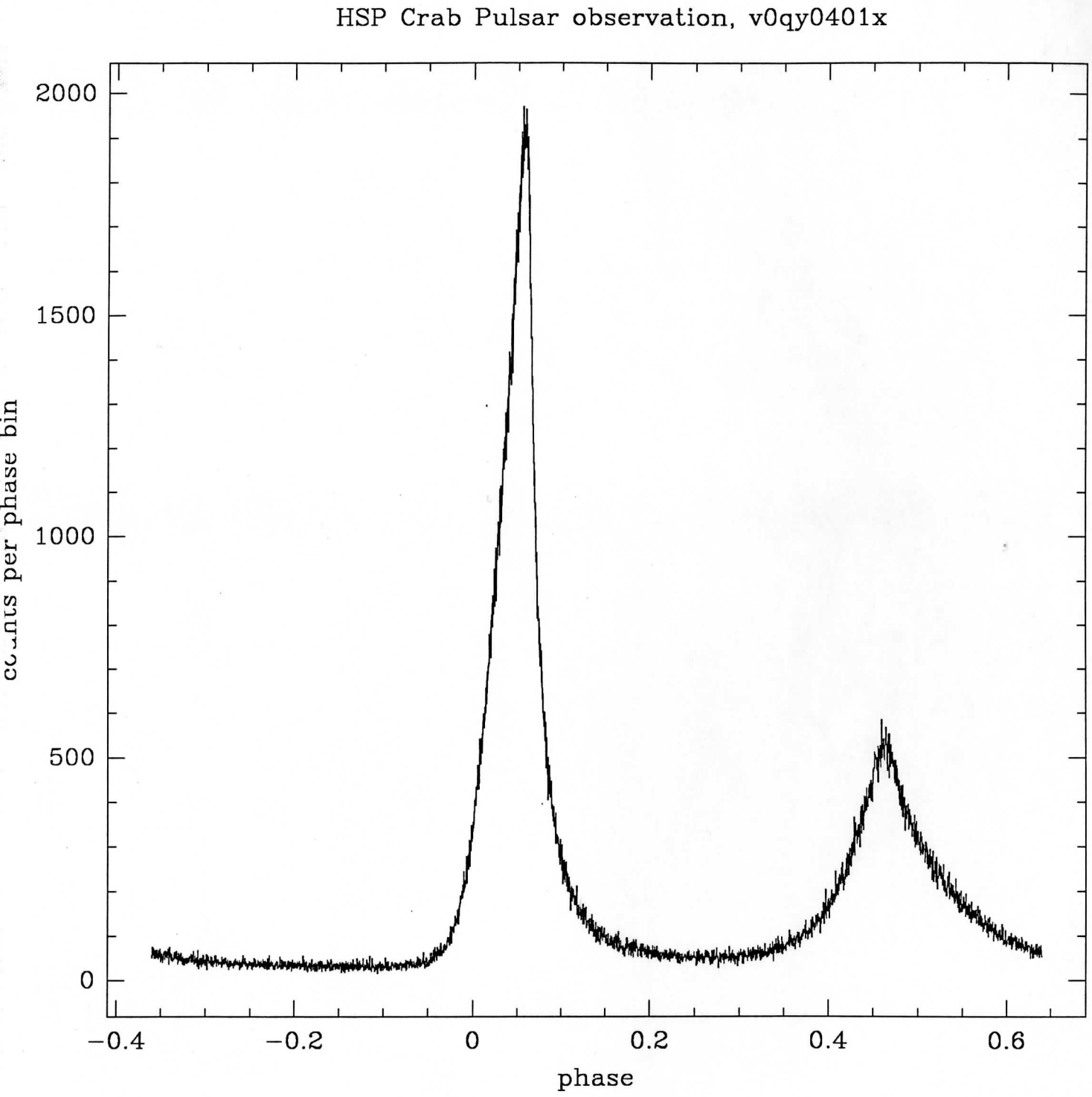

Figure 4: v0qy0401

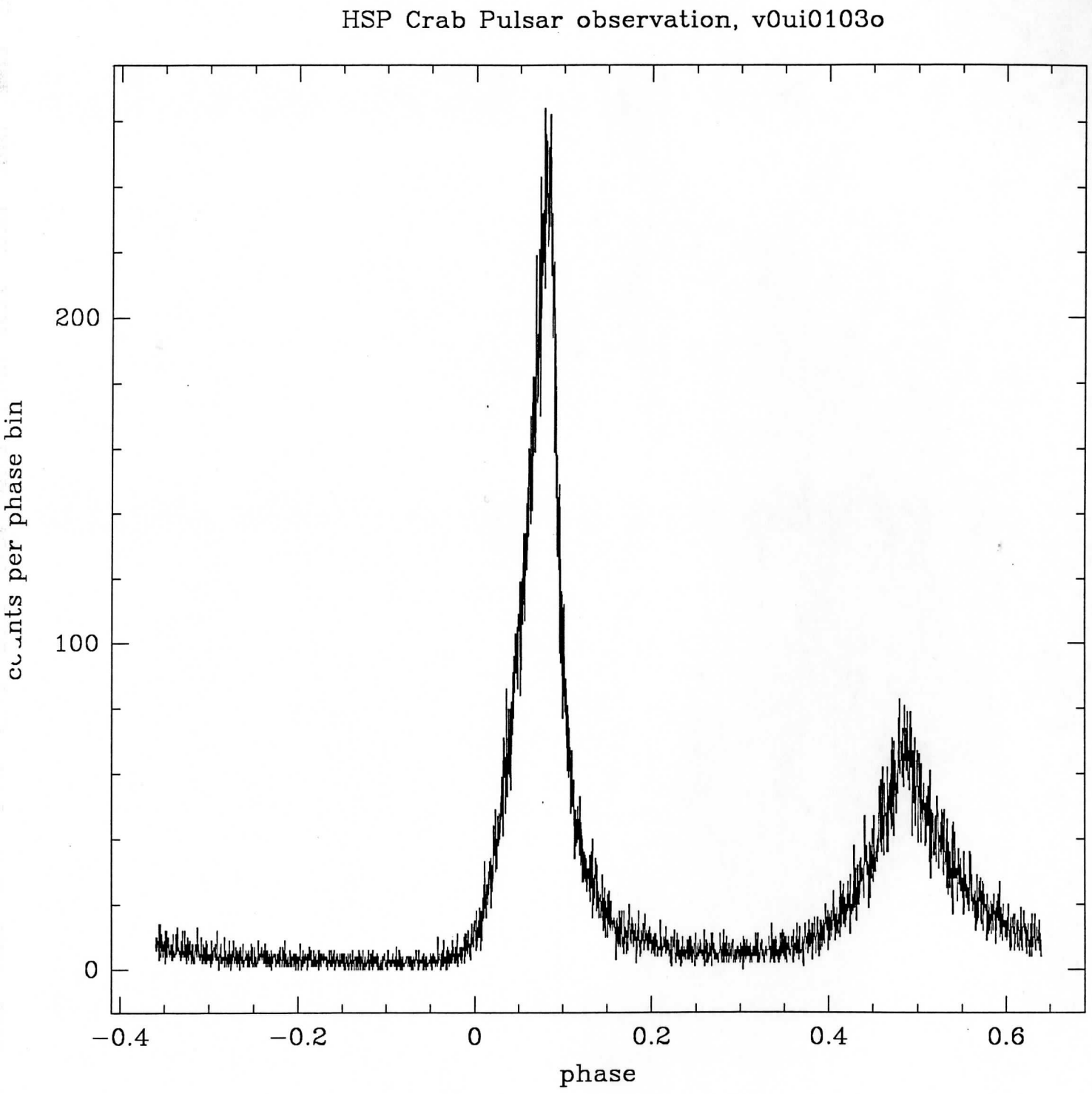

Figure 5: v0ui0103

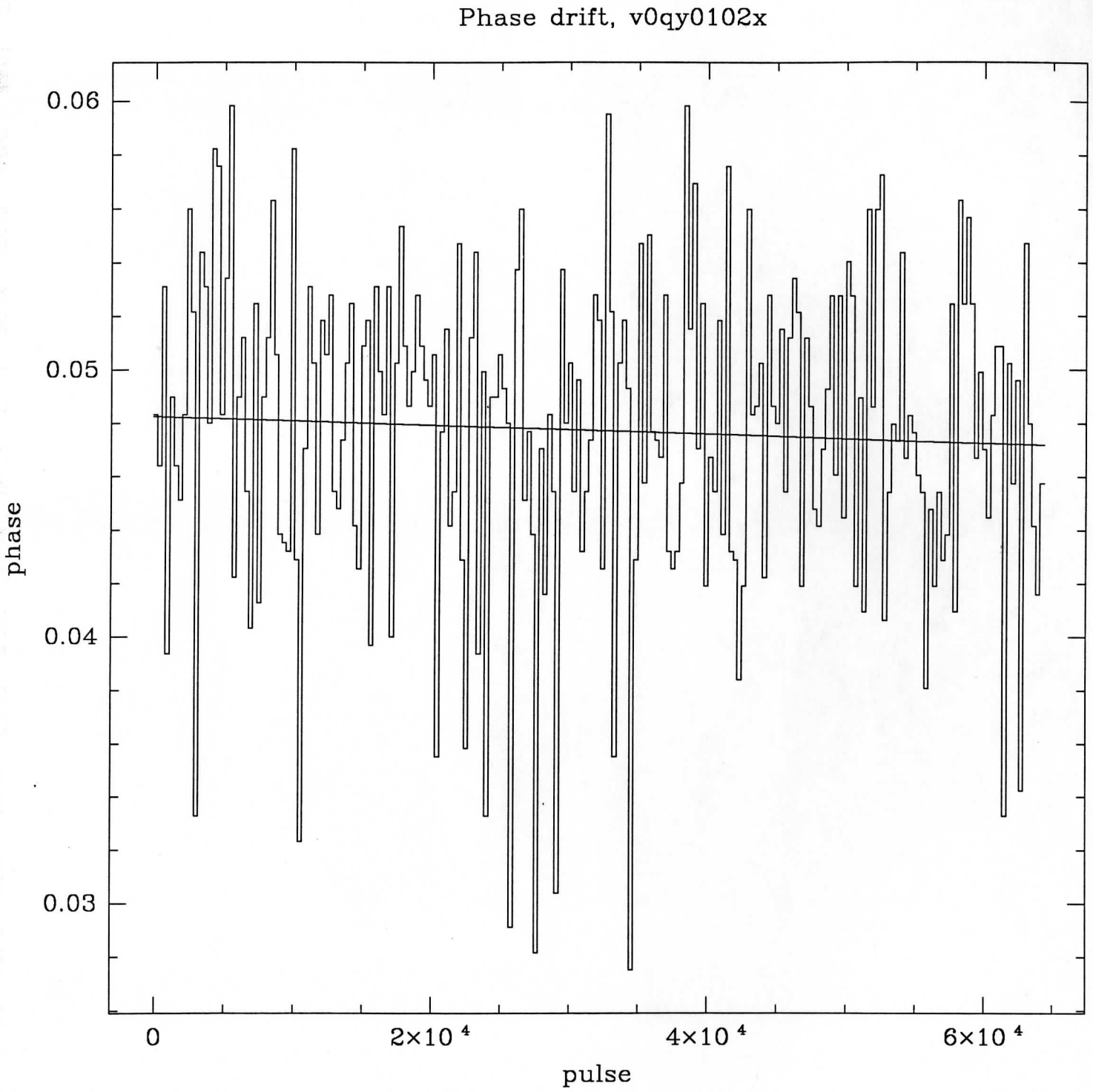

Figure 6: v0qy0102

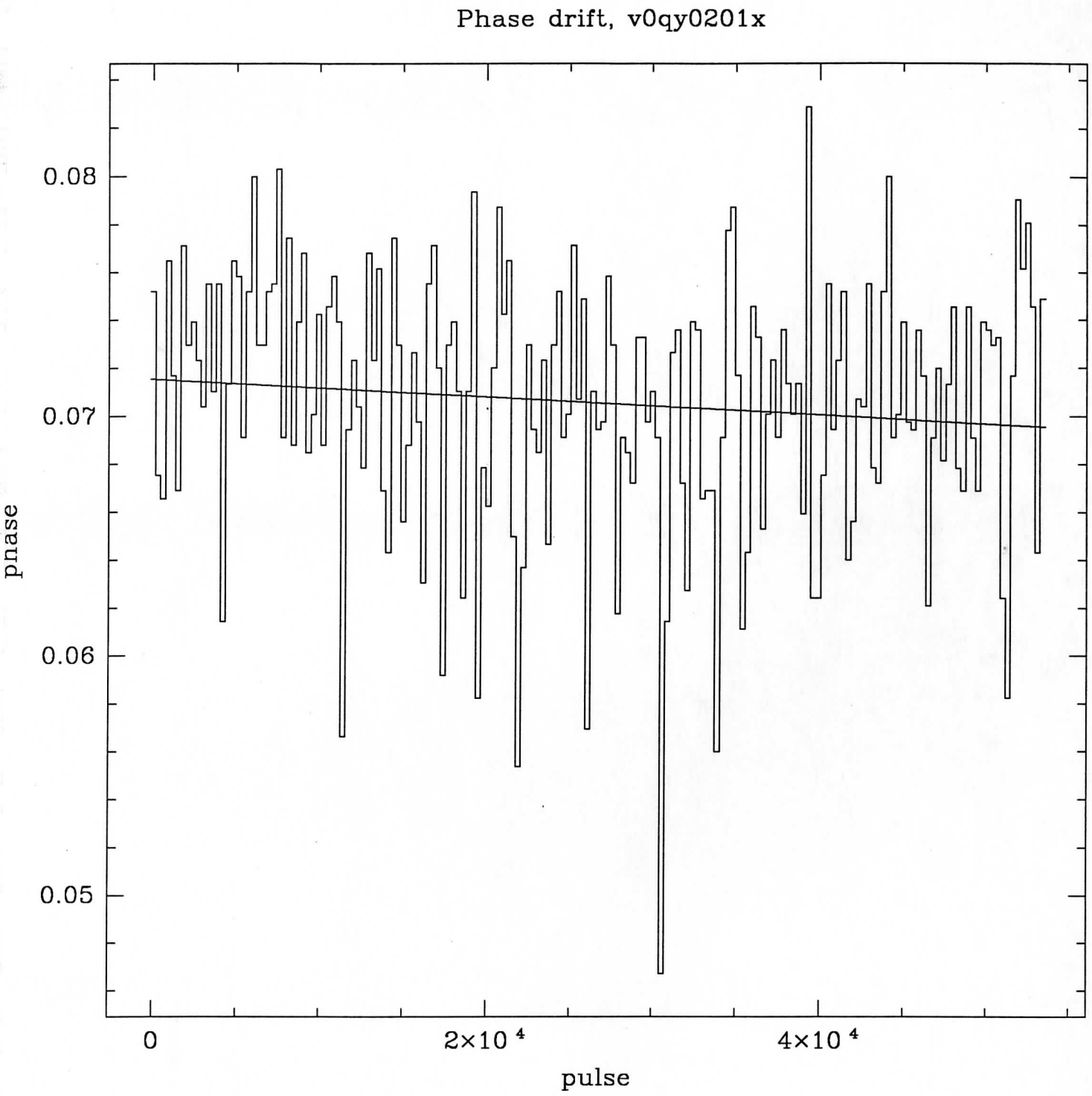

Figure 7: v0qy0201

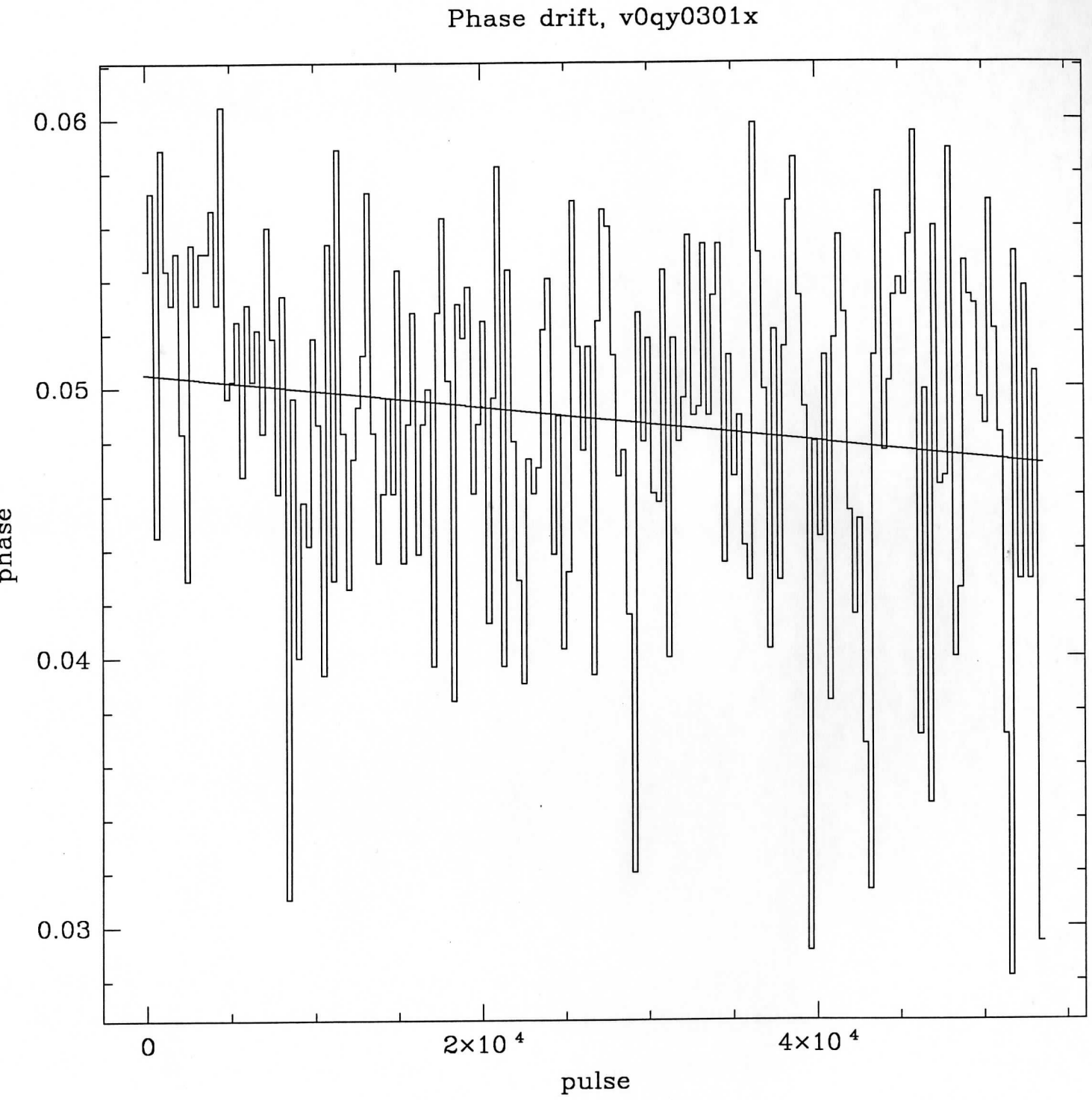

Figure 8: v0qy0301

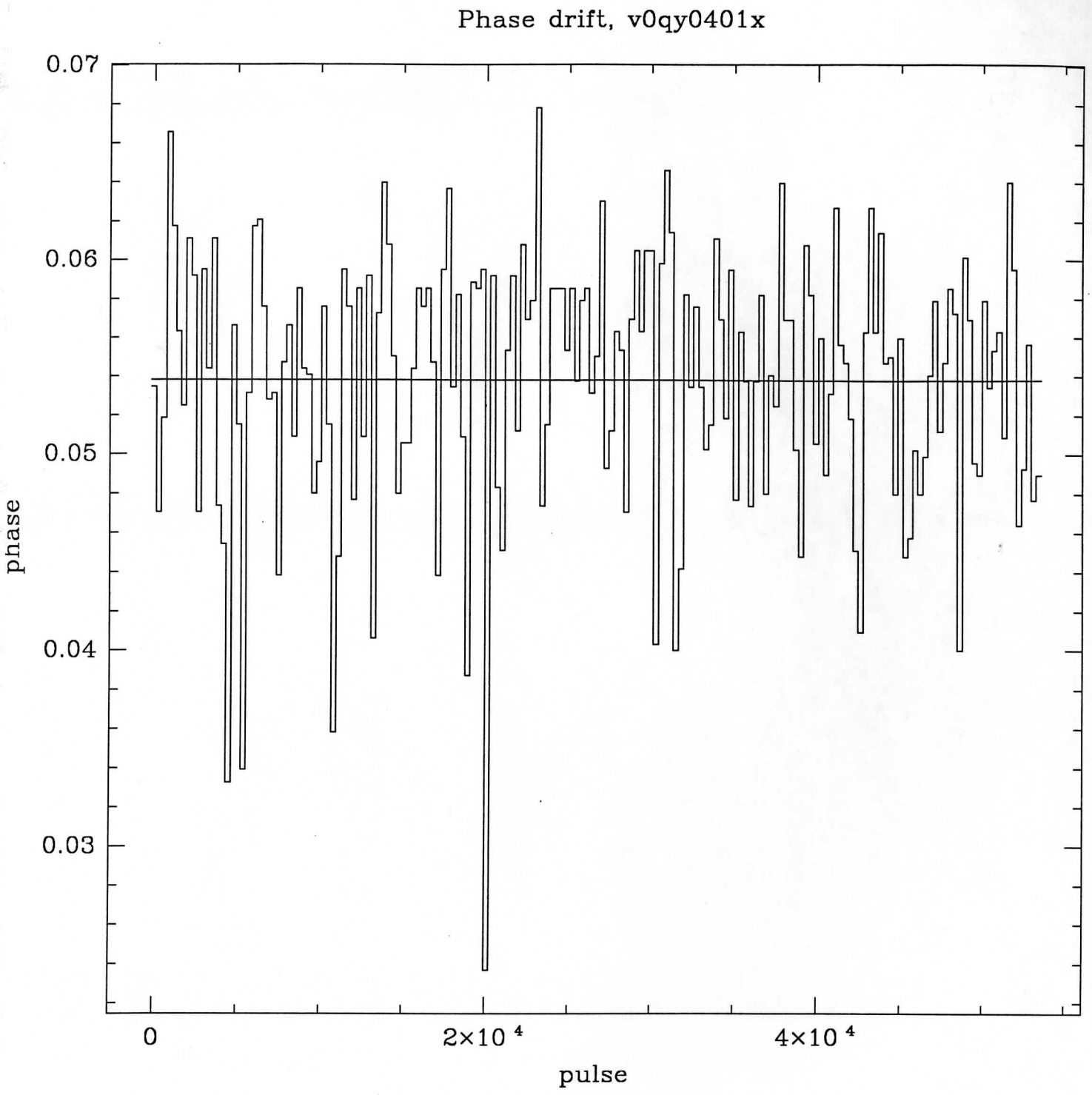

Figure 9: v0qy0401

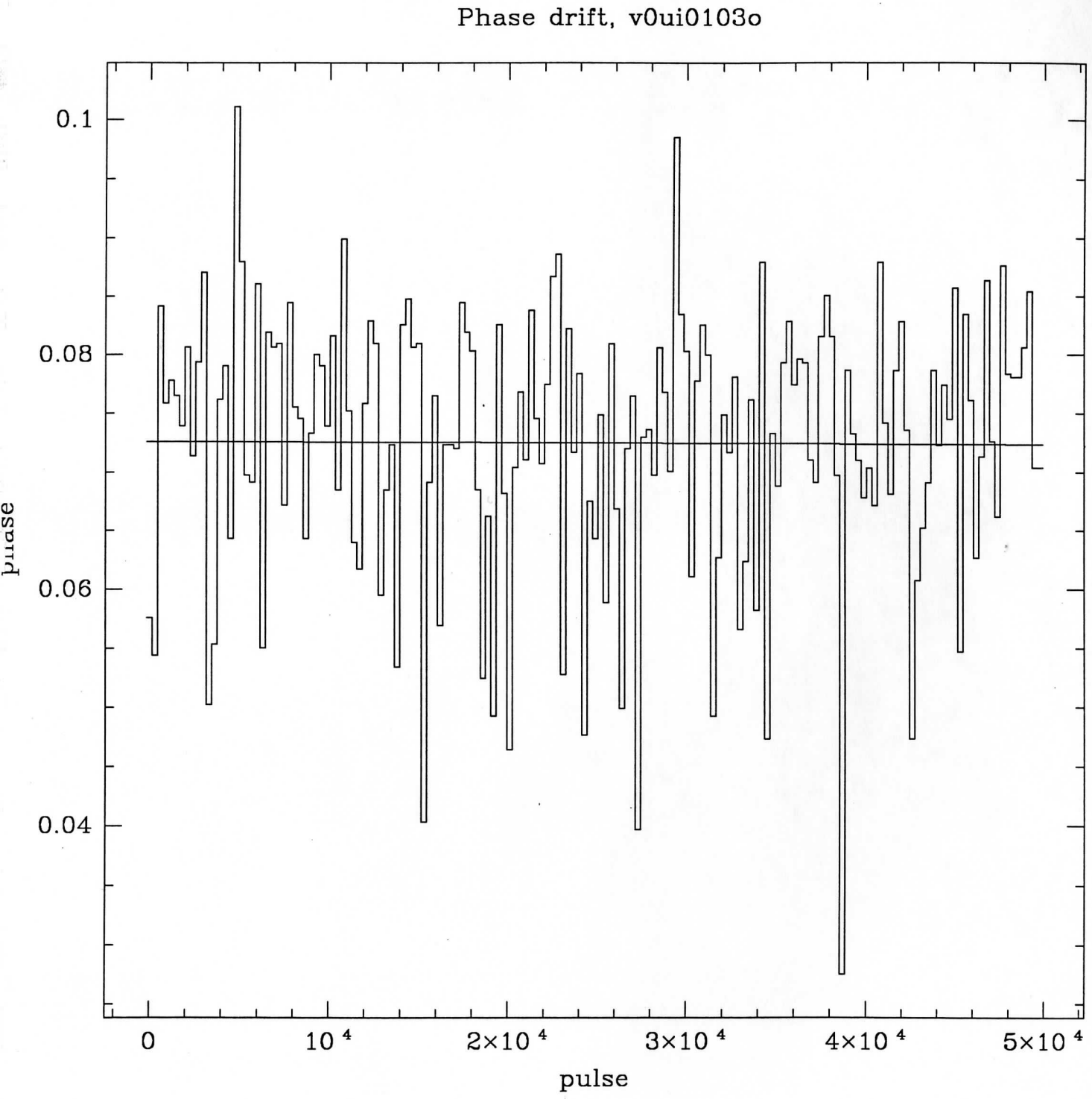

Figure 10: v0ui0103

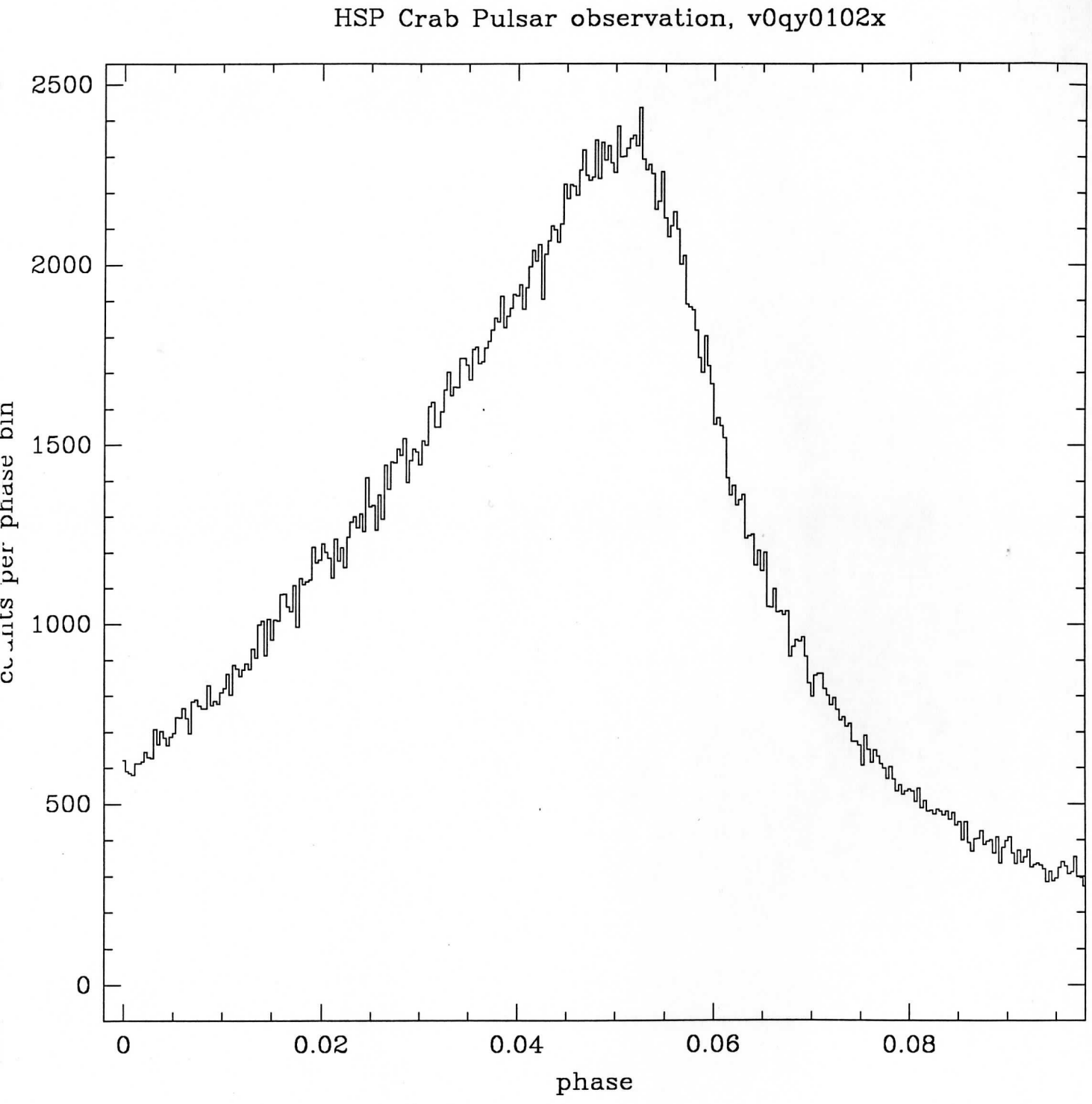

Figure 11: v0qy0102

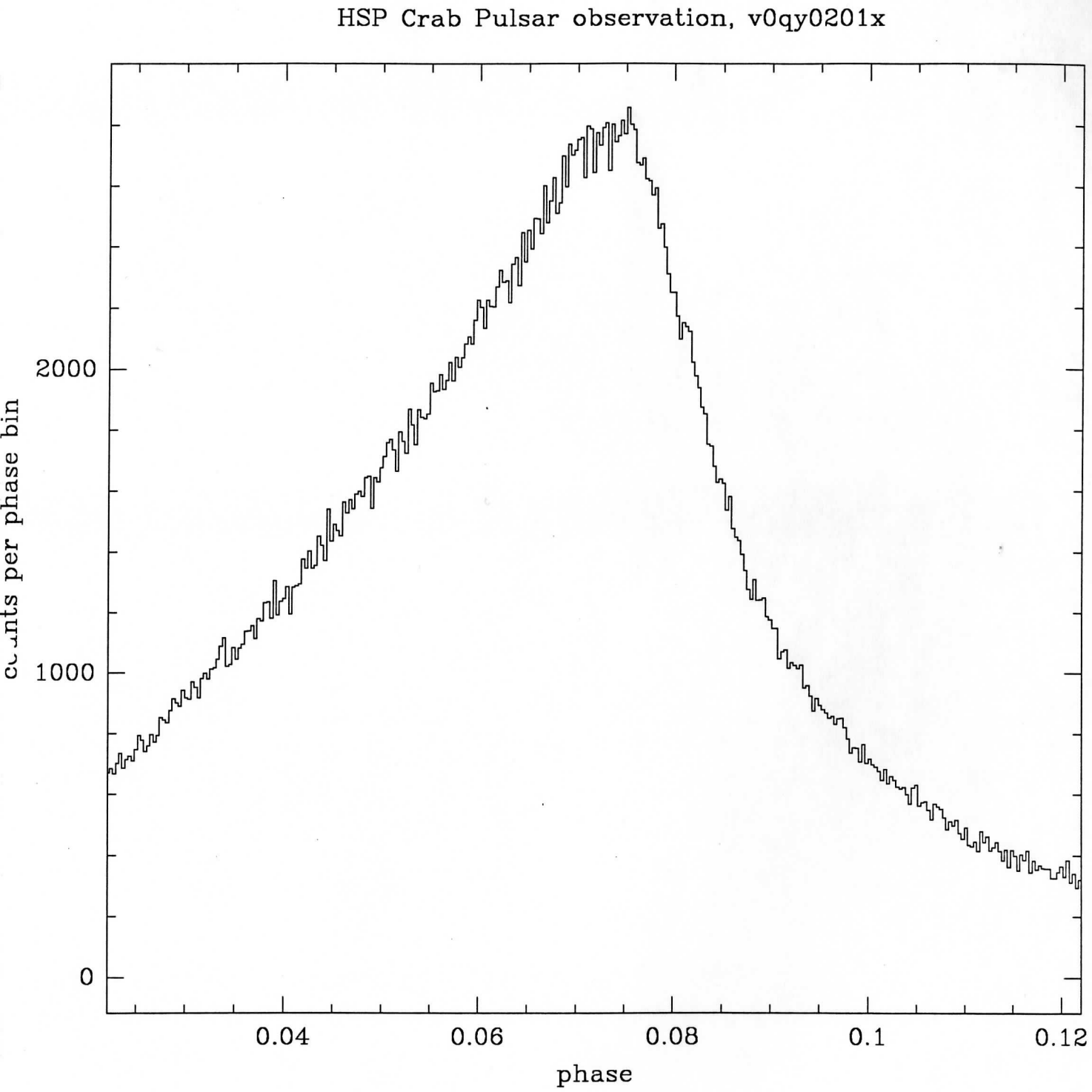

Figure 12: v0qy0201

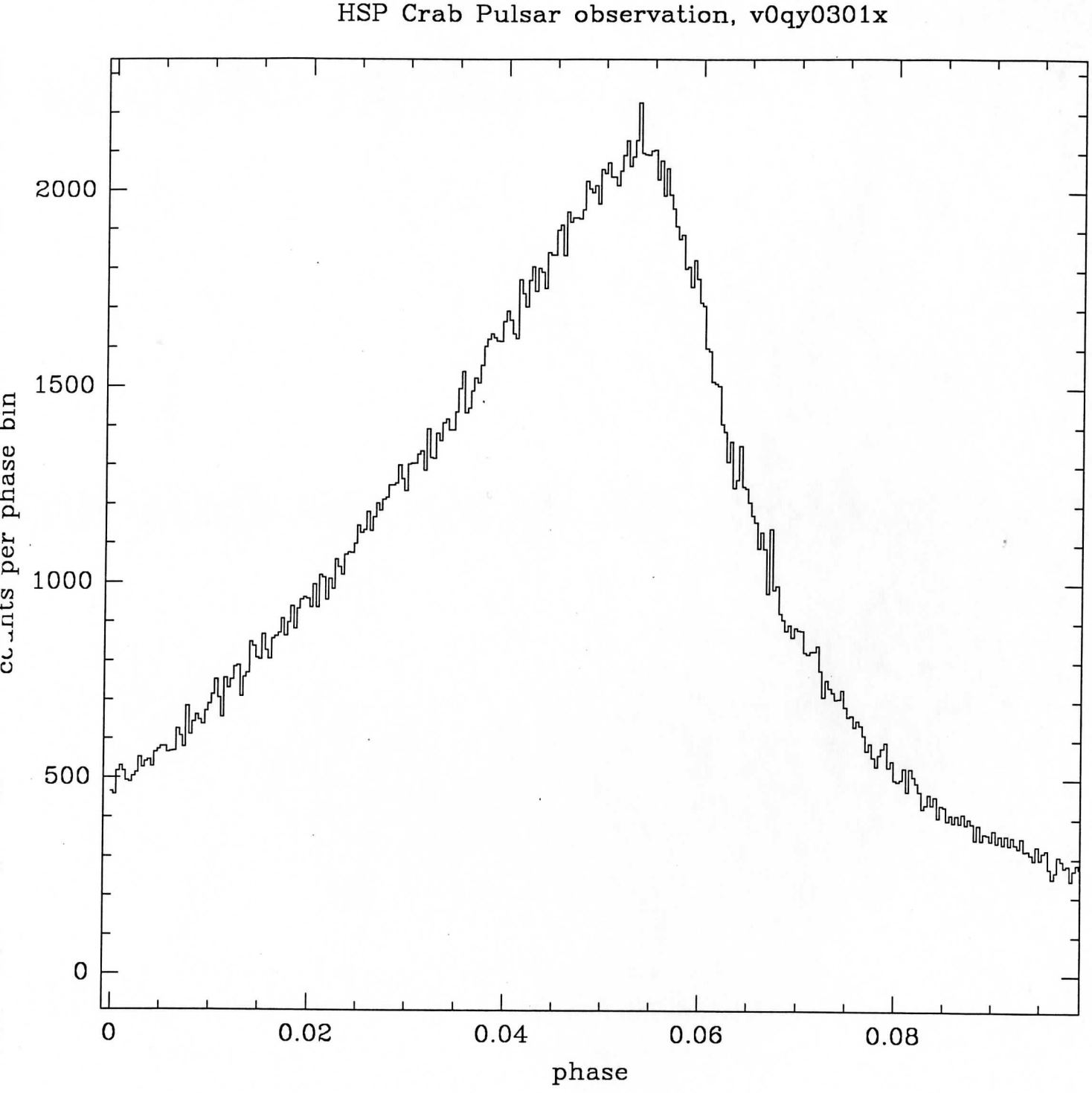

Figure 13: v0qy0301

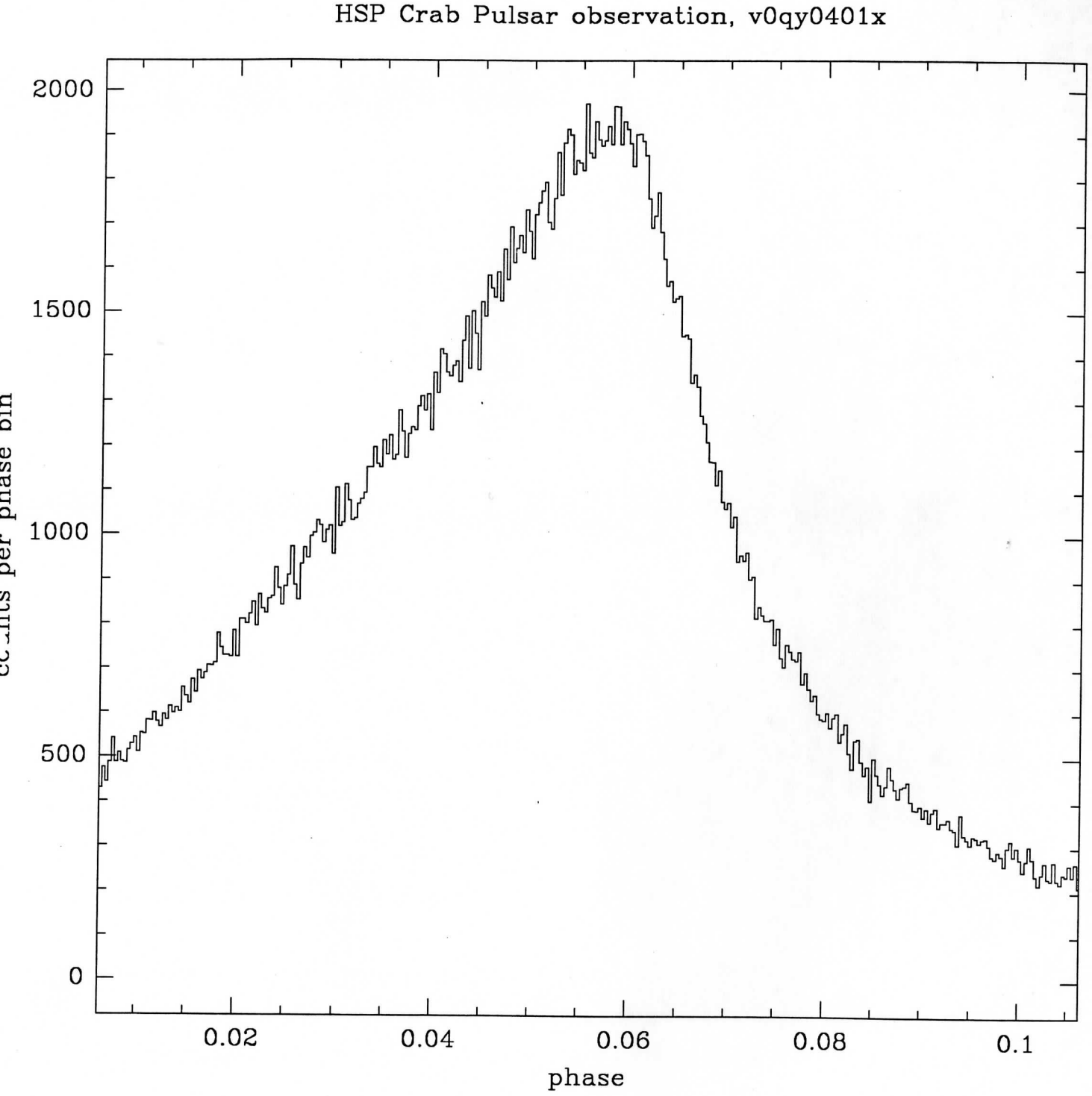

Figure 14: v0qy0401

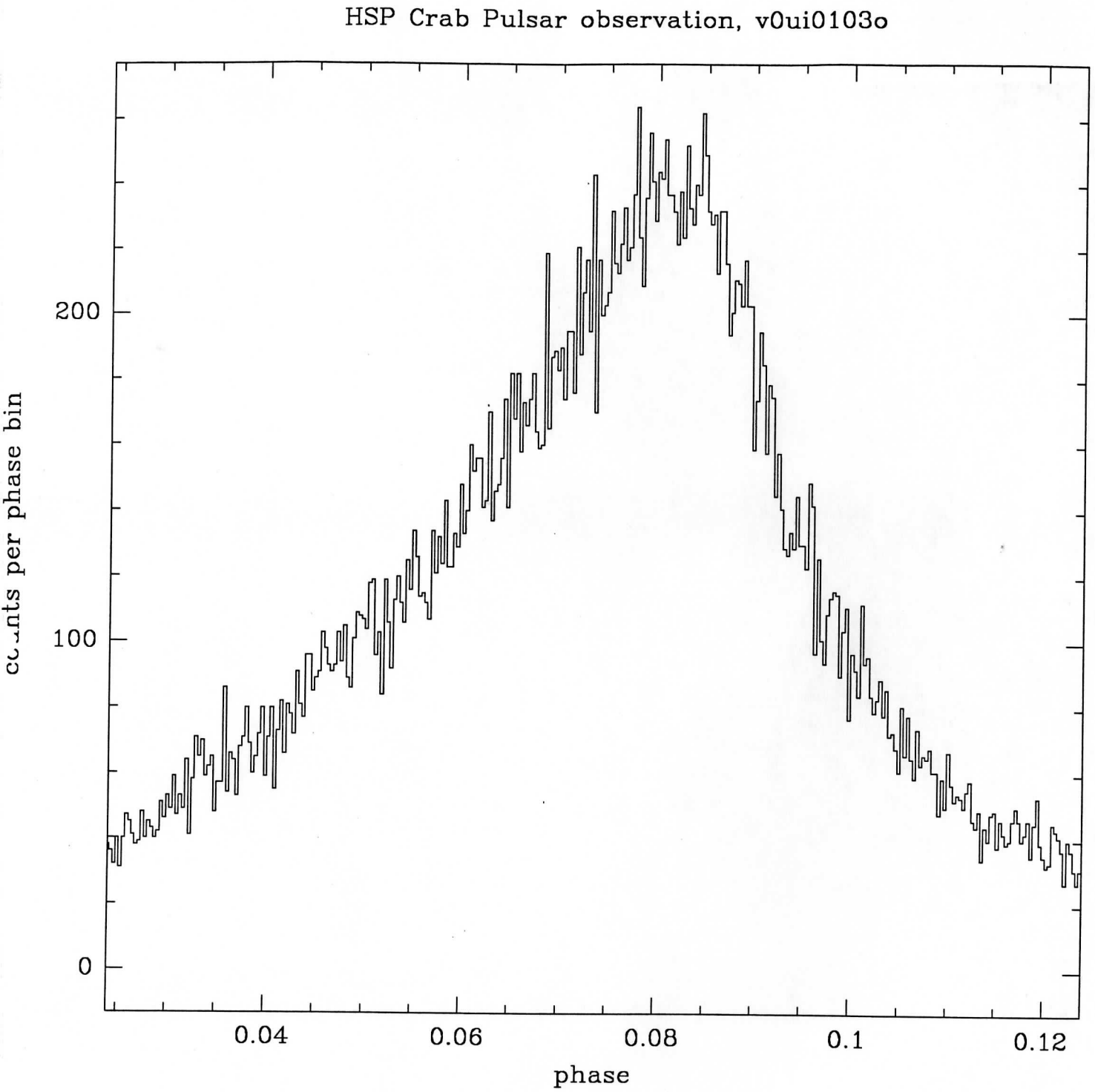

Figure 15: v0ui0103